PSDF

Power Systems Development Facility

Technical Progress Report
Gasification Test Run TC09

September 3, 2002 -
September 26, 2002

DOE Cooperative Agreement Number
DE-FC21-90MC25140

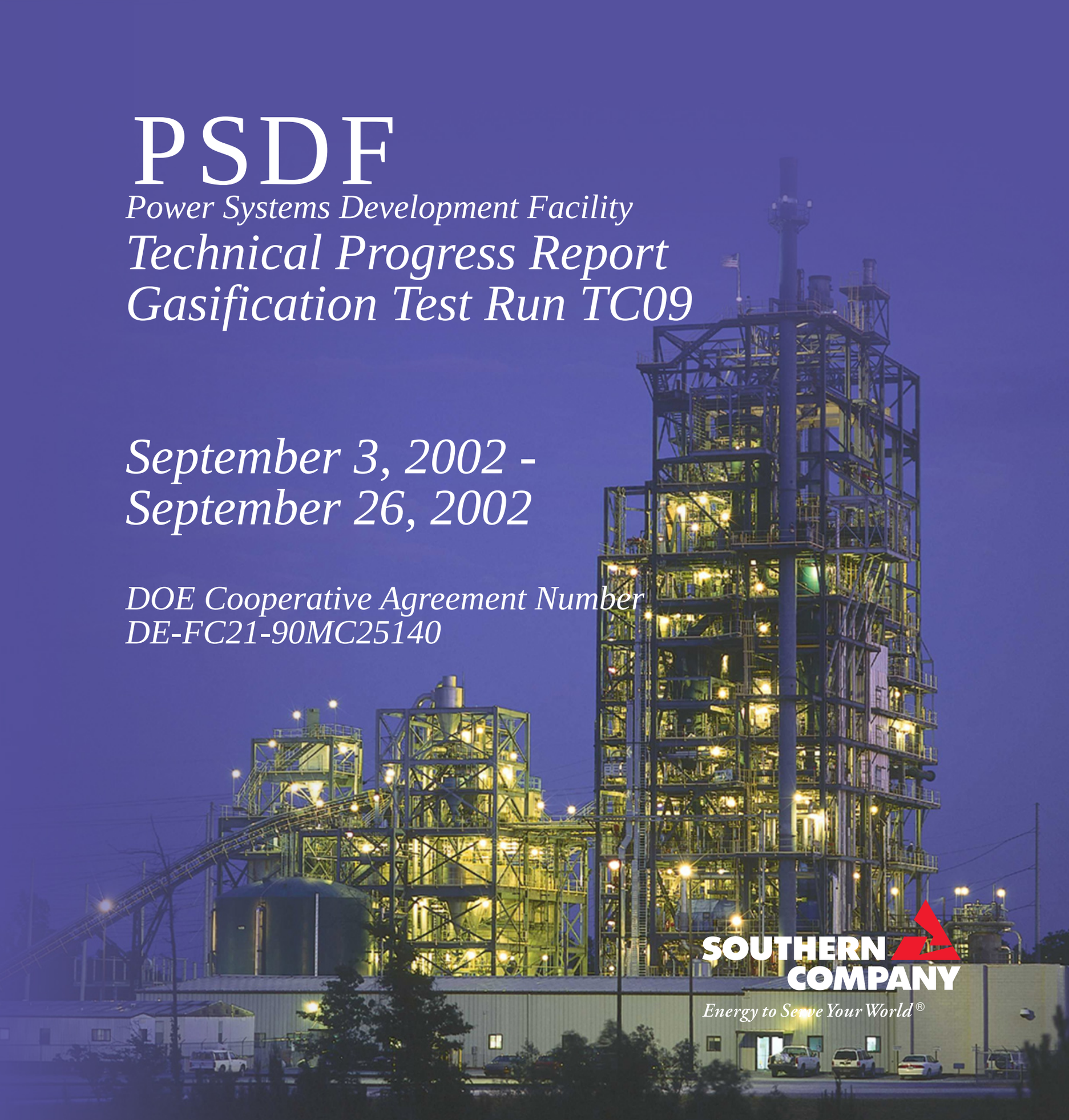

SOUTHERN COMPANY

Energy to Serve Your World®

POWER SYSTEMS DEVELOPMENT FACILITY TECHNICAL PROGRESS REPORT

GASIFICATION TEST RUN TC09

SEPTEMBER 3, 2002 – SEPTEMBER 26, 2002

DOE Cooperative Agreement Number
DE-FC21-90MC25140

Prepared by:
Southern Company Services, Inc.
Power Systems Development Facility
P.O. Box 1069
Wilsonville, AL 35186
Tel: 205-670-5840
Fax: 205-670-5843
http://psdf.southernco.com

October 2004

POWER SYSTEMS DEVELOPMENT FACILITY

DISCLAIMER

Available to the public from the National Technical Information Service, U.S. Department of Commerce, 5285 Port Royal Road, Springfield, VA 22161. Phone orders accepted at (703) 487-4650.

ABSTRACT

This report discusses Test Campaign TC09 of the Kellogg Brown & Root, Inc. (KBR) Transport Gasifier train with a Siemens Westinghouse Power Corporation (Siemens Westinghouse) particle filter system at the Power Systems Development Facility (PSDF) located in Wilsonville, Alabama. The Transport Gasifier is an advanced circulating fluidized-bed gasifier designed to operate as either a combustor or a gasifier in air- or oxygen-blown mode of operation using a particulate control device (PCD). The Transport Gasifier was operated as a pressurized gasifier during TC09 in air- and oxygen-blown modes.

Test Run TC09 was started on September 3, 2002, and completed on September 26, 2002. Both gasifier and PCD operations were stable during the test run, with a stable baseline pressure drop. The oxygen feed supply system worked well and the transition from air to oxygen was smooth. The gasifier temperature varied between 1,725 and 1,825°F at pressures from 125 to 270 psig. The gasifier operates at lower pressure during oxygen-blown mode due to the supply pressure of the oxygen system. In TC09, 414 hours of solid circulation and over 300 hours of coal feed were attained with almost 80 hours of pure oxygen feed.

ACKNOWLEDGMENT

The authors wish to acknowledge the contributions and support provided by various project managers: Jim Longanbach (DOE), Neville Holt (EPRI), Nicola Salazar (KBR), Zal Sanjana (Westinghouse), and Vann Bush (SRI). Also, the enterprising solutions to problems and the untiring endeavors of many personnel at the site are greatly appreciated. The project was sponsored by the U.S. Department of Energy National Energy Technology Laboratory under contract DE-FC21-90MC25140.

CONTENTS

Section Page

Listing of Tables

Listing of Figures

1.0 EXECUTIVE SUMMARY

1.1 SUMMARY

This report discusses Test Campaign TC09 of the Kellogg Brown & Root, Inc. (KBR) Transport Gasifier train with a Siemens Westinghouse Power Corporation (Siemens Westinghouse) particle filter system at the Power Systems Development Facility (PSDF) located in Wilsonville, Alabama. The Transport Gasifier is an advanced circulating fluidized-bed gasifier designed to operate as either a combustor or a gasifier in air- or oxygen-blown mode of operation using a particulate control device (PCD). The Transport Gasifier was operated as a pressurized gasifier during TC09 in air- and oxygen-blown modes.

The Transport Gasifier was modified prior to TC07 to operate with enriched air or pure oxygen mixed with superheated steam by adding a lower mixing zone (LMZ). The LMZ operates like a bubbling fast fluidized bed. TC09 was planned as a 250-hour test run to characterize gasifier and PCD operations using enriched air and pure oxygen with a bituminous coal from the Sufco mine in Utah. The primary test objectives were:

- Bituminous Coal Operation – Evaluate gasifier and PCD operations and performance using a bituminous coal and determine the optimum coal-feed rates, system pressures, temperatures, and steam-flow rate for stable operation.
- Bituminous Oxygen-Blown Operation – Successfully gasify a bituminous coal using oxygen, while maintaining stable gasifier and PCD operation.
- Operational Stability – Characterize gasifier loop and PCD operations for commercial performance with long-term tests by maintaining a near-constant coal-feed rate, air/coal ratio, riser velocity, solids-circulation rate, system pressure, and air distribution.
- PCD operations – Continue to improve reliability and performance by focusing on controlling pressure drop and further develop an understanding of gasification ash (g-ash) bridging.

Secondary objectives included the continuation of the following gasifier characterizations:

- Process performance – Continue to evaluate effect of gasifier operating parameters such as steam/coal ratio, solids-circulation rate, and gasifier temperature on CO/CO_2 ratio, carbon conversion, synthesis gas composition, synthesis gas Lower Heating Value (LHV), sulfur- and nitrogen-compound emissions, and cold and hot gas efficiencies.
- New Steam System Commissioning – Verify the proper operation of the new upper mixing zone (UMZ) steam system, including steam shrouds for two coal feeders, the UMZ steam nozzles, and the steam to the UMZ air nozzles.

- Fluidized-Bed Feeder Commissioning – Use the fluidized-bed feeder for adding sand to the gasifier and determine readiness for use as a coal feeder.
- Standpipe Operations – Determine the causes of standpipe bubbles and packing in the standpipe and eliminate future occurrences.
- PCD Operations – Advance failsafe development by performing online failsafe testing with solids injections.

Test Run TC09 was started on September 3, 2002, and completed on September 26, 2002. Both gasifier and PCD operations were stable during the test run, with a stable baseline pressure drop. The oxygen feed supply system worked well and the transition from air to oxygen was smooth. The gasifier temperature was varied between 1,725 and 1,825°F at pressures from 125 to 270 psig. The gasifier operates at lower pressure during oxygen-blown mode due to the supply pressure of the oxygen system. In TC09, 414 hours of solid circulation and over 300 hours of coal feed were attained with almost 80 hours of pure oxygen feed.

1.2 PSDF ACCOMPLISHMENTS

The PSDF has achieved over 4,985 hours of operation on coal feed and about 6,470 hours of solids circulation in combustion mode and 4,075 hours of solid circulation and 3,017 hours of coal feed in gasification mode of operation. The major accomplishments in TC09 are summarized below. For accomplishments in GCT1 through TC08 see the TC06, TC07, and TC08 Test Campaign technical progress reports.

1.2.1 Transport Gasifier Train

The major accomplishments and observations in TC09 included the following:

Process

- The Transport Gasifier operated for 309 hours in TC09 using a bituminous coal from the SUFCO (Southern Utah Fuel Co.) mine in Utah. The mine, located in the Wasatch Plateau, produces coal from the Hiawatha seam located in the Blackhawk formation. The gasifier operated for over 225 hours in air-blown mode and around 80 hours in oxygen-blown mode.
- The test run consisted of three periods of testing: TC09A, TC09B, and TC09C. A short inspection outage occurred after each period. All oxygen-blown operation occurred in TC09C.
- The Transport Gasifier operated smoothly at a wide range of operating conditions in both air- and oxygen-blown modes. Temperatures ranged from 1,740 to 1,870°F in the gasifier. Although the higher temperature was within 200°F of the coal ash fusion temperature, no clinkers formed during the high-temperature tests.
- Over the course of the run, the gasifier ran at pressures between 125 and 270 psig, the latter being the highest pressure seen to date by the Transport Gasifier. Currently, the design of the oxygen supply system limits the gasifier pressure during oxygen feed to below 175 psig. Thus, the high-pressure tests occurred only during air-blown operations.
- Riser velocities ranged from 30 to 60 ft/s during TC09. Solids circulation rates were between 100,000 and 300,000 lb/s ft^2, assuming a slip factor of 2.
- The new UMZ steam system performed quite well and was able to deliver up to 5,000 pph of steam to the UMZ steam nozzles, the coal-feed line steam shroud, and the gasifier air nozzles. Near the end of the run, operations gradually reduced and eventually terminated steam flow to all locations except the coal-feed line shrouds to improve syngas quality. No clinkers formed during the period of testing with low steam flow.
- During air-blown operations, the raw gas dry heating value averaged 43 Btu/SCF, and it was around 64 Btu/ SCF in oxygen-blown operations. The carbon conversion was around 90 percent during the entire run.

- Although standpipe bubbles and packing continued to pose a problem (especially during the transition from the start-up burner to coke breeze to coal feed), the new nuclear density detector in the standpipe was successful in detecting standpipe bubbles and packing in the standpipe, allowing operations to quickly adjust flows to remove the bubbles and packing.
- The test run ended on schedule after accumulating more than 309 hours for the test run and 3,017 total gasification hours.
- Carbon conversions ranged from 87 to 95 percent in air-blown mode and 80 to 92 percent in oxygen-blown mode. The corrected cold gas efficiencies were up to 72 percent in both air- and oxygen-blown modes of operation. The hot gas efficiencies ranged mostly from 85 to 90 percent.
- The nitrogen-corrected, adiabatic synthesis gas LHVs were up to 106 Btu/SCF for air-blown operation, and 171 Btu/SCF for oxygen-blown operation. The LHVs for both modes of operation were strong functions of the relative amount of oxygen fed to the Transport Gasifier.
- Synthesis gas analyzer data for CO, H_2, CH_4, CO_2, and N_2 were consistent as measured by different analyzers. The in situ H_2O measurements agreed well with calculations using water-gas shift reaction. The syngas H_2S analyzer gave good agreement when compared to the sulfur emissions by the syngas combustor SO_2 analyzer for most of TC09.
- Wet chemistry analyses indicated that NH_3 in the syngas ranged from 1,300 to 2,400 ppm during air-blown operation and 2,500 to 3,400 ppm during oxygen-blown operation.
- The water-gas shift constant using in situ H_2O measurements were between 0.53 and 0.60, despite large variations in syngas constituents during the test run.
- Overall mass balance was excellent at +/- 6 percent. The error in energy balances were less than 15 percent with a positive bias. The carbon, oxygen, and nitrogen component balances were good.

Equipment

- With continuous coal milling, the coal feeder performed reliably, causing no gasifier trips. The coal-feed rate ranged from 1,700 to 2,900 pph during the test run. During TC09A, the PCD became overloaded with solids at higher coal-feed rates and eventually plugged due to a lower than expected fines removal rate of around 550 pph. The slow fines removal rate prohibited testing coal-feed rates in excess of 3,000 pph.
- For the first time in gasification, air was used to convey the coal. TC09 also marked the first use of the coal-feed line steam shroud. Both the steam from the shroud and the transport air proved effective in reducing the chance of clinker formation.

- During TC09, the atmospheric fluidized-bed combustor (AFBC) operated for a total of 457 hours with 161 hours of g-ash feed and 192 hours on fuel oil. The AFBC start-up burner fired for 434 hours. The unit ran generally well during TC09. Temperatures were acceptable; the superheating coils provided plenty of high quality steam to the gasifier and the fuel oil system worked very well including startup. The AFBC g-ash feeder experienced problems controlling the feed rate during the majority of the run. At times, the instantaneous feed rate exceeded the compressors ability to provide sufficient air to combust the PCD fines. The AFBC bed material was also being lost at higher than expected rates due to uneven flow in the cyclone dipleg which necessitated periodic sand additions.
- Sensydine detectors and wet chemistry were used to measure ammonia and HCN concentrations from batch samples of the syngas. The ammonia concentration ranged from 900 to 2,500 ppmv, and the HCN concentration ranged from 5 to 90 ppmv.
- For the majority of the test run, no tar or crystals formed. Thus, the gas analyzers were online for virtually all of the test run, presenting excellent gas composition data. The dry gas compositions added up to between 97.5 and 99.5 percent on a consistent basis.
- The gasifier maintained high circulation rates and riser densities. These characteristics improved the temperature distribution in both the mixing zone and the riser and resulted in higher coal particle heat-up rates.
- The PCD also performed successfully during TC09. The baseline pressure drop across the PCD was low and stable during the final two segments of the run, TC09B and TC09C.

1.2.2 Particulate Control Device

The highlights of PCD operation for TC09 are listed below.

- During the initial testing in TC09A, a higher-than-usual solids loading to the PCD caused solids deposits to appear on the filter elements on the bottom plenum. The solids coverage was detected by instrumentation such as thermocouples, resistance probes, and PCD differential pressure changes. The system was shut down to inspect the PCD. The deposits dislodged during the shutdown and no remaining deposits were found during the manway inspection. As the system operating conditions improved in TC09B and TC09C, the PCD operated successfully without any deposits or g-ash bridging.
- The PCD temperature was higher than that experienced during PRB coal gasification runs, but was stable throughout the run. The inlet temperature ranged from 780 to 940°F. At a face velocity between 2.5 and 4 ft/min, the PCD baseline differential pressure was about 50 to 90 inH_2O. The back-pulse pressure was maintained at

400 psi above system pressure on the top plenum and 600 psi above system pressure on the bottom plenum using a 5-minute cycle frequency.

- All three types of PCD filter elements performed well and maintained their integrity over the course of the run. Pall FEAL, Pall Hastelloy X, and Pall Fluid Dynamics HR-160 filter elements were tested during the run. The total coal exposure time was about 309 hours (including periods in both air-blown and oxygen-blown gasification environments). Some of the FEAL filter elements have a total of 2,381 cumulative on-coal hours. No major material and structural problems have developed with these three types of metal filter elements so far. All of the Hastelloy X filter elements in this run, however, exhibited a thicker dust cake, seemingly a sign of patchy cleaning. Flow test results showed that the filter elements initially had a high flow resistance, but upon water-washing, they exhibited normal flow resistance properties.
- A semidirty shutdown was conducted at the end of TC09C. During the shutdown, the top plenum was not back-pulsed in an effort to preserve a representative transient dust cake, and the bottom plenum was back-pulsed only twice to retain the residual dust cake. The residual cake was very thin except on the Hastelloy X filter elements as mentioned above. No signs of tar effects on the cake were observed.
- Inlet sampling indicated a high inlet loading to the PCD. The inlet loading varied from about 24,000 to 42,000 ppmw during air-blown operation and from about 27,000 to 40,000 ppmw during oxygen-blown operation. The average loading was higher than the loading during PRB coal gasification. The higher loading together with g-ash property changes caused solids conveying problems in the fines removal system. The operation of the FD0502/FD0520 fines removal system was a major concern as the solids rate to the PCD often exceeded its conveying capacity. Work has begun to address the solids conveying capacity, solids level detection, and emergency handling issues.
- Outlet sampling showed that the PCD was leak tight throughout the run, with outlet particulate concentrations below 1 ppmw. Some outlet samples indicated a particle loading as high as 0.23 ppmw, although these samples appeared to be contaminated with condensed organic materials.
- Four types of failsafes were tested in TC09: PSDF-designed failsafes, Pall fuses, and two types of Siemens Westinghouse ceramic failsafes. The two ceramic failsafes, one with Specific Surface material and one with Ceramem material, were tested with g-ash injection to simulate a filter element failure. During both injection tests of the ceramic failsafes, outlet loadings of about 0.45 ppmw were measured. The post run inspection revealed that both failsafes were structurally damaged. Inspections also revealed that one of the Siemens Westinghouse ceramic failsafes (Specific Surface) under gas exposure only had collapsed. The PSDF and Pall fuse failsafes have had no incidences of material or structural problems. Further testing and evaluation of these failsafes are underway.

2.0 INTRODUCTION

This report provides an account of the TC09 test campaign with the Kellogg Brown & Root, Inc. (KBR) Transport Gasifier and the Siemens Westinghouse Power Corporation (Siemens Westinghouse) filter vessel at the Power Systems Development Facility (PSDF) located in Wilsonville, Alabama, 40 miles southeast of Birmingham. The PSDF is sponsored by the U. S. Department of Energy (DOE) and is an engineering-scale demonstration of advanced coal-fired power systems. In addition to DOE, Southern Company Services, Inc., (SCS), Electric Power Research Institute (EPRI), and Peabody Energy are cofunders. Other cofunding participants supplying services or equipment currently include KBR, and Siemens Westinghouse. SCS is responsible for constructing, commissioning, and operating the PSDF.

2.1 THE POWER SYSTEMS DEVELOPMENT FACILITY

SCS entered into an agreement with DOE/National Energy Technology Laboratory (NETL) for the design, construction, and operation of a hot gas clean-up test facility for pressurized gasification and combustion. The purpose of the PSDF is to provide a flexible test facility that can be used to develop advanced power system components and assess the integration and control issues of these advanced power systems. The facility also supports Vision 21 programs to eliminate environmental concerns associated with using fossil fuels for producing electricity, chemicals and transportation fuels. The facility was designed as a resource for rigorous, long-term testing and performance assessment of hot stream clean-up devices and other components in an integrated environment.

The PSDF now consists of the following modules for systems and component testing:

- A Transport Reactor module.
- A hot gas clean-up module.
- A compressor/turbine module.

The Transport Reactor module includes KBR Transport Reactor technology for pressurized combustion and gasification to provide either an oxidizing or reducing gas for parametric testing of hot particulate control devices (PCDs). The Transport Gasifier can be operated in either air- or oxygen-blown modes. Oxygen-blown operations are primarily focused on testing and developing various Vision 21 programs to benefit gasification technologies in general. The hot gas clean-up filter system tested to date at the PSDF is the PCD supplied by Siemens Westinghouse. The gas turbine is an Allison Model 501-KM gas turbine, which drives a synchronous generator through a speed-reducing gearbox. The model 501-KM engine was designed as a modification of the Allison Model 501-KB5 engine to provide operational flexibility. Design considerations include a large, close-coupled external combustor to burn a wide variety of fuels and a fuel delivery system that is much larger than standard.

2.2 TRANSPORT GASIFIER SYSTEM DESCRIPTION

The Transport Gasifier is an advanced circulating fluidized-bed reactor operating in air- or oxygen-blown modes, using a hot gas clean-up filter technology PCDs at a component size readily scaleable to commercial systems. The Transport Gasifier train is shown schematically in Figure 2.2-1. A taglist of all major equipment in the process train and associated balance-of-plant is provided in Tables 2.2-1 and -2.

The Transport Gasifier consists of a mixing zone, a riser, a disengager, a cyclone, a standpipe, a loopseal, and J-legs. Steam and air or oxygen are mixed together and introduced in the lower mixing zone (LMZ) while the fuel, sorbent, and additional air and steam (if needed) are added in the upper mixing zone (UMZ). The steam and air or oxygen along with the fuel, sorbent and solids from the standpipe are mixed together in the UMZ. The mixing zone, located below the riser, has a slightly larger diameter than the riser. The gas and solids move up the riser together, make two turns and enter the disengager. The disengager removes larger particles by gravity separation. The gas and remaining solids then move to the cyclone, which removes most of the particles not collected by the disengager. The gas then exits the Transport Gasifier and goes to the primary gas cooler and the PCD for final particulate cleanup. The solids collected by the disengager and cyclone are recycled back to the reactor mixing zone through the standpipe and a J-leg. The nominal Transport Gasifier operating temperature is 1,800°F. The gasifier system is designed to have a maximum operation pressure of 294 psig with a thermal capacity of about 41 MBtu/hr. Due to a lower oxygen supply pressure, the maximum operation pressure is about 175 psi in oxygen-blown mode.

For startup purposes, a burner (BR0201) is provided at the reactor mixing zone. Liquefied propane gas (LPG) is used as start-up fuel. The fuel and sorbent are separately fed into the Transport Gasifier through lockhoppers. Coal is ground to a nominal average particle diameter between 250 and 400 μ. Sorbent is ground to a nominal average particle diameter of 10 to 30 μ. Limestone or dolomitic sorbents are fed into the reactor for sulfur capture. The gas leaves the Transport Gasifier cyclone and goes to the primary gas cooler, which cools the gas prior to entering the Siemens Westinghouse PCD barrier filter. The PCD uses ceramic or metal elements to filter out dust from the reactor. The filters remove almost all the dust from the gas stream to prevent erosion of a downstream gas turbine in a commercial plant. The operating temperature of the PCD is controlled both by the reactor temperature and by an upstream gas cooler. For test purposes, 0 to 100 percent of the gas from the Transport Gasifier can flow through the gas cooler. The PCD gas temperature can range from 700 to 1,600°F. The filter elements are back-pulsed by high-pressure nitrogen in a desired time interval or at a given maximum pressure difference across the elements. There is a secondary gas cooler after the filter vessel to cool the gas before discharging to the stack or thermal oxidizer (atmospheric syngas combustor). In a commercial process, the gas from the PCD would be sent to a gas turbine in a combined-cycle package. The fuel gas is sampled for online analysis after traveling through the secondary gas cooler.

After exiting the secondary gas cooler, the gas is then letdown to about 2 psig through a pressure control valve. In gasification, the fuel gas is then sent to the atmospheric syngas burner to burn the gas and oxidize all reduced sulfur compounds (H_2S, COS, and CS_2) and reduced nitrogen compounds (NH_3 and HCN). The atmospheric syngas combustor uses propane as a

supplemental fuel. The gas from the atmospheric syngas combustor goes to the baghouse and then to the stack.

The Transport Gasifier produces both fine ash collected by the PCD and coarse ash extracted from the Transport Gasifier standpipe. The two solid streams are cooled using screw coolers, reduced in pressure in lock hoppers, and then combined together. In gasification, any fuel sulfur captured by sorbent should be present as calcium sulfide (CaS). The gasification ash (g-ash) is processed in the sulfator (atmospheric fluidized-bed combustor - AFBC) to oxidize the CaS to calcium sulfate ($CaSO_4$) and burn any residual carbon on the ash. The waste solids are then suitable for commercial use or disposal.

Table 2.2-1

Major Equipment in the Transport Gasifier Train

TAG NAME	DESCRIPTION
BR0201	Reactor Start-Up Burner
BR0401	Thermal Oxidizer
BR0602	AFBC Start-Up/PCD Preheat Burner
CO0201	Main Air Compressor
CO0401	Recycle Gas Booster Compressor
CO0601	AFBC Air Compressor
CY0201	Primary Cyclone in the Reactor Loop
CY0207	Disengager in the Reactor Loop
CY0601	AFBC Cyclone
DR0402	Steam Drum
DY0201	Feeder System Air Dryer
FD0206	Spent Solids Screw Cooler
FD0210	Coal Feeder System
FD0220	Sorbent Feeder System
FD0502	Fines Screw Cooler
FD0510	Spent Solids Transporter System
FD0520	Fines Transporter System
FD0530	Spent Solids Feeder System
FD0602	AFBC Solids Screw Cooler
FD0610	AFBC Sorbent Feeder System
FL0301	PCD — Siemens Westinghouse
FL0302	PCD — Combustion Power
FL0401	Compressor Intake Filter
HX0202	Primary Gas Cooler
HX0204	Transport Air Cooler
HX0402	Secondary Gas Cooler
HX0405	Compressor Feed Cooler
HX0601	AFBC Heat Recovery Exchanger
ME0540	Heat Transfer Fluid System
RX0201	Transport Gasifier
SI0602	Spent Solids Silo
SU0601	Sulfator (Atmospheric Fluidized-Bed Combustor-AFBC)

Table 2.2-2 (Page 1 of 3)

Major Equipment in the Balance-of-Plant

TAG NAME	DESCRIPTION
B02920	Auxiliary Boiler
B02921	Auxiliary Boiler – Superheater
CL2100	Cooling Tower
C02201A-D	Service Air Compressor A-D
C02202	Air-Cooled Service Air Compressor
C02203	High-Pressure Air Compressor
C02601A-C	Reciprocating N_2 Compressor A-C
CR0104	Coal and Sorbent Crusher
CV0100	Crushed Feed Conveyor
CV0101	Crushed Material Conveyor
DP2301	Baghouse Bypass Damper
DP2303	Inlet Damper on Dilution Air Blower
DP2304	Outlet Damper on Dilution Air Blower
DY2201A-D	Service Air Dryer A-D
DY2202	Air-Cooled Service Air Compressor Air Dryer
DY2203	High-Pressure Air Compressor Air Dryer
FD0104	MWK Coal Transport System
FD0111	MWK Coal Mill Feeder
FD0113	Sorbent Mill Feeder
FD0140	Coke Breeze and Bed Material Transport System
FD0154	MWK Limestone Transport System
FD0810	Ash Unloading System
FD0820	Baghouse Ash Transport System
FL0700	Baghouse
FN0700	Dilution Air Blower
H00100	Reclaim Hopper
H00105	Crushed Material Surge Hopper
H00252	Coal Surge Hopper
H00253	Sorbent Surge Hopper
HT2101	MWK Equipment Cooling Water Head Tank
HT2103	SCS Equipment Cooling Water Head Tank
HT0399	60-Ton Bridge Crane
HX2002	MWK Steam Condenser
HX2003	MWK Feed Water Heater

Table 2.2-2 (Page 2 of 3)

Major Equipment in the Balance-of-Plant

TAG NAME	DESCRIPTION
HX2004	MWK Subcooler
HX2103A	SCS Cooling Water Heat Exchanger
HX2103C	MWK Cooling Water Heat Exchanger
LF0300	Propane Vaporizer
MC3001-3017	MCCs for Various Equipment
ME0700	MWK Stack
ME0701	Flare
ME0814	Dry Ash Unloader for MWK Train
ML0111	Coal Mill for MWK Train
ML0113	Sorbent Mill for Both Trains
PG0011	Oxygen Plant
PG2600	Nitrogen Plant
PU2000A-B	MWK Feed Water Pump A-B
PU2100A-B	Raw Water Pump A-B
PU2101A-B	Service Water Pump A-B
PU2102A-B	Cooling Tower Make-Up Pump A-B
PU2103A-D	Circulating Water Pump A-D
PU2107	SCS Cooling Water Make-Up Pump
PU2109A-B	SCS Cooling Water Pump A-B
PU2111A-B	MWK Cooling Water Pump A-B
PU2300	Propane Pump
PU2301	Diesel Rolling Stock Pump
PU2302	Diesel Generator Transfer Pump
PU2303	Diesel Tank Sump Pump
PU2400	Fire Protection Jockey Pump
PU2401	Diesel Fire Water Pump #1
PU2402	Diesel Fire Water Pump #2
PU2504A-B	Waste Water Sump Pump A-B
PU2507	Coal and Limestone Storage Sump Pump
PU2700A-B	Demineralizer Forwarding Pump A-B

Table 2.2-2 (Page 3 of 3)

Major Equipment in the Balance-of-Plant

TAG NAME	DESCRIPTION
PU2920A-B	Auxiliary Boiler Feed Water Pump A-B
SB3001	125-V DC Station Battery
SB3002	UPS
SC0700	Baghouse Screw Conveyor
SG3000-3005	4160-V, 480-V Switchgear Buses
SI0101	MWK Crushed Coal Storage Silo
SI0103	Crushed Sorbent Storage Silo
SI0111	MWK Pulverized Coal Storage Silo
SI0113	MWK Limestone Silo
SI0114	FW Limestone Silo
SI0810	Ash Silo
ST2601	N_2 Storage Tube Bank
TK2000	MWK Condensate Storage Tank
TK2001	FW Condensate Tank
TK2100	Raw Water Storage Tank
TK2300A-D	Propane Storage Tank A-D
TK2301	Diesel Storage Tank
TK2401	Fire Water Tank
XF3000A	230/4.16-kV Main Power Transformer
XF3001B-5B	4160/480-V Station Service Transformer No. 1-5
XF3001G	480/120-V Miscellaneous Transformer
XF3010G	120/208 Distribution Transformer
XF3012G	UPS Isolation Transformer
VS2203	High-Pressure Air Receiver

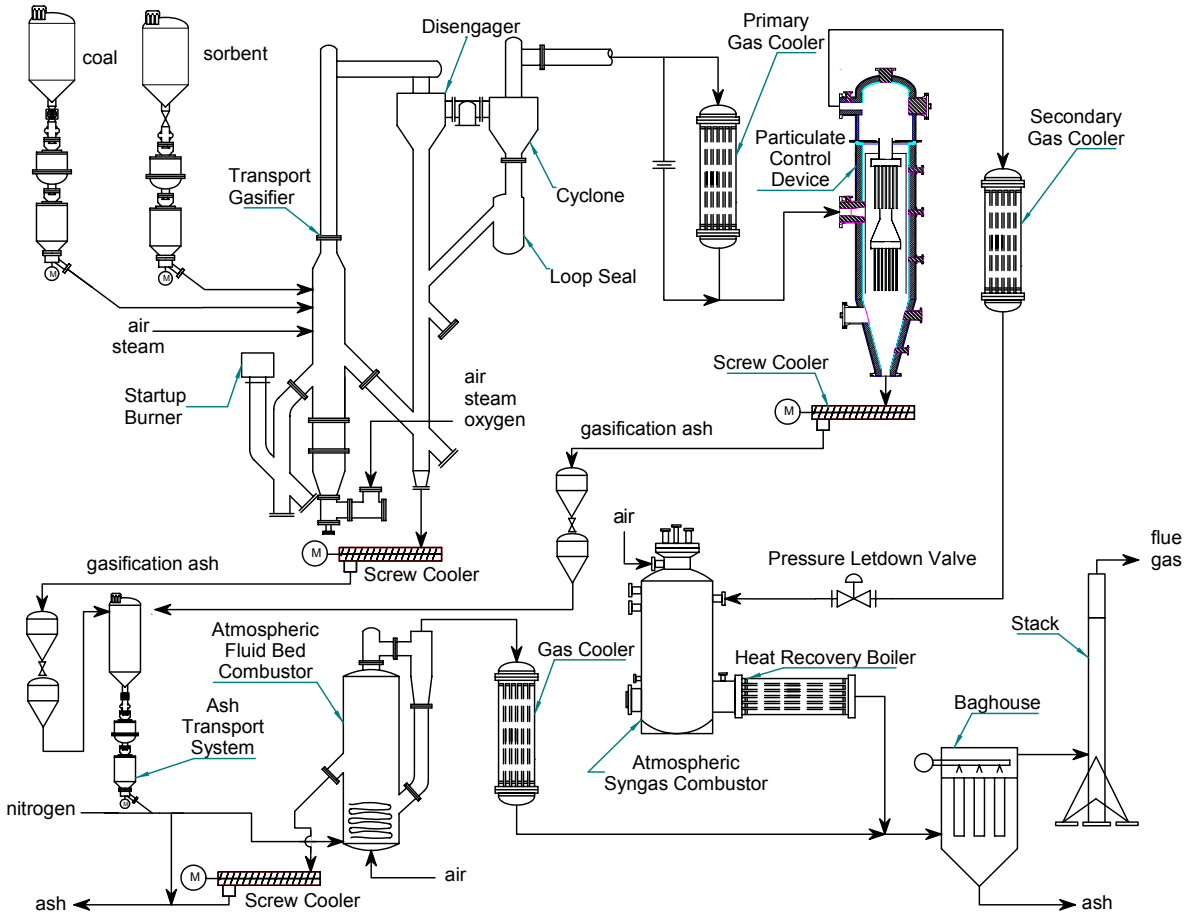

Figure 2.2-1 Flow Diagram of the Transport Gasifier

2.3 SIEMENS WESTINGHOUSE PARTICULATE CONTROL DEVICE

Different PCDs will be evaluated on the Transport Gasifier train. The first PCD that was commissioned in 1996 and has been used in all of the testing to date was the filter system designed by Siemens Westinghouse. The dirty gas enters the PCD below the tubesheet, flows through the filter elements, and the ash collects on the outside of the filter. The clean gas passes from the plenum/filter element assembly through the plenum pipe to the outlet pipe. As the ash collects on the outside surface of the filter elements, the pressure drop across the filter system gradually increases. The filter cake is periodically dislodged by injecting a high-pressure gas pulse to the clean side of the filter elements. The cake then falls to the discharge hopper.

Until the first gasification run in late 1999, the Transport Gasifier had been operated only in the combustion mode. Initially, high-pressure air was used as the pulse gas for the PCD, however, the pulse gas was changed to nitrogen early in 1997. The pulse gas was routed individually to the two-plenum/filter element assemblies via injection tubes mounted on the top head of the PCD vessel. The pulse duration was typically 0.1 to 0.5 seconds.

A sketch of the Siemens Westinghouse PCD is shown in Figure 2.3-1.

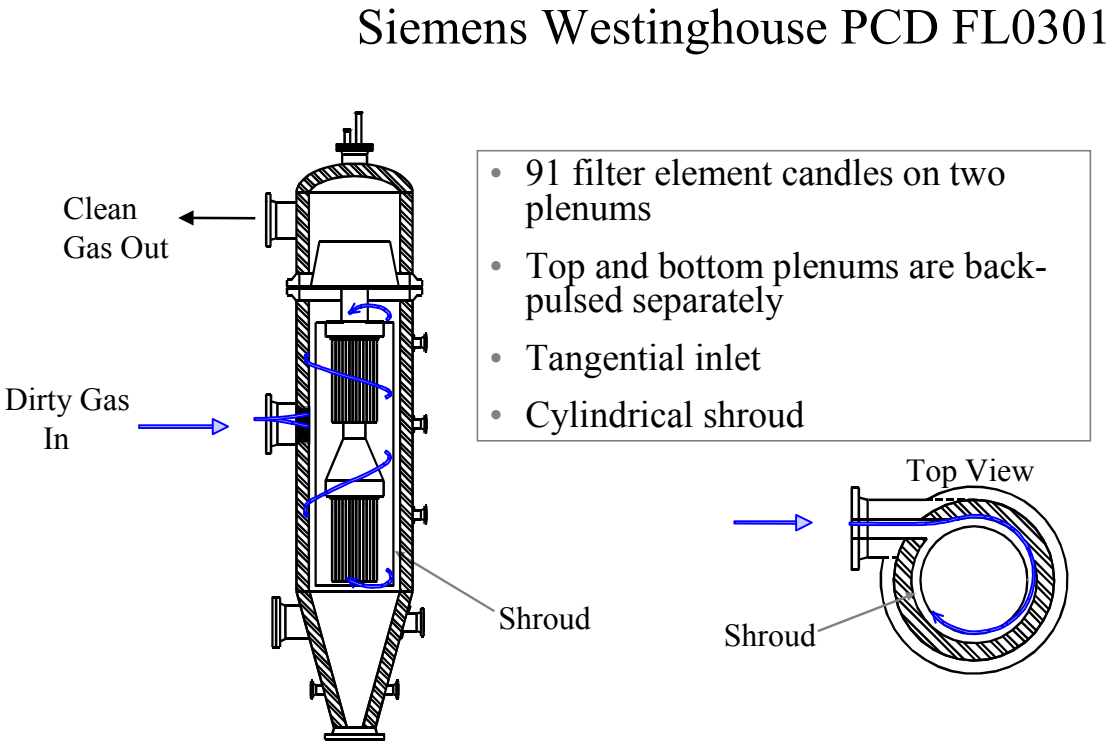

Figure 2.3-1 Siemens Westinghouse PCD

2.4 Operation Status

Conversion of the Transport Gasifier train to gasification mode of operation was performed from May to September 1999. The first gasification test run, GCT1, was planned as a 250-hour test run to commission the Transport Gasifier and to characterize the limits of operational parameter variations. GCT1 was started on September 9, 1999, with the first part completed on September 15, 1999 (GCT1A). The second part of GCT1 was started on December 7, 1999, and completed on December 15, 1999 (GCT1B-D). This test run provided the data necessary for preliminary analysis of gasifier operations and for identification of necessary modifications to improve equipment and process performance. Five different feed combinations of coal and sorbent were tested to gain a better understanding of the gasifier solids collection system efficiency.

GCT2, planned as a 250-hour characterization test run, was started on April 10, 2000, and completed on April 27, 2000. Additional data was taken to analyze effect of different operating conditions on gasifier performance and operability. A blend of several Powder River Basin (PRB) coals was used with Longview limestone from Alabama. In the outage following GCT2, the Transport Gasifier underwent a major modification to improve the operation and performance of the gasifier solids collection system. The most fundamental change was the addition of the loop seal underneath the primary cyclone.

GCT3 was planned as a 250-hour characterization with the primary objective to commission the loop seal. A hot solids circulation test (GCT3A) was started on December 1, 2000, and completed December 15, 2000. After a 1-month outage to address maintenance issues with the main air compressor, GCT3 was continued. The second part of GCT3 (GCT3B) was started on January 20, 2001, and completed on February 1, 2001. During GCT3B, a blend of several PRB coals was used with Bucyrus limestone from Ohio. The loop seal performed well needing little attention and promoting much higher solids circulation rates and higher coal-feed rates that resulted in lower relative solids loading to the PCD and higher g-ash retention in the gasifier.

GCT4, planned as a 250-hour characterization test run, was started on March 7, 2001, and completed on March 30, 2001. A blend of several PRB coals with Bucyrus limestone from Ohio was used. More experience was gained with the loop seal operations and additional data was collected to better understand gasifier performance.

TC06, planned as a 1,000-hour test campaign, was started on July 4, 2001, and completed on September 24, 2001. A blend of several PRB coals with Bucyrus limestone from Ohio was used. Both gasifier and PCD operations were stable during the test run with a stable baseline pressure drop. Due to its length and stability, the TC06 test run provided valuable data necessary to analyze long-term gasifier operations and to identify necessary modifications to improve equipment and process performance as well as progressing the goal of many thousands of hours of candle exposure.

TC07, planned as a 500-hour test campaign, was started on December 11, 2001, and completed on April 5, 2002. A blend of several PRB coals and a bituminous coal from the

Calumet mine in Alabama were tested with Bucyrus limestone from Ohio. Due to operational difficulties with the gasifier (stemming from instrumentation problems), the unit was taken offline several times. PCD operations were relatively stable considering the numerous gasifier upsets.

TC08, planned as a 250-hour test campaign to commission the gasifier in oxygen-blown mode of operation, was started on June 9, 2002, and completed on June 29, 2002. A blend of several PRB coals was tested in air-, enriched air-, and oxygen-blown modes of operation. The transition from different modes of operation was smooth and it was demonstrated that the full transition could be made within 15 minutes. Both gasifier and PCD operations were stable during the test run, with a stable baseline pressure drop.

TC09 (the subject of this report), was planned as a 250-hour test campaign to characterize the gasifier and PCD operations in air- and oxygen-blown modes of operations using a bituminous coal. TC09 was started on September 3, 2002, and completed on September 26, 2002. A bituminous coal from the Sufco mine in Utah was successfully tested in air-blown and oxygen-blown modes of operation. Both gasifier and PCD operations were stable during the test run.

Figure 2.4-1 gives a summary of operating test hours achieved with the Transport Reactor Train at the PSDF.

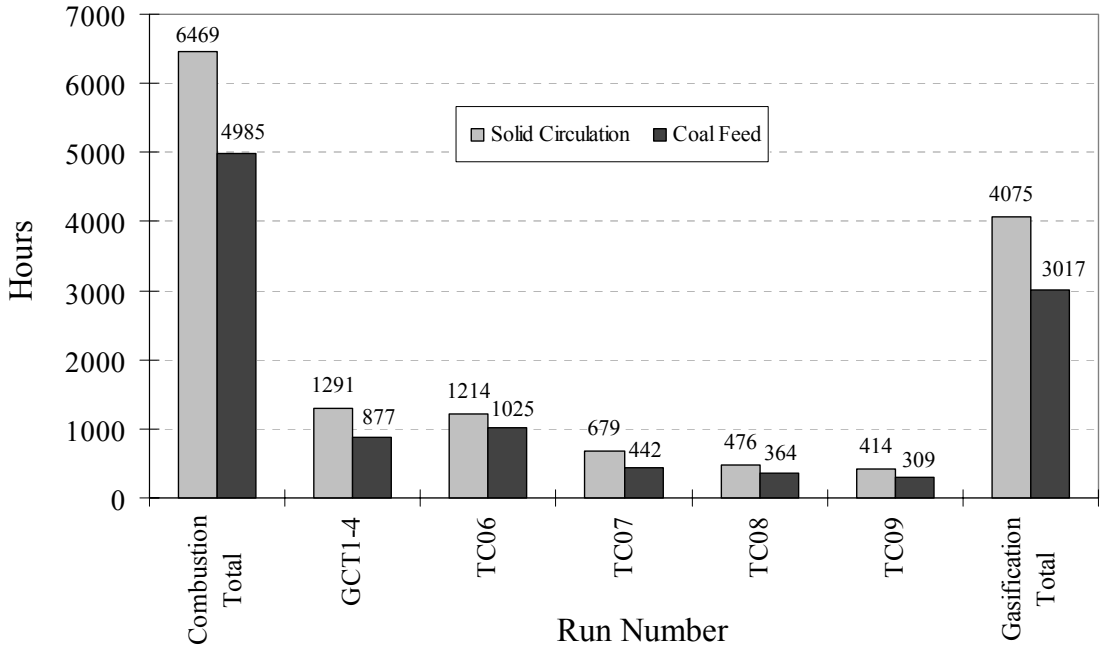

Figure 2.4-1 Operating Hours Summary for the Transport Reactor Train

3.0 PARTICLE FILTER SYSTEM

3.1 TC09 RUN OVERVIEW

In September of 2002, the first test of Hiawatha bituminous coal was completed. This test run, TC09, was only the second one in which the Transport Gasifier operated in oxygen-blown mode. Beginning in January 2002, modifications to the gasifier, specifically the addition of the lower mixing zone which was added for oxygen-blown operation, proved to reduce particle drag. The result was a lower pressure drop in the particulate control device (PCD) and more stable PCD performance. Although gasification ash (g-ash, formerly referred to as char) bridging had been a recurring problem in the 2001 runs, bridging had not occurred since the addition of the lower mixing zone (LMZ) except in the unusual circumstance of g-ash buildup due to overfilling the PCD in TC07C. In TC09, the trend of a lower pressure drop and absence of bridging continued, and PCD operation was stable except for a short period of unstable operation caused by excessive solids carryover. The PCD was leak tight during the run, and no filter element failures occurred. In addition to demonstrating reliable performance, the run provided the opportunity for further characterization of PCD components such as failsafe devices and instrumentation.

TC09 consisted of three major periods of operation including TC09A, 23 on-coal hours that ended due to g-ash buildup in the PCD; TC09B, 161 on-coal hours which ended with a scheduled shutdown; and TC09C, 125 on-coal hours, which also ended in a scheduled shutdown. Because of high solids loading that exceeded the capacity of the fines removal system in TC09A, g-ash buildup occurred and led to bridging between the filter elements. This buildup was indicated by filter element thermocouples and the newly developed resistance probes, as well as by the tube sheet pressure drop. System shutdown was necessitated by the near complete plugging of the bottom plenum of filter elements. The baseline pressure drop rose rapidly during this portion of the run, ranging from about 75 to 200 inH_2O. However, the remainder of TC09 was much more stable, with a baseline pressure drop range of about 50 to 90 inH_2O in TC09B and 50 to 80 inH_2O in TC09C. There was no evidence of g-ash buildup during these portions of TC09.

This report contains the following sections:

- PCD Operation Report, Section 3.2—This section describes the main events and operating parameters affecting PCD operation and includes a discussion of the resistance probe instrumentation. Operation of the fines removal system is also included in this section.

- Inspection Report, Section 3.3—The partial inspection performed following TC09A and the full inspection completed after TC09C are discussed in this section, this includes details of the post-run conditions of various PCD components and of the fines removal system.

- G-ash, characteristics, and PCD Performance, Section 3.4—This section includes a detailed discussion of g-ash physical and chemical properties, as well as the effects of these characteristics on PCD performance. The results of PCD inlet and outlet solids concentration sampling is also presented in this section.

- Failsafe Testing, Section 3.5—Results from the ongoing failsafe testing program are presented in this section, including details of the g-ash injection testing completed during TC09.

3.2 TC09 PCD OPERATION REPORT

3.2.1 Introduction

The first test of Hiawatha bituminous coal (TC09) was a demonstration of successful PCD operation. Although excessive solids carryover caused unstable operation in the short period of TC09A operation, PCD operation was stable for the remainder of TC09. The filter vessel was leak tight during the run, and no filter element failures occurred. The run provided the opportunity to test the newly developed resistance probes as well as to perform failsafe testing with solids injection with the Westinghouse ceramic failsafes.

In TC09A, the solids loading to the PCD exceeded the fines removal system capacity, and shortly after coal feed began, the PCD cone filled up. (Note that the solids loading to the PCD was higher than in previous runs due to the higher ash content of the bituminous coal.) After only a few hours on coal, pressure drop measurements as well as filter element thermocouples and resistance probes indicated that the gasification ash (g-ash) had built up between the filter elements. (Details of the resistance probe measurements are included in Section 3.2.5.) This buildup almost completely blocked flow through the bottom plenum of filter elements, which caused unsustainable operating conditions. Therefore, the system was shut down so that the g-ash could be removed.

The remainder of the run, which comprised TC09B and C, was stable despite some gasifier upsets occurring at startups. During TC09C, failsafe testing with g-ash injection was completed on two types of Siemens Westinghouse ceramic failsafes. (Refer to Section 3.5 for details on failsafe testing.) Both TC09B and C ended with scheduled shutdowns.

The fines removal system operated reliably during the majority of the run. However, high solids loading following gasifier upsets occasionally caused trips of the FD0502 screw cooler and the FD0520 lock hopper system. Because of the high solids loading during coal feed, the FD0520 lock hopper system required frequent cycle-time adjustment. Also, the FD0502 screw cooler required daily maintenance attention to control leaking seals.

Run statistics for TC09 are shown in Table 3.2-1. Layout 25, the filter element layout implemented for the run, is shown in Figure 3.2-1.

3.2.2 Test Objectives

For TC09, the primary objectives for the filter system were the following:

- G-ash Bridging – Although g-ash bridging had occurred in several of the previous test runs, it did not occur in the latest runs, TC07D and TC08. Prior to TC07D, several measures were taken to prevent g-ash bridging and these were also evaluated in TC09. The measures include using six blanks in the place of a partial row of elements on the bottom plenum, removing support that may be needed for g-ash bridging. Also, the bottom plenum back-pulse pressure was consistently kept at 600 psid, that is, 600 psi above gasifier pressure, with the pulse frequency of 5 minutes during coal feed.

To track g-ash bridging that may occur during the run, filter element surface temperatures were monitored for its presence and growth. More thermocouples were added, for a total of 33 thermocouples attached to the filter element surfaces. These were installed primarily on the bottom plenum and placed at various locations and levels. In addition, six resistance probes were installed on two adjacent elements to detect g-ash bridging between the elements. These probes protruded about half an inch from the element surfaces, and, when covered by g-ash, measure change in electrical resistance.

The inverted filter design by Siemens Westinghouse was incorporated into the TC08 filter element layout for initial evaluation. Because the two inverted assemblies functioned without apparent plugging or sealing problems, they were left in place for further evaluation in TC09.

- Filter Element Testing – Exposure of metallic filter elements continued in TC09. Many of the filter elements from TC08 were reinstalled and included Pall Iron Aluminide (FEAL), Pall Hastelloy X, and U.S. Filter HR-160 filter elements. A greater number of Hastelloy X and HR-160 filter elements were installed to more extensively characterize these materials.

- Failsafe Device Testing – Several types of failsafe devices were exposed during TC09, including the Pall fuse, the PSDF design, and the Siemens Westinghouse ceramic failsafes. Also, on-line tests of the Siemens Westinghouse ceramic failsafes were conducted, which entailed g-ash injection into the clean side of two filter elements beneath the tested failsafes. The effectiveness of each failsafe device was evaluated by monitoring pressure drop measurements across the filter elements and failsafes tested, and by SRI outlet sampling during the injections.

- Dustcake Characterization – As in previous runs, PCD pressure drop was monitored throughout TC09, and the rate of pressure drop rise was used in combination with the measured particulate loadings and face velocities to determine the drag of the transient dustcake under various conditions. At the conclusion of TC09, the PCD was shut down "semidirty," that is, the top plenum of the PCD was shut down dirty (last back-pulse initiated 5 minutes before coal feed ended) while the bottom plenum was back-pulsed twice after coal feed ended. The contributions of the transient and residual dustcakes to the PCD pressure drop were examined by comparing laboratory drag measurements with the drag values calculated from the PCD pressure drop rise and baseline pressure drop.

- Inlet Particulate Sampling and Characterization – TC09 allowed evaluation of the effects of a new coal on the characteristics of Transport Gasifier g-ash. To better understand these effects, the in situ g-ash samples collected at the PCD inlet under the various operating conditions were thoroughly characterized. The goal was to document the effects of coal type on the g-ash particle concentration, size distribution, surface

area, porosity, and drag. Data was collected in both air- and oxygen-blown operating modes during the Hiawatha coal tests.

- Outlet Particulate Sampling and Monitoring – Particulate sampling was conducted at the PCD outlet throughout TC09 to document the ability of the PCD to maintain acceptable levels of particulate control. The output from the PCME DustAlert-90 was also monitored and evaluated for accuracy and sensitivity. Outlet sampling and monitoring was conducted during the tests of g-ash injection into a filter element to evaluate the effectiveness of failsafes.

3.2.3 Observations/Events – September 3, 2002, Through September 26, 2002

Refer to Figures 3.2-2 through 3.2-19 for operating trends corresponding to the following list of events.

A. System Startup. Back-pulsing began at 06:30 on September 3, 2002, and the start-up burner was lit at 18:10. At 14:20 on September 4, 2002, the back-pulse pressure was set at 400 psid on the top plenum and 600 psid on the bottom plenum, and the frequency was set at 5 minutes as coke breeze feed started.

B. Coal Feed Started. At 19:12 on September 4, 2002, coal feed was started. The feeder tripped at 20:25, and coal feed was reestablished at 22:40. The fines removal system tripped shortly thereafter due to a high level in the FD0530 surge bin, but the system operation was quickly restored.

C. PCD Cone Filled. At 05:00 on September 5, 2002, several temperatures in the lower cone noticeably dropped, indicating solids accumulation. By 05:20, the mid-cone thermocouples were showing solids coverage, and by 06:00, upper cone thermocouples were covered.

D. G-ash Buildup/Bridging Became Apparent. By 09:15 on September 5, 2002, filter element temperatures, resistance probe readings, tube sheet, and venturi pressure drops all indicated solids buildup between the filter elements.

E. Back-pulse Pressure Increased. At 09:50 on September 5, 2002, the bottom plenum back-pulse pressure was increased in an attempt to dislodge the g-ash from the filter elements.

F. Fines Removal System Trips. Beginning around 12:15 on September 5, 2002, the fines removal system tripped several times due to a problem with the FD0530 outlet line.

G. Air Compressor Trip. At 14:50 on September 5, 2002, the main air compressor tripped, although the coal feed continued, and the compressor operation was quickly restored.

H. System Shutdown. Due to the presence and severity of the g-ash accumulation, system shutdown was initiated late on September 5, 2002. This marked the end of TC09A. By 04:00 on September 6, 2002, the resistance probes all showed that they were not covered. A manway inspection was completed, and this showed that the g-ash was no longer present on the filter elements.

I. System Startup. After an inspection revealed that the g-ash had dislodged completely from the filter elements, system operation resumed. TC09B began on September 7, 2002, with back-pulsing started at 20:30. Coke breeze feed was started at 11:10 on September 8, 2002, and at that time, the back-pulse pressure was set to 400 psid for the top plenum and 600 psid for the bottom plenum with a 5-minute cycle frequency.

J. Gasifier Upsets. Several gasifier upsets occurred beginning at 14:35 on September 8, 2002. The first upset was followed by an upset 2 minutes later; These upsets caused rapid increases of the inlet and filter surface temperatures and triggered several rate-of-change alarms, which were initiated by a temperature increase of 2°F/sec. At 16:01, another gasifier upset occurred which also caused rapid increases in filter element temperatures and rate-of-change alarms. This upset apparently carried more than 1,000 lb of solids, and due to the high loading, the FD0502 screw cooler tripped on high outlet temperature. Another upset occurred at 20:00, causing a spike in filter element temperatures and high solids carryover. Again, the FD0502 screw cooler tripped due to the high loading.

K. Coke Breeze Feed Started. Coke breeze feed was established at 14:25 on September 9, 2002, and back-pulse pressure was increased to 400 psid on the top plenum and 600 psid on the bottom plenum with a 5-minute cycle time.

L. Gasifier Upsets. Two gasifier upsets occurred beginning at 18:00 on September 9, 2002. The FD0502 screw cooler tripped, but operation was quickly reestablished.

M. Coal Feed Started. At 19:55 on September 9, 2002, coal feed was started.

N. Gasifier Upset. At 15:30 on September 10, 2002, a gasifier upset occurred which caused a high solids carryover. The FD0502 screw cooler tripped following this incident.

O. Fines Removal System Trip. Due to a leaking valve, the FD0520 lock hopper system tripped at 13:50 on September 14, 2002. As a result, solids accumulated in the PCD cone until the system could be put back online. At 16:00, the coal-feed rate was reduced slightly to reduce solids loading. The fines removal system operation was restored at 17:25, and the coal-feed rate was increased to its previous level at 18:00.

P. System Shutdown. At 13:30 on September 16, 2002, the system was shut down. This marked the conclusion of TC09B.

Q. System Restart. The run resumed with TC09C on September 20, 2002, as back-pulsing began at 06:40. At 18:00, coke breeze was started, and the back-pulse pressures were set at 400 psid on the top plenum and 600 psid on the bottom plenum.

R. Gasifier Upset. At 01:38 on September 21, 2002, a gasifier upset caused heavy solids carryover to the PCD, which led to a trip of the fines removal system. Another upset occurred at 02:15. Due to the loss of gasifier inventory and temperature, coke breeze was discontinued, and heatup was continued with the start-up burner. The back-pulse pressures were lowered to 220 psid on the top plenum and 250 psid on the bottom plenum with a 15-minute cycle frequency.

S. Coke Breeze Feed Started. At 07:10 on September 21, 2002, coke breeze feed was started again, and at 09:50, the back-pulse pressure was increased to 400 psid on the top plenum and 600 psid on the bottom plenum with a 5-minute timer.

T. Gasifier Upset. A gasifier upset occurred at 11:10 on September 21, 2002, causing heavy solids carryover and filter element temperature spikes of about 285°F in 1.25 minutes.

U. Coal Feed Started. At 11:53 on September 21, 2002, coal feed was started.

V. Reduced Coal-Feed Rate. Cone temperatures showed solids accumulation beginning at 01:30 on September 22, 2002. Therefore, the coal-feed rate was reduced slightly at around 02:00.

W. System Shutdown. At 16:40 on September 26, 2002, coal feed was stopped. The PCD was shut down "semidirty," as the top plenum was not back-pulsed clean after coal feed stopped, but the bottom plenum was back-pulsed twice after coal feed stopped.

3.2.4 Run Summary and Analysis

TC09 began on September 3, 2002, as the system was pressurized and the back-pulsing sequence was first started. Shortly after coal feed was established at 22:40 on September 4, 2002, the particulate loading to the PCD exceeded the fines removal system capacity. The loading was, at times, in excess of 1,000 lb/hr, whereas the capacity of the solids removal system is about 500 to 700 lb/hr for g-ash. By about 05:00 on September 5, 2002, the PCD cone thermocouples showed solids accumulation, and by 08:30, various measurements indicated g-ash buildup between the filter elements. The first indication of buildup between the filter elements was abnormal pressure drop measurements across the venturi devices of each plenum. These devices indicated an unusually high flow through the top plenum and virtually no flow through the bottom plenum. At 08:45, filter element thermocouples indicated g-ash bridging between the filters, and by 09:11, the resistance probes began to indicate bridging as well. In addition, the pressure drop across the tube sheet was unusually high, and traces of pressure drop data showed no effect from bottom plenum back-pulsing by around 11:30.

Further details of the g-ash buildup and instrumentation responses can be found in Section 3.2.5.

Because of the severity of the g-ash buildup and the potential of filter element damage, the system was shut down to remove the g-ash, marking the end of TC09A. During shutdown, the resistance probes indicated that the solids dislodged from the filter elements. A video inspection through the lower PCD manway was completed, which confirmed that the g-ash was gone. Therefore, the system was reheated and the run was resumed.

TC09B began with system heatup on September 7, 2002. During heatup, several gasifier upsets occurred which caused a surge of gasifier bed material. These upsets caused rapid increases in filter element temperatures, and, at times, overwhelmed the fines removal system, causing trips. Coal feed was introduced on September 9, 2002. A gasifier upset occurred the next day while on coal feed, again causing high solids loading that was problematic for the fines removal system. The remainder of TC09B was fairly stable, and this portion of the run ended with a scheduled shutdown on September 18, 2002.

TC09C began on September 20, 2002. A delay in heatup occurred following a gasifier upset that caused a significant loss of gasifier inventory and temperature. Another gasifier upset occurred later, but did not cause a run delay. Coal feed was established on September 21, 2002. Shortly thereafter, solids accumulation in the PCD cone became a concern, and the coal-feed rate was therefore reduced. System operation was stable, and this portion of the run also ended in a scheduled shutdown.

Of major concern during the run were the frequent gasifier upsets usually occurring at startups while feeding coke breeze. These upsets caused rapid temperature increases of the filter elements, although they apparently did not cause permanent damage to the elements. Often, the fines removal system tripped in response to the solids carryover, so solids accumulation in the PCD cone was a concern, particularly in light of the bridging incident in TC09A.

Overall, TC09 was a successful run with no filter element failures and good sealing of the filter vessel. Although g-ash buildup led to the end of TC09A, this experience was helpful in understanding one method of g-ash bridging growth. In addition, the resistance probes were well tested during this incident and proved to be reliable and useful. TC09 was also an opportunity to continue the failsafe injection testing, which will help tremendously in the development of reliable failsafes.

3.2.5 Resistance Probe Measurements

Due to the recurrence of g-ash bridging in the PCD in recent runs, new instrumentation was jointly developed by Siemens Westinghouse and SRI to help characterize the development of bridging deposits so that the bridging issue could be effectively addressed. The instrumentation, called resistance probes, were first installed prior to TC07D and have been installed for each run since then. TC09A was the first run during which g-ash bridged the filter elements and the resistance probes responded as designed.

3.2.5.1 Description of Resistance Probe Installation

Due to the high carbon content of g-ash, the resistance between two electrical conductors inserted into a bulk g-ash sample, with a path length of about 1.5 inches between the conductors, is on the order of 100 Ω. Due to the low resistivity of the g-ash, it was thought that a measurement of the resistance between a probe located between filter elements and the grounded metal filter element surface might be useful for detecting bridging. Resistance probes were constructed from 1/16-inch Inconel-sheathed, mineral-insulated Type K thermocouples, as shown in Figure 3.2-20. The end of the Inconel sheath was removed to expose the thermocouple wire. An alumina insulator was cemented over the exposed thermocouple wire and potted with ceramic cement to insulate the wire from the metal sheath. In lab tests it was found that a light coating of g-ash on the ceramic insulator, such as would exist during normal gasifier operation, did not reduce the resistance between the thermocouple wire and the metal sheath significantly. Resistance between the thermocouple wire and sheath was still greater than 10,000 Ω with a dirty insulator.

Prior to TC09, six resistance probes were installed between the filter elements at locations B30 and B43. Three sets of two probes were located at distances 1/6, 1/2, and 5/6 from the top of the filter elements. Both filter elements were 1.5m Pall FEAL with three filter segments. A set of probes was located about the midpoint of each filter segment. In each set of probes, one was located at 1/4 of the minimum filter element-to-filter element spacing and the other was located at 1/2 of the minimum filter element-to-filter element spacing, as shown in Figure 3.2-21. Photos of the probe installation are shown in Figure 3.2-22.

The resistance from probe tip to ground was monitored using the circuit shown in Figure 3.2-23. A DC potential of about 6 volts was applied between the probe conductor and ground and voltage drops across the unknown probe-tip-to-ground resistance and across a known resistor were monitored using a PC-based data acquisition system. The probe-tip-to-ground resistance can be calculated from these voltage measurements.

3.2.5.2 Measurements

The first indication of bridging in the PCD was noted at 08:30 on September 5, 2002, when the PCD venturi ΔP measurements (PDI3029 and PDI3030) started to deviate from their normal values. These measurements provide an indication of the relative amounts of flow through the top and bottom plenums. At 08:30, the top venturi ΔP started increasing and the bottom venturi ΔP started decreasing, which indicated that a larger-than-normal fraction of the flow was going through the top plenum. Shortly thereafter, the PCD baseline and peak ΔPs also started increasing. The first resistance probe shorted at 09:11 and the other five shorted between that time and 09:53.

Resistance probe measurements between 09:00 and 10:10 are plotted in Figure 3.2-24 along with a filter element ΔP measurement. The times each probe shorted and the elapsed time between events are listed below.

Probe	Time When Short Occurred	Elapsed Time Since Last Probe Shorted
Bottom 1/4	09:11:24	—
Bottom 1/2	09:13:46	2:22
Middle 1/4	09:26:27	12:41
Middle 1/2	09:27:44	1:17
Top 1/4	09:52:55	25:11
Top 1/2	09:52:55	0:00

From these measurements, it seems clear that the bridging started at the bottom and progressed toward the top. Once the spaces between the filter elements are plugged at the bottom, most of the g-ash removed from the active part of the filter elements during back-pulsing will pile on top of what is already there. Therefore, the key question is how the bottom first starts to plug. With the exception of the probe at 1/4 spacing on the bottom, every time the various probes shorted it corresponded to either a top or bottom back-pulse. The brief delay between the times when the probes at 1/4 and 1/2 spacing shorted at lower and mid levels may be attributed to "valleys" in the g-ash between the filter elements.

Coal-fired Transport Gasifier operation continued at a more-or-less normal firing rate until about 18:00, at which time it was decided to shut down to remove the bridging. From 18:00 until 20:00 the coal flow was gradually reduced and coal flow was completely stopped at about 20:00. All six of the resistance probes remained shorted (resistance < 200 Ω) until about 19:00 when the resistances began increasing. Following shutdown the PCD back-pulse sequence was continued at 5-minute intervals with both back-pulse tanks at 400 psi above the process pressure. The probe resistances continued increasing until about 04:00 on the following morning September 6, 2002, when all six were open circuit (resistances > 100 kΩ). Resistance measurements during this period are plotted in Figure 3.2-25. No discernable pattern was detected in the resistance measurements during the period when the bridged material was falling out. A video inspection of the lower plenum was performed through the lower manway on September 7, 2002, and confirmed that there was no bridged material left between the lower plenum filter elements at that time.

3.2.5.3 Analysis

After reviewing the test data, it seems reasonable to conclude that bridging was initiated by overfilling of the PCD cone, due to inability of the FD0502/FD0520 conveying system to remove the g-ash as fast as it was being collected. The maximum amount of g-ash the 502/520 system can transport is around 500 to 700 lb/hr; while during TC09A, the g-ash carryover rate to the PCD was as much as 1,000 lb/hr. G-ash carryover rates have always been higher when operating on bituminous coal as compared to PRB due to lower carbon conversion in the gasifier and the higher ash content of the bituminous coal.

Overfilling of the cone was detected when the cone thermocouples were covered by g-ash. TI3021, located at the mid-cone level, covered at 05:21 and TI3022, located at the upper-cone level, covered at 06:06 as shown in Figure 3.2-26. Locations of these thermocouples relative to the bottom of the filter elements are shown in Figure 3.2-27. Assuming that the cone filled uniformly (probably not a very accurate assumption) and at a constant rate, the predicted time when the cone should have filled to the bottom of the filter elements was about 07:50 (see Figure 3.2-28). The first indication of bridging was at about 08:30, so the predicted and actual times seem to be in reasonable agreement.

After reviewing the data from the earlier bridging episode during TC07C on February 8, 2002, it appears that the bridging on that occasion was also caused by overfilling the cone. Alabama bituminous coal was fired during TC07C. Therefore, cone overfilling seems to explain both bridging episodes that have occurred while firing bituminous coal. The bituminous coal produces more solids loading than does PRB because it contains higher ash content. Cone overfilling does not appear to have been responsible for most of the earlier bridging experienced when firing PRB.

The PCD pressure recovery during the onset of bridging was also compared with the resistance probe measurements to see how the ΔP performance correlated with the assumed progress of bridging. The ratio of ΔP recovery after the top back-pulse vs. the total recovery (peak ΔP minus ΔP after the bottom back-pulse) was calculated. A Visual Basic program was used to sort the test data to find the ΔP values before the top back-pulse (PK), after the top back-pulse (BL1) and after the bottom back-pulse (BL2). Results are plotted in Figure 3.2-29. Since there is a time difference between the top and bottom back-pulse, this is not an exact comparison, but the expected ratio during normal operation should be about 49 (number of filter elements on bottom plenum) / 49 + 36 (total filter elements) = 0.576. As the plot shows, the actual ratio was around 0.576 before 09:00. Assuming that 1/6 of the bottom filter element area was inactive at 09:12 when the bottom probes shorted, 1/2 was inactive at 09:27 when the middle probes shorted, and 5/6 was inactive at 09:53 when the top probes shorted, the expected ratios are 0.531, 0.405, and 0.185 respectively. Those points are shown as triangles on the plot and they seem to be in reasonable agreement with the test data during the period from 09:00 to 10:00. Between 10:00 and 11:00, the test data did not follow the established trend, but during that period most of the back-pulses were the emergency type where the top and bottom back-pulses are only 22 seconds apart – that could be a factor in the poor agreement. The negative ratios between 11:00 and 12:00 are because there was essentially no recovery from the bottom back-pulse, so BL1-BL2 is a negative number. Thus the ΔP recovery data seems to support the conclusion that the bridging progressed more or less uniformly from the bottom of the filter elements to the top.

The resistance probes installed during TC09A successfully demonstrated that they would signal in the event of bridging. Not only did they signal, but they assisted in the understanding of how the bridging material progressed during TC09. These probes will continue to be tested in upcoming runs.

Table 3.2-1

TC09 Run Statistics and Steady-State Operating Parameters
September 3, 2002 Through September 26, 2002

Start Time:	09/03/02 06:30 (for back-pulse system)
End Time:	09/26/02 17:00
Coal Type:	Upper Hiawatha Seam Bituminous
Hours on Coal:	Approx. 309 hr
Number of Filter Elements:	85
Filter Element Layout No.:	25 (Figure 3.2-1)
Filtration Area:	241.4 ft^2 (22.4 m^2)
Pulse Valve Open Time:	0.2 sec
Pulse Time Trigger:	5 min
Pulse Pressure, Top Plenum	400 psi above System Pressure
Pulse Pressure, Bottom Plenum:	600 psi above System Pressure
Pulse dP Trigger:	275 inH_2O
Inlet Gas Temperature:	Approx. 775 to 925°F (410 to 500°C)
Face Velocity:	Approx. 2.5 to 3.5 ft/min (1.2 to 1.8 cm/sec)
Inlet Loading Concentration:	Approx. 22,000 to 42,000 ppmw
Outlet Loading Concentration:	Below detection limit of 0.1 ppmw to 0.23 ppmw
Baseline Pressure Drop:	Approx. 50 to 90 inH_2O (125 to 225 mbar)

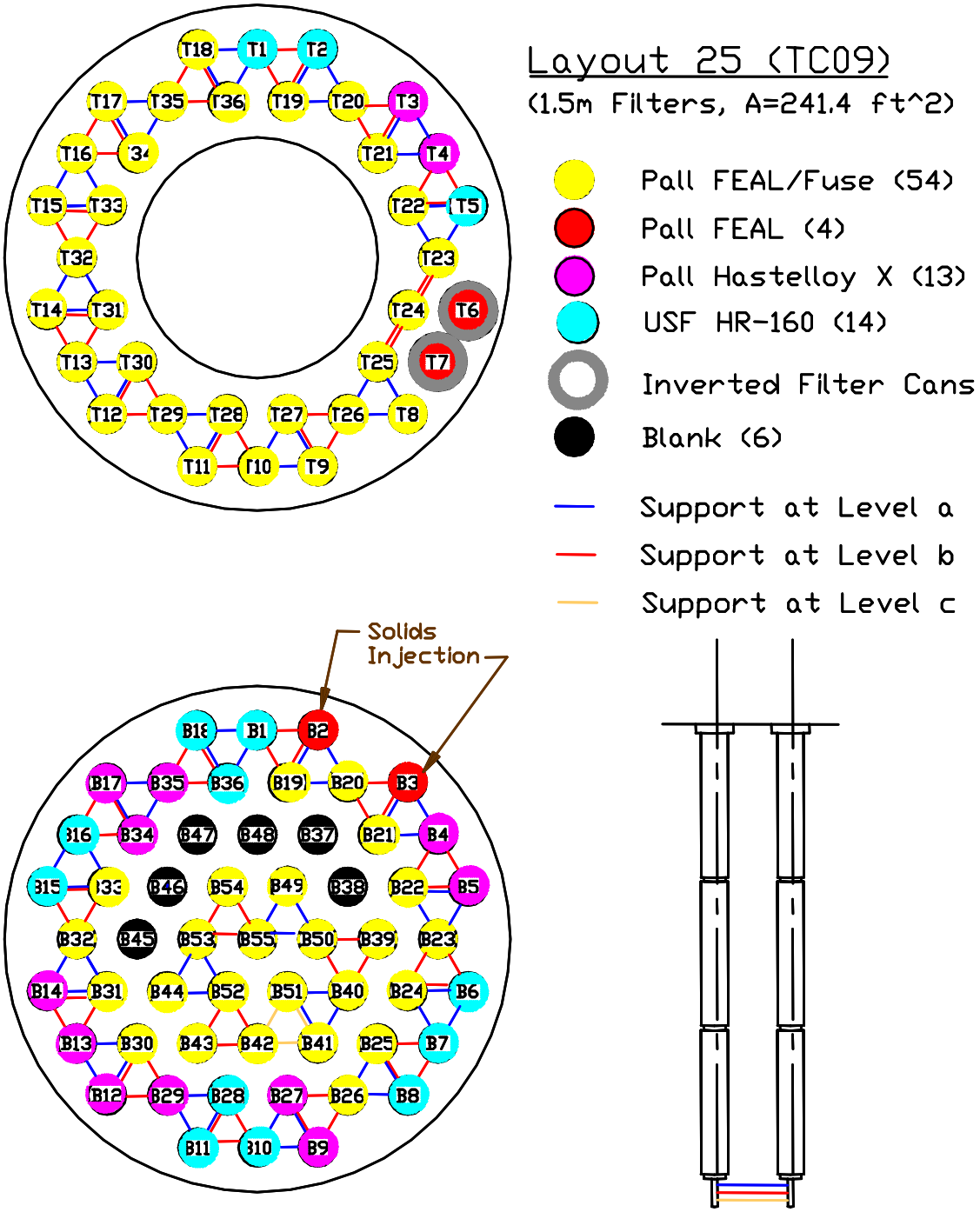

Figure 3.2-1 Filter Element Layout 25

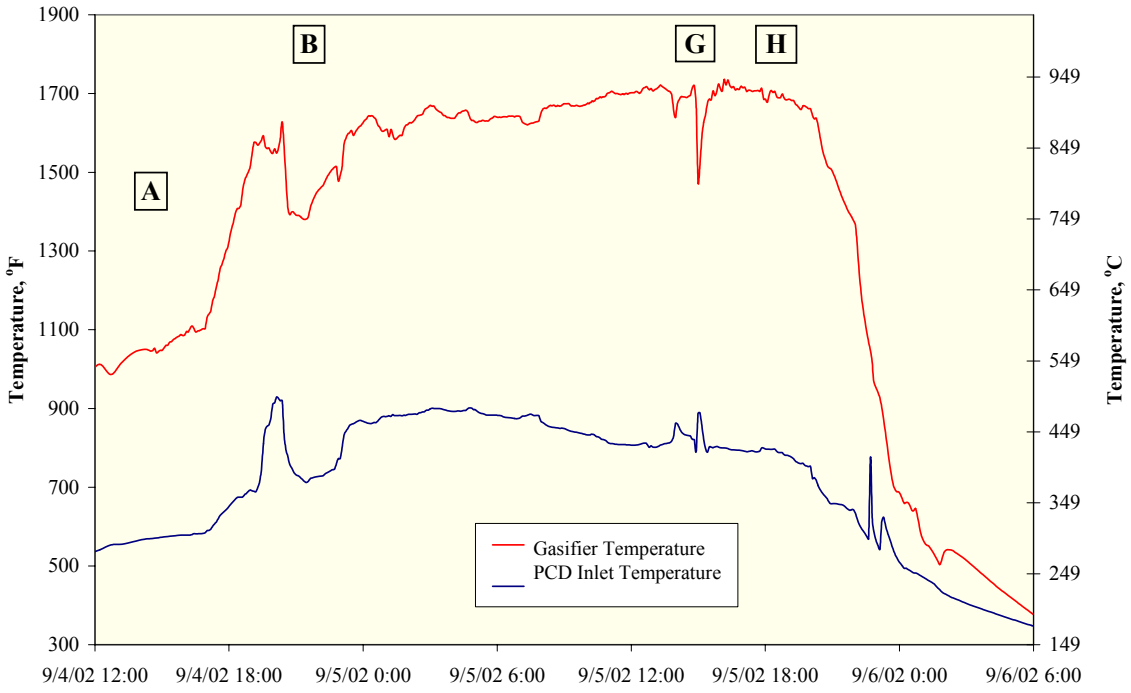

Figure 3.2-2 Gasifier and PCD Temperatures, TC09A

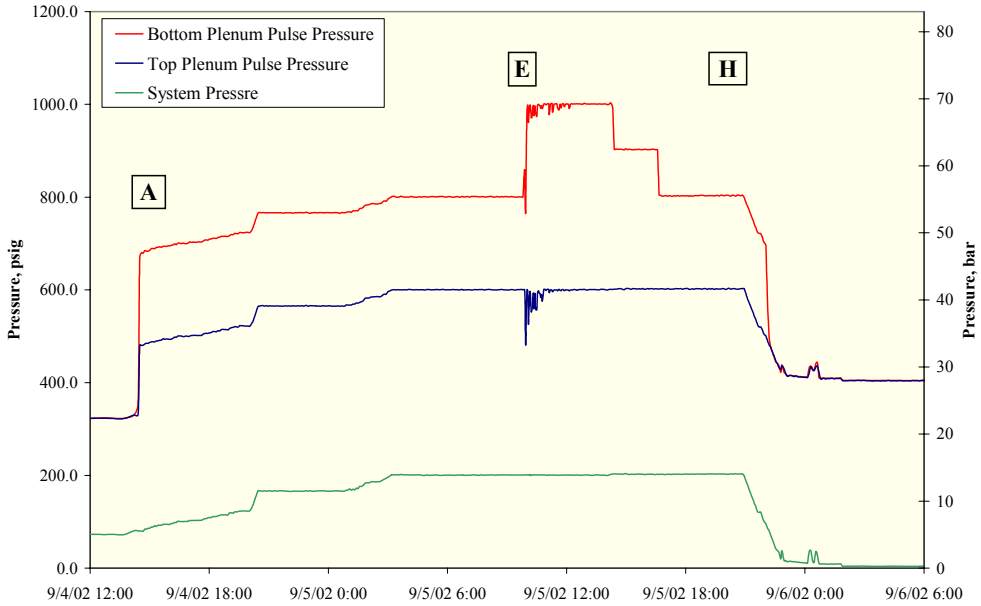

Figure 3.2-3 System and Pulse Pressures, TC09A

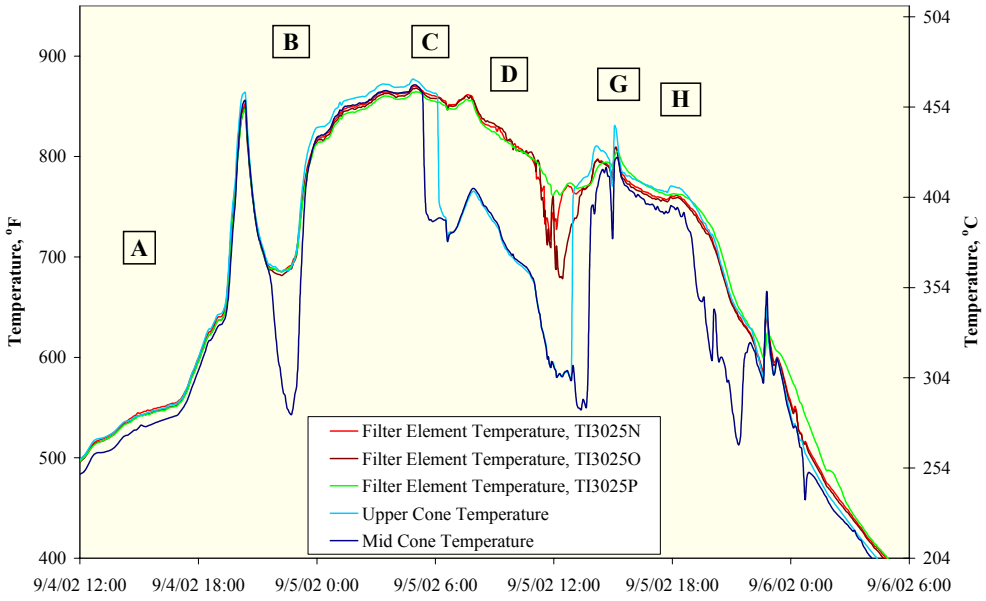

Figure 3.2-4 Filter Element and Cone Temperatures, TC09A

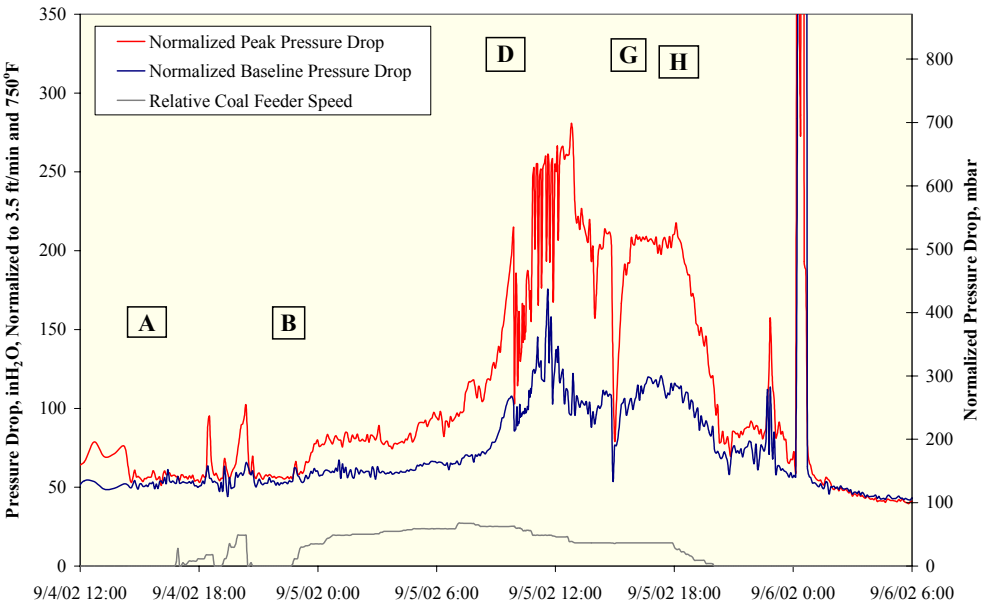

Figure 3.2-5 Normalized PCD Pressure Drop, TC09A

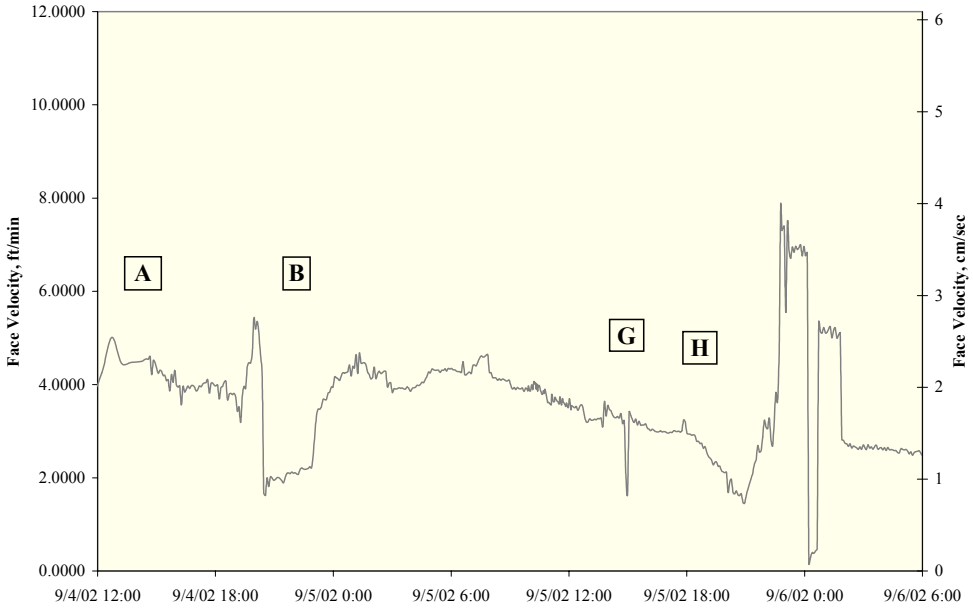

Figure 3.2-6 PCD Face Velocity, TC09A

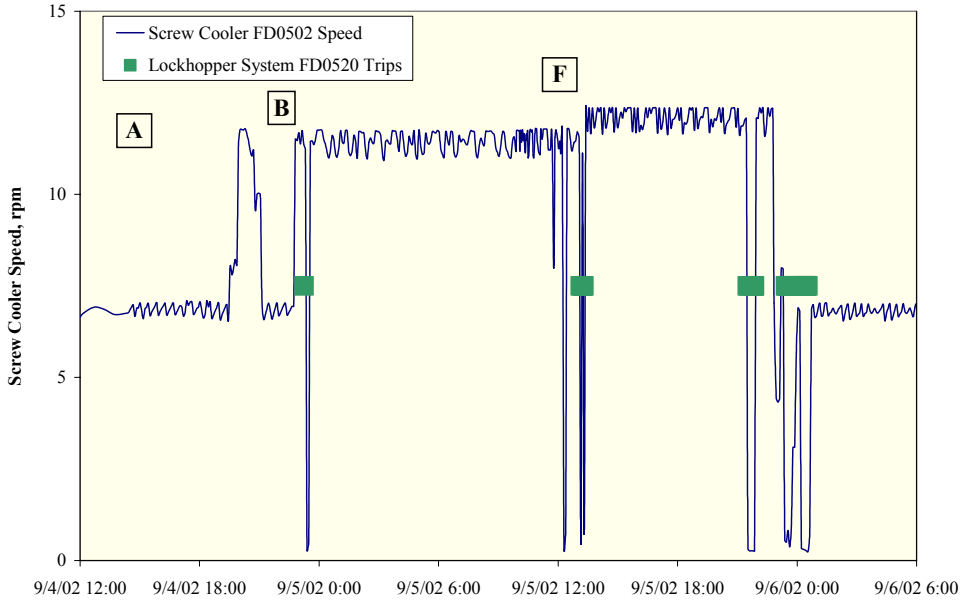

Figure 3.2-7 Fines Removal System Operation, TC09A

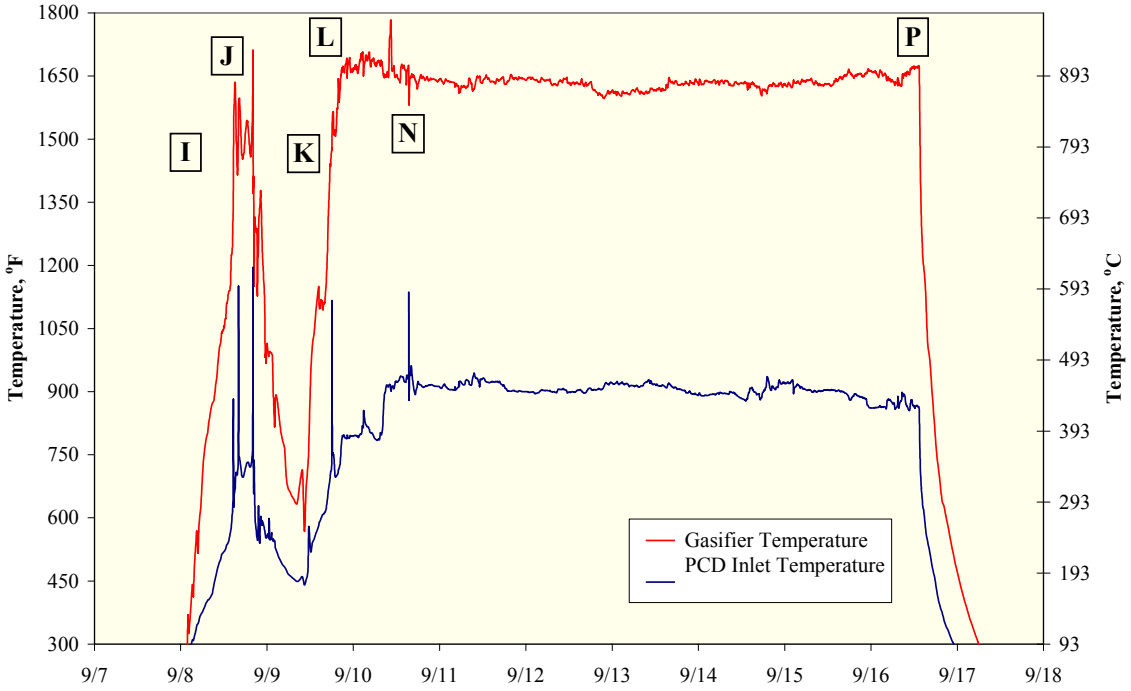

Figure 3.2-8 Gasifier and PCD Temperatures, TC09B

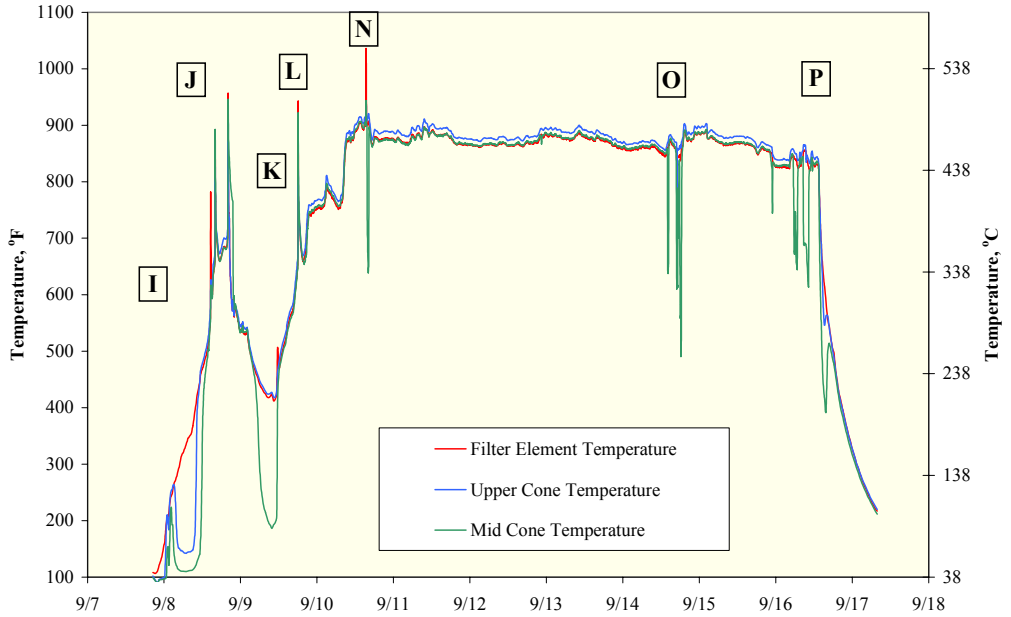

Figure 3.2-9 Filter Element and Cone Temperatures, TC09B

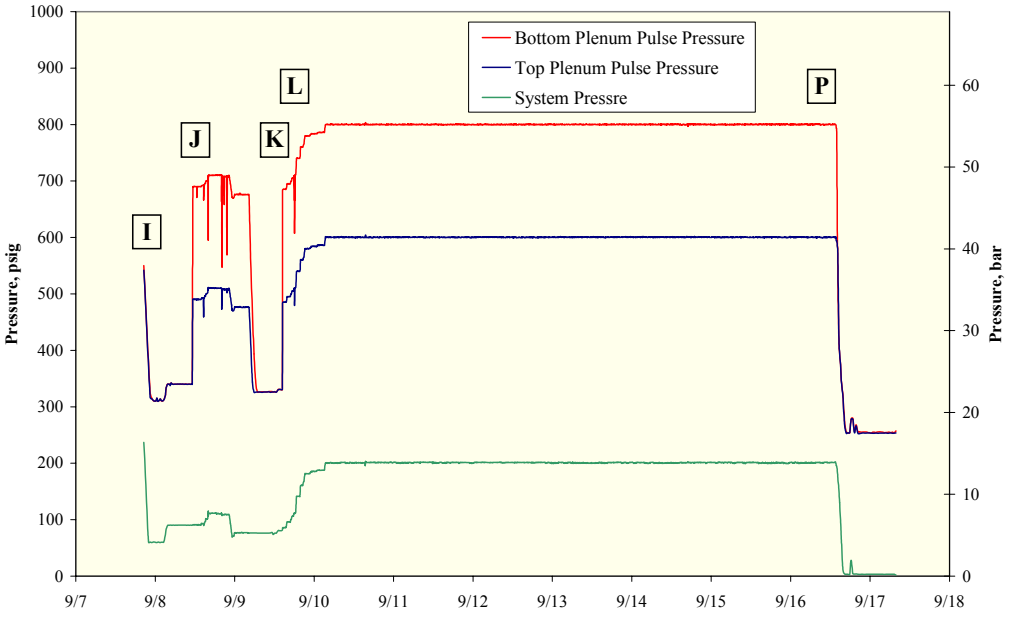

Figure 3.2-10 System and Pulse Pressures, TC09B

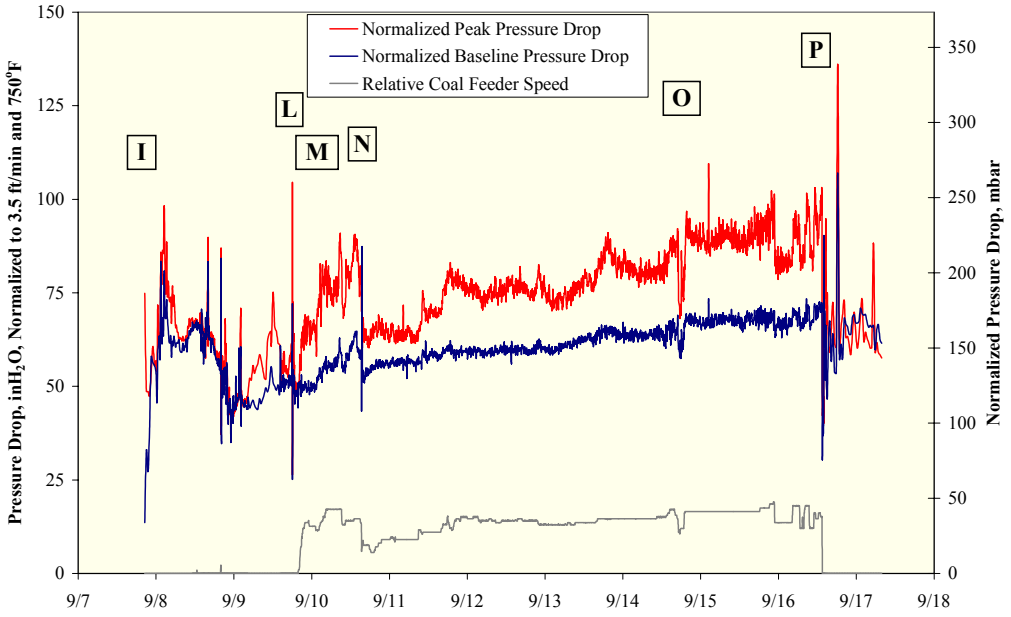

Figure 3.2-11 Normalized PCD Pressure Drop, TC09B

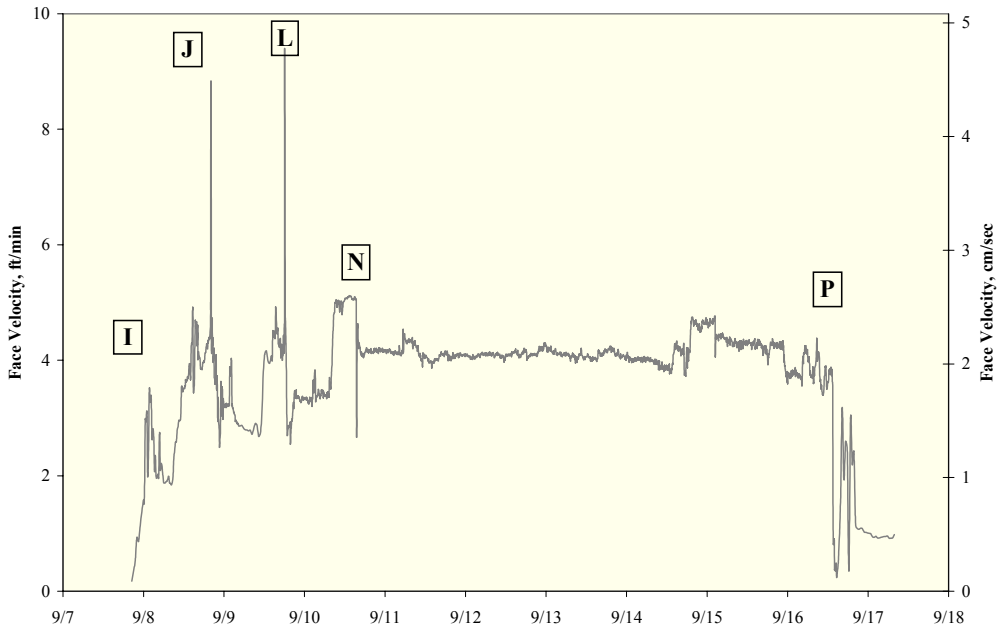

Figure 3.2-12 PCD Face Velocity, TC09B

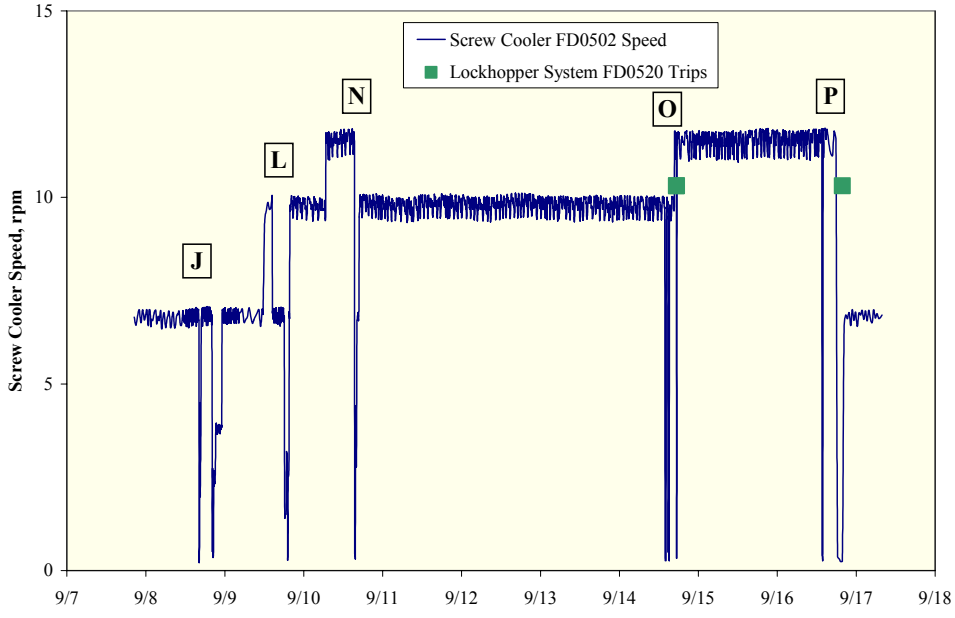

Figure 3.2-13 Fines Removal System Operation, TC09B

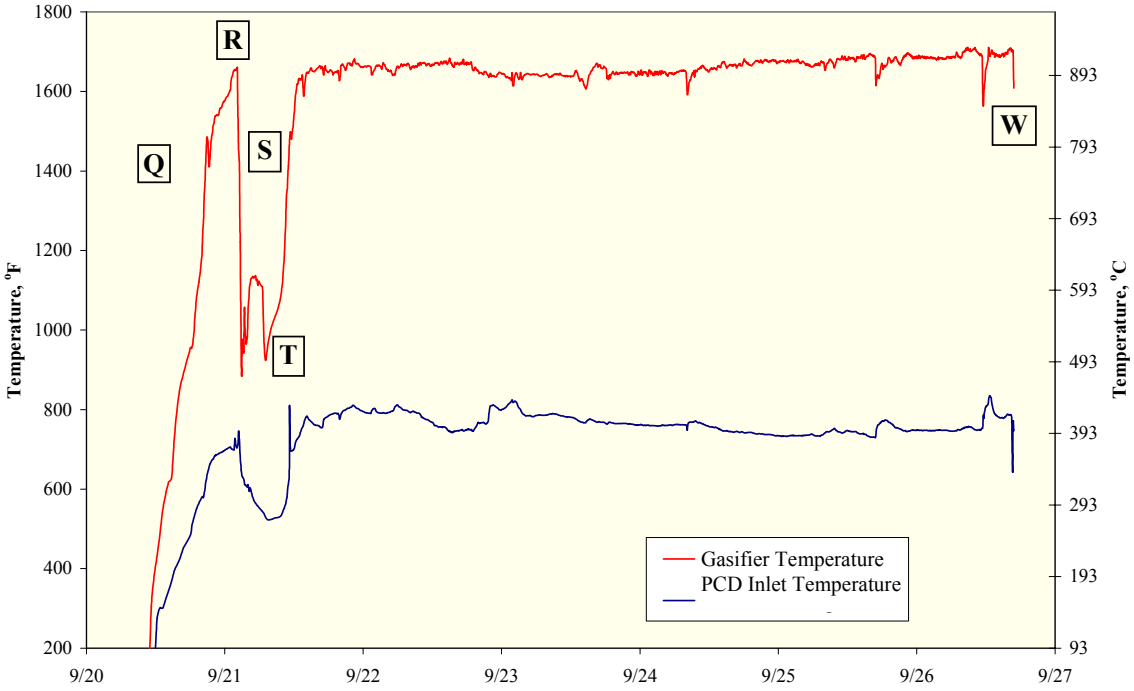

Figure 3.2-14 Gasifier and PCD Temperatures, TC09C

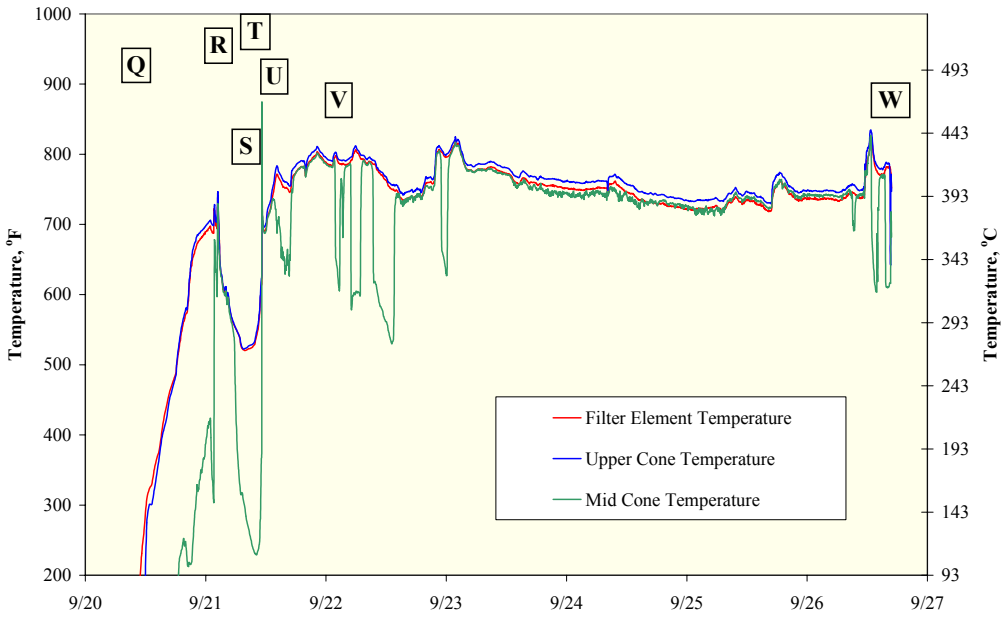

Figure 3.2-15 Filter Element and Cone Temperatures, TC09C

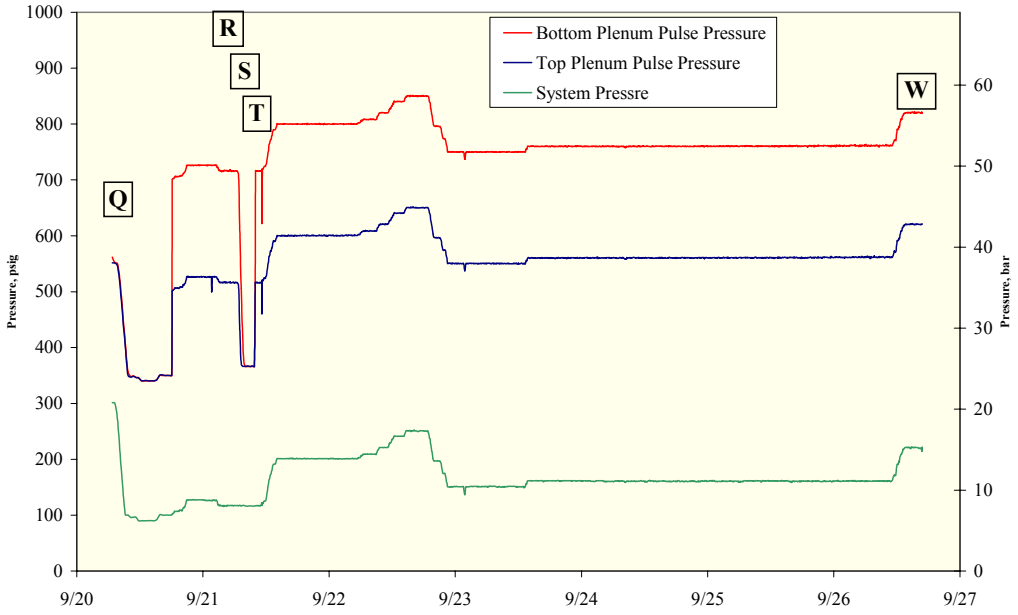

Figure 3.2-16 System and Pulse Pressures, TC09C

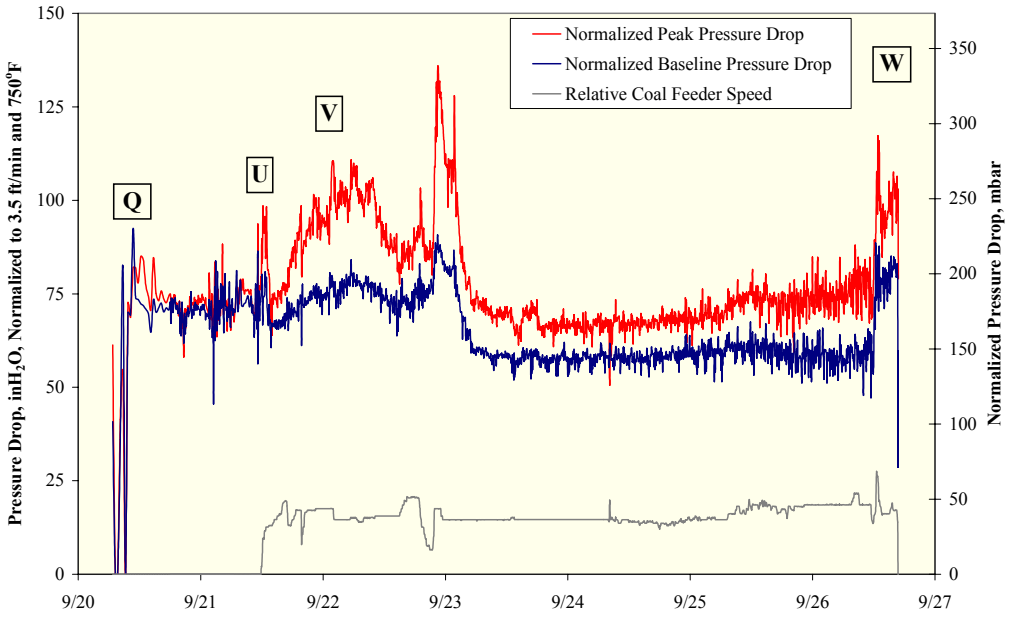

Figure 3.2-17 Normalized PCD Pressure Drop, TC09C

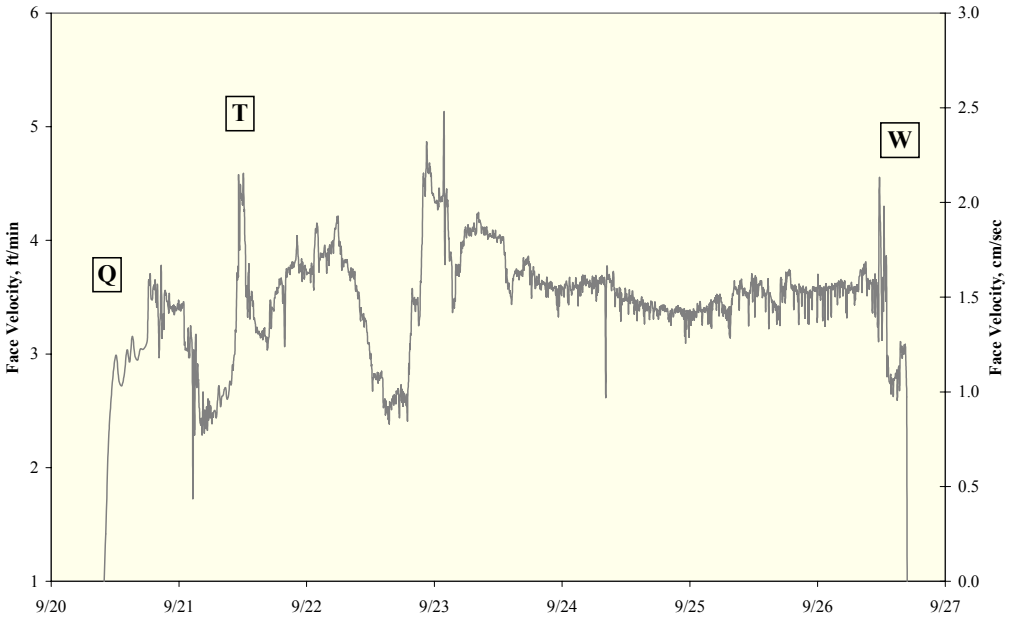

Figure 3.2-18 PCD Face Velocity, TC09C

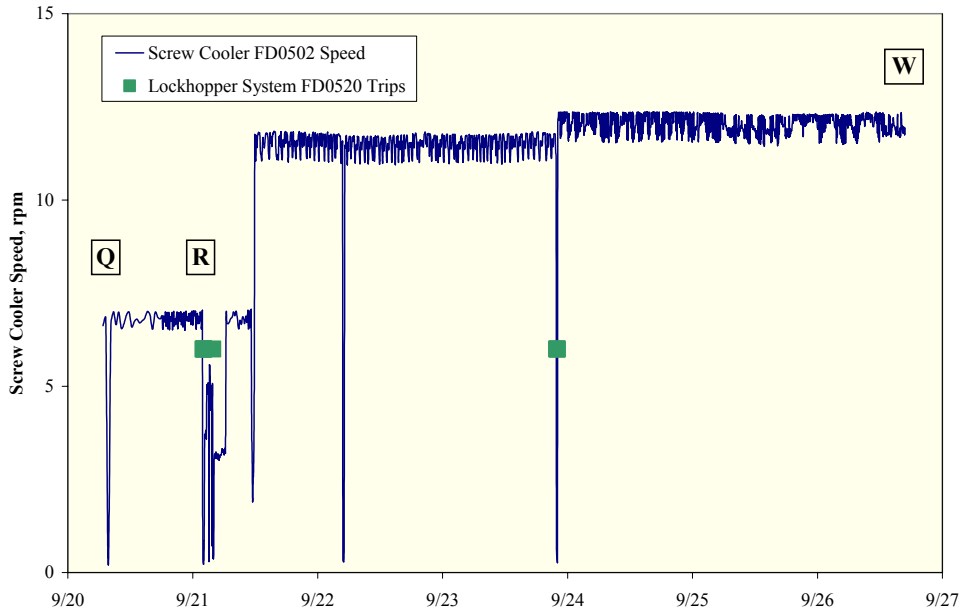

Figure 3.2-19 Fines Removal System Operation, TC09C

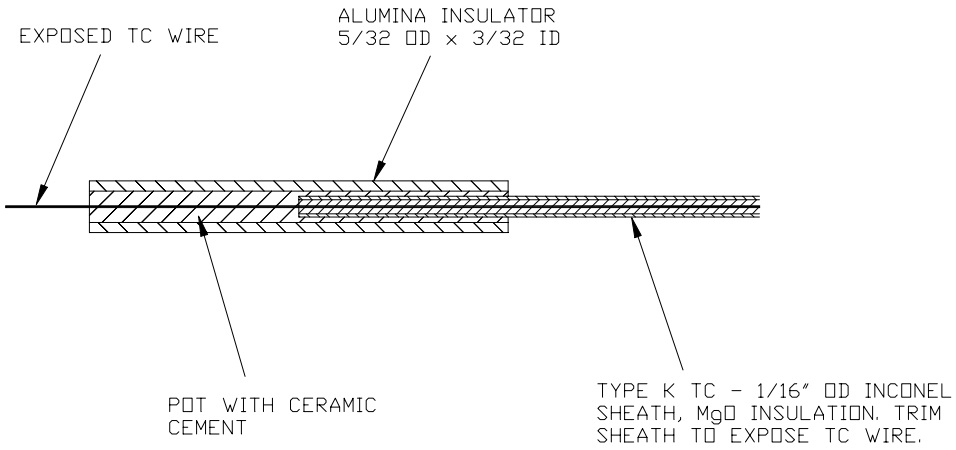

Figure 3.2.20 Resistance Probe Construction

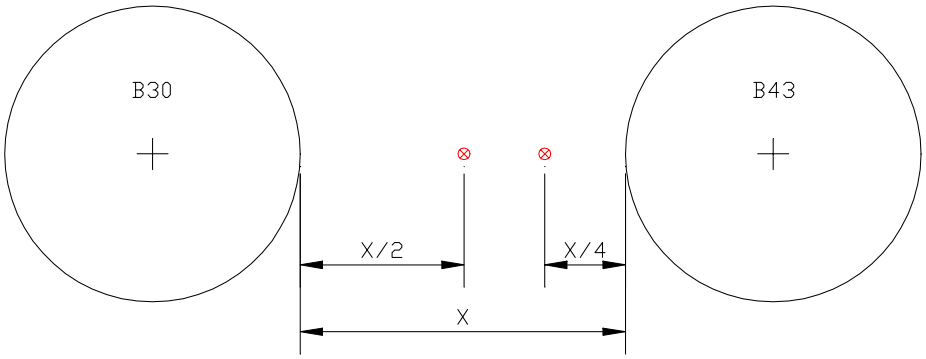

Figure 3.2-21 Bridge Resistance Probe Arrangement

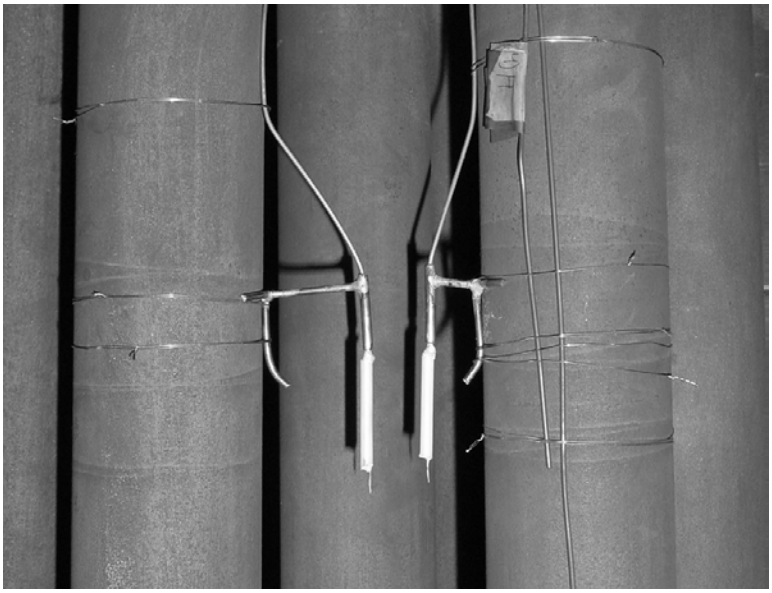

Figure 3.2-22a Close-Up View of Resistance Probe Installation

Figure 3.2-22b Overall View of Resistance Probe Installation

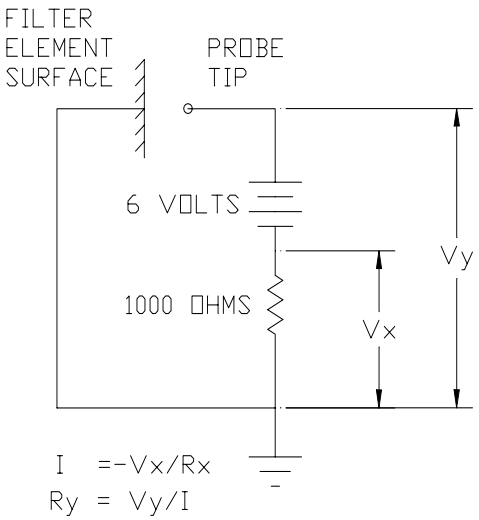

Figure 3.2-23 Resistance Probe Circuit

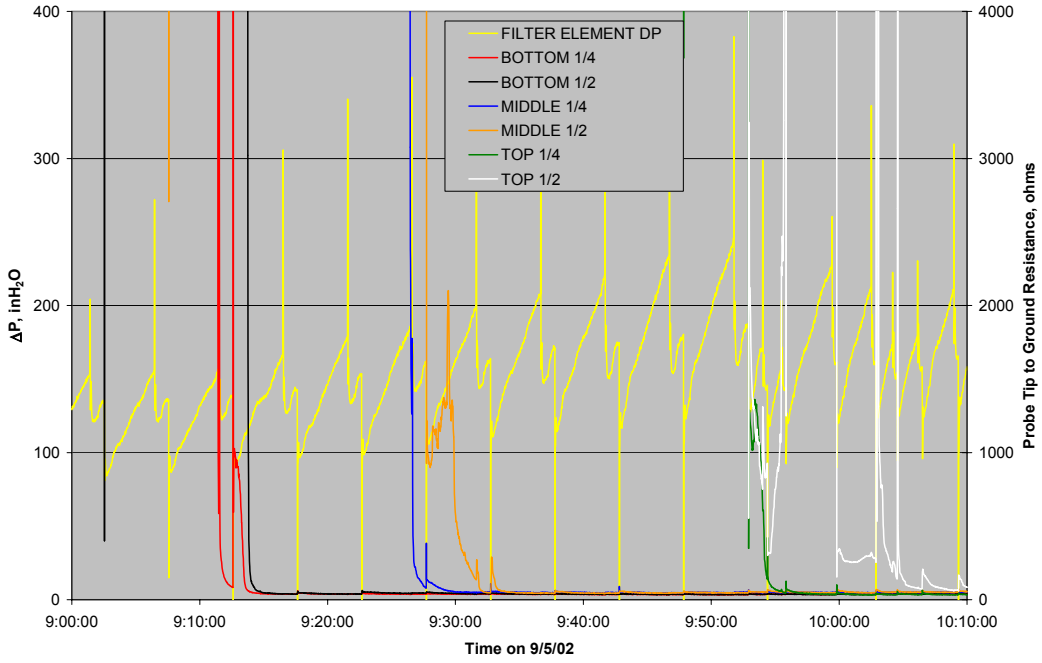

Figure 3.2-24a Resistance Probe Measurements During Initiation of Bridging

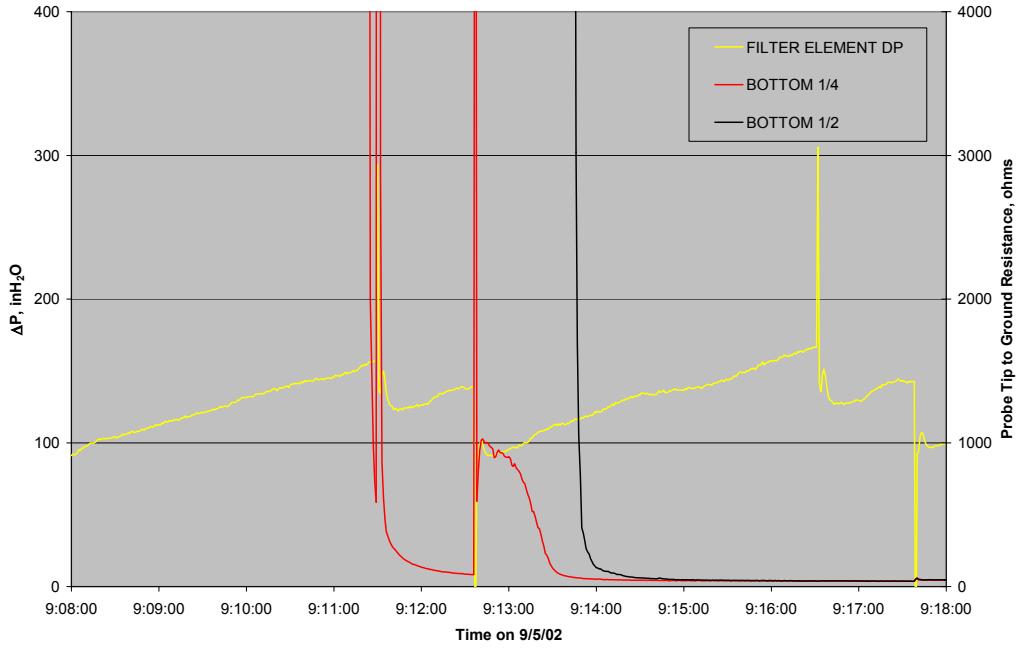

Figure 3.2-24b Resistance Probe Measurements When Bottom Probes Shorted

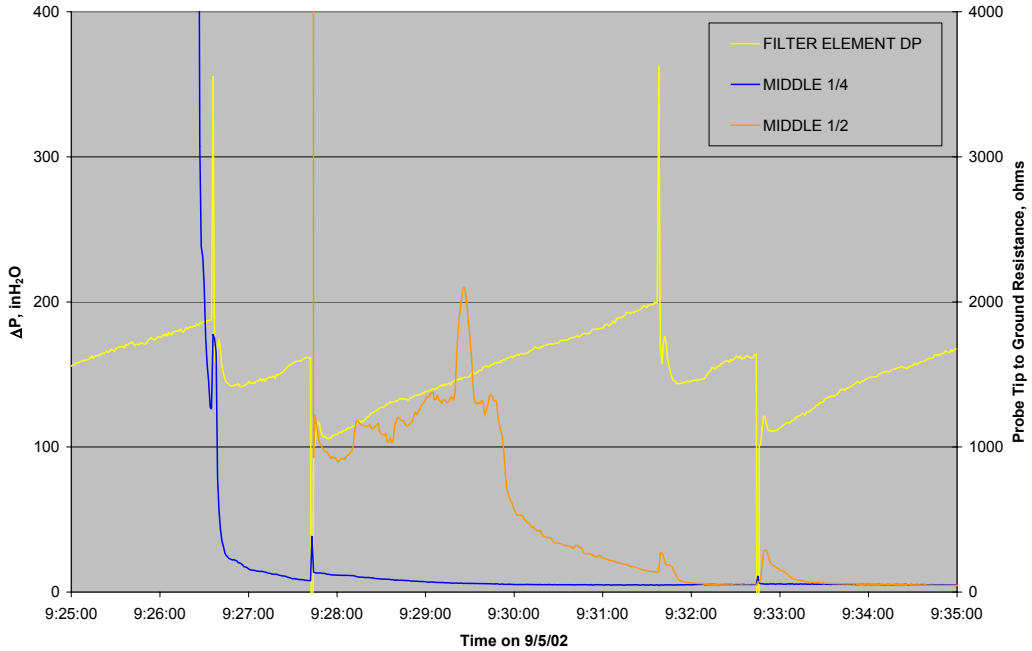

Figure 3.2-24c Resistance Probe Measurements When Middle Probes Shorted

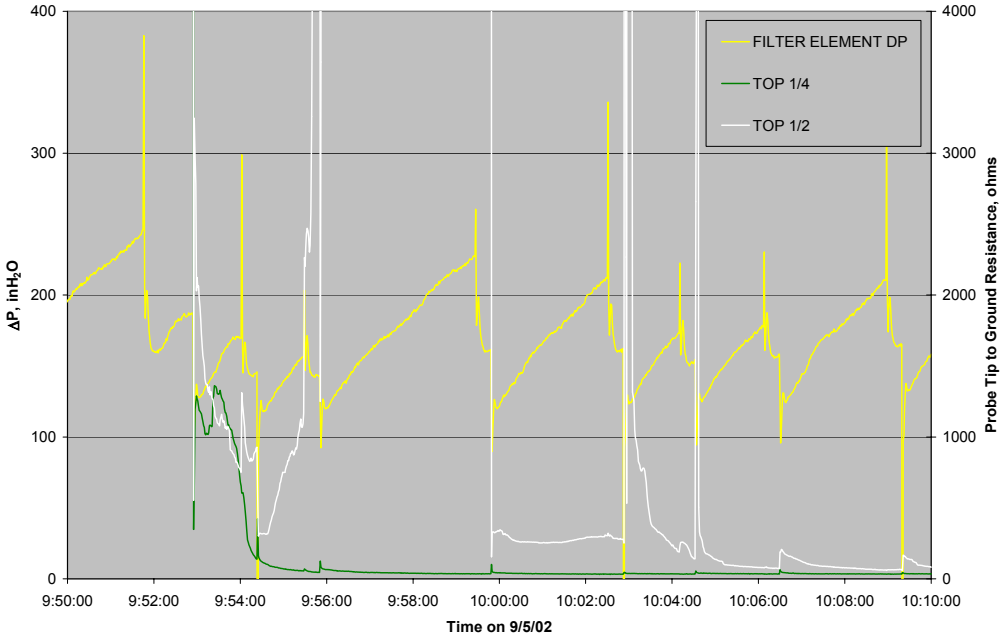

Figure 3.2-24d Resistance Probe Measurements When Top Probes Shorted

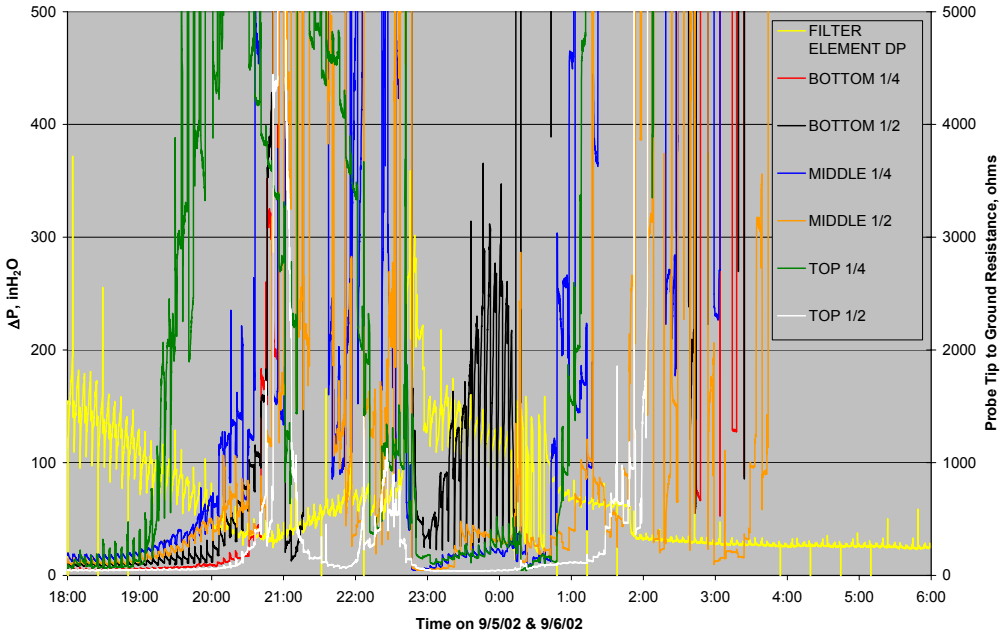

Figure 3.2-25 Resistance Probe Measurements When Bridging Dislodged

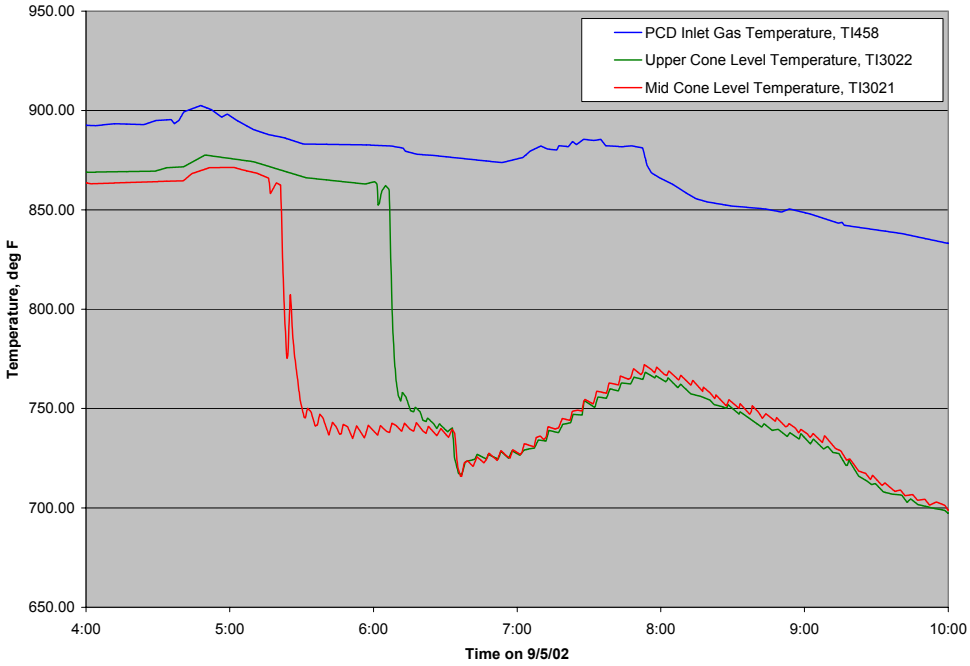

Figure 3.2-26 PCD Inlet Gas Temperature and Cone Temperature Measurements

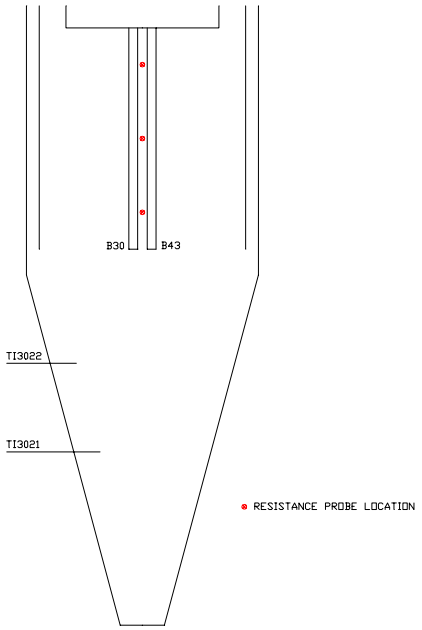

Figure 3.2-27 PCD Cone Thermocouple Locations

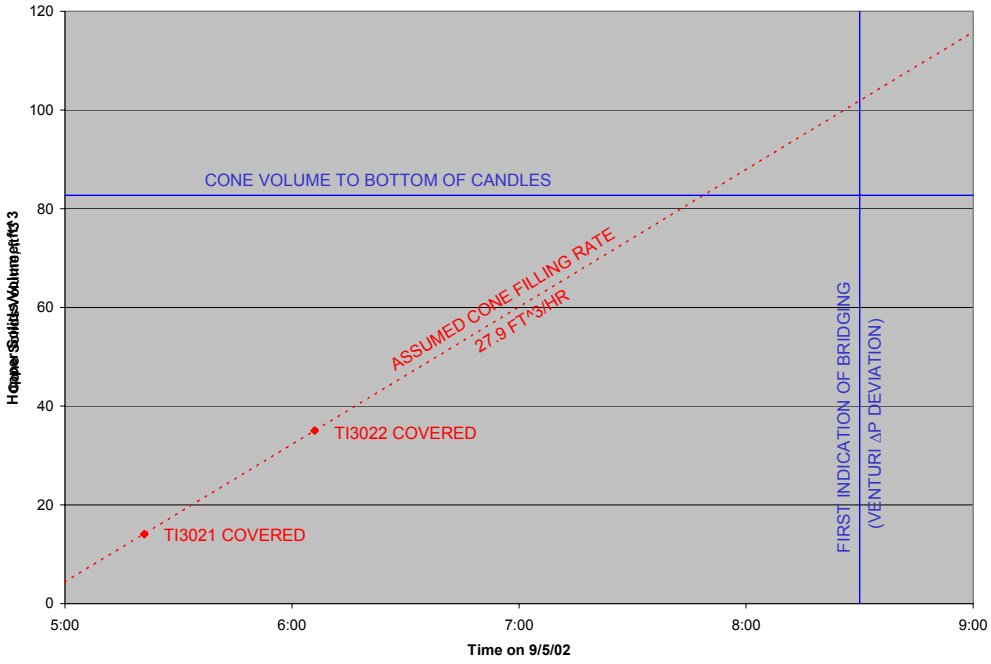

Figure 3.2-28 Estimation of Time Required for Cone to Fill to Bottom of Filter Elements

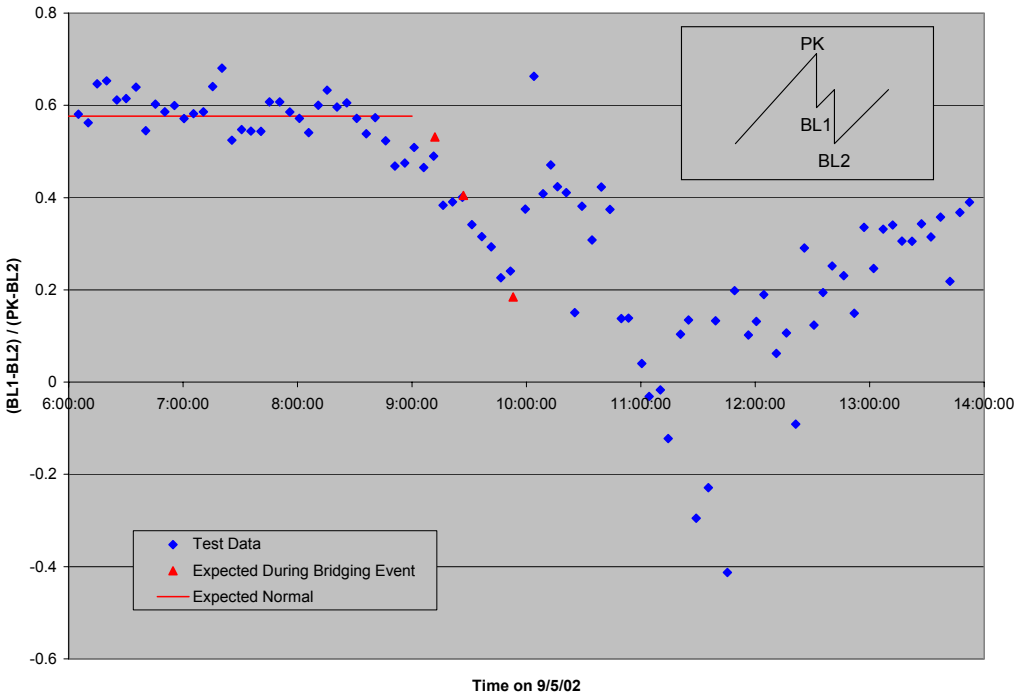

Figure 3.2-29 PCD ΔP Recovery During Bridging Event

3.3 TC09 PCD INSPECTION REPORT

3.3.1 Introduction

During the TC09 outage, the PCD internals were removed from the vessel and inspected. The outage inspection included examinations of the filter elements, their fixtures to the plenums, solids deposition, filter element gaskets, and auxiliary equipment. The inspection revealed that there were no obvious problems with the PCD at the end of TC09. The subsequent sections will detail the findings of the inspection.

3.3.2 Filter Elements

For TC09, the following filter elements were installed (See Figure 3.2-1):

- Four 1.5-meter Pall Fe_3Al filter elements.
- Fifty-four 1.5-meter Pall Fe_3Al filter elements with fuse (safeguard device welded in the filter).
- Thirteen 1.5-meter Hastelloy X filter elements.
- Fourteen 1.5-meter Pall Fluid Dynamics Division HR-160 sintered metal fiber filter elements.

During the outage all of the filter elements were removed and inspected.

Shutdown after TC09 was "semidirty," this means that the bottom plenum elements were back-pulsed after the coal feed was shutdown, but the top plenum was not. All loose g-ash was blown off the outside surface of the elements using compressed air before flow testing. Therefore, dirty condition, in this discussion, refers to elements with the loose g-ash blown off the surface but had no further cleaning such as water washing. All flow tests mentioned in this section were conducted using air at ambient temperature and pressure.

Fifty-eight 1.5-meter Pall Fe_3Al filter elements were removed. Each element was closely inspected, and no obvious damage was noted. The welds were examined and no separation from the candle media or cracks was noticed.

The Pall Fe_3Al filter elements have accumulated many gasification exposure hours since they were first installed in GCT3. The following table outlines the exposure hours of the Pall Fe_3Al elements that were installed during TC09.

Exposure Hours After TC09	Number of Fe_3Al Filters Exposed
2,381	9
2,268	1
2,085	1
1,911	2
1,114	3
968	40
818	1
308	1

Several of the Pall Fe_3Al filter elements were flow tested. The pressure drop versus face velocity for the Pall Fe_3Al filter elements with a fuse is plotted in Figure 3.3-1. Where available, flow test results on these elements on virgin condition are included in this plot. Figure 3.3-1 shows that at a face velocity of 3 ft/min, the pressure drop ranged from 11 to 29 inH_2O. At the same face velocity the pressure drop for virgin elements ranged from 4 to 6 inH_2O. The elements from the bottom plenum had a greater pressure drop than the elements from the top plenum. This is surprising since the bottom plenum was back-pulsed after the coal feed was stopped. There was no correlation between hours in operation and pressure drop measured. Based on these flow measurements, the Fe_3Al that remained in operation for TC10 were installed without further cleaning such as water washing or chemical cleaning.

Fourteen HR-160 filter elements were tested during TC09. One HR-160 element has been in operation from TC07 through TC09 and has accumulated 1,114 on-coal hours of exposure. Another HR-160 filter element was in operation during TC07B and C, then removed for TC08 and reinstalled for TC09. By the end of TC09, this filter element had accumulated 454 on-coal hours of exposure. The other 12 HR-160 filter elements that were installed prior to TC09 were virgin.

All 14 HR-160 filter elements were inspected and flow tested. There was no damage noted. Pressure drop versus face velocity for HR-160 elements are plotted in Figure 3.3-2. Virgin flow test results are included in this plot. At a face velocity of 3 ft/min, the pressure drop ranged from 8 to 20 inH_2O. At that same face velocity, the pressure drop for virgin elements was less than 1 inH_2O. Based on these flow measurements, the HR-160 that remained in operation for TC10 were reinstalled without cleaning such as water washing or chemical cleaning.

Thirteen Pall 1.5-meter Hastelloy X filter elements were tested. By the end of TC09, one of the Hastelloy X filter elements had accumulated 2,139 hours of exposure, while two other filter elements accumulated 1,114 hours of exposure. The other 10 elements were virgin when installed prior to TC09. All 13 Hastelloy X filter elements were removed and inspected. There was no damage noted with all the welds in good condition.

Eleven out of the 13 were flow tested. Pressure drops versus face velocity for Pall Hastelloy X elements are plotted in Figure 3.3-3. At a face velocity of 3 ft/min, the pressure drop ranged from 25 to 52 inH_2O. Testing was not conducted at higher flow rates on these elements, because the differential pressure gauge will not read above 50 inH_2O. This high flow resistance on dirty Hastelloy X elements, in comparison with the flow resistance of other types of

elements, has been measured after some previous runs such as TC06B but not after others such as TC08. The reason for the higher flow resistance in the dirty Hastelloy X elements has not been determined; however, future testing must address this issue if these elements are to be considered for use in commercial hot-gas filtration systems.

The pressure drops measured were too high for reinstallation for TC10, so the elements were cleaned by water washing and then retested. The results measured after water washing are shown on Figure 3.3-3. The pressure drops at a face velocity of 3 ft/min ranged from 4 to 14 inH_2O. This is slightly higher than the typical pressure drop for virgin Hastelloy X elements of ~ 2 inH_2O but acceptable for reinstallation for TC10.

3.3.3 G-Ash Deposition

TC09A

There was an unscheduled shutdown in the initial hours of TC09. Operational evidence indicated that there was bridging on the lower plenum of the PCD.

During TC09A, the solids loading to the PCD was higher than seen in past gasification runs. The solids loading to the PCD during past runs on Powder River Basin (PRB) coal has been between 300 and 400 lb/hr. The solids loading to the PCD during the initial hours was as high as 950 lb/hr as measured by Southern Research Institute (SRI).

It is believed that the increase in solids loading to the PCD during this time contributed to the bridging. The solids loading to the PCD exceeded the fine solids removal system conveying capacity. This resulted in solids building up in the cone of the PCD. Bridging became evident when the baseline pressure drop began to significantly increase. Also, the filter element thermocouples began to deviate and the g-ash resistance probes began to indicate that they were covered with solids (see Section 3.2).

Based on all the operational evidence, it was decided to shut down and inspect the PCD. During the shutdown procedure, the resistance probes indicated that the bridging began to dislodge. Therefore, by the time the inspection could be performed, the bridging had completely dislodged. The lower manway on the PCD was removed in order to inspect the filter elements on the lower plenum. The inspection did not reveal any bridging.

TC09C

The plenum was pulled out of the PCD vessel after TC09C on October 1, 2002. Figure 3.3-4 shows the tube sheet as it is removed from the PCD vessel. Figure 3.3-4 shows that there was no bridging present after TC09.

As mentioned above, the shutdown after TC09 was "semidirty," which means that the bottom plenum elements were back-pulsed after the coal feed was shut down, but the top plenum was not. The purpose of the semidirty shut down was to allow inspection of transient dustcake on the top plenum and the residual dustcake on the lower plenum. The results of the dustcake measurements are discussed in Section 3.4.

3.3.4 Filter Element Gaskets

The gasket arrangement used in past gasification runs has proved to be very reliable; therefore, they were used during TC09. The gasket types have been outlined in past run reports (See TC06 Run Report). During this outage all the gaskets of the filter elements and failsafe devices that were removed were inspected. Figure 3.3-5 shows all the primary gaskets on the lower plenum before they were removed. Figure 3.3-5 shows that the primary gaskets were relatively clean indicating no obvious particulate penetration through the gasket. Inspection of the top plenum gaskets revealed the same findings. The gaskets between the failsafe and plenum were clean as well indicating a tight seal.

3.3.5 Failsafe Inspection

During TC09, the following failsafe devices were tested: fifty-four Pall fuses, twenty-one PSDF-designed devices, and ten SWPC ceramic failsafe devices. Also, six metal fiber failsafe devices designed by SWPC were installed above blanks to expose different alloys to reducing environment. Figure 3.3-6 shows the layout of the different failsafe devices during TC09. During TC09, two SWPC ceramic failsafe devices were tested online by g-ash injection.

During the outage, all the Pall Fe_3Al filter elements with fuses were removed and inspected. All of the fuses appeared to be in good condition. The welds seemed to be in good condition with no evidence of cracking. Thirteen of the Pall filters with fuses were flow tested. The flow tests did not reveal a significant increase in the flow resistance that would indicate that the fuse was blinding. However, it is difficult to determine the actual difference in flow resistance without cutting the fuse out of the filter element. Future plans include installing several Pall fuses into the tube sheet separate from the filter element. This will provide information on whether or not the fuse is blinding over time.

Before TC09, 21 PSDF-designed failsafe devices were installed. After TC09, all the PSDF-designed failsafe devices were removed for inspection. The failsafe devices appeared to be in good condition with no evidence of failsafe damage. After each failsafe was inspected, they were flow tested. The table below summarizes the results of the flow tests by taking the ratio of flow coefficients. The ratio of flow coefficients is determined by dividing the flow coefficient after TC09 by the flow coefficient before TC09. In addition to the ratio of flow coefficients, the corresponding exposure hours are included in the following table. The table shows that the flow coefficients decreased to varying degrees for each failsafe during TC09.

Failsafe ID	Total Exposure Hours	Ratio of Flow Coefficients
PSDF-Designed Failsafe #10	308	0.68
PSDF-Designed Failsafe #11	308	0.58
PSDF-Designed Failsafe #12	308	0.64
PSDF-Designed Failsafe #13	308	0.66
PSDF-Designed Failsafe #1	2,137	0.44
PSDF-Designed Failsafe #14	308	0.59
PSDF-Designed Failsafe #15	308	0.66
PSDF-Designed Failsafe #16	308	0.62
PSDF-Designed Failsafe #17	308	0.52
PSDF-Designed Failsafe #18	308	0.82
PSDF-Designed Failsafe #19	308	0.55
PSDF-Designed Failsafe #5	967	0.93
PSDF-Designed Failsafe #3	2,140	0.82
PSDF-Designed Failsafe #2	1,842	0.81
PSDF-Designed Failsafe #20	308	0.63
PSDF-Designed Failsafe #21	308	0.65
PSDF-Designed Failsafe #22	672	0.88
PSDF-Designed Failsafe #23	672	0.80
PSDF-Designed Failsafe #24	672	0.85
PSDF-Designed Failsafe #4	967	0.98

Each failsafe device was visually inspected under a microscope to determine whether or not the porous material was blinding due to corrosion or to particle accumulation in the pores. Figure 3.3-7 shows a considerable amount of particles that penetrated into the porous media of the failsafe. The porous material appeared to be coated with smaller black particles that appeared to be fine g-ash particles. Also, larger particles that appeared to be sand or mineral ash were seen within the pores. All the failsafe devices revealed similar results. None of the failsafe devices inspected under the microscope revealed any corrosion product. Therefore, it appears that the increase in flow resistance was due to particle penetration into the porous material.

It was not clear, based on this visual observation, where the particles came from. Three possible suggestions have been offered to explain where the particles originated:

1. PCD Tube sheet – Over the past 7 years there have been many filter failures. These failures resulted in contamination of the clean side of the filter vessel. Therefore, it is possible that the solid particles within the tube sheet are being back-pulsed into the failsafe and blinding them over time. This might explain where the sand particles came from.

2. Leaking Gaskets – It is possible that as solid particles leak past the gasket material, they are collected by the failsafe.

3. Filter Leak – It is possible that particles are penetrating through the filter elements and being collected over time.

In order to determine where the solid particles originated, a small sample was cut from one of the failsafe devices to view both the inner and outer surfaces of the fiber material. Figure 3.3-8 shows the outer surface of the prepared sample, while Figure 3.3-9 shows the inner surface. The outer surface shows large particles of sand or mineral ash. When viewing the inner surface and comparing it to the outer surface, the inner surface didn't appear to be as contaminated with particles as the outer surface. This finding might support the idea that the particles are being entrained into the porous media from the clean side of the tube sheet during back-pulsing. Also, it is important to note that some of the particles seen within the fibers of the failsafe were greater than 25 μ. Therefore, it would seem that if particles this large penetrated through the filter elements or gaskets, it would result in a PCD outlet loading greater than the outlet loadings reported in Section 3.4. At this point, it is difficult to say with any certainty the origin of these particles; therefore, test plans are being considered to determine the source of these particles.

During TC08, two prototype ceramic failsafe devices supplied by SWPC were tested. Two different suppliers, Specific Surface and CeraMem, provided the ceramic (silicon carbide) material. The ceramic material was contained in stainless steel housing. During TC08, these failsafe devices were installed in the tube sheet and exposed to actual operating conditions which including back-pulsing. Both of the failsafe devices were inspected, and no evidence of damage was noticed after TC08. Therefore, further testing was performed during TC09 by installing 10 ceramic failsafe devices in the PCD.

During TC09, eight CeraMem and two Specific Surface ceramic failsafe devices were installed into the PCD. The collection efficiency of two ceramic failsafe devices (one CeraMem and one Specific Surface) was determined during TC09 as well. The collection efficiency was determined by injecting g-ash into two filter elements to simulate a filter leak (see Section 3.5 for results of the injection test).

After TC09, all 10 of the ceramic failsafe devices were visually inspected. The two failsafe devices that were subjected to the g-ash injection test had small amounts of material missing from the top of the silicon carbide filter media. The other eight ceramic failsafe devices were removed, inspected, and flow tested. Upon removal, the Specific Surface failsafe device that was not tested with the g-ash injection test was severely damaged (see Figure 3.3-10). None of the other seven CeraMem failsafe devices that were installed for gas-only exposure had any obvious damage to the filter media, and the flow test results did not indicate a significant change in their porosity compared to the pretest condition. All 10 of the ceramic failsafe devices have been sent to the SWPC Science and Technology Center for further evaluation.

It appears that the structural design of the ceramic failsafe devices needs further development. The current design can not handle the repeated thermal and mechanical stresses imposed on it during the numerous back-pulse events. Based on these findings, all of the ceramic failsafe devices were removed from the test plan until Specific Surface and CeraMem can resolve these problems associated with the ceramic failsafes.

3.3.6 Auxiliary Equipment

During TC09, two prototype inverted filter assemblies supplied by SWPC were installed in the PCD and tested. The inverted filter assembly was developed primarily as a possible solution for bridging. One of the concerns with respect to the inverted filter assembly was the sealing mechanism. During the post-test inspection, no indication of dust leakage was noted. The flow resistance of the failsafe devices installed above the inverted filter assemblies was within acceptable limits after TC09, implying that the inverted filter assemblies did not leak. Therefore, more inverted filter assemblies will be tested during TC10.

The back-pulse pipes were removed and inspected during this outage. There was no significant damage on the pulse pipes. Figure 3.3-11 shows one of the back-pulse pipes after TC09. Figure 3.3-11 shows a thin layer of condensed tar on the pipe. In the past, some pitting has been noted on the back-pulse pipe near the flange. The pitting did not seem any worse than after the last outage. Finally, the inner liner of each back-pulse pipe was inspected and appeared to be in good condition with no obvious damage (see Figure 3.3-12).

3.3.7 Fine Solids Removal System

The screw cooler (FD0502) performed well during TC09. This is based on the fact that during the 307 hours of on-coal operation it did not fail. Other than minor packing adjustments, FD0502 did not require any attention from maintenance during operation. Before TC07, several modifications were made to the drive end stuffing box to increase reliability. These modifications were documented in the TC07 run report. Since the modifications improved the performance during TC07, the same changes were implemented to the nondrive end before TC08. FD0502 performed well during TC08, so the modifications were tested during TC09 without disassembling the stuffing box. The current modification has accumulated 671 on-coal hours.

One of the methods that has been used to determine the success of the new stuffing box modifications is tracking the stuffing box gap. Figure 3.3-13 shows the packing follower gap that is being measured. The packing follower is used to compress the shaft seal rings to prevent process gas from leaking. Once there is no more room to compress the follower, the seals must be replaced. The packing follower gap has been monitored since TC08. The following table summarizes the packing follower measurements:

Run	Drive-End Gap, inches	Nondrive-End Gap, inches
Before TC08	1.75	1.75
After TC08/Before TC09	1.375	1.625
After TC09	1.125	1.375

The table above shows that both the drive and nondrive end packing follower gaps still has plenty of room for compression. Therefore, FD0502 was not disassembled during this outage in order to accumulate operating experience with the new modifications.

The fine solids depressurization system (FD0520) required a large amount of attention by process engineers and operations during TC09. Many of the problems associated with FD0520 were associated with Transport Gasifier upsets, high solids loading, or FD0530 trouble. The fine solids removal system tripped on several different occasions due to high temperature alarms that were due to Transport Reactor upsets. Also, FD0520 tripped due to problems associated with FD0530. The following table outlines the different upset events that tripped the fine solids removal system.

Date	Time	Reason for Trip
9-4-02	23:00	FD0530 Tripped
9-8-02	16:10	High Temperature Alarm* Due to Transport Reactor Upset
9-8-02	16:30	High Temperature Alarm* Due to Transport Reactor Upset
9-8-02	20:00	High Temperature Alarm* Due to Transport Reactor Upset
9-8-02	20:20	High Temperature Alarm* Due to Transport Reactor Upset
9-9-02	19:00	High Temperature Alarm* Due to Transport Reactor Upset
9-10-02	15:30	High Temperature Alarm* Due to Transport Reactor Upset

* The purpose for the high temperature alarm is to protect the seals in FD0520. These seals must not be exposed to temperatures above 400 °F.

In order to prevent these unscheduled trips in the future, a control scheme to slow down FD0502's speed during high solids carryover will be implemented.

During TC09, one of the vent valves failed, which prevented the lock vessel from pressurizing to process pressure. The other vent valve was brought into service while the failed valve was isolated and replaced.

Since a reliable level detector has not been found for FD0520, the process engineers spent a large amount of time adjusting the lock-vessel cycle timer to ensure the solids were not accumulating in the PCD cone. Figure 3.3-14 shows how the solids loading to the PCD fluctuated during TC09. The solids loading in Figure 3.3-14 was determined by the weigh cell in FD0530. In order for a commercial unit to run efficiently and cost effectively, a reliable level detector designed for these harsh conditions needs to be developed.

During the outage, FD0520 was disassembled and thoroughly inspected. Figure 3.3-15 shows the lock-vessel ring plate. The ring plate appeared to be in good condition; therefore, it was reinstalled. During the inspection of FD0520, it was noticed that the seal material on the top sphere valve was cracked. Figure 3.3-16 shows the location of the crack. Although this did not result in a failure during operation, it appears that this seal was near failure. The seal is made of Nomex-filled Viton, which is brittle at lower temperatures (< 200 °F). The vendor has suggested that a more pliable seal be used; therefore, Nomex-filled Silicon material will be used in TC10.

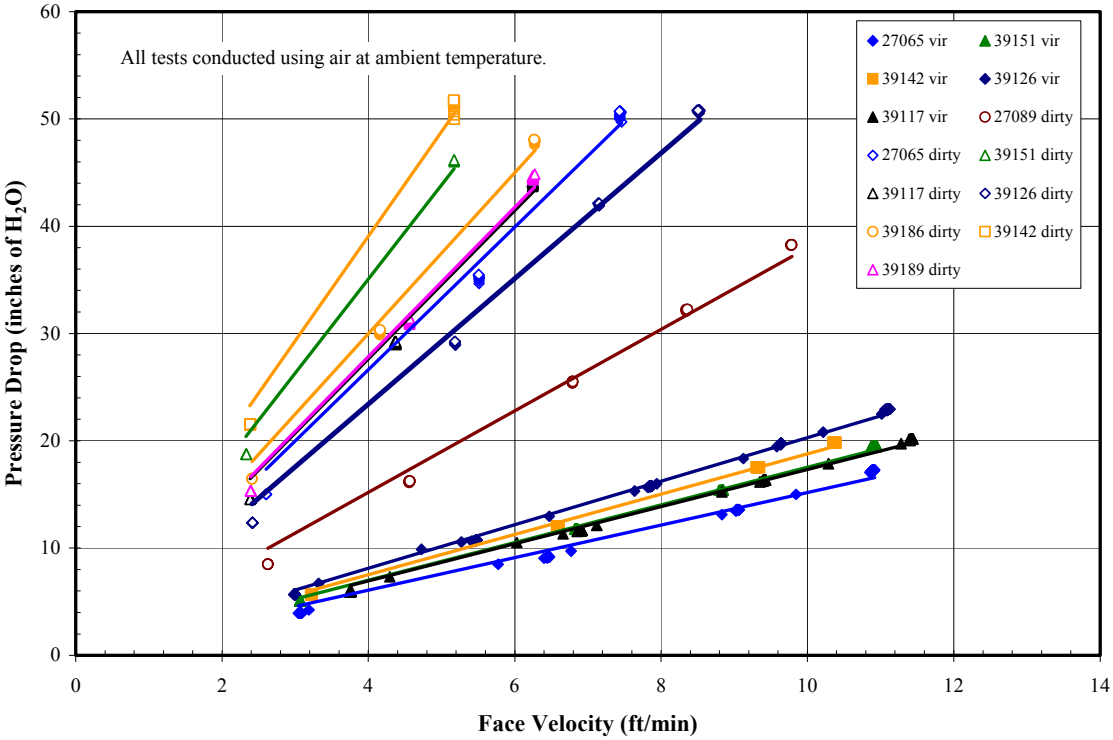

Figure 3.3-1 Pressure Drop Versus Face Velocity for Pall Fe_3Al After TC09

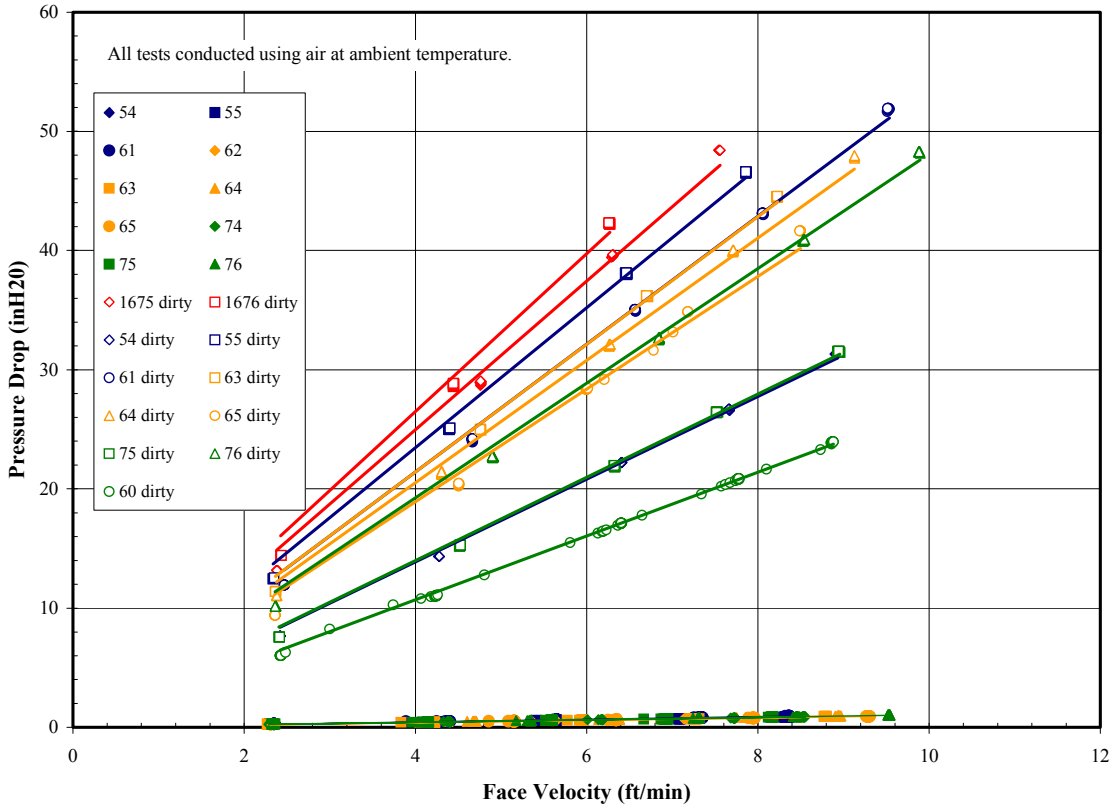

Figure 3.3-2 Pressure Drop Versus Face Velocity for HR-160 After TC09

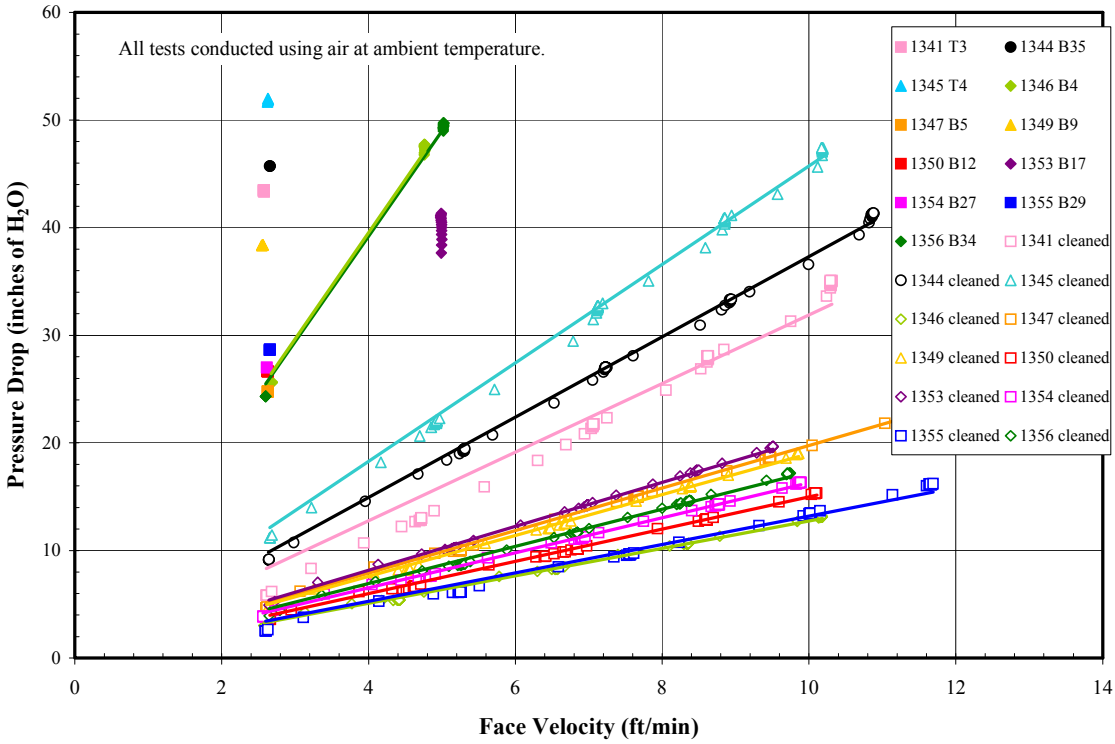

Figure 3.3-3 Pressure Drop Versus Face Velocity for Hastelloy X After TC09

Figure 3.3-4 Tubesheet Removal After TC09

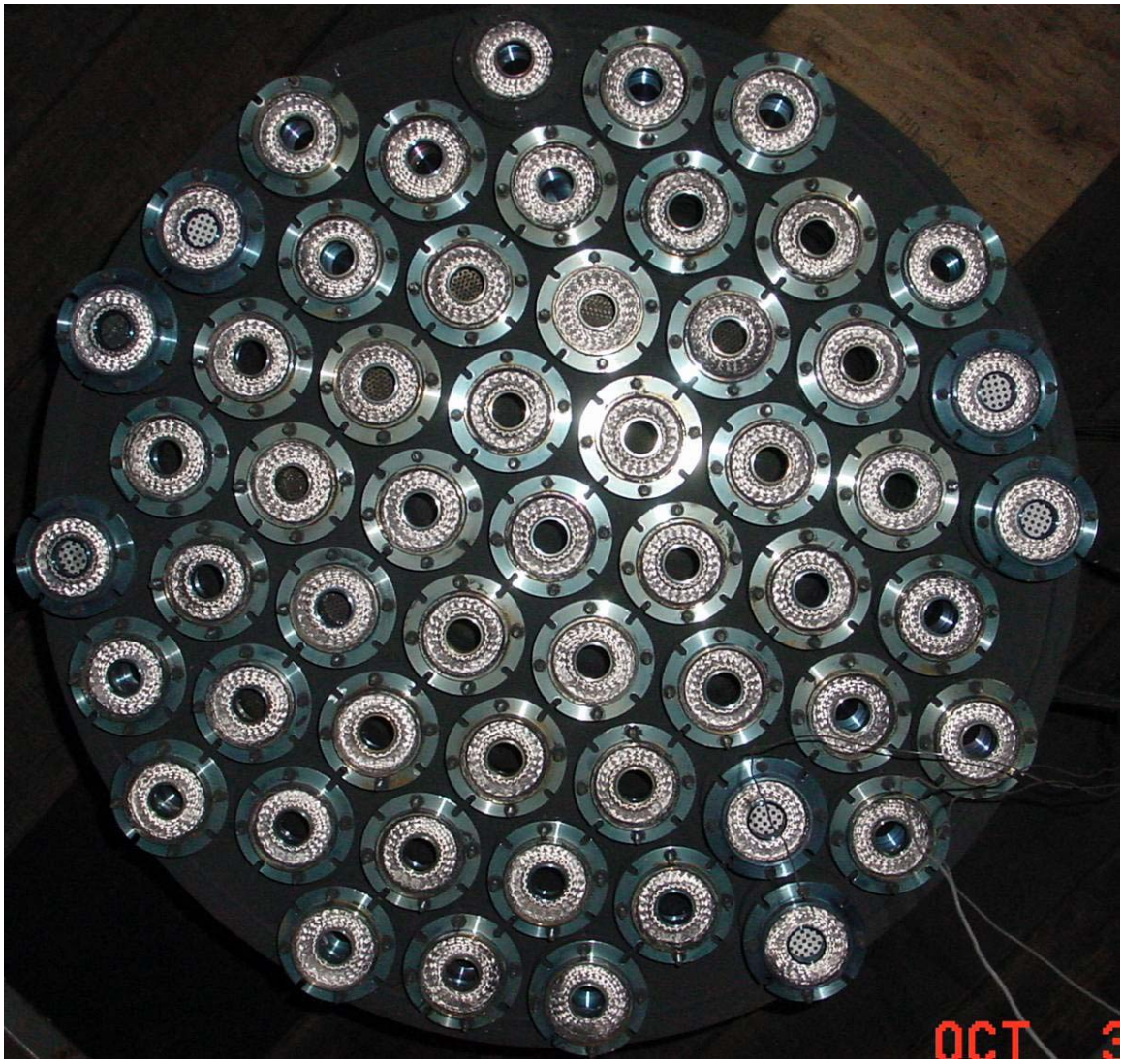

Figure 3.3-5 Primary Gaskets on Lower Plenum After TC09

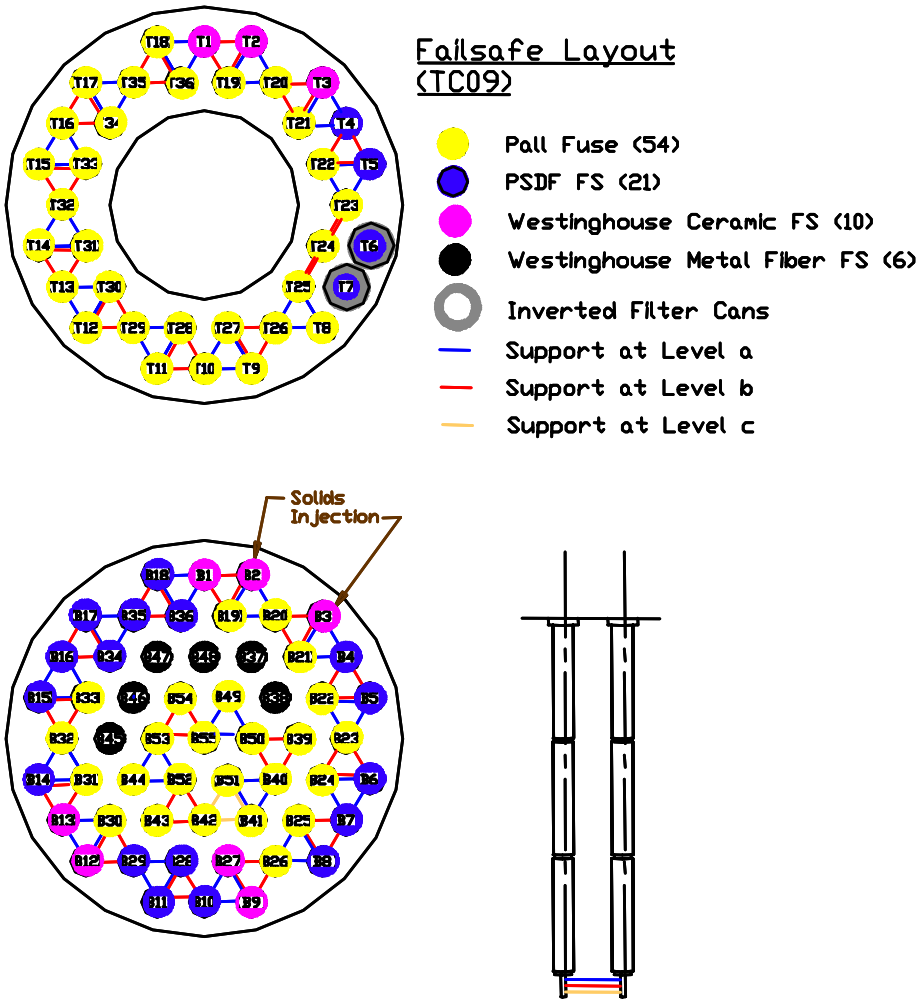

Figure 3.3-6 Failsafe Layout for TC09

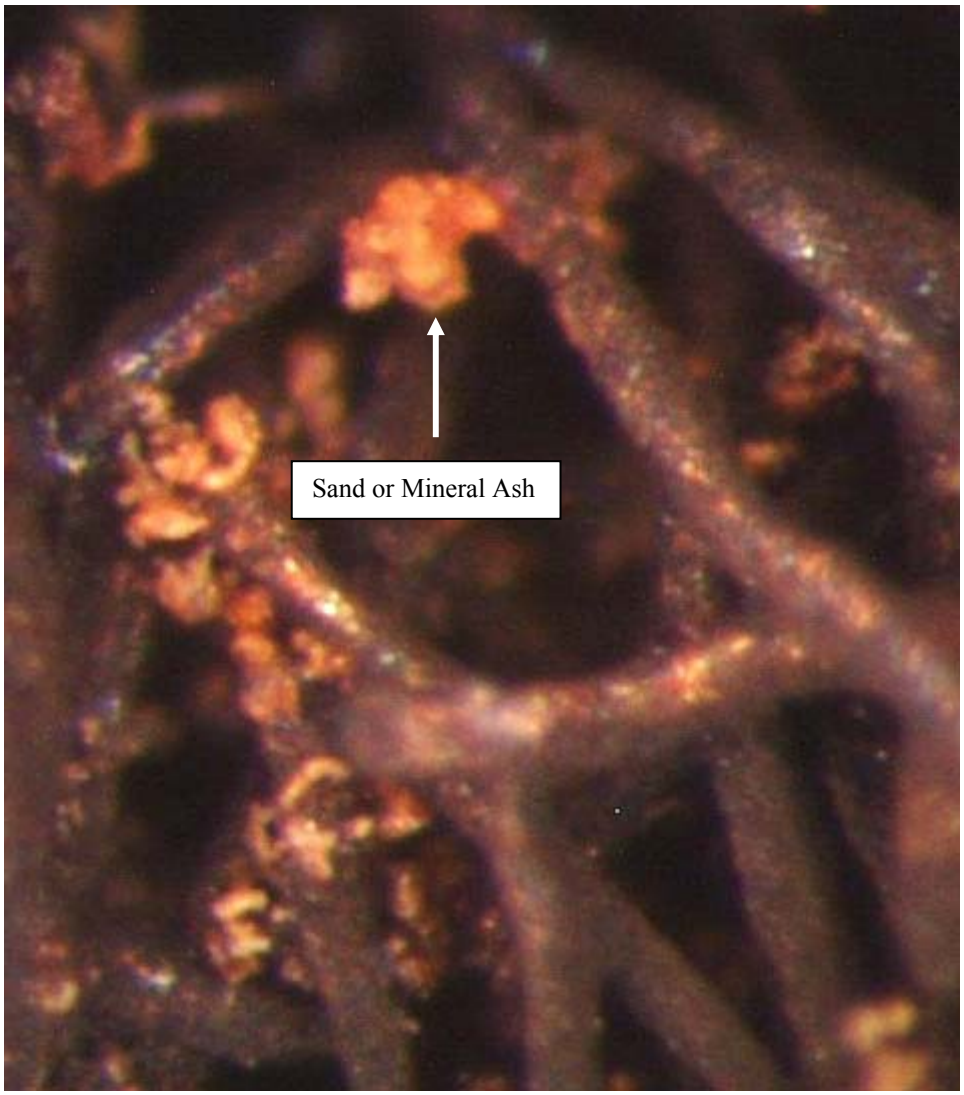

Figure 3.3-7 PSDF-Designed Failsafe #5 After TC09

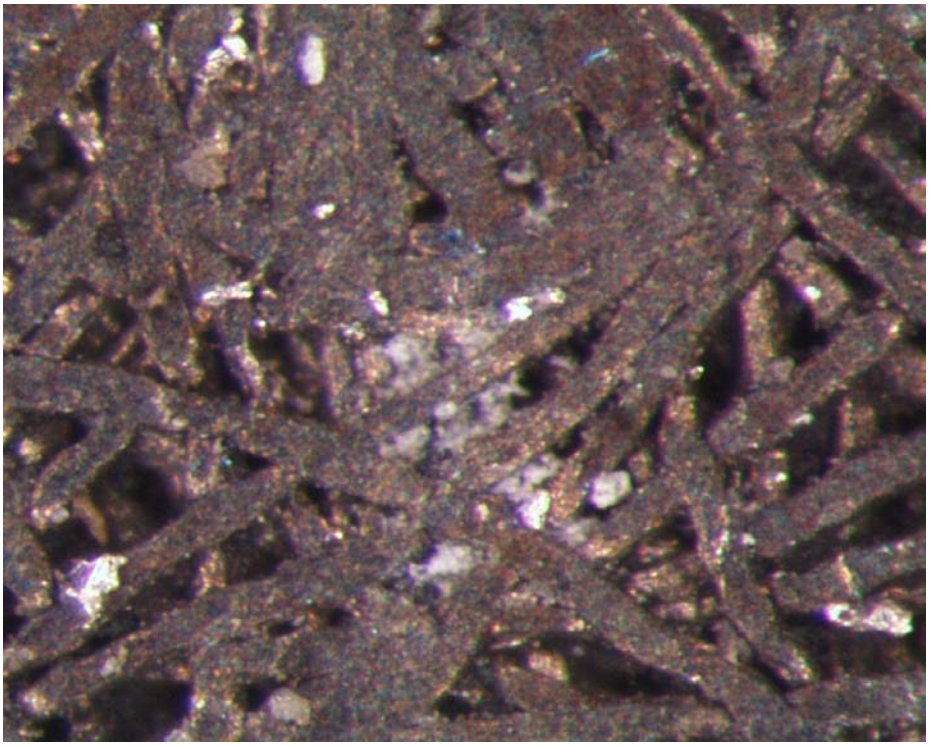

Figure 3.3-8 PSDF-Designed Failsafe #21 Outside Surface After TC09

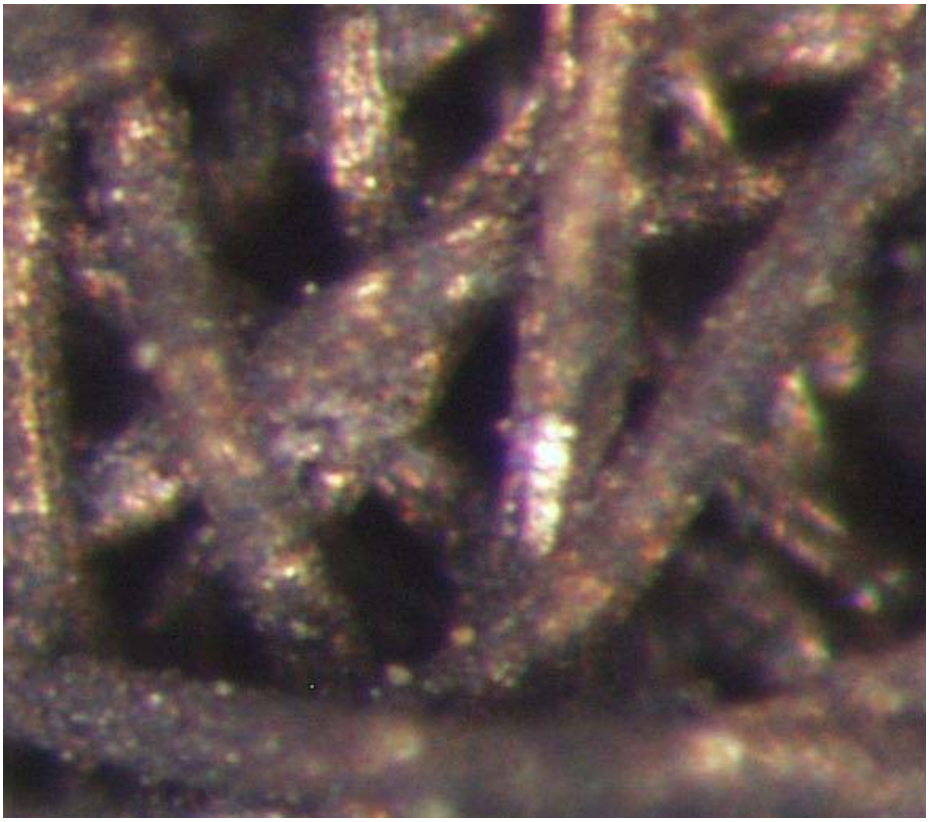

Figure 3.3-9 PSDF-Designed Failsafe #21 Inside Surface After TC09

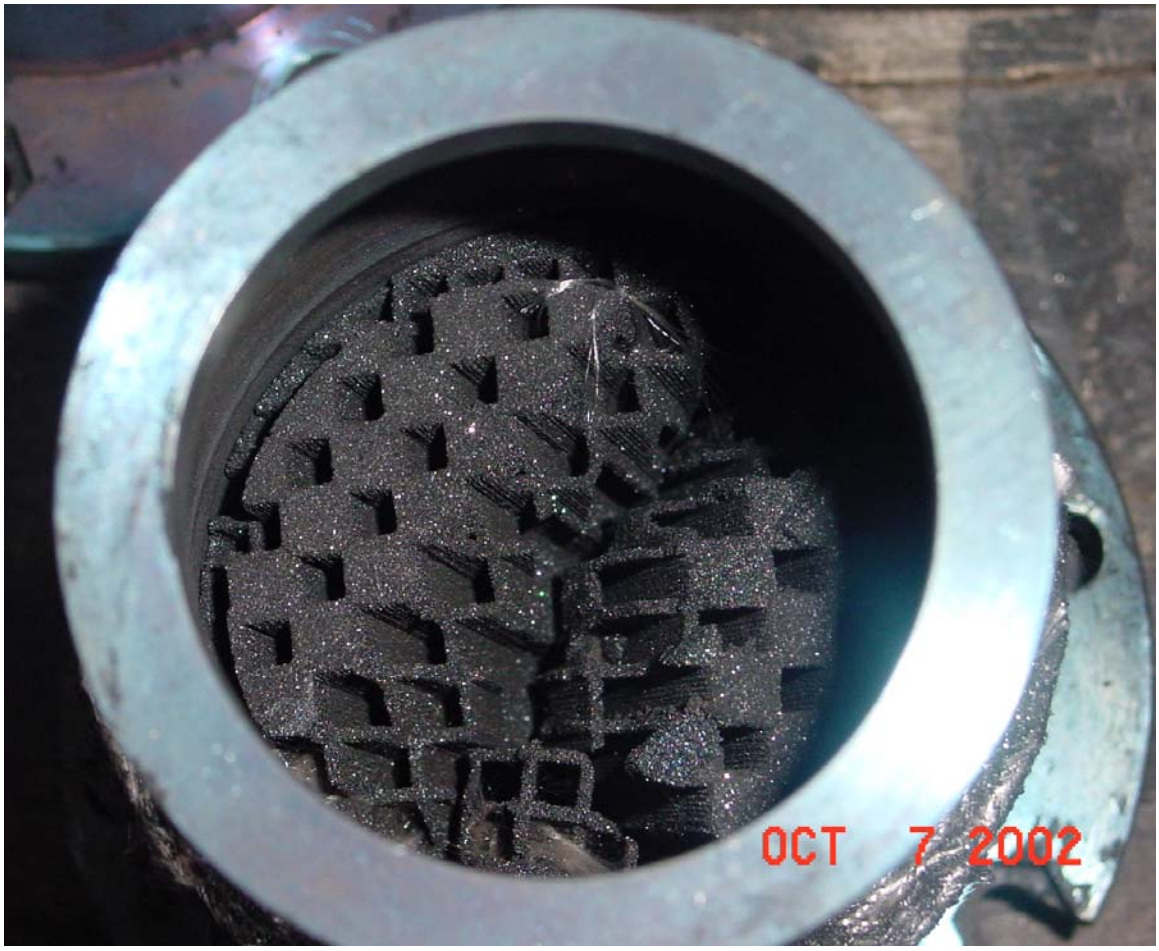

Figure 3.3-10 Specific Surface Failsafe Device After TC09

Figure 3.3-11 Back-Pulse Pipe After TC09

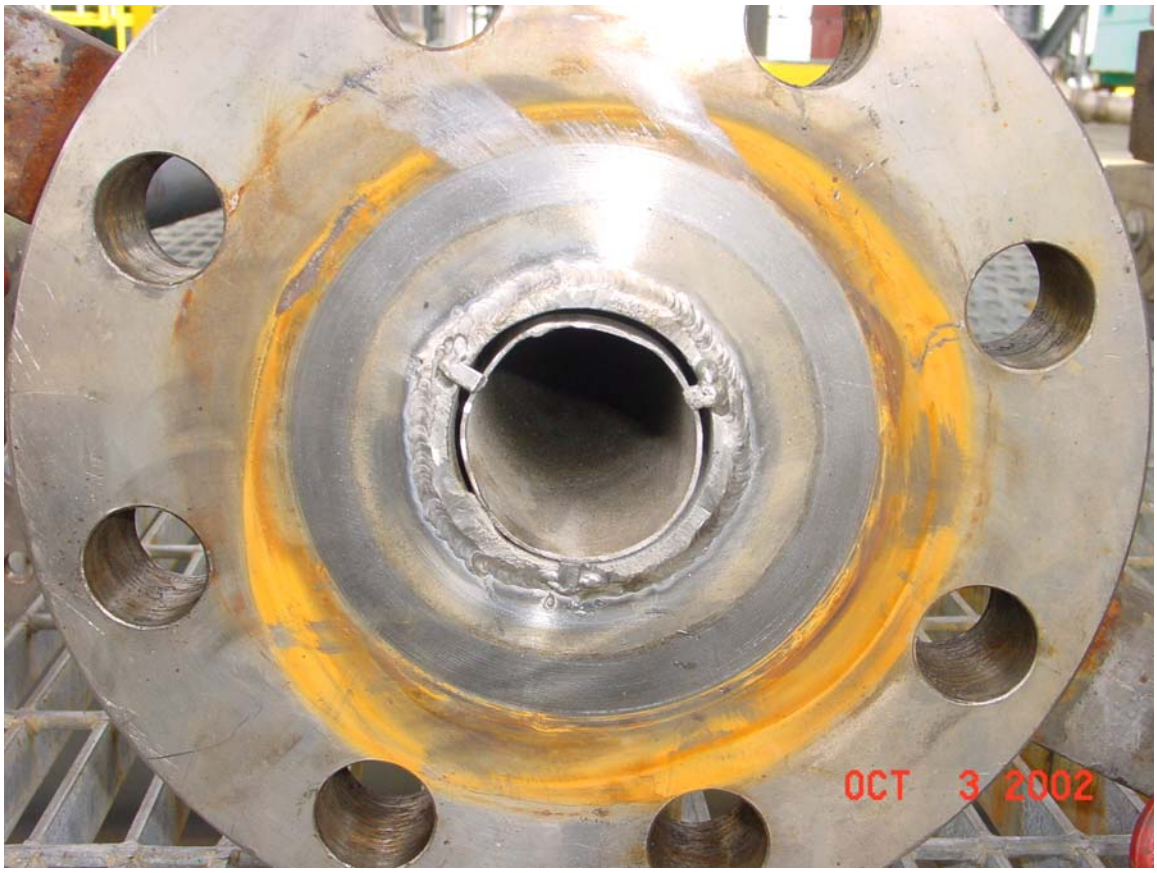

Figure 3.3-12 Back-Pulse Pipe Inner Liner After TC09

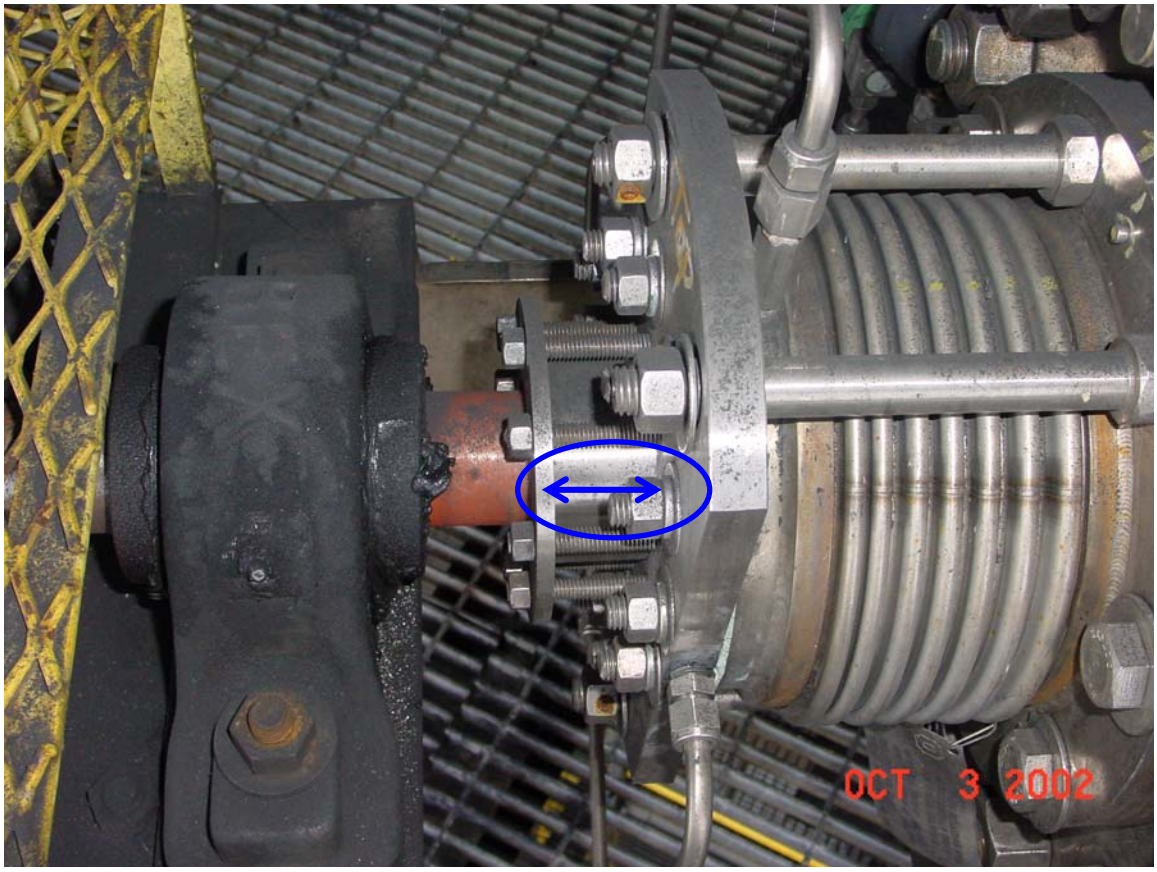

Figure 3.3-13 FD0502 Drive-End Packing Follower Gap

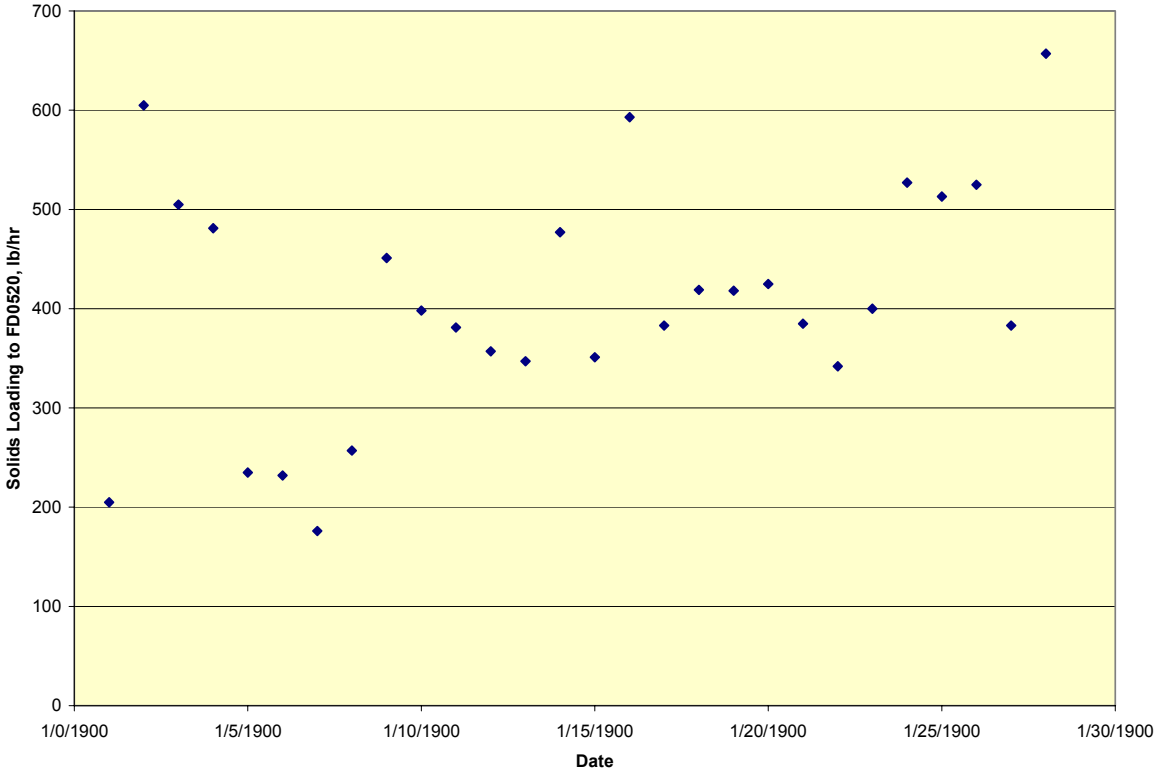

Figure 3.3-14 Solids Loading to FD0520 During TC09

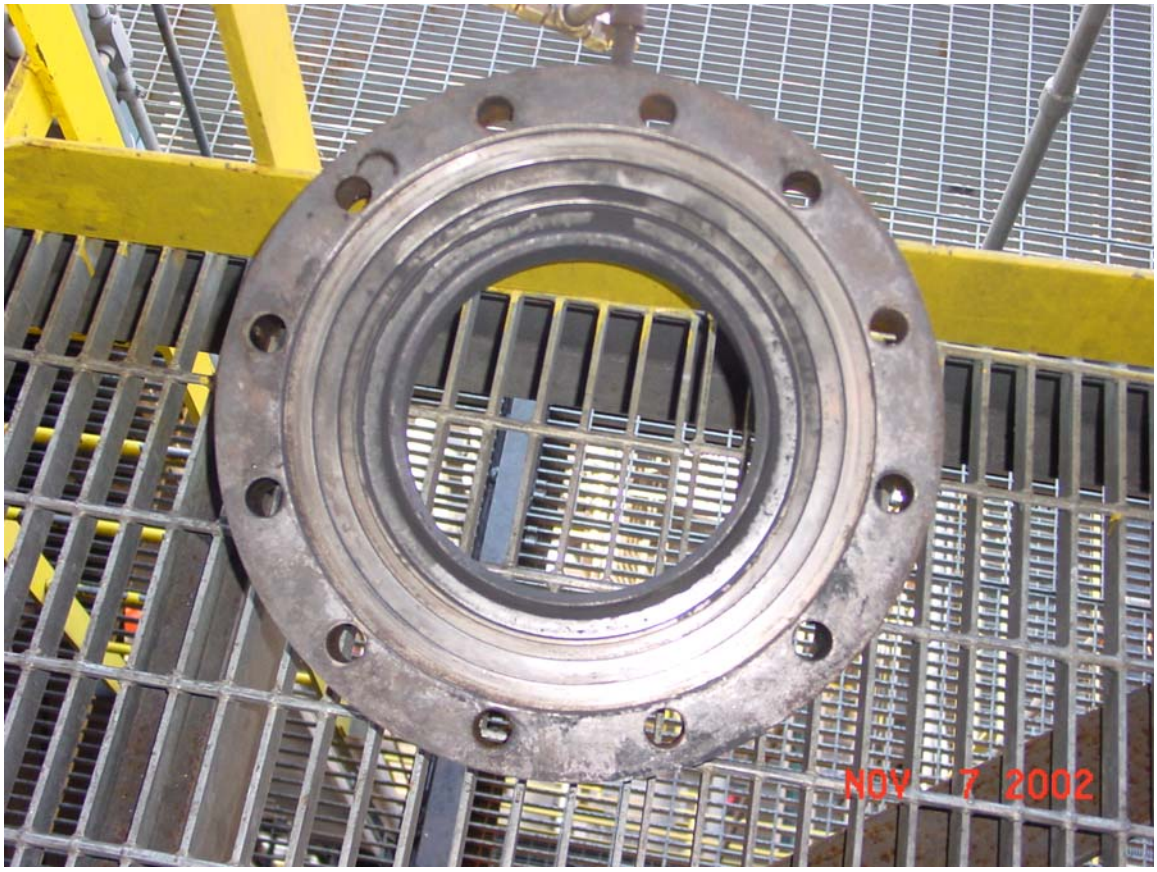

Figure 3.3-15 Lock-Vessel Ring Plate After TC09

Figure 3.3-16 Cracked Upper Spheri Valve Seal After TC09

3.4 G-ASH CHARACTERISTICS AND PCD PERFORMANCE

This section deals with the characteristics of the g-ash produced during TC09 and the relationship between the g-ash characteristics and PCD performance. As discussed previously, the main purpose of TC09 was to successfully operate the Transport Gasifier system and PCD with the Hiawatha (SUFCo) bituminous coal in both air- and oxygen-blown modes of operation. Since most of the previous testing has been done with PRB coal, this report will be focused on understanding the differences between the Hiawatha bituminous coal and the PRB coal. The effects of air- and oxygen-blown operation will also be examined.

As in previous tests, characterization of the in situ g-ash samples and dustcake samples included measurements of the true particle density, bulk density, uncompacted bulk porosity, specific-surface area, chemical analyses, particle-size analyses, and laboratory drag measurements. Drag measurements, as a function of particle size, were made using the resuspended ash permeability tester (RAPTOR), and these measurements were compared to transient drag values determined from PCD performance data. The results were used to better understand the contribution of the dustcake to PCD ΔP and to gain insight into the effect of particle size and morphology on drag. As suggested earlier, the results presented here will also provide insight into the effects of operating mode (air- or oxygen-blown) and coal type on g-ash characteristics and PCD performance.

3.4.1 In situ Sampling and Monitoring

In situ sampling with the SRI batch sampling systems was conducted at both the inlet and the outlet of the PCD throughout the TC09 test program. These measurements were used to quantify the concentration and characteristics of the dust entering the PCD, the particulate emission rate, and the syngas moisture content. This section will present the concentration data obtained with these measurements, while the physical and chemical characteristics of these samples will be discussed in later sections. Comparison of real-time particle monitor results to the outlet in situ measurements will also be discussed in this section. The system and procedures used for the in situ particulate sampling and real-time monitoring have been described in previous reports.

3.4.1.1 PCD Inlet Particle Mass Concentrations

A total of 12 in situ particulate measurements were obtained at the PCD inlet during TC09. Eight runs were obtained in air-blown mode, and four measurements were made in 100 percent oxygen-blown mode. The results are shown in Table 3.4-1.

During air-blown operation, the inlet mass concentrations varied from 22,000 to 42,400 ppmw, corresponding to mass-flow rates of 471 to 965 lb/hr. These particle concentrations and solids flows were much higher than those measured during previous tests with PRB coal. During TC08, for example, the measured particle concentrations varied from 12,500 to 16,700 ppmw, corresponding to mass flows of 260 to 395 lb/hr. Much of the difference in particle mass is attributable to the higher ash content of the Hiawatha bituminous coal compared to the PRB subbituminous coal. Based on coal samples taken from the FD210 coal feeder during TC09, the

Hiawatha bituminous coal had an average ash content of 11.2 wt percent on a dry basis, while the average ash content of the PRB coal samples taken during TC08 was only 6.2 wt percent.

During the oxygen-blown portion of TC09, the inlet particulate concentration varied from 26,900 to 39,700 ppmw, corresponding to mass flows of 390 to 594 lb/hr. The variations that are seen within all the TC09 data can be largely explained by changes in the coal-feed rate, as illustrated in Figure 3.4-1. Although there is considerable scatter in the data, the linear regression suggests that the coal feed accounts for the majority of the variation observed. The oxidant used did not affect the particulate loading entering the PCD. The one data point in the upper left corner of the graph (2,670, 855) was collected during a period when Transport Gasifier standpipe inventory was dropping continuously resulting in more mass exiting the gasifier than expected. The exact reason for the unstable operation during this period is unknown. This data point was excluded from the linear regression.

3.4.1.2 PCD Outlet Particle Mass Concentrations

The particle concentrations which penetrated the PCD are shown in the rightmost column of Table 3.4-1 and compared to the results of recent test programs in Figure 3.4-2. After the first 2 days of operation and in the absence of injected dust for failsafe testing, and with the exception of one case of tar contamination, the PCD outlet mass concentration varied from below the detection limit of 0.10 up to 0.12 ppmw.

During TC09, a different type of sample filter material was used at the outlet of the PCD for several tests. This filter material is much more dense than used previously, which will keep collected particles close to the surface of the filter rather than letting them penetrate deeply into the filter media. Keeping the particles on the filter surface will allow microscopic examination of the particles even when the collected mass is too small to weigh. Particles were observed on all of the sampling filters in TC09, even those that had a mass that was below the detection limit. Figure 3.4-3 shows an optical microscope photograph of the filter from outlet Run Number 12. Although the filter was only very slightly gray in color to the naked eye, particles are clearly visible with the microscope. The largest particles are around 10 μm in diameter and the smallest specks that are visible are around 1 μm. Particles below 1 μm cannot be seen with the optical microscope. These particles are not believed to be reentrained debris from the duct but are probably resulting from some rate of penetration through the PCD. Whether this number of particles of this size would be a problem for a downstream turbine is unknown.

The first two tests during TC09 indicated slightly elevated levels of dust in the PCD outlet gas stream. The first outlet sampling run was conducted 10 hours after start of coal feed and indicated a loading of 0.23 ppmw. After about 21 hours of coal feed, the unit was shut down for several days. The second test was conducted 12 hours after restart on coal and indicated a particle concentration of 0.22 ppmw. The third measurement, which indicated a much lower mass concentration (0.11 ppmw), was made after 36 continuous hours on coal. Some process appeared to be contributing particles to the PCD outlet during the first hours on coal which cleared up with time. The size distribution of these particles included large concentrations of small particles. In the past, the presence of small (<10 μm) particles for any significant period of time has indicated a PCD leak. This elevated emission issue is different from the problem

discussed in past reports of large (>10 μm) particle contamination on the sample filters. In the latter case, there were no small particles present, which we believe is not indicative of a leak.

There was also a slightly elevated outlet particulate loading at the beginning of the next test program, TC10, which was completed prior to the preparation of this report. Again, the fine-size distribution of the particles suggested that they came from penetration through the PCD. Subsequent tests conducted in a PCD cold-flow model showed that certain types of filter elements allow particle penetration, especially when the filter elements are new. Elements of the same type that had been used in previous runs did not allow as much particle penetration in the cold-flow tests, suggesting that there is a "conditioning" effect similar to that observed in baghouses and other types of "nonbarrier" filters. This may explain why the outlet loading was initially above 0.2 ppmw and then dropped to 0.1 ppmw or less after the first two measurements.

Out of the 85 filter elements that were installed in the PCD in TC09, 27 of them were of the types that allowed some particle penetration in the cold-flow model tests. Out of these 27 elements, 22 were new elements installed for the first time before TC09. Based on the testing done in the cold-flow model, particle penetration through these new elements seems to be a likely source for the particles observed on the outlet sampling filters at the beginning of TC09.

Elevated particle concentrations were also measured during the testing of two different failsafes in which g-ash was injected into the space between the filter element and the failsafe being tested. The tests were done on a Ceramem cross-flow ceramic failsafe and a Specific Surface ceramic honeycomb failsafe and resulted in outlet particle loadings of 0.46 ppmw and 0.45 ppmw, respectively. Inspection of the failsafes after TC09 revealed that both failsafes had apparently experienced some type of structural damage during the run and were no longer intact. The failsafe suppliers are currently investigating the problem. Results of the failsafe injection tests are discussed in more detail in Section 3.5.

3.4.1.3 Syngas Moisture Content

Measurements of the syngas moisture content were made in conjunction with the outlet particulate sampling runs by collecting the condensate from the syngas sample in an ice-bath condenser. The values determined for individual runs are included in Table 3.4-1. In air-blown operation the moisture content ranged from 12.3 to 30.3 percent, whereas in oxygen-blown mode the moisture content was generally higher at 32.2 to 38.6 percent. The higher moisture content measured in the oxygen-blown mode is a result of the additional steam injected for cooling the lower mixing zone during oxygen-blown operation. There is no evidence that this would have an adverse effect on PCD operation, other than to increase the face velocity as a result of the additional gas volume.

3.4.1.4 Real-Time Particle Monitoring

During TC09, the PCME Dustalert-90 particle monitor exhibited unusual behavior. Elevated readings were common and the output varied considerably. At times the monitor reading appeared to correspond to system events and at other times seemed random. For example, during the first two in situ mass concentration measurements, discussed above, that returned

actual concentrations of 0.23 and 0.22 ppmw, the Dustalert-90 gave values of 0.44 percent and 3.26 percent, respectively. At the conclusion of TC09, the instrument was removed and inspected. Although the instrument was in good physical condition (no insulator contamination or other problems), the erratic elevated readings continued in the lab. PCME, Inc. determined that the sensor head circuit board was faulty and provided a new board. This new board was installed prior to TC10.

3.4.2 Particle-Size Analysis of In situ Samples

Particle-size distributions of the TC09 in situ samples were measured using a Microtrac X-100 Particle-Size Analyzer. Figures 3.4-4 and -5 show the particle-size distributions measured in air-blown mode and in oxygen-blown mode, respectively. The symbols indicate the results from individual tests while the solid lines are the average for all runs. Although there is some scatter in the data, the runs are in acceptable agreement.

The averages for the air- and oxygen-blown data are compared on an actual mass basis in Figure 3.4-6. The slight differences between these distributions are almost entirely a result of differences in coal-feed rate or gas volume flow. Figure 3.4-7 compares the air- and oxygen-blown distributions on a percent-mass basis and indicates that there is no difference in the relative concentrations of particle sizes emitted from the Transport Gasifier. Therefore, under the conditions of these tests, the choice of oxidant (air or oxygen) does not seem to affect the size distribution of the particles carried over to the PCD. The same conclusion was reached with regard to the size distributions measured in TC08 with PRB coal.

The average particle-size distributions obtained during gasification of the Hiawatha bituminous coal are compared with those of PRB g-ash from TC08 in Figure 3.4-8. This comparison indicates that the bituminous coal produced a lower concentration of particles smaller than 5 μm than did the PRB coal. Interestingly, increased concentrations of fine particles are typical of fly ash from pulverized coal-fired boilers that burn PRB coal. The increased production of fine particles results from a relatively high degree of char fragmentation that occurs during coal devolatilization. Compared to bituminous chars, subbituminous chars tend to undergo a higher degree of fragmentation because of their higher volatiles content and the resulting increased release of volatiles during rapid heating. The rapid release of this volatile matter creates fissures in the char particles and ultimately leads to a greater degree of fragmentation (Sarofim et al, 1977). With all other factors being equal, a coarser size distribution would be expected to produce a lower pressure drop dustcake with the bituminous coal.

3.4.3 Sampling of PCD Dustcakes

In an effort to preserve the residual and transient dustcakes, TC09 was concluded with a "semidirty" shutdown of the PCD. The semidirty shutdown procedure has been described in previous reports. The procedure was implemented successfully at the end of TC09, presumably preserving the residual cake on the bottom filter elements and the entire cake (transient plus residual) on the top elements. In addition to the residual cake, there were also some thicker patches of dustcake on the Hastelloy-X elements in the bottom plenum. The thicker patches appeared to contain some of the transient cake as well as the entire residual cake. The table

below summarizes the thickness and areal loading measurements that were made in each of these areas along with the corresponding calculated values of porosity.

Location, type of cake	Cake Thickness, in.	Areal Loading, lb/ft^2	Calculated Porosity, percent
Top plenum, entire dustcake (transient plus residual)	0.051 to 0.069	0.087 to 0.10	85.2 to 87.4
Bottom plenum, residual cake only	0.006 to 0.01	0.004 to 0.007	93.4 to 94.8
Bottom plenum, patches (residual and some transient)	0.044 to 0.055	0.032 to 0.037	93.5 to 93.7

As expected, the bottom plenum (residual) cake was the thinnest, and the dustcake on the top elements, which represents the entire cake (transient plus residual), was the thickest. The patches on the bottom elements were only slightly thinner than the transient-plus-residual cake on the top plenum, implying that the patches contained most of the transient cake in addition to the entire residual cake. While the top plenum cake was only slightly thicker than the patches, it was much heavier, giving it a much lower porosity than the patches. Previous tests with PRB coal have not shown such a large difference in porosity between the residual and transient cakes, but such a difference may not be too surprising given the different histories of the residual and transient dustcakes. While the residual cake and patches have presumably been subjected to multiple cycles of back-pulse cleaning, the transient cake that was collected in the semidirty shutdown was never subjected to any back-pulsing. The back-pulsing would tend to open flow channels (pores) through the residual material, thereby increasing porosity in the residual cake and patches.

The residual dustcake that remained on the bottom elements after TC09 was extremely thin, with an average thickness of only 0.008 in. As mentioned above, the dustcake that remained on the top elements (residual plus transient) was much thicker, with an average thickness of 0.06 in. The average thicknesses of the TC08 dustcakes that were produced from PRB coal were 0.01 in. for the residual and 0.09 in. for the entire (residual-plus-transient) cake. Thus, the Hiawatha dustcakes were actually somewhat thinner than the PRB dustcakes, even though the Hiawatha coal has a higher ash content than does the PRB coal. The explanation for this apparent discrepancy can be found in the solids carryover rates that were calculated from the in situ sampling. The last measurement that was made at the end of TC09 indicated a solids carryover rate of 390 lb/hr, while the last TC08 measurement indicated a carryover rate of 617 lb/hr. Thus, the TC08 solids carryover exceeded the TC09 solids carryover by a ratio of 617:390, or about 1.6:1. The ratio of the total (residual-plus-transient) dustcake thicknesses was 0.09:0.06, or about 1.5:1. As might be expected, the total cake thickness is largely controlled by the solids carryover, since the transient cake accounts for most of the total cake thickness. The residual cake thickness is apparently not as strongly influenced by the carryover rate, since the ratio of residual cake thicknesses was 0.01:0.008, or about 1.25:1. This result is not too surprising, since the thickness of the residual cake would be more strongly influenced by other effects associated with the prolonged exposure of the cake to syngas. These effects could involve various mechanisms (chemical reactions, sintering, etc.) that would tend to cause cake consolidation.

3.4.4 Physical Properties of In situ Samples

Table 3.4-2 gives the physical properties of the TC09 in situ samples and the composite PCD hopper samples that were used for the RAPTOR drag measurements. The physical characteristics do not reveal any significant differences between the air- and oxygen-blown portions of the run. All of the in situ samples collected during both the air- and oxygen-blown portions have fairly consistent physical properties, with the exception of the first sample (Run No. 1), which was collected on September 5, 2002. The specific-surface area of the first sample was well below the range of all the other in situ samples (49 m^2/g versus 80 to 149 m^2/g). As discussed later in the section on chemical analysis, the lower surface area of the first sample may be related to its chemical composition, which suggests that it was more highly sulfidized than any of the other samples (0.98-percent CaS versus 0.36 to 0.71-percent CaS for the other samples).

The composite hopper samples also had relatively low surface areas compared to the in situ samples, but their chemical compositions do not suggest an unusual degree of sulfidation. In previous tests, it has been noted that hopper samples usually have lower surface areas than do in situ samples. This difference suggests that the g-ash undergoes some sort of change during its additional residence time on the filter elements and in the hopper. The mechanism of the change is not understood, but this sort of surface area reduction can be caused by sintering or by chemical reactions with various syngas components. Despite this reduction in surface area, past experience has shown that the drag characteristics of the PCD hopper samples are consistent with the actual PCD ΔP. This result suggests that the surface area reduction that occurs in the hopper samples results mainly from the closure of small pores that do not affect the drag characteristics.

The following table compares the average properties of the air- and oxygen-blown g-ashes produced in TC08 and TC09.

	TC09 Air	TC09 Oxygen	TC08 Air	TC08 Oxygen
Bulk density, g/cc	0.24	0.23	0.25	0.25
Skeletal particle density, g/cc	2.25	2.19	2.39	2.35
Uncompacted bulk porosity, percent	89.3	89.6	89.5	89.4
Specific surface area, m^2/g	89	111	235	217
Mass-median diameter, μm	19.0	19.3	18.7	18.7

Again, the average physical properties of the g-ash are not significantly influenced by the type of oxidant (air or oxygen). However, the type of coal (Hiawatha bituminous in TC09 versus PRB subbituminous in TC08) clearly has a significant effect on the properties of the g-ash. The most striking effect is on the specific-surface area (89 to 111 m^2/g for the bituminous g-ash versus

217 to 235 m^2/g for the subbituminous g-ash). It is not known whether this trend applies to bituminous and subbituminous g-ashes in a more generalized sense, but there is definitely a substantial difference in the g-ashes from these particular coals. Based on the difference in surface area alone, we would expect the Hiawatha g-ash to exhibit less flow resistance (i.e., lower normalized drag) than the PRB g-ash. Of course, the higher ash content of the Hiawatha coal will result in heavier dustcakes, which will tend to offset the lower normalized drag. These effects will be discussed in more detail in the section on analysis of PCD pressure drop.

3.4.5 Chemical Composition of In situ Samples

Table 3.4.3 gives the chemical compositions of the TC09 in situ samples. The methods used for calculating these compositions from the elemental analyses have been described in previous reports. Like the physical properties, the chemical compositions do not indicate any significant differences between the air- and oxygen-blown g-ashes. As indicated earlier, the first sample had a higher concentration of CaS than any of the other samples. The first sample also had the lowest concentration of CaO. This result suggests that this first sample was more highly sulfidized than the other samples. This may explain why this sample also had an unusually low surface area compared to all of the other TC09 samples. The additional sulfidation would presumably block some of the pores and thereby reduce the internal surface area of the g-ash.

The following table compares the average compositions of the air- and oxygen-blown g-ashes produced in TC08 and TC09.

Component, wt percent	TC09 Air	TC09 Oxygen	TC08 Air	TC08 Oxygen
$CaCO_3$	1.30	0.96	4.41	4.20
CaS	0.59	0.51	1.03	0.36
CaO	5.03	3.82	8.75	7.33
Noncarbonate carbon	53.93	53.48	37.73	49.85
Inerts	39.15	41.24	48.08	38.27

As stated earlier, there does not appear to be any significant difference between the chemical compositions of the TC09 air-blown solids and the TC09 oxygen-blown solids. In terms of the main ingredients -- noncarbonate carbon and inerts (or ash) – the air- and oxygen-blown g-ashes produced in TC09 are essentially identical. As shown in the table above, however, this was not the case with the air- and oxygen-blown g-ashes produced from PRB coal in TC08. The TC08 air-blown g-ash contained less carbon (or more inerts) than did the TC08 oxygen-blown g-ash. In TC08, the coal-feed rate was generally higher during the oxygen-blown portion of the testing than during the air-blown portion, which might lead to speculation that the difference in g-ash composition is somehow related to the difference in coal-feed rate. Because of the higher ash content of the Hiawatha coal, the coal-feed rates that were used in TC09 were generally lower than those used in TC08 in order to avoid overloading the ash discharge system. In TC09, the coal-feed rates covered essentially the same range in both the air- and oxygen-blown modes

(2,300 to 3,100 lb/hr for all but two of the runs). For comparison, the coal-feed rates used in TC08 were about 2,900 to 4,400 lb/hr in air-blown operation and about 4,300 to 5,100 lb/hr in oxygen-blown mode. These differences in coal feed apparently do *not* explain the differences in chemical composition, however, because the bulk compositions are similar for TC09 air- and oxygen-blown and TC08 oxygen-blown, even though the coal-feed rate was substantially higher in the latter case. Apparently, the chemical composition of the g-ash is being influenced by other factors such as gasifier temperature, steam flow, residence time, etc. In any case, the differences in composition noted here are not believed to be significant in terms of their effect on the flow resistance of the g-ash. Flow resistance is probably more directly related to physical parameters such as morphology, surface area, and porosity.

3.4.6 Physical Properties of Dustcake Samples

Physical properties of the TC09 dustcake samples are compiled in Table 3.4-4, and the properties of the TC09 dustcake samples are compared to those of the TC09 in situ samples in the table below. This comparison is based on average in situ properties for both air- and oxygen-blown operation since there was no significant difference in the physical properties of the g-ash generated in the two modes of operation.

	TC09 In situ	TC09 Residual Dustcake	TC09 Transient + Residual
Bulk density, g/cc	0.24	0.24	0.22
Skeletal particle density, g/cc	2.2	2.1	2.1
Uncompacted bulk porosity, percent	89	89	89
Specific surface area, m^2/g	100	114	119
Mass-median diameter, μm	19	12	13

This comparison shows that the only substantial difference between the dustcake and the inlet g-ash is in the particle size. This difference could reflect the effects of fine particle enrichment in the dustcake or large particle removal or particle dropout ahead of the filter elements. The operating conditions in the last cleaning cycle before shutdown may also be different than the conditions measured with the in situ samples. Unfortunately, dustcake samples were not collected after TC08, because the TC08 dustcake was damaged by an oxygen excursion that occurred during shutdown. Therefore, it is not possible to present a comparison of the TC09 and TC08 dustcake properties. However, comparisons with earlier dustcake samples suggest that the TC09 dustcake had a much lower surface area than the dustcakes from PRB coal (110 to 120 m^2/g versus > 200 m^2/g) and a slightly larger mean particle size than the dustcakes from PRB coal (12 to 13 μm versus 9 to 11 μm). With all other factors being equal, the lower surface area and larger particle size would suggest that the Hiawatha dustcake should exhibit less flow resistance than the PRB dustcake. However, differences in dustcake areal loading must also be taken into consideration to understand the net effect on PCD ΔP. These effects will be discussed in more detail in the section on the analysis of PCD pressure drop.

3.4.7 Chemical Composition of Dustcake Samples

Table 3.4-5 summarizes the chemical compositions of the TC09 dustcake samples. These compositions were calculated from the elemental analyses using the same techniques that were applied to the in situ samples. The table below compares the average composition of the dustcakes to that of the in situ samples. Since the concentrations of the non-carbonate carbon and inerts did not vary substantially between the air-blown and the oxygen-blown samples, the table below gives average concentrations based on combining these two sets of data.

	TC09 In situ	TC09 Residual Dustcake	TC09 Transient + Residual
$CaCO_3$, Wt percent	1.1	3.1	0.2
CaS, Wt percent	0.6	1.6	1.5
Free Lime (CaO), Wt percent	4.5	2.7	5.0
Noncarbonate Carbon, Wt percent	53.7	52.3	54.9
Inerts (Ash/Sand), Wt percent	40.1	40.3	38.4

While this comparison shows considerable similarity in the major constituents (non-carbonate carbon and inerts), there is an obvious difference in the degree of sulfidation in the dustcakes versus the in situ samples. Based on the average compositions given above, the degree of sulfidation (expressed as the molar ratio of sulfur to calcium) is 0.084 in the incoming g-ash, 0.22 in the residual dustcake, and 0.19 in the entire cake (transient plus residual). These results suggest that the calcium present in the g-ash continues to capture a significant amount of H_2S after it is collected as a dustcake on the filter elements, and this additional sulfidation continues during the long-term exposure of the residual cake. This additional sulfidation apparently did not cause any significant degree of pore closure, since the dustcake samples had surface areas that were comparable to or even slightly greater than the surface areas of the incoming g-ash. The additional sulfidation has apparently had no significant effect on the physical properties of the dustcake, and, therefore, would not be expected to have a significant impact on dustcake flow resistance or drag.

3.4.8 Laboratory Measurements of Dustcake Drag

The drag of the TC09 g-ash was measured as a function of particle size using the RAPTOR system with various combinations of cyclones to adjust the particle-size distribution reaching the filter. Measurements were made on dust samples collected from the PCD hopper during stable operating periods for both air- and oxygen-blown operating periods. The measured drag as a function of particle size is shown in Figure 3.4-9, where it can be compared with data from all tests since GCT1. Rather than grouping the prior results by test program, in the TC08 report we established three natural groups of data indicated by the dashed lines on the figure. The three

groups represent: 1) PRB coal prior to the modification of the Transport Gasifier recycle loop, 2) PRB coal after the recycle loop modification, but before the LMZ was placed into service (GCT3, GCT4, TC06, and TC07-B), and 3) PRB coal with the new LMZ (TC07D and TC08). The TC09 data collected with the Hiawatha bituminous coal are represented by the solid circles. The air- and oxygen-blown results for TC09 are randomly mixed, indicating no difference between these two operating modes. The TC09 results fall generally in the region of the other data collected with the LMZ, roughly in the middle between the highest and lowest data sets. However, the Hiawatha results do seem to indicate a different slope or relationship between drag and particle size. The data represented by the squares on the figure are results from dust generated with the Alabama bituminous coal during TC07-C. Interestingly, the slope of the Alabama coal matches the Hiawatha suggesting that bituminous coals may produce different drag relationships than PRB coals.

3.4.9 Analysis of PCD Pressure Drop

In this section the flow resistance of the transient dustcake collected in the PCD during TC09 will be analyzed and compared to the drag measurements obtained in the laboratory with the RAPTOR device. This is a valuable comparison because mismatches between these two methods of determining drag can indicate that other factors (e.g., tar deposition, failsafe plugging, element blinding, etc.) may be influencing the filter ΔP. The normalized drag of the PCD transient dustcake was determined by using the same procedure described in previous reports. For each in situ particulate sampling run, the transient PCD drag during the run was determined from the rate of ΔP rise ($\Delta P/\Delta t$) during the run and the rate of g-ash accumulation in the transient cake. The latter was determined from the measured particulate loading and the syngas mass flow rate during the run.

The results of the calculations for TC09 are shown in Table 3.4-6. The PCD drag results are compared to the laboratory drag measurements in the rightmost two columns. The column labeled "PCD@RT" is the PCD drag value normalized to laboratory conditions using the ratio of the syngas viscosity at process temperature to the viscosity of air at laboratory room temperature. The RAPTOR drag value for each particulate sampling run was taken from Figure 3.4-9 using the MMD of each in situ g-ash sample. The RAPTOR and "PCD (@RT)" drag values are plotted in Figure 3.4-10 to graphically illustrate the good agreement of the values computed in Table 3.4-6.

From both Table 3.4-6 and Figure 3.4-10, it is apparent that there is excellent agreement between the PCD drag values and the RAPTOR drag values for 10 out of the 12 sampling runs. The two exceptions are Run Nos. 1 and 8. Run No. 1 was previously identified as an outlier in terms of both physical properties (much lower surface area than the other in situ samples) and chemistry (highest degree of sulfidation of any of the in situ samples). Therefore, Run No. 1 may be disregarded when comparing the lab and PCD drag values. Unlike Run No. 1, the sample from Run No. 8 appears to be typical of the other in situ samples in terms of both physical properties and chemistry. There were no indications of unstable coal feed or abnormal gasifier operations that could have affected Run No. 8, but it was the first sampling run conducted after the Transport Gasifier system was restarted following the outage between TC09B and TC09C. Even though there is no satisfactory explanation for the lack of agreement

on Run No. 8, the important point is that excellent agreement was achieved with 10 out of the remaining 11 runs (excluding Run No. 1).

The average drag values for the air- and oxygen-blown portions of the test are compared in the summary table below. While the average values given in Table 3.4-6 included all runs, the averages given below were calculated excluding Run No. 1 since it was an obvious outlier and had atypical physical properties and chemistry. Run No. 8 was included in the average even though it was an outlier because we could not identify anything unusual about the operating conditions or the properties of the sample.

	Drag, inWc/(lb/ft^2)/(ft/min)	
	Air-Blown	Oxygen-Blown
Average from PCD ΔP/Δt	28.1	22.5
Average from RAPTOR Data	23.4	22.9
Percent difference	18.3	1.8

The comparison of the average drag values again shows good agreement between the RAPTOR measurements and the PCD ΔP. Even with Run No. 8 included, the percent difference for the air-blown portion is acceptable (about 18 percent). If Run No. 8 were disregarded, this difference would shrink to 12 percent. In the oxygen-blown mode, the agreement is excellent (1.8 percent difference between RAPTOR and PCD drags). This comparison shows that the PCD performance calculations and the RAPTOR measurements agree well for both test conditions. It also indicates that the PCD operation agrees with the laboratory measurements that oxygen-blown operation was not significantly different from air-blown operation in terms of the flow resistance of the g-ash.

3.4.10 Conclusions

During TC09, the effects on the PCD of the Hiawatha bituminous coal were evaluated under both air- and oxygen-blown modes of operation. The main effect observed was a much higher PCD inlet particle concentration compared to that obtained with PRB coal in TC08. This result was expected based on the higher ash content and lower carbon conversion of the Hiawatha bituminous coal. During the oxygen-blown portion of TC09, the average solids carryover rate to the PCD was slightly lower than it was during the air-blown portion. This difference was a result of differences in the coal-feed rate and was not directly related to the type of oxidant (air or oxygen). In comparing the g-ash characteristics generated in the air- and oxygen-blown modes, no significant differences in particle-size distribution or other physical properties were noted.

Compared to PRB g-ash generated in previous tests, the Hiawatha g-ash contains a lower concentration of fine (<5-μm) particles and a much lower specific-surface area (typically about 110 m^2/g versus >200 m^2/g for PRB g-ash). With all other factors being equal, the lower concentration of fine particles and the lower surface area would suggest a lower drag.

The higher particle loading associated with the Hiawatha coal would be expected to produce a higher transient dustcake areal loading than has been observed in the past with PRB coal. However, the transient areal loading measured at the end of TC09 was actually lower than the transient areal loadings that have been measured with PRB coal in past runs. The relatively thin transient cake was attributed to the relatively low rate of solids carryover at the end of TC09 (only 390 lb/hr compared to a rate of about 600 lb/hr at the end of TC08). This difference in solids carryover was a direct result of differences in the coal-feed rate.

The physical properties and chemistry of the TC09 dustcakes were similar to those of the in situ samples, except that the size distributions of the dustcakes were finer. This difference in particle size between the in situ samples and the dustcakes has been observed in previous tests, and suggests that operating conditions at shutdown are not typical or that some large particles may be dropping out before they reach the filter elements. Nevertheless, the drag measurements made on the TC09 hopper samples resulted in a good correlation with the actual PCD ΔP. Drag measurements from previous tests have also confirmed that hopper samples give a good indication of PCD performance even though they may not be completely representative of the material that reaches the filter elements.

Measurements of drag as a function of particle size showed no significant difference between the air- and oxygen-blown g-ashes produced in TC09. As in previous tests, the TC09 drag versus particle-size data fell on a straight line when plotted on log-log coordinates. The trend line for the TC09 data was steeper than the trend lines for PRB g-ash and ran parallel to the trend line for the Alabama bituminous g-ash from TC07-C. This may suggest that the drag of bituminous g-ash is more sensitive to particle size than is the drag of PRB g-ash. Because of the different slopes of the Hiawatha and PRB trend lines, the two trend lines intersect at a mean particle size of about 5 μm. As a result of this effect, the normalized drag of the Hiawatha g-ash is actually lower than the normalized drag of the PRB g-ash at the mean particle size of the dust entering the PCD (about 18 μm). However, if the inlet particle-size distribution were made much finer (e.g., by increasing the cyclone efficiency), the drag measurements suggest that the Hiawatha g-ash may offer more flow resistance than does the PRB.

During TC09, three episodes of elevated outlet particle concentrations occurred in the absence of g-ash injection for failsafe testing. Two of the elevated measurements were obtained just after startup. The particle-size distributions suggested that the elevated loadings came from a PCD leak. Subsequent tests in the PCD cold flow model showed that some of the filter element types that were used in TC09 allowed some particle penetration, especially when the elements were new. Elements of the same type that had been used in previous runs did not allow as much particle penetration, suggesting that there is a "conditioning" effect similar to that observed with other types of "nonbarrier" filters. This may explain why the outlet loading was initially about 0.2 ppmw and then dropped to 0.1 ppmw or less after the first two measurements.

The outlet particle loading remained at or below 0.1 ppmw for the rest of TC09 with one exception. The one exception was a case of contamination of the outlet sampling filter with a yellow liquid, which was presumably some oil or tar-like substance that was driven off the coal. This oil/tar type of contamination should not be a problem for turbine operation, since the oil/tar would presumably be burned in the combustor upstream of the turbine.

During injection of g-ash upstream of the Ceramem and the Specific Surface failsafes, outlet particle concentrations of 0.46 and 0.45 ppmw were measured with the in situ sampling system. The results of the failsafe testing suggest that neither of the failsafes plugged completely, and it was later found that both failsafes had undergone some type of structural damage to their ceramic substrates. The damaged failsafes were returned to the suppliers for inspection and analysis of the damage, and the suppliers have recommended changes to the failsafe packaging to eliminate this problem in the future. The structural integrity and collection efficiency of the modified failsafes will be evaluated in future tests.

3.4.11 References

1. Sarofim, A.F., J.B. Howard, and A.S. Padia. "The Physical Transformations of Mineral Matter in Pulverized Coal under Simulated Combustion Conditions" Combustion Science and Technology. Vol. 16. pp. 187-204. 1977.

Table 3.4-1 PCD Inlet and Outlet Particulate Measurements From TC09

Test Date	PCD Inlet					PCD Outlet				
	SRI Run No.	Start Time	End Time	Particle Loading, ppmw	Mass Rate, lb/hr	SRI Run No.	Start Time	End Time	H_2O Vapor, vol. %	Particle Loading, ppmw
Air-Blown										
9/05/02	1	9:15	9:30	42,400	965	1	9:00	13:00	12.3	0.23
9/10/02	2	8:55	9:10	32,000	855	2	8:40	10:40	30.3	0.22
9/11/02	3	10:15	10:30	22,000	471	3	10:00	14:00	22.9	0.11
9/12/02	4	10:30	10:45	24,600	525	4	9:00	13:00	25.6	< 0.10
9/13/02	5	10:10	10:25	25,000	533	5	10:00	14:07	24.4	0.23 (1)
9/14/02	6	9:30	9:45	24,700	513	6	8:30	12:30	21.3	< 0.10
9/16/02	7	11:15	11:25	42,200	901	7	9:00	13:00	18.5	0.10
9/22/02	8	8:45	9:00	24,400	546	8	8:30	12:30	14.8	0.12
Average				29,700	664	Average			21.3	< 0.1 (2)
Standard Deviation				8,300	205	Standard Deviation			5.9	
Oxygen-Blown										
9/23/02	9	9:15	9:30	39,700	594	9	8:30	12:30	38.5	< 0.10
9/24/02	10	11:00	11:15	36,500	504	10	10:50	12:50	38.6	0.46 (3)
9/25/02	11	9:30	9:45	37,100	546	11	8:30	10:30	34.5	< 0.10
9/25/02	--	--	--	--	--	12	13:30	15:30	33.8	0.10
9/26/02	12	9:30	9:45	26,900	390	13	8:50	10:50	32.2	0.45 (4)
Average				35,100	509	Average			35.5	< 0.1 (5)
Standard Deviation				5,600	87	Standard Deviation			2.9	
Air-Blown										
9/26/02	--	--	--	--	--	14	13:45	14:45	12.4	0.31 (6)

1. Filter contaminated with light yellow liquid (tar).
2. Outlet Runs 1, 2, and 5 excluded from average.
3. Ceramem failsafe injection test.
4. Specific Surface failsafe injection test.
5. Outlet Runs 10 and 13 excluded from average due to bias from failsafe testing.
6. Dust injection into PCD outlet piping to check PCME.

Table 3.4-2 Physical Properties of TC09 In situ Samples

Date	SRI Run No.	Bulk Density, g/cm^3	True Density, g/cm^3	Uncompacted Bulk Porosity, %	Specific Surface Area, m^2/g	Mass-Median Diameter, μm
Air-Blown						
9/05/02	1	0.29	2.17	86.6	49	18.7
9/10/02	2	0.33	2.25	85.3	80	16.4
9/11/02	3	0.20	2.42	91.7	101	20.4
9/12/02	4	0.23	2.25	89.8	85	19.1
9/13/02	5	0.21	2.21	90.5	93	19.0
9/14/02	6	0.22	2.22	90.1	98	20.1
9/16/02	7	0.18	2.22	91.9	116	18.7
9/22/02	8	0.25	2.23	88.8	88	19.7
Average		0.24	2.25	89.3	89	19.0
Composite Hopper Sample Used for RAPTOR Drag Measurements						
9/14/02	N/A	0.30	2.25	86.7	55	19.6
Oxygen-Blown						
9/23/02	9	0.24	2.20	89.1	90	20.4
9/24/02	10	0.25	2.18	88.5	98	19.6
9/25/02	11	0.22	2.22	90.1	105	19.1
9/26/02	12	0.20	2.16	90.7	149	18.2
Average		0.23	2.19	89.6	111	19.3
Composite Hopper Sample Used for RAPTOR Drag Measurements						
9/25/02	N/A	0.30	2.21	86.4	77	20.0

Table 3.4-3 Chemical Composition of TC09 In situ Samples

Date	SRI Run No.	$CaCO_3$, Wt %	CaS, Wt %	Free Lime (CaO), Wt %	Non-Carbonate Carbon, Wt %	Inerts (Ash/ Sand), Wt %
Air-Blown						
9/05/02	1	1.41	0.98	2.65	59.02	35.94
9/10/02	2	1.16	0.36	5.78	47.66	45.04
9/11/02	3	1.84	0.53	5.65	51.39	40.59
9/12/02	4	1.05	0.49	6.17	50.58	41.71
9/13/02	5	2.09	0.51	5.10	54.44	37.86
9/14/02	6	1.75	0.49	5.88	54.93	36.96
9/16/02	7	0.82	0.71	4.92	59.49	34.06
9/22/02	8	0.25	0.67	4.07	53.94	41.08
Average		1.30	0.59	5.03	53.93	39.15
Composite Hopper Sample Used for RAPTOR Drag Measurements						
9/14/02	N/A	1.36	0.40	6.10	44.10	48.04
Oxygen-Blown						
9/23/02	9	0.48	0.47	4.98	50.14	43.94
9/24/02	10	2.30	0.49	3.10	48.18	45.93
9/25/02	11	0.70	0.51	3.60	55.47	39.72
9/26/02	12	0.36	0.56	3.59	60.12	35.37
Average		0.96	0.51	3.82	53.48	41.24
Composite Hopper Sample Used for RAPTOR Drag Measurements						
9/25/02	N/A	0.59	0.42	4.47	49.34	45.18

Table 3.4-4 Physical Properties of TC09 Dustcake Samples

Plenum	Type of Sample	Bulk Density, g/cm^3	True Density, g/cm^3	Uncompacted Bulk Porosity, %	Specific Surface Area, m^2/g	Mass-Median Diameter, μm
Top	Entire Dustcake (Transient plus residual)	0.22	2.09	89.5	119	13.1
Bottom	Residual Dustcake Only	0.24	2.12	88.7	114	12.4
Bottom	Thicker Patch (Residual plus Some Transient)	0.17	2.12	92.0	94	13.9

Table 3.4-5 Chemical Composition of TC09 Dustcake Samples

Plenum	Type of Sample	$CaCO_3$, Wt %	CaS, Wt %	Free Lime (CaO), Wt %	Non-Carbonate Carbon, Wt %	Inerts (Ash/ Sand), Wt %
Top	Entire Dustcake (Transient plus residual)	0.16	1.53	5.00	54.92	38.39
Bottom	Residual Dustcake Only	3.11	1.56	2.70	52.29	40.34
Bottom	Thicker Patch (Residual plus Some Transient)	6.16	1.53	2.51	47.43	42.37

Table 3.4-6 TC09 Transient Drag Determined From PCD ΔP and from RAPTOR

Run No.	ΔP/Δt, inwc/min	Δ(AL)/Δt, lb/min/ft^2	FV, ft/min	MMD, μm	Drag, inwc/(lb/ft^2)/(ft/min)		
					PCD	PCD@RT	RAPTOR
Air-Blown							
1	23.7	0.063	3.51	18.7	107.0	60.9	23.8
2	11.6	0.056	4.32	16.4	48.1	26.6	28.2
3	5.2	0.031	3.49	20.4	48.5	26.5	21.3
4	5.5	0.034	3.42	19.1	46.4	25.6	23.2
5	5.9	0.035	3.48	19.0	48.2	26.4	23.3
6	5.3	0.034	3.31	20.1	47.7	26.5	21.7
7	9.6	0.059	3.36	18.7	48.2	27.0	23.8
8	7.7	0.036	3.26	19.7	66.5	38.4	22.2
Avg	9.3	0.044	3.52	19.6	57.6	32.2	23.4
Oxygen-Blown							
9	4.1	0.039	2.93	20.4	35.7	20.8	21.3
10	2.3	0.033	2.48	19.6	27.8	16.5	22.4
11	3.8	0.036	2.64	19.1	40.3	24.1	23.2
12	3.2	0.026	2.61	18.2	47.9	28.5	24.7
Avg	3.4	0.034	2.67	19.3	37.9	22.5	22.9

1. ΔP/Δt = rate of PCD pressure drop rise during particulate sampling run, inwc/min.
2. Δ(AL)/Δt = rate of increase in dustcake areal loading during sampling run, lb/ft^2/min.
3. FV = average PCD face velocity during sampling run, ft/min.
4. MMD = mass-median diameter of in situ particulate sample, μm.
5. RT = room temperature air, 77°F (25°C).
6. RAPTOR = resuspended ash permeability tester.

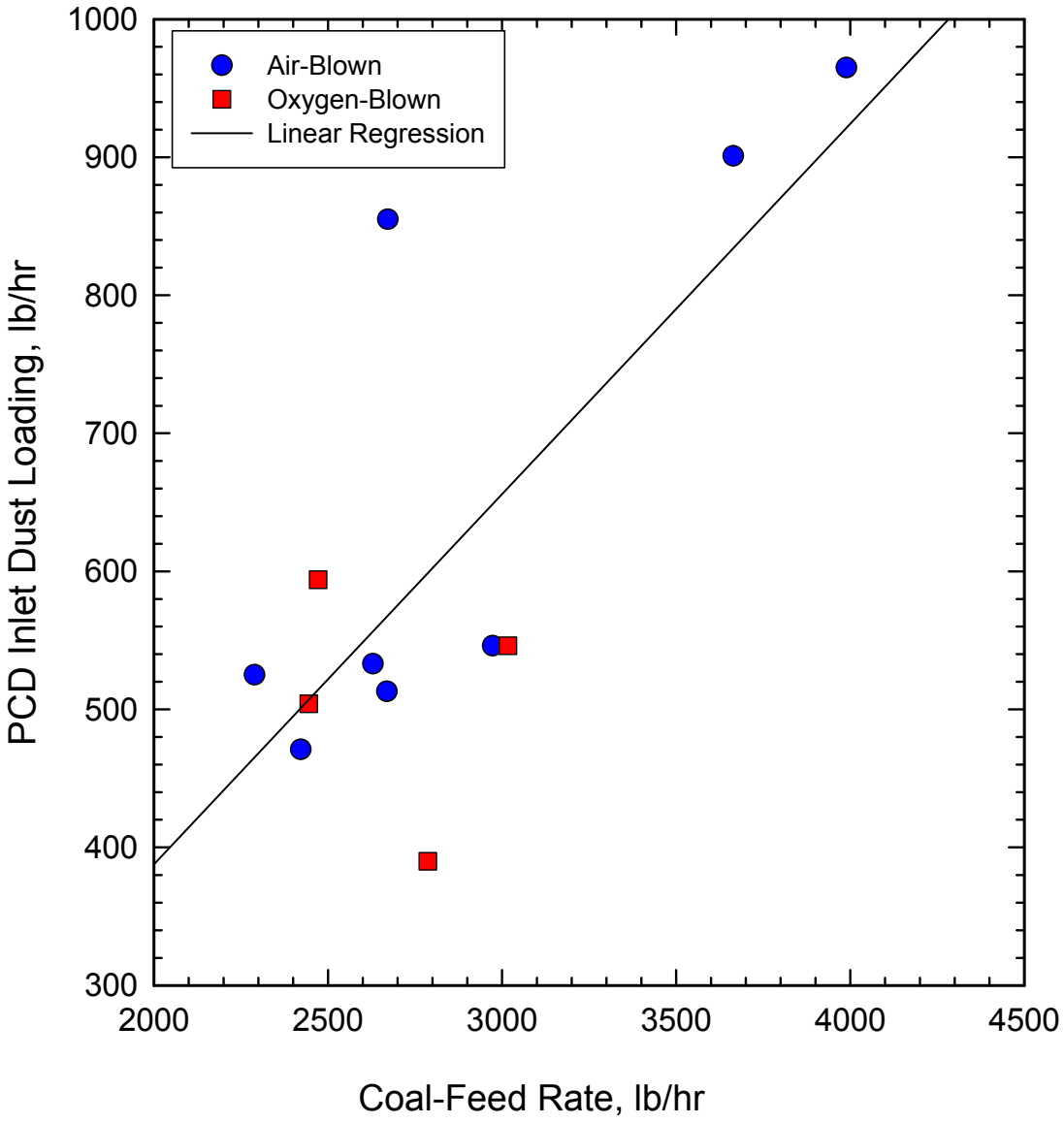

Figure 3.4-1 PCD Inlet Loadings as a Function of Coal-Feed Rate

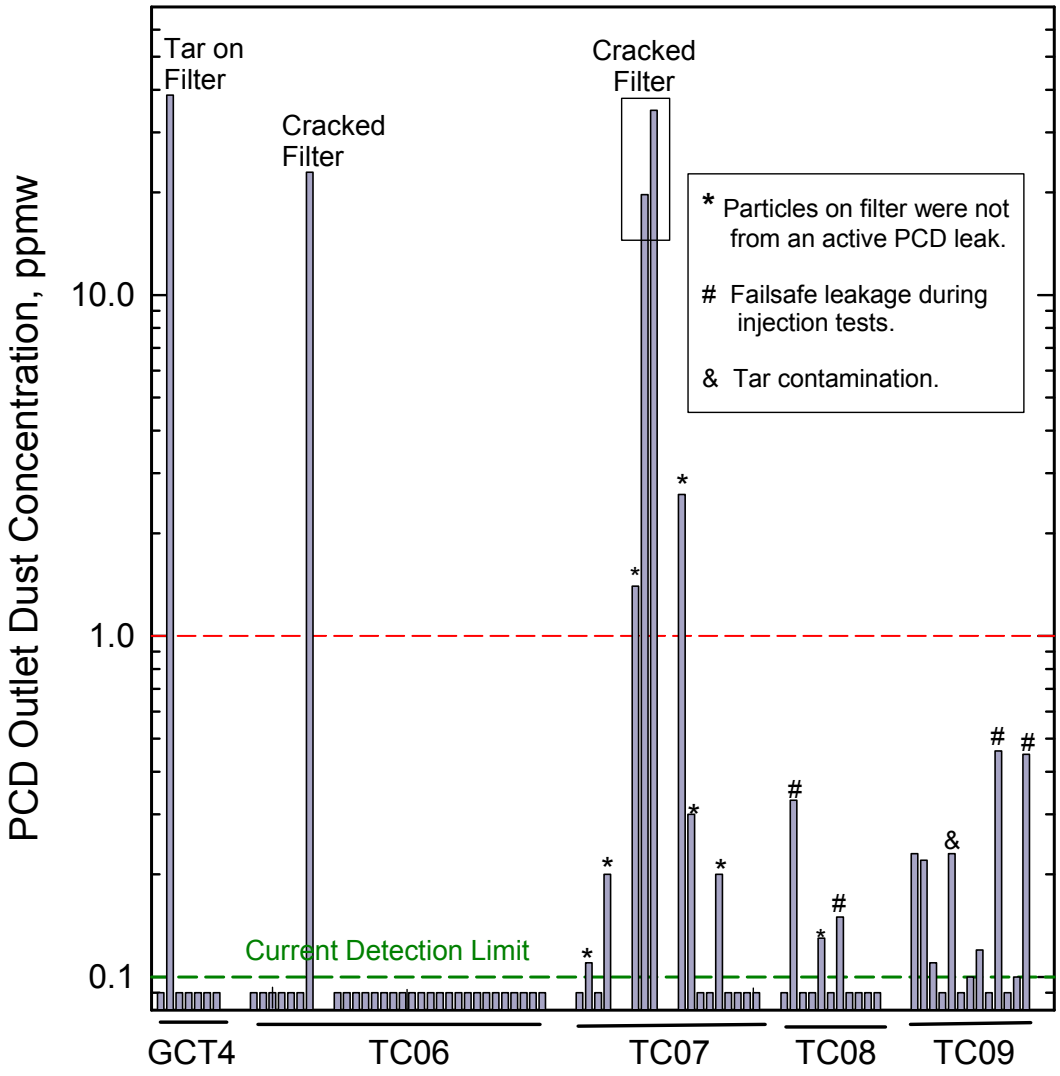

Figure 3.4-2 PCD Outlet Emissions for Recent Test Programs

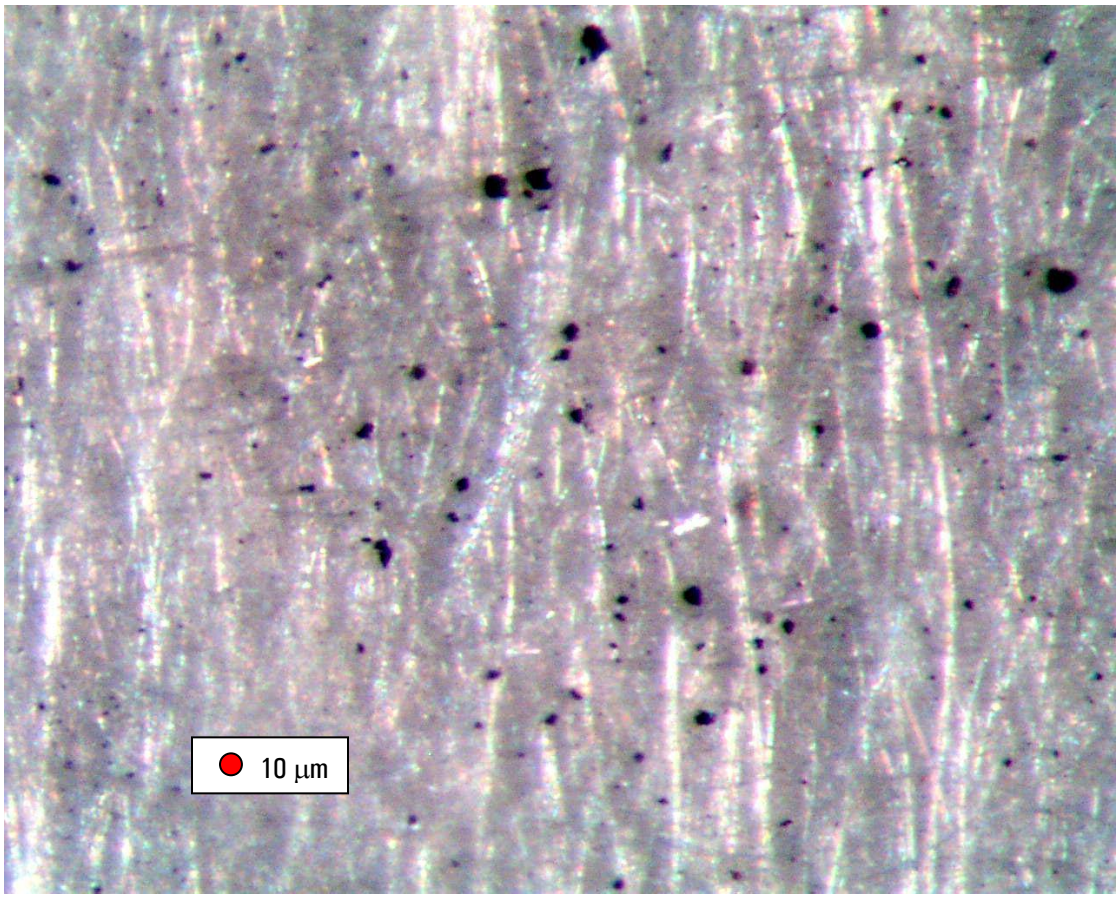

Figure 3.4-3 Optical Photograph of Particles Collected During Outlet Run 12

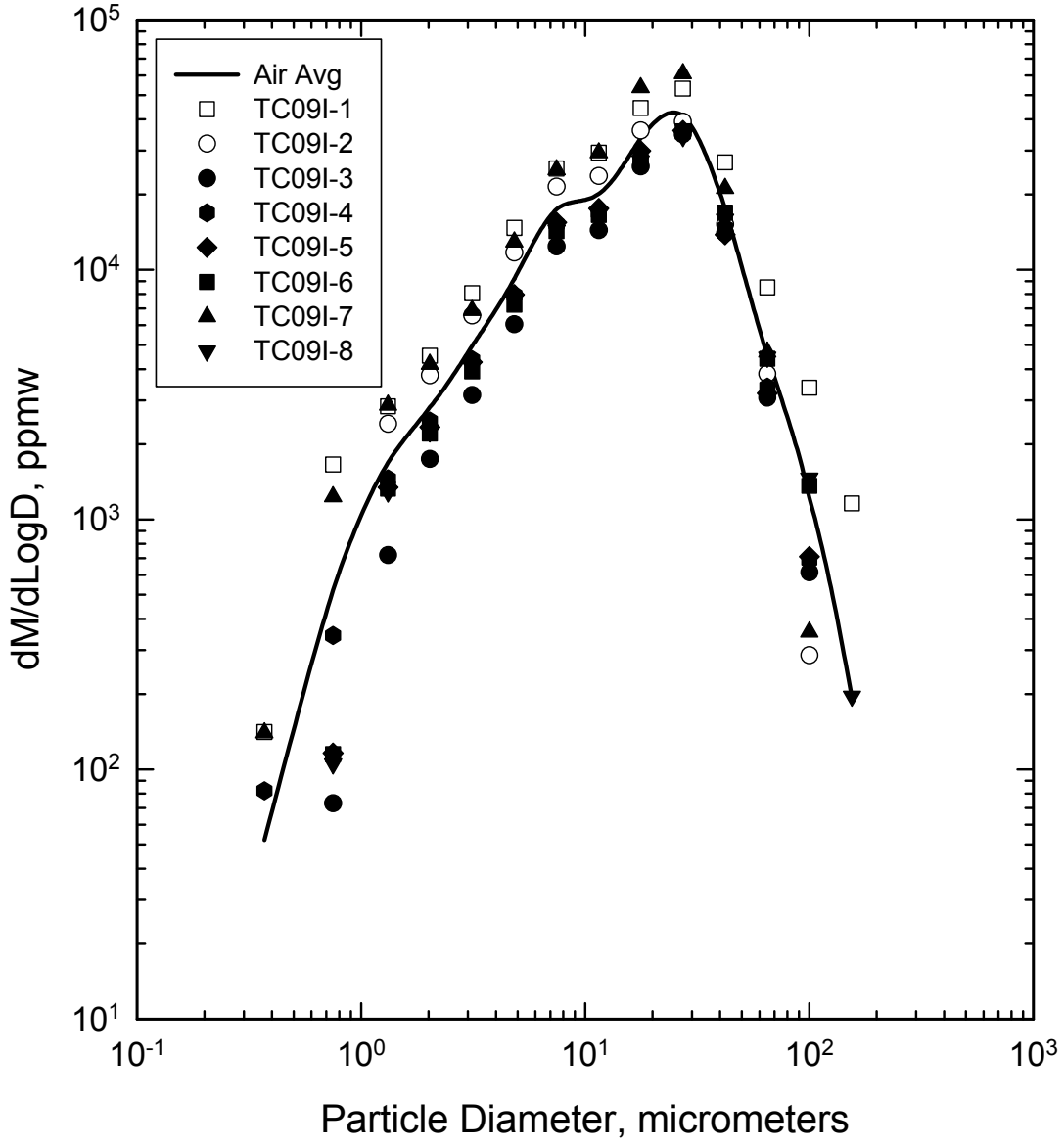

Figure 3.4-4 Particle-Size Distribution Measured During Air-Blown Operation

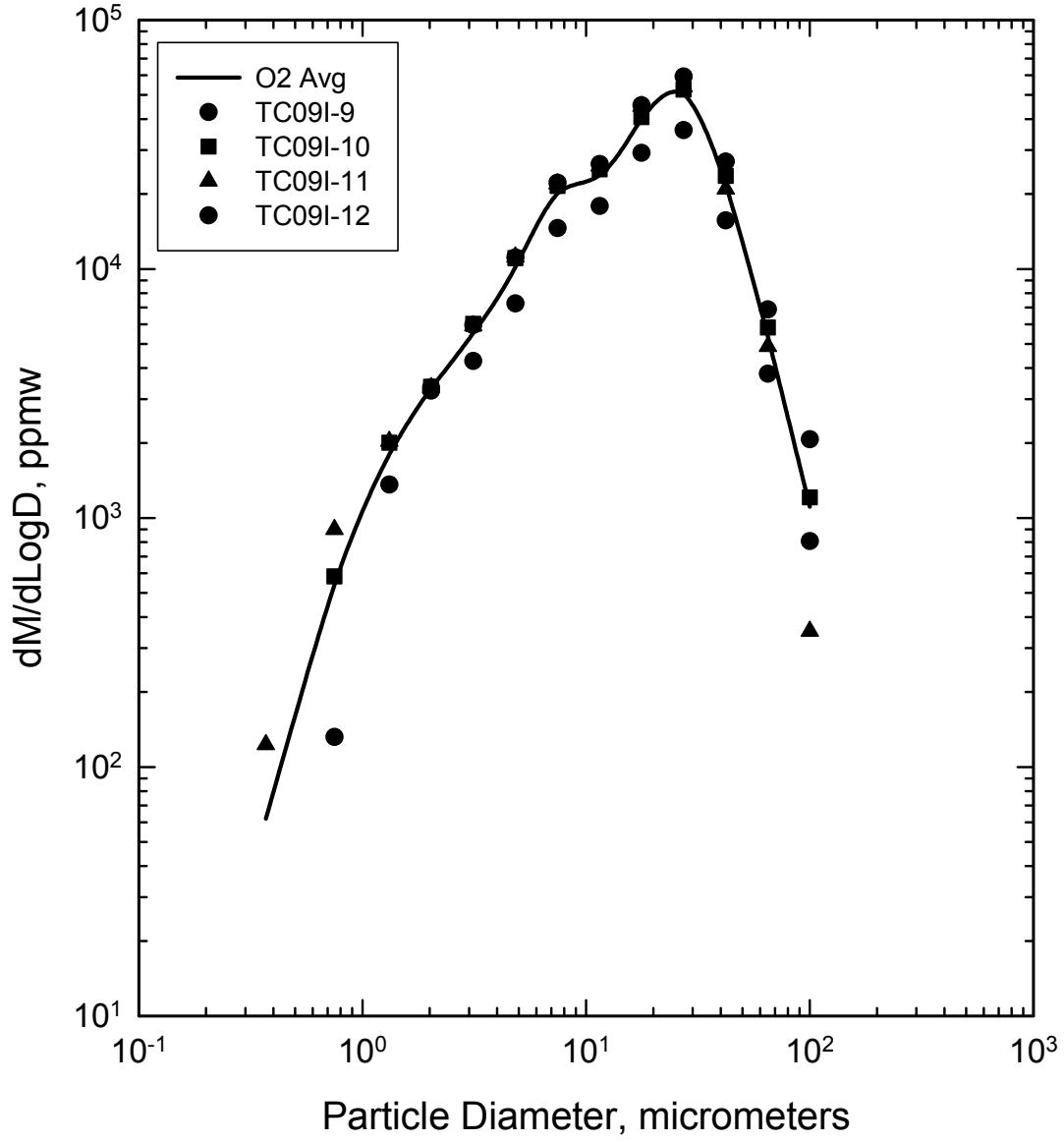

Figure 3.4-5 Particle-Size Distribution Measured During Oxygen-Blown Operation

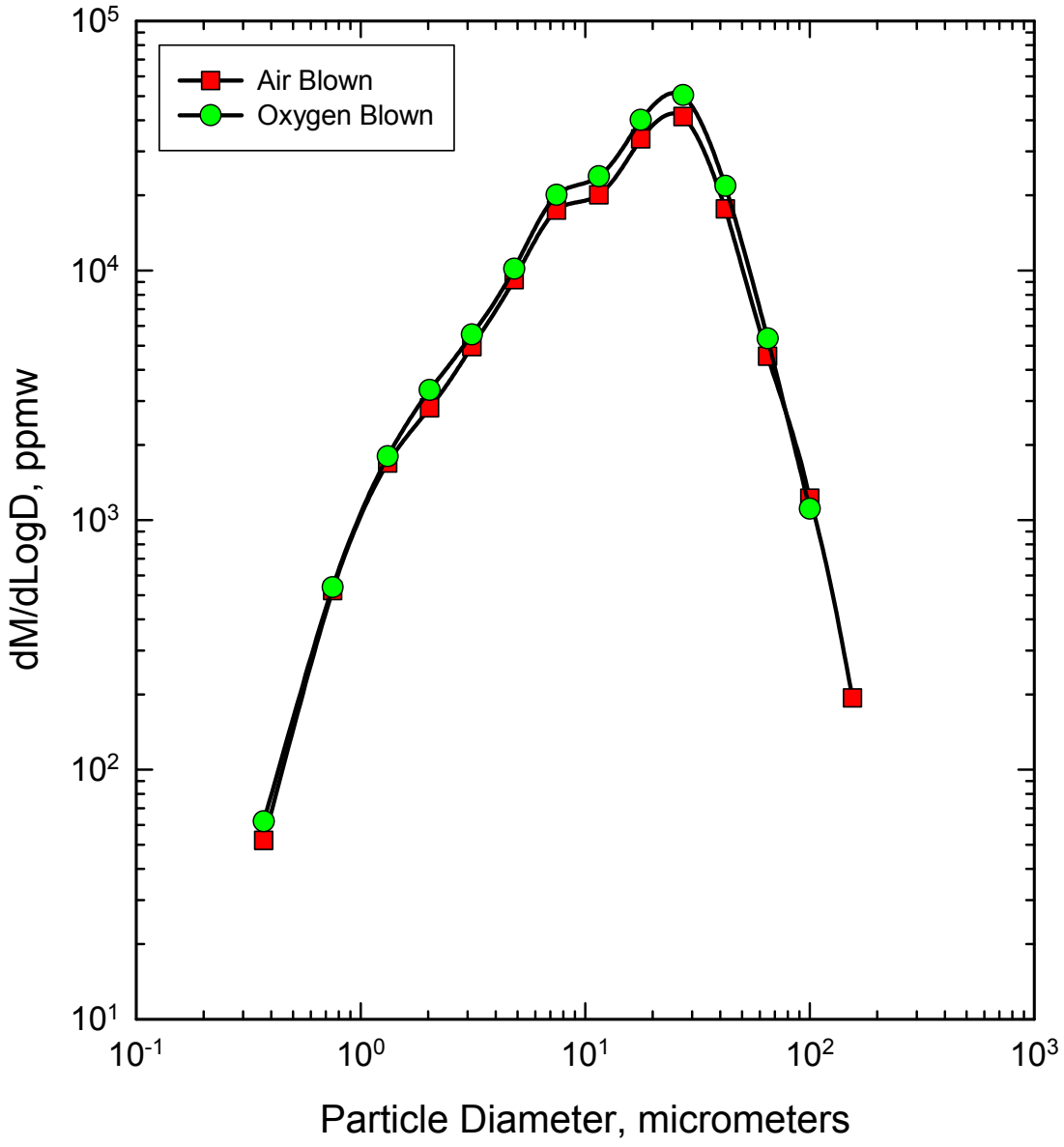

Figure 3.4-6 Comparison of Particle-Size Distributions on Actual Mass Basis

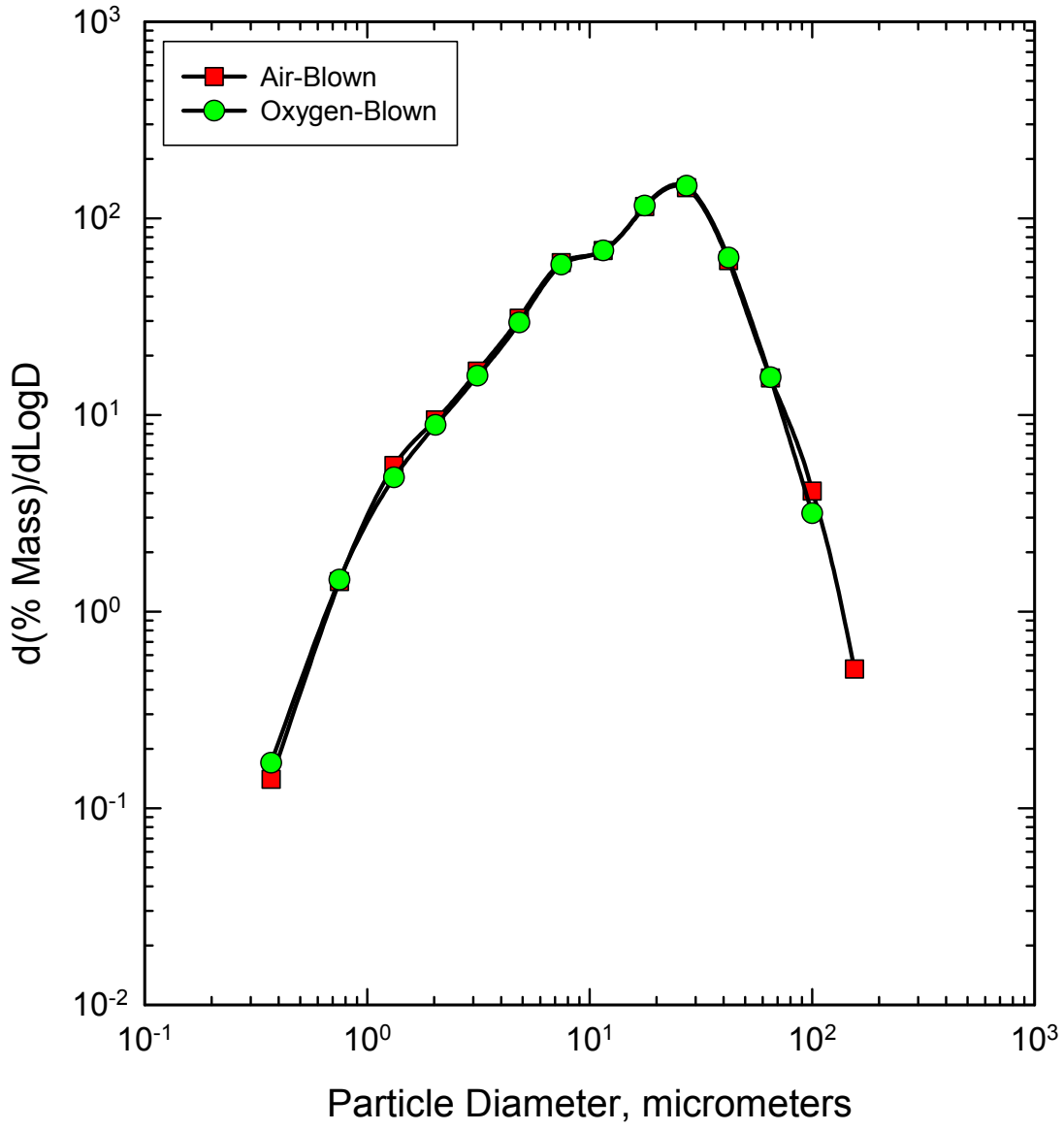

Figure 3.4-7 Comparison of Particle-Size Distributions on Percent Mass Basis

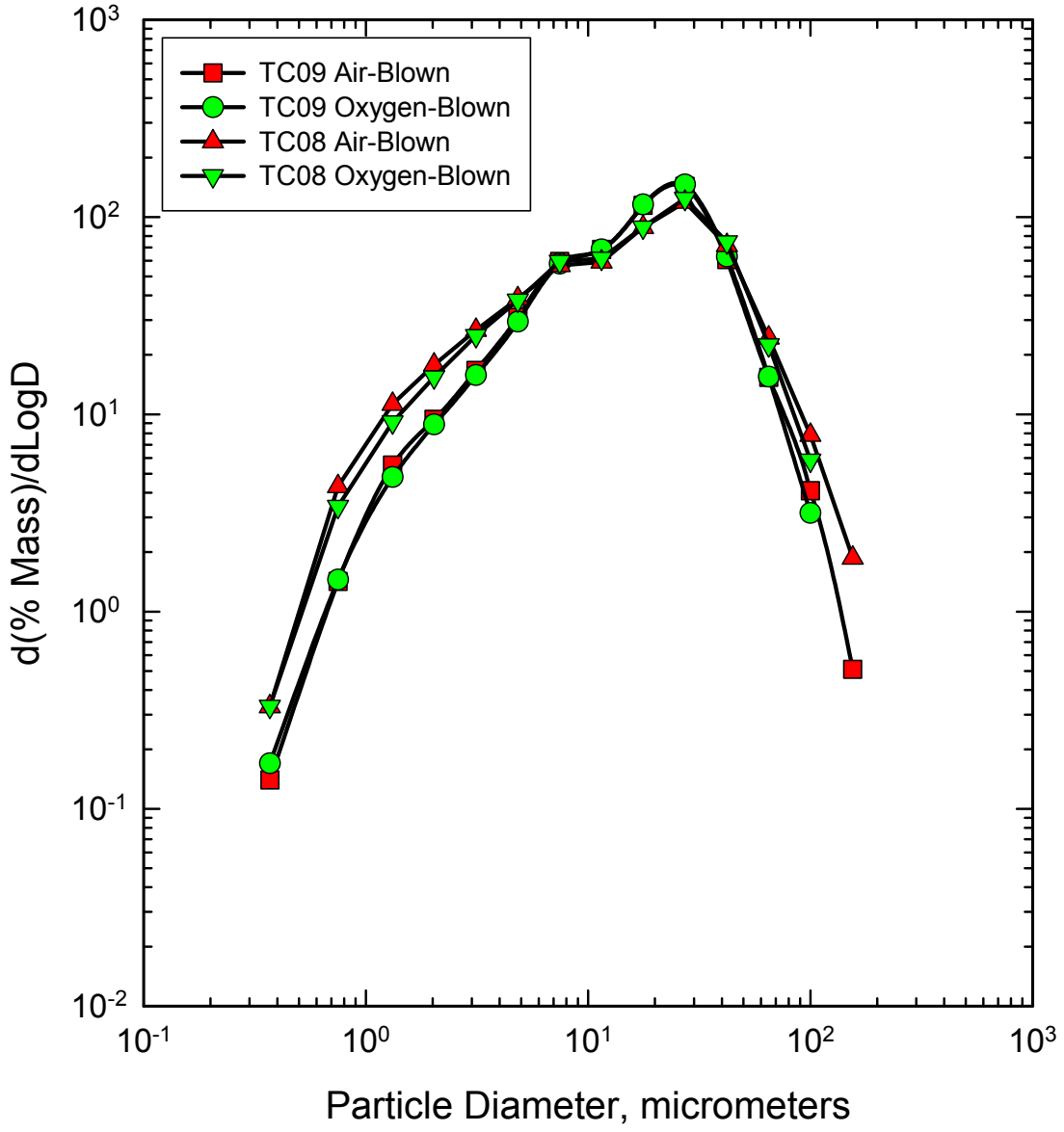

Figure 3.4-8 Comparison of Hiawatha and PRB Particle-Size Distributions

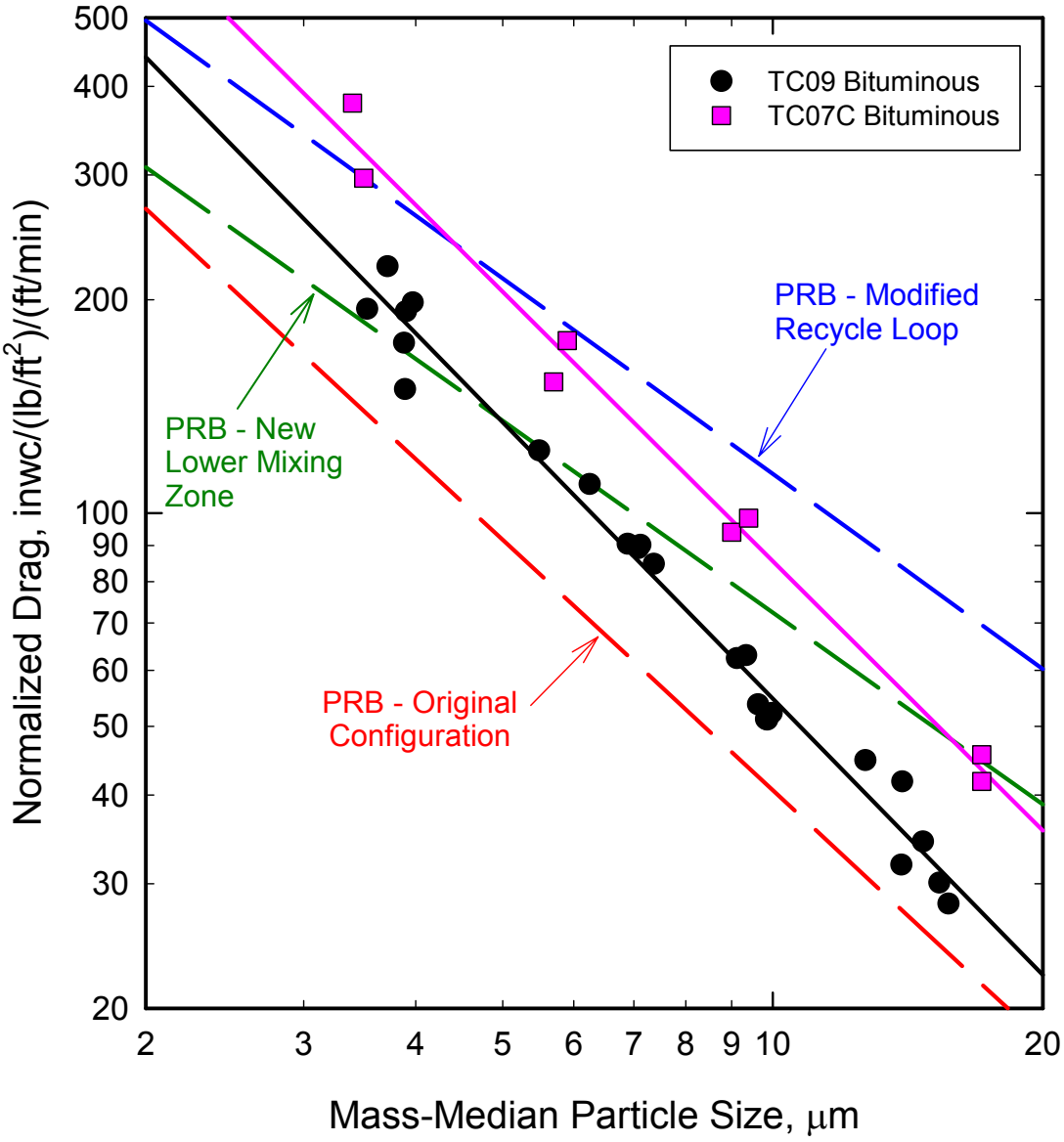

Figure 3.4-9 Effect of Particle Size on Dustcake Drag

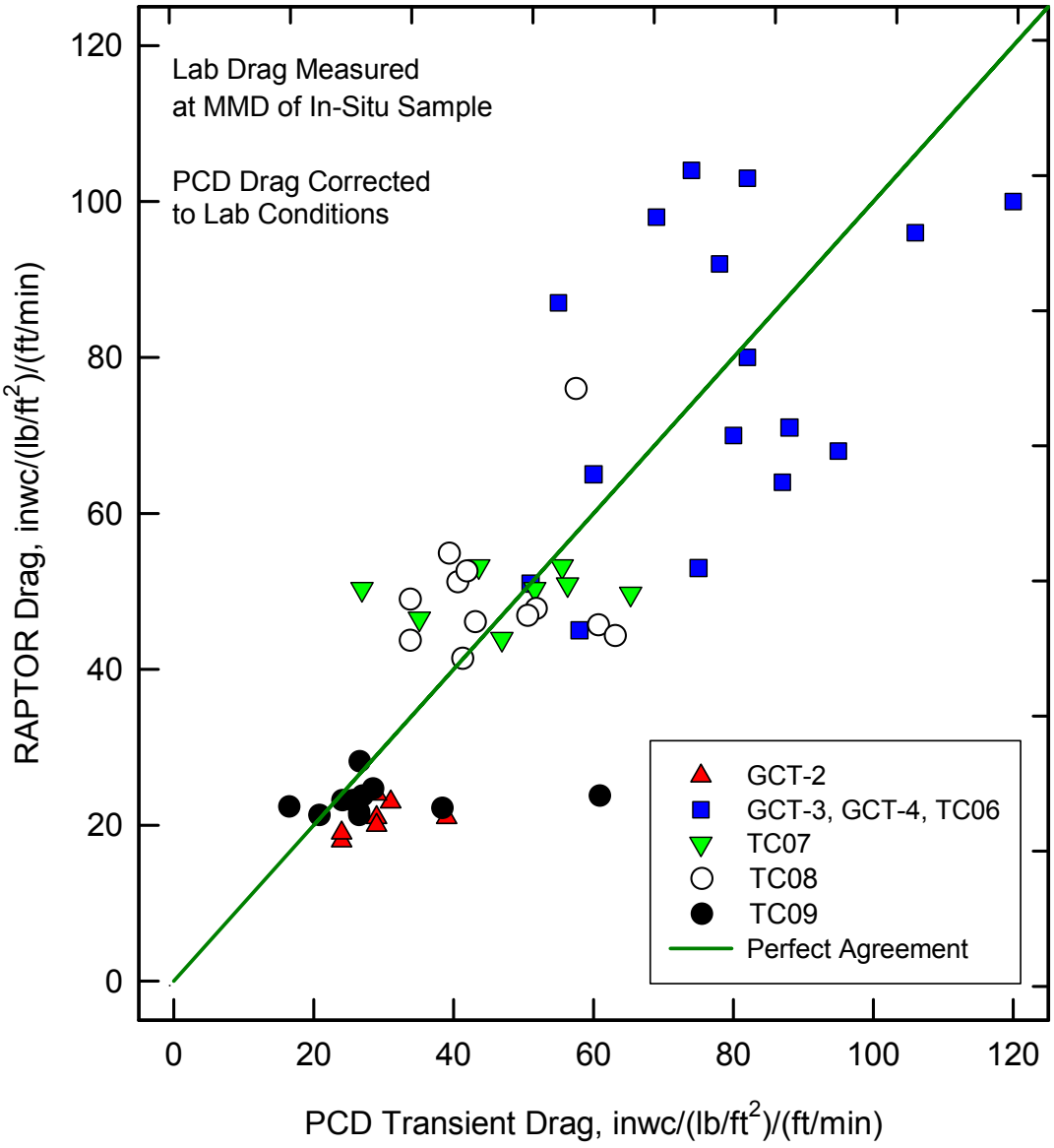

Figure 3.4-10 Comparison of PCD Drag With Laboratory Measurements

3.5 TC09 FAILSAFE INJECTION TEST

3.5.1 Introduction

One of the main objectives of the PSDF is to improve the commercial readiness of high temperature, high pressure (HTHP) gas filtration technology. HTHP gas filtration systems have established that they can achieve high collection efficiencies during stable operations; however, process upsets can cause filter element failure resulting in an outlet loading that exceeds turbine requirements. In order to reduce the risk of an unscheduled shutdown due to filter failure, a reliable failsafe device is required. The failsafe device acts as a safeguard by mechanically closing or plugging in the event of a filter element failure. Currently, a successful failsafe has not been identified; therefore, the PSDF has established a failsafe testing program to identify failsafe devices that will protect the downstream turbine while screening out poor performing failsafes. This program was developed to allow testing and performance comparison of different failsafe devices under comparable testing conditions (refer to TC08 Run Report Section 3.5 for PSDF Failsafe Test Criteria, Plan, and Setup).

3.5.2 TC09 Solids Injection Test

During TC08, two prototype ceramic failsafe devices supplied by SWPC were tested. The failsafe devices were constructed of silicon carbide honeycomb filter. The ceramic material was contained in a stainless steel housing. Two different suppliers, Specific Surface and CeraMem, provided the silicon carbide material. During TC08, these failsafe devices were installed in the tube sheet and exposed to actual operating conditions, which included back-pulsing. Both of the failsafe devices were inspected, and no evidence of damage was noticed. Therefore, it was decided to do further testing on the ceramic failsafes during TC09. During TC09, eight CeraMem and two Specific Surface ceramic failsafe devices were installed into the PCD. The collection efficiency of two ceramic failsafe devices (one CeraMem and one Specific Surface) was tested during TC09 as well.

The CeraMem failsafe was tested on September 24, 2002, with g-ash injection starting at 10:17 and continuing until 14:31. The pressure drop measurements that were recorded during the entire first injection test are shown in Figure 3.5-1. The failsafe pressure drop increased slowly from an initial value of less than 1 inH_2O to about 8 inH_2O over a period of about 4 hours. The rate of increase was much slower than was observed during injection testing of the PSDF-designed failsafe and the Pall fuse during TC08. The difference was attributed to the much larger filtration surface area of the ceramic failsafe compared to the PSDF-designed failsafe and Pall fuse. The ceramic failsafe devices have approximately five times the filtration area of the metal failsafe devices. During the CeraMem failsafe test, an outlet loading test was conducted from 10:50 until 12:50. The PCD outlet loading measured by SRI was 0.46 ppmw.

After the injection test, a baseline outlet loading test was conducted on September 25, 2002, to verify that there were no solids present in the outlet duct of the PCD. The outlet loading measured by SRI was below their detection limit, so it was decided to proceed with the Specific Surface injection test on September 26, 2002.

G-ash injection into the Specific Surface failsafe device started at 08:23 on September 26, 2002, and continued until 10:50. The pressure drop measurements that were recorded during the Specific Surface injection test are shown in Figure 3.5-2. The failsafe pressure drop increased by less than 2 inH_2O during the 2.5-hour injection test. An outlet loading test was conducted from 08:50 until 10:50. The PCD outlet loading measured by SRI was 0.45 ppmw.

In addition to meeting turbine inlet loading requirements, a failsafe device must be able to maintain its structural integrity in a gasification environment. Therefore, all the ceramic failsafe devices installed during TC09 were removed and inspected for failures.

During the outage, two Specific Surface ceramic failsafe devices were removed and inspected. One failsafe was exposed to the injection test (designated SS SiC-2), while the other was exposed to gas only exposure (designated SS SiC-1). SS SiC-1 was in much worse shape than the failsafe from the injection test. The silicon carbide material in SS SiC-1 was severely damaged (see Figure 3.3-10). Inspection of SS SiC-2 revealed that some of the ceramic material on the top surface was missing. This could explain why the Specific Surface failsafe had a higher outlet loading than the PSDF-designed failsafe or Pall fuse (see TC08 Run Report for results of PSDF-designed failsafe and Pall Fuse solids injection tests). According to SWPC, it appeared that the damage could have been due to chemical attack; however, silicon carbide filter elements have been tested before and during gasification at the PSDF without any signs of chemical attack. Therefore, it is possible that the structural design of the Specific Surface failsafe needs further development. The current design may not be able to handle the repeated thermal and mechanical stresses imposed on it during a back-pulse event.

Eight CeraMem ceramic failsafe devices were removed and inspected. One failsafe was exposed to the g-ash injection test, while the other seven were exposed to gas only. The CeraMem failsafe used during the g-ash injection test had some ceramic material missing from the top surface. This could explain why the CeraMem failsafe had a higher outlet loading than the PSDF-designed failsafe or Pall Fuse. The other seven failsafe devices were removed for inspection. These seven failsafe devices did not reveal any apparent damage. These failsafe devices were sent back to SWPC Science and Technology Center for further evaluation. SWPC cut one of the CeraMem failsafe devices apart, and did not notice any interior damage. CeraMem is planning on repackaging the ceramic material in the stainless steel housing to offer more support.

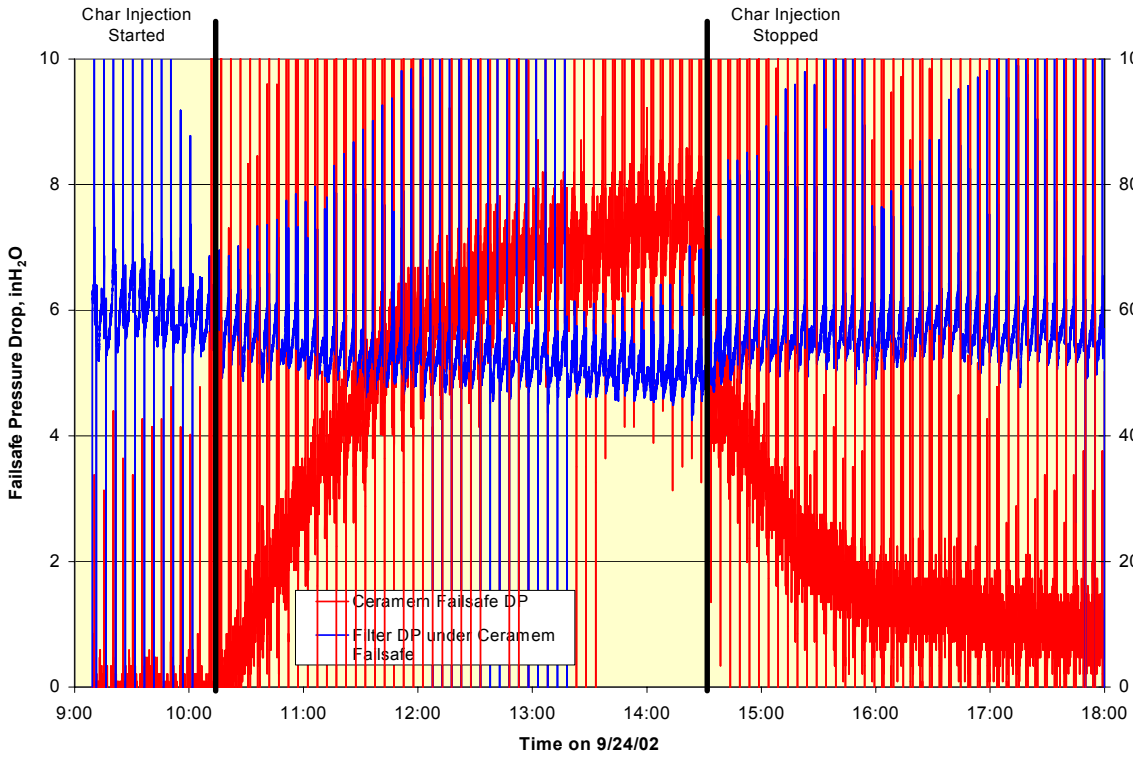

Figure 3.5-1 Failsafe and Filter Pressure Drop During CeraMem Injection Test on September 24, 2002

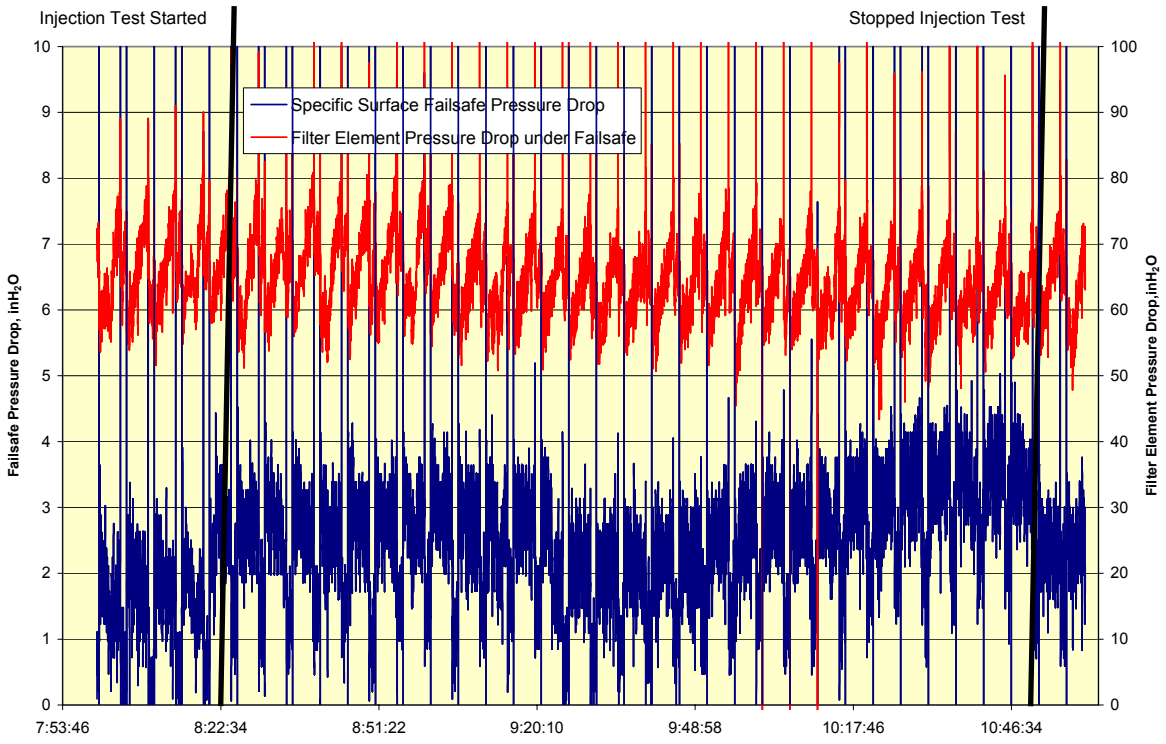

Figure 3.5-2 Failsafe and Filter Pressure Drop During Specific Surface Injection Test on September 26, 2002

4.0 TRANSPORT GASIFIER

4.1 TRANSPORT GASIFIER OPERATIONS

4.1.1 TC09 Run Summary

Test Run TC09 began on September 3, 2002, with the startup of main air compressor and lighting of the start-up burner, and ended on September 26. The test run had two interruptions in service: the first between September 6 and 7 to inspect for possible gasification ash (g-ash) bridging in the Particulate Control Device (PCD), and the second between September 17 and September 19 to inspect the PCD and gasifier interiors before attempting oxygen-blown operations. During the test run, the gasifier temperature was varied between 1,725 and 1,825 °F at pressures from 125 to 270 psig.

During TC09, the gasifier successfully operated with bituminous coal from the Sufco mine in Utah gasifying over 396 tons of coal. Over 300 hours of coal feed, almost 80 hours of which were in oxygen-blown operation, were accumulated. Sorbent was not used during the run.

Primary objectives of test run TC09 were as follows:

- Bituminous Coal Operation – Evaluate gasifier and PCD operations and performance using a bituminous coal and determine the optimum coal-feed rates, system pressures, temperatures, and steam-flow rate for stable operation.
- Operational Stability – Characterize gasifier loop and PCD operations for commercial performance with long-term tests by maintaining a near-constant coal-feed rate, air/coal ratio, riser velocity, solids circulation rate, system pressure, and air distribution.

Secondary objectives included the following:

- Gasifier Operations – Study the devolatilization and tar cracking effects from transient conditions during the transition from start-up burner to coke breeze to coal. Evaluate the effect of process operations on heat release, heat transfer and accelerated fuel particle heatup rates. Study the effect of changes in gasifier conditions on transient temperature profiles, pressure balance and product gas composition. Observe performance of new gasifier temperature and coal-feed rate controllers.
- Effects of Gasifier Conditions on Syngas Composition – Evaluate the effect of air distribution, steam/coal ratio, solids circulation rate and gasifier temperature on synthesis gas Lower Heating Value (LHV), carbon conversion, and cold and hot gas efficiencies.
- New Steam System Commissioning – Verify the proper operation of the new upper mixing zone (UMZ) steam system, including steam shrouds for two coal feeders, the UMZ steam nozzles, and the steam to the UMZ air nozzles.

- Fluidized Bed Feeder Commissioning – Use the fluidized-bed feeder for adding sand to the gasifier. Evaluate potential issues with using as a coal feeder.
- Standpipe Operations – Determine the causes of bubble formation and packing in the standpipe to eliminate future occurrences.

Outage activities preceding test run TC09 included 26 equipment revisions. Those revisions that most affected the process are listed below:

- Improving the steam system to ensure high steam-flow rates at high temperatures to the UMZ steam nozzles, the coal feeder shrouds, and adding the capability to mix steam with air in the UMZ air nozzles.
- Creating the ability to feed coke breeze through the FD0220 sorbent feeder to ensure a stable fuel supply in the event of a FD0210 coal feeder trip.
- Modifying the standpipe screw cooler to prevent heat transfer fluid (HTF) leaks.
- Installing a batch syngas trace metals sampling system.

A summary of the events that occurred in TC09 is shown below:

The main air compressor was started on September 3, 2002, to begin test run TC09. Before lighting the start-up burner, the sulfator (atmospheric fluidized-bed combustor – AFBC) air compressor discharge pressure was too high, and the air flow to the AFBC was restricted, indicating the AFBC air distributor had plugged. By using higher pressure air from the main air compressor through the AFBC air lines, operations dislodged the material, and the AFBC air flow returned to normal. After the main air compressor was lined back to the gasifier, the start-up burner preheated the system, while the sorbent feeder charged the gasifier with sand. To bring the gasifier from 1,200°F (the maximum temperature attainable by the start-up burner) to an optimum gasifier temperature above the tar dewpoint, coke breeze was introduced as a start-up fuel on September 4. Later that day, once the gasifier had reached 1,650°F, coal feed began, coke breeze was stopped, and the start-up burner was tripped.

As the gasifier pressure was being increased shortly after starting coal feed, a standpipe bubble occurred. Coal feed was stopped until the gasifier stabilized, then resumed once the bubble dissipated. That night the gasifier ran at moderately low temperatures of around 1,700°F to reduce the chance of forming deposits. The pressure was around 200 psig.

The next morning the PCD cone began to fill with solids, and, based on both the PCME and the thermocouples, it was suspected that g-ash was bridging between the filter elements. The PCD cone was fluffed and the gasifier temperature was increased in an attempt to reduce the g-ash loading to the PCD, but the bridge was not affected. The PCD cone was full of solids and it appeared that the high level in the cone aided in the formation of a bridge between filter elements. Later that afternoon, the main air compressor surged causing the gasifier air valve to close, but the momentary

event did not interrupt coal feed. The PCD bridging, however, worsened, and the decision was made to shut down and inspect the PCD. Coal feed ended at 20:00 on September 5, 2002.

After the PCD cone was emptied, the bridged material in the PCD apparently dislodged itself. On September 7, 2002, after the gasifier had cooled, maintenance opened the PCD to inspect the filter elements. The filters were clean, and no bridging was present. Maintenance closed the manway, and the normal start-up procedure began again.

The main air compressor was started and the start-up burner was lit early in the morning on September 8, 2002. By noon of the same day coke breeze feed was started, and coal feed was resumed around 20:00. As soon as the coal feeder was started, a standpipe bubble occurred sending material to the PCD and thus reducing the solids inventory in the gasifier. Operations suspended coal feed immediately, but continued to feed coke breeze to keep the gasifier warm. A restriction formed between the cyclone solids exit and the loop seal downcomer during the upset making it impossible to add sand to the loop seal or resume normal gasifier operations. After adjusting aeration flows, the restriction dislodged itself several hours later. After several more J-leg upsets, coal feed resumed around 20:00 on September 9, 2002.

During the next few days, the gasifier operated in a much more stable manner with the riser just below 1,800°F. A low coal-feed rate and a high steam-flow rate were used to avoid bridging in the PCD and forming deposits in the gasifier. Figures 4.1-1 to -4 indicate typical operating conditions for this air-blown portion of the run.

Over the next few days, some of the mixing zone and LMZ thermocouple readings began to steadily decrease, indicating the possibility of deposit formation in the gasifier. High steam flows had some success in restoring the LMZ thermocouples, but had mixed results with the thermocouples in the mixing zone. To reduce chances of forming a large deposit, the gasifier was run conservatively. The coal feeder performed excellently throughout this portion of the test run.

After a few days of conservative operation, the steam flow was reduced and the coal-feed rate and gasifier temperatures were increased. The synthesis gas heating value improved significantly. Occasionally the coal-feed rate was lowered to prevent filling the PCD cone with g-ash. The thermocouple readings in the mixing zone neither improved nor worsened. On Monday, September 16, 2002, the Transport Gasifier was shut down on schedule to inspect the PCD filter elements and gasifier interior for bridging and deposits.

Inspections during the short outage showed that the PCD was quite clean with no g-ash bridging present. The gasifier had only a very thin coating of material that crumbled easily when touched. The coating did not seem to be thick enough to cause the thermocouple to read as low as they did. The steam-flow rate to the mixing zone may have been much higher than shown by the flowmeters, and the excess steam-flow rate coupled with the thin deposit may have caused the thermocouples to read low. Steam rates by hydrogen balances were 30 to 50 percent higher than the measured steam rates, see Section 4.5.9.

Since the gasifier appeared to be in good order, maintenance resealed the gasifier, and the start-up procedure began once again. The main air compressor and start-up burner were restarted on Friday,

September 20, 2002. Coke breeze feed began at 18:00 the same day. The gasifier ran until 01:30 the next morning when a standpipe bubble formed forcing some of the gasifier inventory to the PCD. Sand was added, but the material packed in the upper standpipe rather than settling in the loop seal and J-leg. After several hours of adjusting aeration flows and running the standpipe screw cooler, the sand settled, and coke breeze feed was resumed at 11:30 on September 21, 2002. Coal feed began 30 minutes later. The gasifier was operated at a higher coal-feed rate and at a higher temperature than it was during the first two parts of the test run.

After operating in air-blown operations for almost 37 hours, the transition to oxygen-blown operations occurred on September 23, 2002. The transition was smooth and took place in under 3 hours. The gasifier ran in oxygen-blown mode for almost 80 hours. The oxygen-blown period was quite stable, except when the oxygen tank was being filled. During tank filling, the oxygen pressure fluctuated and the oxygen flow changed rapidly, making it difficult to control gasifier temperatures. During the last few fillings, a new filling procedure minimized the oxygen flow and temperature fluctuations.

On September 25, 2002, the pressure, temperature, and coal-feed rate were increased, and the steam-flow rate was decreased to achieve a higher synthesis quality. Figures 4.1-5 to -8 indicate the gasifier conditions at that time. Once gasifier temperatures around 1,850°F were reached, the gasifier was transitioned quickly back to air-blown operations, and operated in air-blown mode at the higher temperatures with virtually no steam addition. The gasifier was shut down on September 26, 2002, after completing a total of 309 hours of coal-feed.

Tables 4.1-1 and -2 give general operating conditions for the Transport Gasifier operations in TC09 in air- and oxygen-blown modes, whereas the coal analysis data are given in Table 4.1-3. The steady-state test periods that were selected for data analysis are given in Table 4.1-4 with details of operating conditions in Tables 4.1-5 and -6

4.1.2 Gasifier Inspections

At the end of TC09, the gasifier was inspected by using a borescope for most items and by removing spool pieces to allow for visual inspections. First the borescope was inserted above the primary cyclone. After finding that the cyclone and its gas exit were in good shape, the borescope continued to be lowered to inspect the loop seal and the solids downcomer to the loop seal. Near the top of the downcomer there were some soft deposits. Towards the bottom of the downcomer the walls started showing more deposits. The last few feet of the downcomer looked rough.

The riser and the mixing zone were inspected next. The top of the riser was coated in a dark grey shiny material. This coating went away as the borescope went lower into the riser. The walls of the riser were textured, implying that there may have been a very thin layer of deposits on the surface. The riser refractory still appeared to be in good shape with some cracking and lost material evident. The riser crossover was in overall good shape. It was also coated in a dark, shiny material. There was a small amount of loose material in the bottom of the crossover.

The top of the mixing zone looked good with only some small deposits on the wall opposite the coal-feed nozzle within the first few feet below the coal-feed point. These deposits have been known for some time. Other minor deposits were found lower in the mixing zone. One deposit was perhaps an inch wide, 1 to 2 inches across, and several inches long. Another looked to be about the size of a baseball. Just above the J-legs was a thin deposit several inches wide and about a foot long that looked like material flowing down the wall. None of these were deemed large enough to warrant removal before TC10.

The primary gas cooler was inspected by removing the spool piece above the cooler. Figure 4.1-9 shows the top of the tube sheet during the inspection. About half of the tubes appeared to be partially or fully plugged just at the inlet to the tubes. The tubes and tube sheet were cleaned. The ferrules were found to be in good shape. The bottom flange of the secondary gas cooler was removed to check for tar deposits. A moderate amount of tar was found and chipped out. Figure 4.1-10 shows the tar that was removed. The amount of tar shown in the picture was an accumulation from the last three test runs.

The gasifier was also inspected with the infrared camera during the run. The IR scan did not reveal any significant problems. It did reveal some insulation needs for personnel protection.

Table 4.1-1

TC09 Operating Conditions for Transport Gasifier During Air-Blown Operations

Start-up Bed Material	Sand, ~120 μm
Start-up Fuel	Propane / Coke Breeze
Fuel Type	Blackhawk Formation, Upper Hiawatha Seam (Sufco) Bituminous
Fuel Particle Size (mmd)	275 - 300 μm
Average Fuel Feed Rate, pph	2,300
Sorbent Type	None
Gasifier Temperature, °F	1,750 – 1,850
Gasifier Pressure (Mixing Zone), psig	200 – 220
Riser Gas Velocity, fps	40 – 56
Riser Mass Flux, $lb/s \cdot ft^2$	225-450 (average slip ratio = 2)
Standpipe Level, inH_2O	120 – 250
Primary Gas Cooler Bypass	0%
PCD Temperature, °F	750 – 850
Total Gas Flowrate, pph	18,000 – 25,000
Air/Coal Ratio	4.2 to 6.1
Primary Air Split ($1^{st}/2^{nd}$ levels)	50/50
Steam/Coal Mass Ratio	0.7 to 3.2
AFBC Operating Temperature, °F	1,600 – 1,650
Duration of Coal Feed	229 hours

Table 4.1-2

TC09 Operating Conditions for Transport Gasifier During Oxygen-Blown Operations

Start-Up Bed Material	Process Derived Solids
Start-Up Fuel	Propane / Coke Breeze
Fuel Type	Blackhawk Formation, Upper Hiawatha Seam (Sufco) Bituminous
Fuel Particle Size (mmd)	325 - 350 μm
Average Fuel Feed Rate, pph	2,200
Sorbent Type	None
Gasifier Temperature, °F	1,750 – 1,850
Gasifier Pressure, psig	160 - 170
Riser Gas Velocity, fps	39 - 44
Riser Mass Flux, $lb/s \cdot ft^2$	150 - 450 (average slip ratio = 2)
Standpipe Level, inH_2O	120 – 250
Primary Gas Cooler Bypass	0%
PCD Temperature, °F	750 – 850
Total Gas Flowrate, pph	14,000 to 15,500
Oxygen/coal Mass Ratio	0.9 – 1.0
Oxygen/steam Mass Ratio	0.4 – 0.5
Steam/coal Mass Ratio	1.7 – 2.3
AFBC Operating Temperature, °F	1,600 – 1,650
Duration of Coal Feed	80 hours

Table 4.1-3

Coal Analyses as Fed

	Hiawatha
Moisture	6.85
Ash	10.29
Sulfur	0.38
C	66.36
H	4.34
N	1.08
O	10.71
Vol	35.61
Fix C	47.25
HHV (Btu/lb)	11,246

Table 4.1-4

Selected Steady-State Periods

TC09A-1	First steady-state period.
TC09A-2	Increased steam flow.
TC09A-3	Decreased coal-feed rate.
TC09A-4	Decreased coal-feed rate.
TC09B-1	Lowered pressure.
TC09B-2	Increased coal feed, pressure.
TC09B-3	Increased steam flow, decreased coal-feed rate.
TC09B-4	Increased steam flow.
TC09B-5	Increased coal feed.
TC09B-6	Increased coal feed.
TC09B-7	Decreased temperature.
TC09B-8	Decreased steam flow, increased temperature.
TC09B-9	Increased steam and coal feeds.
TC09B-10	Decreased steam flow.
TC09B-11	Lowered riser temperature.
TC09B-12	Lowered coal-feed rate.
TC09B-13	Increased coal, circ rates.
TC09B-14	Increased temperatures.
TC09C-1	Decreased steam flow.
TC09C-2	Decreased coal feed.
TC09C-3	Increased pressure.
TC09C-4	Increased pressure.
TC09C-5	Transitioned to oxygen.
TC09C-6	Resume after brief interruption.
TC09C-7	Reduced coal feed, increased pressure.
TC09C-8	Increased circulation rate.
TC09C-9	Increased temps, reduced circulation
TC09C-10	Increased circulation rate.
TC09C-11	Increased temperatures.
TC09C-12	Slightly increased temperatures.
TC09C-13	Increased coal-feed rate.
TC09C-14	Increased coal-feed, temps.
TC09C-15	Decreased coal-feed rate.
TC09C-16	Air mode, high press, low steam.

Table 4.1-5

Operating Periods With Coal Feed, Temperature, and Pressure Data (Page 1 of 2)

	Start	End	LMZ temp deg F	Rsr Temp deg F	LMZ Press Psig	Rxr Exit Pres psig	Coal Fd[1] Rate lb/hr	SP Level in H_2O
TC09A-1	9/5/2002 04:45	9/5/2002 06:45	1,742	1,636	216	200	5,525	131
TC09A-2	9/5/2002 08:15	9/5/2002 10:00	1,773	1,754	215	200	4,141	122
TC09A-3	9/5/2002 11:00	9/5/2002 12:30	1,779	1,762	214	200	3,187	94
TC09A-4	9/5/2002 15:30	9/5/2002 17:45	1,768	1,792	219	202	2,565	177
TC09B-1	9/9/2002 23:15	9/10/2002 00:45	1,767	1,765	200	184	1,449	106
TC09B-2	9/10/2002 03:30	9/10/2002 06:30	1,518	1,795	216	200	2,786	156
TC09B-3	9/10/2002 23:15	9/11/2002 05:15	1,679	1,777	214	200	1,885	130
TC09B-4	9/11/2002 05:30	9/11/2002 08:45	1,667	1,775	215	200	1,792	143
TC09B-5	9/11/2002 12:15	9/11/2002 15:15	1,722	1,774	215	200	2,116	149
TC09B-6	9/11/2002 20:00	9/12/2002 17:30	1,733	1,771	217	200	2,714	186
TC09B-7	9/12/2002 22:15	9/13/2002 14:30	1,711	1,755	216	200	2,594	185
TC09B-8	9/13/2002 16:30	9/14/2002 12:00	1,742	1,781	217	200	2,785	193
TC09B-9	9/14/2002 19:00	9/15/2002 02:00	1,714	1,786	217	200	3,053	183
TC09B-10	9/15/2002 03:00	9/15/2002 07:30	1,728	1,794	217	200	2,943	185
TC09B-11	9/15/2002 08:00	9/15/2002 16:00	1,727	1,782	217	200	3,029	191
TC09B-12	9/15/2002 23:15	9/16/2002 03:30	1,753	1,792	217	200	2,653	182
TC09B-13	9/16/2002 04:30	9/16/2002 06:15	1,768	1,787	218	200	3,100	212
TC09B-14	9/16/2002 11:00	9/16/2002 13:15	1,788	1,814	217	200	3,018	177

[1] Based on coal feeder weigh cell.

Table 4.1-5

Operating Periods With Coal Feed, Temperature, and Pressure Data (Page 2 of 2)

	Start	End	LMZ temp deg F	Rsr Temp deg F	LMZ Press Psig	Rxr Exit Pres psig	Coal Fd[1] Rate lb/hr	SP Level in H_2O
TC09C-1	9/21/2002 22:15	9/22/2002 02:00	1,798	1,790	219	200	3,190	194
TC09C-2	9/22/2002 02:15	9/22/2002 04:00	1,796	1,793	219	200	3,020	199
TC09C-3	9/22/2002 09:30	9/22/2002 11:00	1,800	1,807	239	220	3,324	210
TC09C-4	9/22/2002 12:30	9/22/2002 14:15	1,802	1,810	260	240	3,047	214
TC09C-5	9/23/2002 04:00	9/23/2002 07:30	1,799	1,774	166	150	2,753	181
TC09C-6	9/23/2002 07:45	9/23/2002 11:45	1,782	1,774	166	150	2,642	191
TC09C-7	9/23/2002 19:15	9/24/2002 05:30	1,801	1,781	175	160	2,619	182
TC09C-8	9/24/2002 11:00	9/24/2002 13:30	1,807	1,795	176	160	2,600	195
TC09C-9	9/24/2002 13:45	9/25/2002 01:15	1,815	1,811	175	160	2,529	178
TC09C-10	9/25/2002 01:30	9/25/2002 05:30	1,813	1,814	176	160	2,571	200
TC09C-11	9/25/2002 09:00	9/25/2002 11:15	1,833	1,824	175	160	2,863	188
TC09C-12	9/25/2002 11:30	9/25/2002 14:45	1,836	1,831	175	160	3,074	195
TC09C-13	9/25/2002 21:15	9/26/2002 06:15	1,829	1,826	175	160	3,014	188
TC09C-14	9/26/2002 08:00	9/26/2002 09:00	1,842	1,851	175	160	3,339	184
TC09C-15	9/26/2002 09:15	9/26/2002 10:30	1,821	1,848	175	160	3,155	192
TC09C-16	9/26/2002 13:30	9/26/2002 16:30	1,827	1,844	237	220	3,184	209

Table 4.1-6

Operating Periods With Temperature and Gas Flow Data (Page 1 of 2)

	Start	End	Air Flow lb/hr	Air/Coal	Air/C	O_2 Flow lb/hr	O_2/Coal	O_2/C	O_2 Conc %	Steam Flow[1] lb/hr	Stm/Coal	Total GasRate lb/hr
TC09A-1	9/5/2002 04:45	9/5/2002 06:45	12,163	2.20	3.32	0	0.00	0.00	23	316	0.06	23,839
TC09A-2	9/5/2002 08:15	9/5/2002 10:00	12,466	3.01	4.53	0	0.00	0.00	23	1,188	0.29	23,013
TC09A-3	9/5/2002 11:00	9/5/2002 12:30	11,072	3.47	5.23	0	0.00	0.00	23	1,235	0.39	21,481
TC09A-4	9/5/2002 15:30	9/5/2002 17:45	10,093	3.94	5.93	0	0.00	0.00	23	945	0.37	18,947
TC09B-1	9/9/2002 23:15	9/10/2002 00:45	9,514	6.56	9.89	0	0.00	0.00	23	834	0.58	19,249
TC09B-2	9/10/2002 03:30	9/10/2002 06:30	10,844	3.89	5.86	0	0.00	0.00	23	886	0.32	20,750
TC09B-3	9/10/2002 23:15	9/11/2002 05:15	10,070	5.34	8.04	0	0.00	0.00	23	2,875	1.53	22,289
TC09B-4	9/11/2002 05:30	9/11/2002 08:45	10,350	5.77	8.70	0	0.00	0.00	23	3,489	1.95	23,015
TC09B-5	9/11/2002 12:15	9/11/2002 15:15	10,171	4.81	7.24	0	0.00	0.00	23	2,527	1.19	21,362
TC09B-6	9/11/2002 20:00	9/12/2002 17:30	10,772	3.97	5.98	0	0.00	0.00	23	2,834	1.04	21,651
TC09B-7	9/12/2002 22:15	9/13/2002 14:30	10,547	4.07	6.12	0	0.00	0.00	23	2,651	1.02	21,532
TC09B-8	9/13/2002 16:30	9/14/2002 12:00	10,971	3.94	5.93	0	0.00	0.00	23	2,303	0.83	21,578
TC09B-9	9/14/2002 19:00	9/15/2002 02:00	11,941	3.91	5.89	0	0.00	0.00	23	3,035	0.99	24,346
TC09B-10	9/15/2002 03:00	9/15/2002 07:30	11,606	3.94	5.94	0	0.00	0.00	23	2,553	0.87	23,040
TC09B-11	9/15/2002 08:00	9/15/2002 16:00	11,335	3.74	5.64	0	0.00	0.00	23	2,573	0.85	22,660
TC09B-12	9/15/2002 23:15	9/16/2002 03:30	10,437	3.93	5.92	0	0.00	0.00	23	1,909	0.72	20,631
TC09B-13	9/16/2002 04:30	9/16/2002 06:15	11,365	3.67	5.52	0	0.00	0.00	23	1,941	0.63	22,084
TC09B-14	9/16/2002 11:00	9/16/2002 13:15	11,120	3.68	5.55	0	0.00	0.00	23	1,482	0.49	20,718

[1]Steam rate by PI tag 'KBR_Steam_Total.'

Table 4.1-6

Operating Periods With Temperature and Gas Flow Data (Page 2 of 2)

	Start	End	Air Flow lb/hr	Air/Coal	Air/C	O_2 Flow lb/hr	O_2/Coal	O_2/C	O_2 Conc %	Steam Flow lb/hr	Stm/Coal	Total Gas Rate lb/hr
TC09C-1	9/21/2002 22:15	9/22/2002 02:00	11,379	3.57	5.37	0	0.00	0.00	23	1,262	0.40	22,318
TC09C-2	9/22/2002 02:15	9/22/2002 04:00	11,611	3.85	5.79	0	0.00	0.00	23	1,319	0.44	22,634
TC09C-3	9/22/2002 09:30	9/22/2002 11:00	11,652	3.51	5.28	0	0.00	0.00	23	1,019	0.31	21,726
TC09C-4	9/22/2002 12:30	9/22/2002 14:15	10,852	3.56	5.36	0	0.00	0.00	23	958	0.31	20,333
TC09C-5	9/23/2002 04:00	9/23/2002 07:30	0	0.00	0.00	2,015	0.73	1.10	100	4,107	1.49	15,655
TC09C-6	9/23/2002 07:45	9/23/2002 11:45	0	0.00	0.00	2,015	0.76	1.15	100	4,091	1.55	15,349
TC09C-7	9/23/2002 19:15	9/24/2002 05:30	0	0.00	0.00	1,857	0.71	1.07	100	3,626	1.38	14,510
TC09C-8	9/24/2002 11:00	9/24/2002 13:30	0	0.00	0.00	1,870	0.72	1.08	100	3,366	1.29	14,100
TC09C-9	9/24/2002 13:45	9/25/2002 01:15	0	0.00	0.00	1,869	0.74	1.11	100	3,147	1.24	13,923
TC09C-10	9/25/2002 01:30	9/25/2002 05:30	0	0.00	0.00	1,869	0.73	1.09	100	3,429	1.33	14,159
TC09C-11	9/25/2002 09:00	9/25/2002 11:15	0	0.00	0.00	2,061	0.72	1.08	100	3,357	1.17	14,565
TC09C-12	9/25/2002 11:30	9/25/2002 14:45	0	0.00	0.00	2,111	0.69	1.03	100	3,199	1.04	14,867
TC09C-13	9/25/2002 21:15	9/26/2002 06:15	0	0.00	0.00	2,060	0.68	1.03	100	2,924	0.97	14,620
TC09C-14	9/26/2002 08:00	9/26/2002 09:00	0	0.00	0.00	2,275	0.68	1.03	100	3,005	0.90	15,086
TC09C-15	9/26/2002 09:15	9/26/2002 10:30	0	0.00	0.00	2,139	0.68	1.02	100	3,034	0.96	14,605
TC09C-16	9/26/2002 13:30	9/26/2002 16:30	10,783	3.39	5.10	0	0.00	0.00	23	276	0.09	18,653

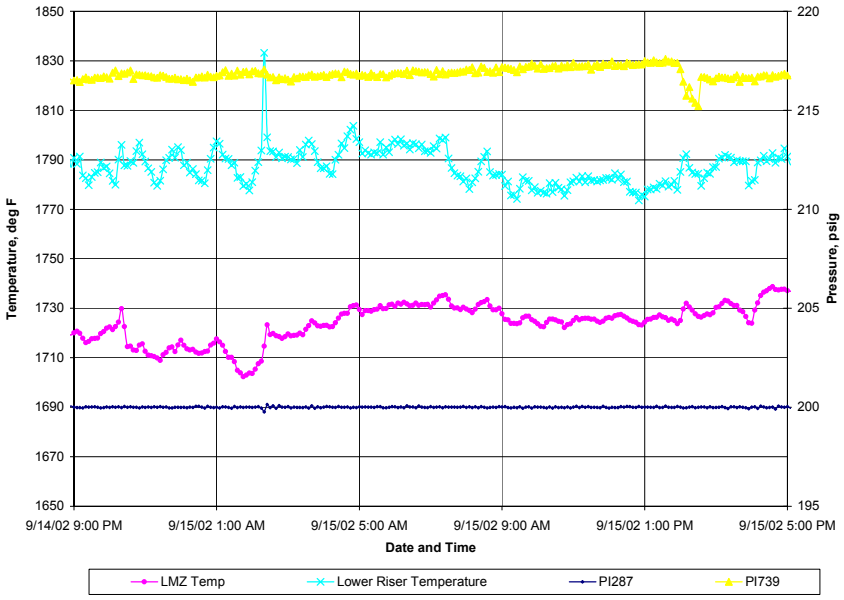

Figure 4.1-1 Gasifier Temperature and Pressure During Test Periods TC09B-9 and TC09B-10 in the Air-Blown Portion of TC09.

PI287 is the controlling pressure at the cyclone exit. PI739 is the pressure in the lower mixing zone.

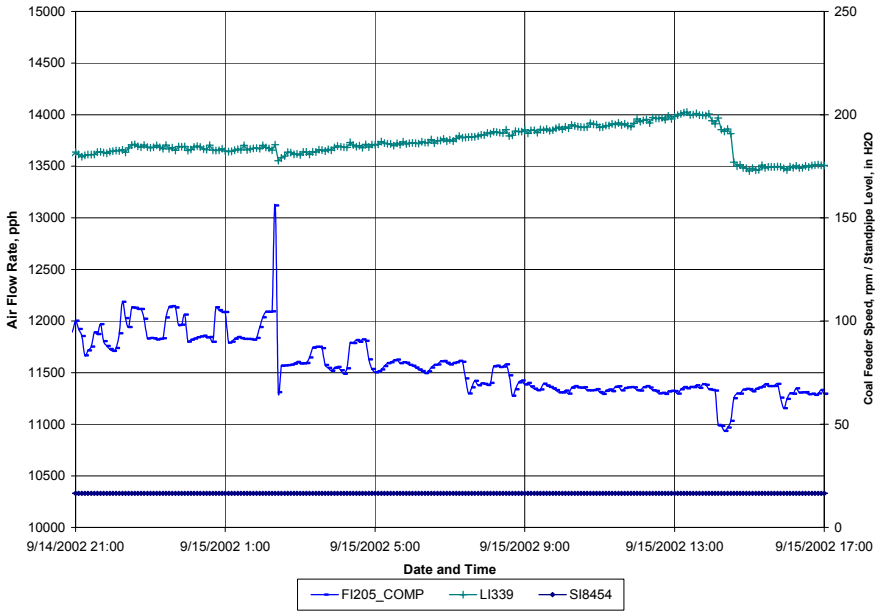

Figure 4.1-2 Typical Standpipe Level, Coal Feeder Speed, and Air-Flow Rate During Test Periods TC09B-9 and TC09B-10 in the Air-Blown Portion of TC09.

FI205_COMP is the total compensated air flow rate. LI339 is the standpipe level based on the standpipe differential pressure, and SI8454 is the coal feeder speed.

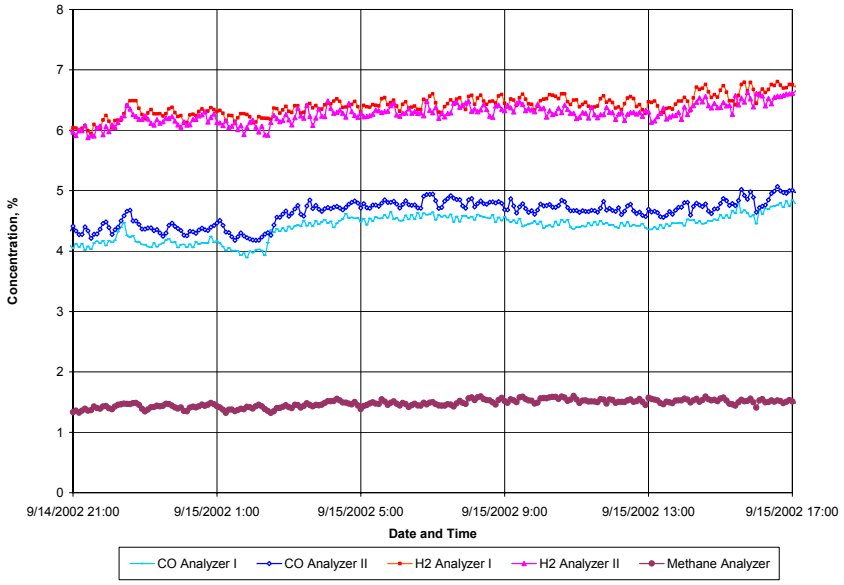

Figure 4.1-3 Typical Gas Analysis Data During Test Periods TC09B-9 and TC09B-10 in the Air-Blown Portion of TC09.

All measurements are taken downstream of the PCD.

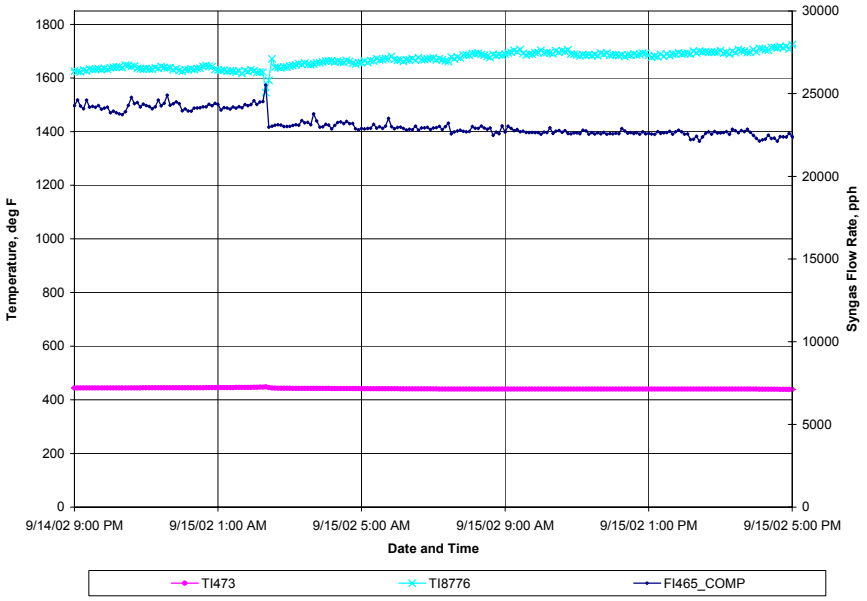

Figure 4.1-4 Total Syngas Flow Rate and Atmospheric Syngas Burner Inlet and Exit Temperatures During Test Periods TC09B-9 and TC09B-10 in the Air-Blown Portion of TC09.

FI465_COMP is the compensated syngas flow rate. TI473 and TI8776 are the burner inlet and exit temperatures, respectively.

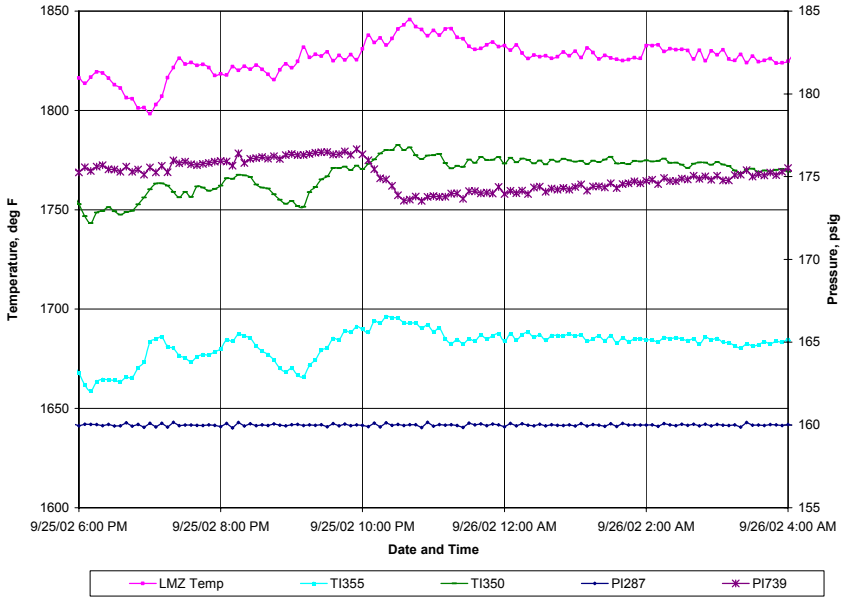

Figure 4.1-5 Gasifier Temperature and Pressure During Test Period TC09C-13 in Oxygen-Blown Operations in TC09.

PI287 is the controlling pressure at the cyclone exit. TI350 is a thermocouple in the middle of the gasifier mixing zone. TI355 is a thermocouple at the top of the riser. PI739 is the pressure in the lower mixing zone.

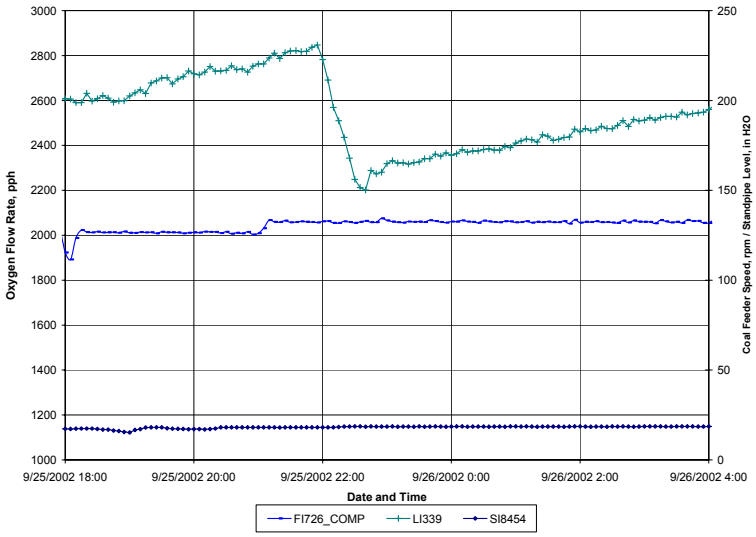

Figure 4.1-6 Coal Feeder Speed, Standpipe Level, and Oxygen-Flow Rate During Test Period TC09C-13 in Oxygen-Blown Operations in TC09.

FI726_COMP is the total compensated oxygen flow rate. LI339 is the standpipe level based on the standpipe differential pressure, and SI8454 is the coal feeder speed.

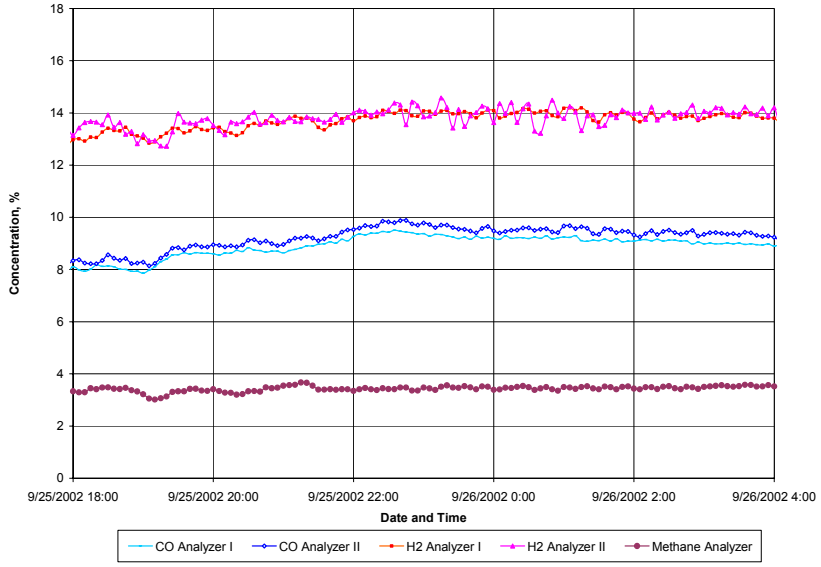

Figure 4.1-7 Gas Analysis Data During Test Period TC09C-13 in Oxygen-Blown Operations in TC09. All measurements are taken downstream of the PCD.

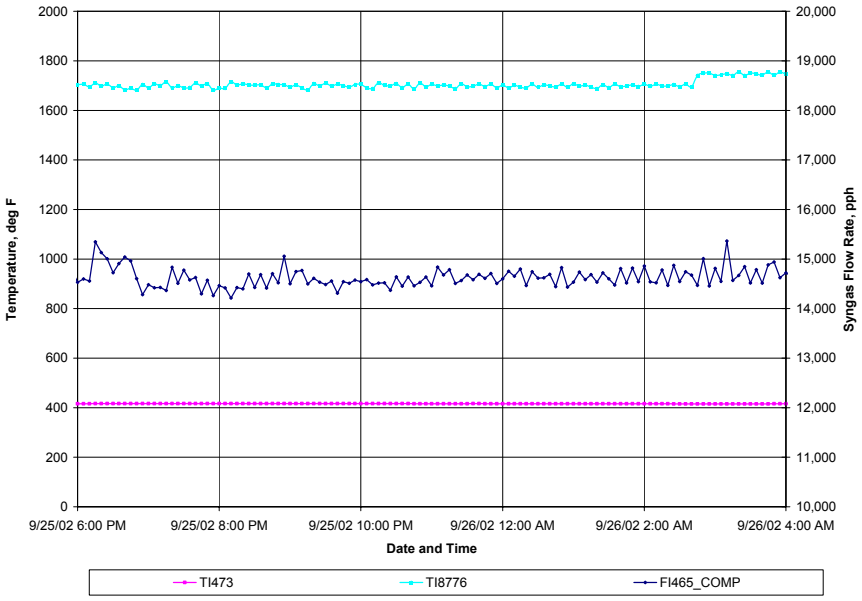

Figure 4.1-8 Total Syngas Flow Rate and Atmospheric Syngas Burner Inlet and Exit Temperatures During Test Period TC09C-13 in Oxygen-Blown Operations in TC09.
FI465_COMP is the compensated syngas flow rate. TI473 and TI8776 are the burner inlet and exit temperatures, respectively.

Figure 4.1-9 HX0202 Tube Sheet

Figure 4.1-10 Tar Removed From HX0402 Gas Exit

4.2 GASIFIER TEMPERATURE PROFILES

Section 4.2 describes the temperature profiles in TC09. A schematic of the gasifier with relative thermocouple locations is given in Figure 4.2-1. The gasifier was operated in air- and oxygen-blown modes during TC09, with a bituminous coal from the Sufco mine in Utah. The temperature profiles for steady-state periods for air- and oxygen-blown modes are shown in Figures 4.2-2 and -3, respectively, along with temperature profiles from TC08. There were some erroneous temperature readings in the upper mixing zone (UMZ) and riser throughout the run due to thermowell erosion and corrosion, and deposition around the thermowells. Thus, the temperature profile for TC09 is incomplete. The steady-state periods used for analysis for air- and oxygen-blown modes in TC09 were TC09A-1 and TC09C-9, respectively.

Figure 4.2-2 compares the temperature profile for air-blown operations in TC08 (PRB coal) and TC09. In air-blown mode in TC09, the temperature in the lower mixing zone (LMZ), T1-T4, increased quickly as the heat released from gasification ash (g-ash, formerly referred to as char) combustion heats the air, steam, and solids in the LMZ. The temperature then decreased as cooler solids from the J-leg, T14, entered the UMZ, T5. Air and steam added in the UMZ decreased the temperature, T6, slightly. The temperature in the UMZ, T7-T8, began to increase as g-ash combustions occured. The temperatures, T9-T10 (not shown) likely increased further. Coal was added as the UMZ transitioned into the riser, see Figure 4.2-1. Coal and conveying gas heat-up, coal devolatilization, and endothermic gasification reactions combined with heat losses decreased the temperature, T11, as the gas and solids flowed up through the riser. The solids removed by the disengager and cyclone cooled as they flowed down the standpipe (T12-T14). The temperature profile in air-blown mode for TC09 is very similar to TC08.

The temperature profile for the oxygen-blown case is shown in Figure 4.2-3. Similar to air mode, the LMZ temperature, T1-T4, increased quickly as the heat released from g-ash combustion heated the oxygen, steam, and solids in the LMZ. The temperature then decreased as cooler solids from the J-leg, T14, entered the UMZ, T5. Excess oxygen from the LMZ combusted the g-ash in circulating solids and again the temperature, T6 rose. The temperatures, T7-T8 (not shown), likely increased further. When all of the oxygen was consumed, the temperatures, T9 and T10 (not shown), likely decreased. The temperature, T11, decreased further through the riser due to the coal and conveying gas heat-up, coal devolatilization, endothermic gasification reactions, and heat losses. The solids removed by the disengager and cyclone cooled as they flowed down the standpipe (T12-T14). The temperature profile in oxygen-blown mode for TC09 is also similar to TC08.

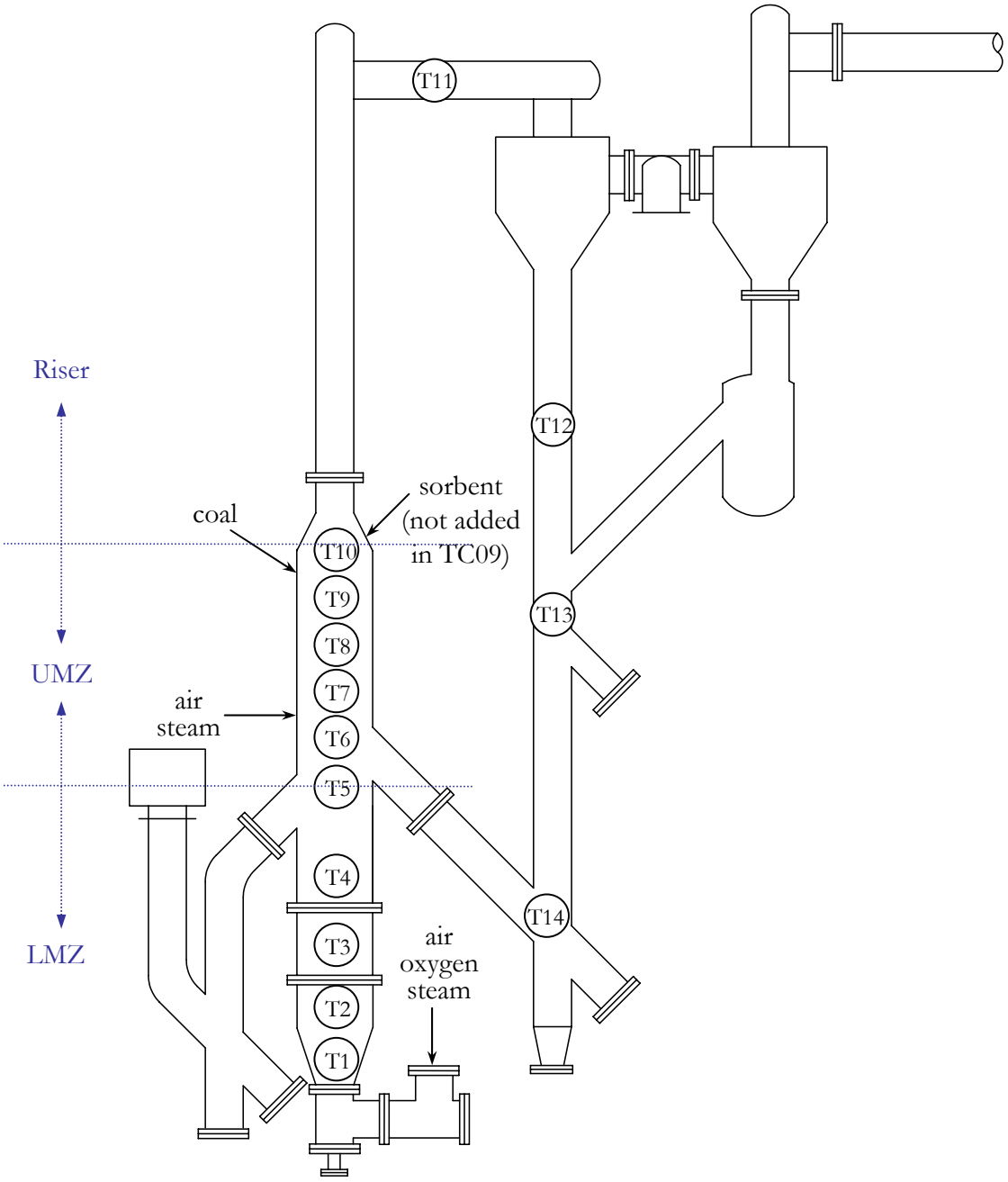

Figure 4.2-1 Transport Gasifier Schematic

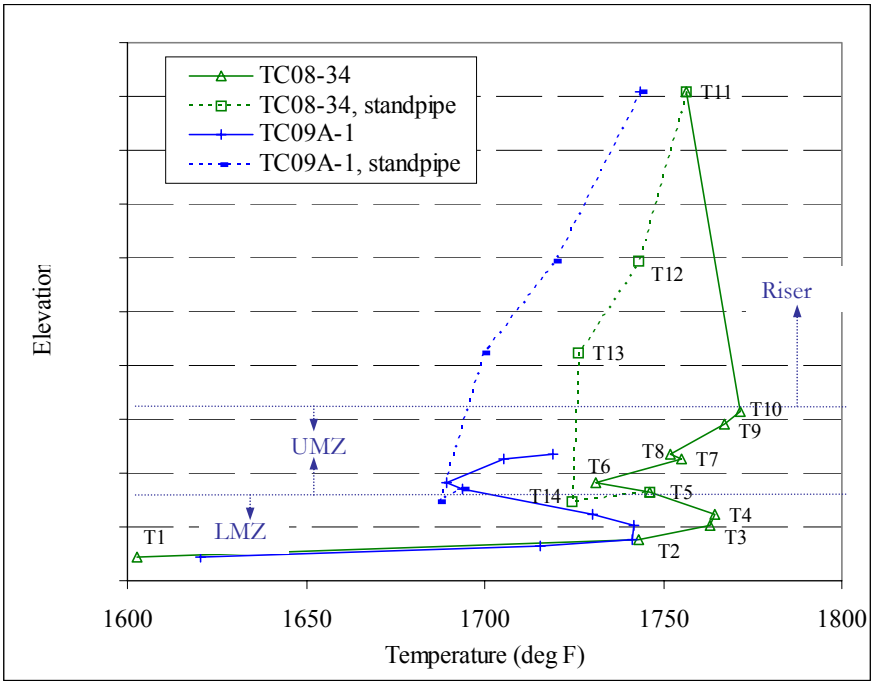

Figure 4.2-2 Temperatures Profile in Air-Blown Mode for TC08 (TC08-34) and TC09 (TC09A-1)

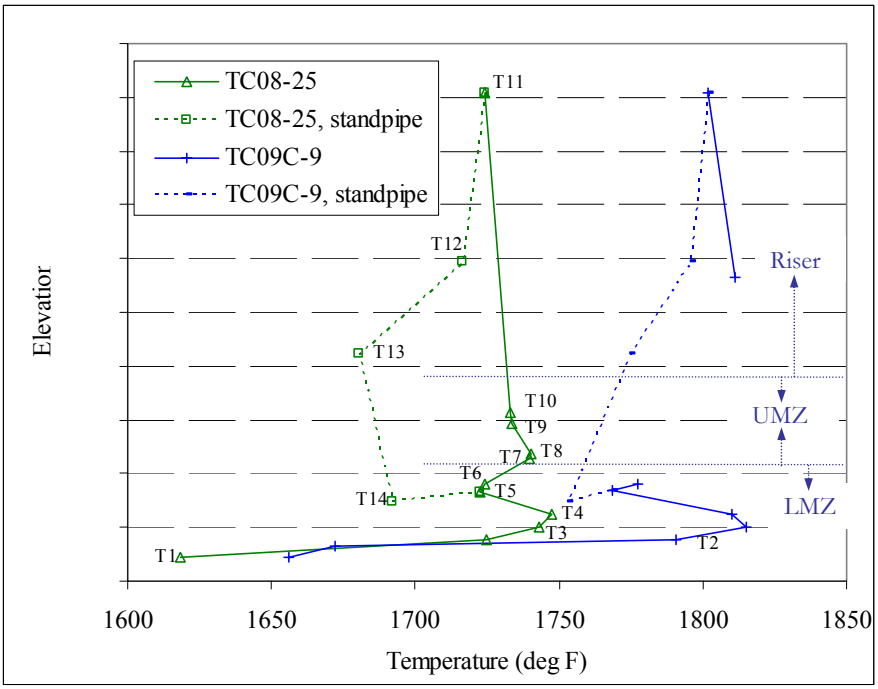

Figure 4.2-3 Temperature Profile in Oxygen-Blown Mode for TC08 (TC08-12) and TC09 (TC09C-9)

4.3 GAS ANALYSIS

4.3.1 Summary and Conclusions

- The raw synthesis gas lower heating values (LHV) were between 22 and 62 Btu/scf for air-blown operation and between 56 and 76 Btu/scf for oxygen-blown operation.
- The LHV for both modes of operation were strong functions of the relative amount of oxygen fed to the Transport Gasifier.
- The nitrogen-corrected, adiabatic synthesis gas LHVs were between 37 and 106 Btu/scf for air-blown operation and between 140 and 171 Btu/scf for oxygen-blown operation.
- Total reduced sulfur (TRS, mostly H_2S) emissions were between 192 and 578 ppm. The concentrations were consistent with about 8-percent sulfur capture.
- Synthesis gas analyzer data for CO was excellent, with all five analyzers in agreement with each other for most of the run.
- Synthesis gas analyzer data for H_2 was good, with both gas chromatographic analyzers within a few percent for most of the run.
- Synthesis gas analyzer data for CH_4 was good in that both the GCs (AI464 & AI419) were in agreement for oxygen-blown mode. Analyzer AI419E was slightly higher than AI464E for air-blown mode.
- Synthesis gas analyzer data for C_2^+ was poor for air-blown mode in that the AI419 read about 0.275 percent higher than AI464. Both analyzers agreed during oxygen-blown mode.
- Synthesis gas analyzer data for CO_2 was excellent in that all three analyzers were in agreement for most of the run.
- Synthesis gas analyzer data for N_2 was good in that both GCs (AI464 & AI419) were in agreement for most of the run.
- The synthesis gas H_2O was calculated using the thermodynamic equilibrium of the water-gas shift reaction at the mixing zone temperature. The water-gas shift H_2O agreed with 13 out of the 14 in situ H_2O measurements.
- The sum of the dry-gas analyzer concentrations was between 97.5 and 99.5 percent.
- The syngas H_2S analyzer gave good agreement when compared to the sulfur emissions by the syngas combustor SO_2 analyzer for most of TC09.
- Wet chemistry NH_3 data indicated 1,300 to 2,400 ppm for air-blown operation and 2,500 to 3,400 ppm for oxygen-blown operation.
- The CO/CO_2 ratio was between 0.2 and 0.8 for air-blown mode and between 0.3 and 0.6 for oxygen-blown mode.

- The water-gas shift constant used the in situ H_2O measurements were between 0.53 and 0.60, despite large variations in H_2O, H_2, CO, and CO_2 concentrations.
- The synthesis gas molecular weight was between 25.0 and 26.9 lb/mole for air-blown mode and between 23.8 and 24.2 lb/mole for oxygen-blown mode.
- The synthesis gas combustor oxygen balance was good.
- The synthesis gas combustor hydrogen balance was excellent for air-blown mode and good for oxygen-blown mode.
- The synthesis gas combustor carbon balance was good for air-blown mode and poor for oxygen-blown mode.

4.3.2 Introduction

The major goal for TC09 was the demonstration of the Transport Gasifier on oxygen and enhanced air operation with Upper Hiawatha bituminous coal (SUFCO mine) from the Blackhawk Formation. TC09 was the first run in which bituminous coal was used for an entire test run at the PSDF Transport Gasifier. Hiawatha coal feed was established with air on September 4, 2002. After about 21 hours, the Transport Gasifier was tripped for examination of potential g-ash bridging. Coal testing resumed on September 8, 2002, and operated for about 161 hours before the unit was tripped for an inspection prior to oxygen-blown mode. The unit was then started up on air with coal feed resuming on September 21, 2002, and operated on air for about 37 hours and then transitioned to oxygen-blown mode on September 23, 2002. The Transport Gasifier operated on oxygen for about 78 hours. The gasifier was then transitioned to air-blown mode on September 25, 2002, and the unit was then shut down on September 26, 2002, ending TC09.

There were 34 steady periods of operation between September 5 and 26. The steady periods of operation are given on Table 4.3-1. Three periods (TC09-6, -7, -8) were longer than 16 hours and were split into periods of about 8 hours each. This resulted in 37 operating periods.

Sorbent was not injected into the Transport Gasifier during TC09; all sulfur removal was from the alkali contained in the Hiawatha coal.

Table 4.3-2 lists some of the TC09 operating conditions for TC09, including mixing zone temperatures, pressure control valve pressures, PCD inlet temperatures, air rate, oxygen rate, syngas rate, steam rate, and nitrogen rate. The system pressure was at 200 psig for most of the air-blown periods, with the exceptions of 184 psig (TC09B-1), 220 psig (TC09C-3 and TC09C-16), and 240 psig (TC09C-4).

4.3.3 Raw Gas Analyzer Data

During TC09, Transport Gasifier and synthesis gas combustor outlet gas analyzers were continuously monitored and recorded by the Plant Information System (PI). Fourteen in situ grab samples of synthesis gas moisture content were measured during PCD outlet loading sampling.

The gas analyzer system analyzed synthesis gas for the following gases during TC09 using the associated analyzers:

CO	AI425, AI434B, AI453G, AI464C, AI419C
CO_2	AI434C, AI464D, AI419D
CH_4	AI464E, AI419E
C_2^+	AI464F, AI419F
H_2	AI464G, AI419G
H_2O	AI419H
N_2	AI464B, AI419B
H_2S	AI419J

Analyzer AI475 was out of service for repair and was not available for TC09. The AI464 and AI419 analyzers use a gas chromatograph and typically have about a 6-minute delay. The other three CO analyzers (AI425, AI434B, and AI453G) and CO_2 analyzer (AI434C and) are IR based and give more real-time measurements. All analyzers require that the gas sample be conditioned to remove water vapor, therefore all the analyzers report gas compositions on a dry basis.

The locations of the synthesis gas analyzers are shown on Figure 4.3-1. The gas analyzers obtain synthesis gas samples from three different locations:

- Two between the PCD and the secondary gas cooler (HX0202).
- One between the secondary gas cooler and the pressure letdown valve (PCV-287).

With five CO analyzers, there is a measure of self-consistency when all or several of the five analyzers read the same value. There is also the choice of which analyzer to use if all the analyzers do not agree. The TC09 hourly averages for the five CO analyzers are given in Figure 4.3-2. For most of TC09, analyzers AI453G, AI419C, AI464C AI434B, and AI425 were in good agreement. Except for the first 10 hours, at least four of the five analyzers were in agreement. The analyzer selection for each operating period is given in Table 4.3-3. The good agreement between the CO analyzers gives confidence to the accuracy of the CO data. The low CO measurements are either periods when the gas analyzers were being calibrated or analyzer measurements made during coal feeder trips. The CO data used in calculations were interpolated for times when the gas analyzers were being calibrated.

The two unit outages are shown on Figure 4.3-2. During the period shown as oxygen-blown operation, each trip was restarted on air, and then transitioned to enriched air for a brief period before the oxygen-blown operation was resumed.

TC09 hourly averages data for the H_2 analyzers are shown on Figure 4.3-3. Both analyzer AI464G and analyzer AI419G gave reasonable results for the entire run and agreed with each other, except for a few periods of calibration. Either gas analyzer was used for the operating periods. The analyzer used is given on Table 4.3-3 and which operating periods used interpolated data.

The TC09 hourly average gas analyzer data for CH_4 is given in Figure 4.3-4. Analyzer AI419E gave more reasonable results for the first 100 hours of TC09. For the next 75 hours, until the second outage, AI419E was about 0.25 percent higher than AI464E. For the remainder of TC09, through the oxygen-blown mode, both analyzers agreed with each other. AI419E gave reasonable results for the entire run, while AI464H usually agreed with AI419E; there were several periods where AI464E was not reading correctly. The choice of which analyzer, AI464E or AI419E to use is given on Table 4.3-3. Analyzer AI419E was used for all operating periods except TC09B-7a.

The TC09 hourly average gas analyzer data for C_2^+ is given in Figure 4.3-5. AI419F read about 0.3 percent for the first 260 hours of TC09. AI464F read less than 0.1 percent for the first 110 hours, and then increased to 0.1 percent from hour 110 to the second outage at 183 hours. After the second outage, AI464F read between 0.05 and 0.18 percent. During oxygen-blown mode, AI464F agreed with AI419F. AI419F was used for the first 226 hours of TC09, and AI464F was used for the remainder of TC09.

The CO_2 analyzer data is given on Figure 4.3-6. Analyzers AI419D and AI434C agreed with each other for all of TC09. Analyzer AI464D was erratic until about hour 90, and then agreed with the other two CO_2 analyzers for the rest of the run. The TC09 CO_2 data were excellent. All of the three analyzers were used for the operating periods. The analyzers used for each operating periods are given on Table 4.3-3.

The nitrogen analyzer data is given in Figure 4.3-7. Analyzer AI464B and AI419B agreed with each other for the entire run with a few periods of disagreement. Either analyzer was used for the operating period data. The analyzer used for data analysis is given on Table 4.3-3.

Since both GC analyzers AI419 and AI464 analyze for nearly the entire spectrum of expected gas components, a useful consistency check of each analyzer is to plot the sum of the gases measured by each bank of analyzers to see how close the sum of compositions is to 100 percent. The sum of both of the GC analyzer banks is given on Figure 4.3-8. AI419 was fairly consistent during TC09 after hour 20, usually between 98 and 100 percent. The AI464 sums agreed with AI419 for long portions of TC09 in both air- and oxygen-blown modes.

The H_2O analyzer AI419H is part of the AI419 GC. Since AI419 operates dry, and the synthesis gas H_2O is removed prior to analysis, AI419H always read 0.0 percent, and will not be discussed further.

The raw H_2S analyzer AI419J data is shown on Figure 4.3-9. The H_2S data seems reasonable in that it was lower during the air-blown mode than in oxygen-blown mode, and seemed to

be in the expected range for Hiawatha coal with no sorbent added. The AI419J data will be compared with synthesis gas combustor SO_2 analyzer data in Section 4.3.8.

During TC09 several point analyses were made for H_2S, COS, and CS_2 using Sensydine tubes. Sensydine tubes take a small sample of a gas stream and analyze for only one compound. (They report gas concentrations wet.) The Sensydine H_2S data will be compared with the H_2S analyzer, AI419J, concentrations on a wet basis for the operating periods in Section 4.3-8. The COS Sensydine data will be compared with the difference of the total reduced sulfur concentration and the H_2S analyzer, AI419J, for the operating periods.

There were no operating NH_3 analyzers during TC09. During TC09 several point analyses were made for NH_3 and HCN using Sensydine tubes and using wet chemistry extract sampling. The wet chemistry sampling usually lasted about 15 minutes. The ammonia data is given on Figure 4.3-10. The NH_3 wet chemistry data was 1,300 to 2,400 ppm in air-blown mode and 2,500 to 3,400 ppm in oxygen-blown mode. The TC09 (Hiawatha coal) NH_3 wet chemistry data was in the same range as the TC08 (PRB coal) analyzer data in air-blown mode and consistent with the TC08 oxygen-blown mode (TC08 NH_3 analyzer was over the maximum range of 2,000 ppm NH_3). The Sensydine NH_3 data was consistently lower than the wet chemistry NH_3 data. Based on past results, the wet chemistry NH_3 data appears better than the Sensydine NH_3 data.

The HCN data is given on Figure 4.3-11. The wet chemistry HCN data was from 4 to 35 ppm for air-blown mode and 78 to 96 for oxygen-blown mode. This is the first HCN data for the Transport Gasifier syngas. It appears reasonable in that the HCN should be less than the NH_3, and the HCN increases during oxygen-blown operation. The Sensydine HCN data were higher than the wet chemistry HCN at 60 to 167 ppm for air-blown operation and 250 to 286 for oxygen-blown operation. It appears that interference from other components results in the Sensydine HCN reading higher than the actual HCN measurement. The wet chemistry HCN is the more accurate.

4.3.4 Gas Analysis Results

The dry, raw synthesis gas analyzer data was adjusted to produce the best estimate of the actual gas composition in three steps:

1. Choice of CO, H_2, CH_4, N_2, and CO_2 analyzer data to use (see Table 4.3-3).
2. Normalization of dry gas compositions (force to 100 percent total).
3. Conversion of dry compositions to wet compositions.

For the rest of this section, the data analysis is based only on the TC09 operating periods. The operating period averages of the sum of the dry gas analyses selected are shown on Figure 4.3-12. All of the operating periods have the sum of dry gas compositions between 97.5 and 99.5 percent indicating that the data is biased low, in that the GCs are not picking up all of the syngas components. The average of all the operating sum of the dry gas composition is 98.6 percent. During the normalization process all of the dry gas

compositions will be increased slightly due to the sum of the dry gas compositions being biased low.

In previous gasification runs, the water-gas shift reaction was used to interpolate H_2O measurements between in situ H_2O measurements and to check the consistency of the H_2O analyzer. Since there were no operating H_2O analyzers during TC09, water-gas shift equilibrium was used to interpolate H_2O data between in situ H_2O measurements. The water-gas shift equilibrium constant should be a function of a Transport Gasifier mixing zone or riser temperature. Plotted on Figure 4.3-13 are the H_2O concentrations calculated from the water-gas shift equilibrium constant based on the mixing zone temperature TI368 at an approach temperature of 50ºF, and using the measured H_2, CO, and CO_2 concentrations. The approach temperature of 50ºF seemed to give the best fit of the in situ data. These interpolated H_2O measurements analyzer readings will be used for further data analyses.

The water-gas shift (WGS) reaction and equilibrium constant are as follows:

$$CO + H_2O \leftrightarrow H_2 + CO_2 \quad (1)$$

$$Kp = \frac{(H_2)(CO_2)}{(H_2O)(CO)} \quad (2)$$

The synthesis gas H_2O concentration should be a function of the amount of steam added to the Transport Gasifier and the amount of nitrogen dilution. Figure 4.3-14 plots the synthesis gas H_2O content against the amount of steam added to the gasifier. Due to the wide range of steam rates during air-blown mode (1,500 to 5,500 lb/hr), the moisture content of the syngas varied from 12 to 33 percent. As expected, the syngas H_2O was a strong function of the steam rate. During oxygen-blown mode, the steam rate effect was less because the steam rate only varied by about 700 lb/hr (4,200 to 4,900 lb/hr).

The best estimates of the wet gas compositions for the TC09 operating periods are given on Table 4.3-4 and shown on Figure 4.3-15. Also shown on Table 4.3-4 are the synthesis gas molecular weights for each operating period.

The CO concentration was erratic between 4.4 to 7.3 percent from the start of TC09 to hour 31. The CO then decreased to 1.5 percent for two operating periods (hour 52 and 57) when the steam rate was increased by about 3,000 lb/hr, increasing the H_2O concentration. The increase in H_2O concentration diluted the CO and decreased the CO concentration by reaction via the water-gas shift reaction to CO_2 and H_2. The CO concentration then slowly increased to 6 percent until the oxygen-blown mode, as the steam rates and resulting H_2O concentrations decreased. At the beginning of the oxygen-blown mode the CO decreased to 4 percent, again as a result of the steam rate being increased by 2,000 lb/hr to nearly 5,000 lb/hr. The H_2O concentration increased at the same time by over a factor of two from 16 to 36 percent. During the oxygen-blown mode, the CO concentration slowly increased from 4 to 7 percent as the steam rate was decreased from 5,000 to 4,500 lb/hr at the end of the oxygen-blown mode. For the last air-blown mode operating period the CO remained at 7.1 percent, as the steam rate decreased to 1,700 lb/hr.

The H_2 concentration was erratic, between 4 and 6 percent, at the start of TC09 to hour 31. When the steam rate was increased at hour 52, the H_2 decreased to less than 4 percent. The H_2 concentration then increased from 4 to 6 percent until the end of the air-blown modes as the steam rate was decreased. During oxygen-blown mode, the H_2 increased from 7.5 to 10 percent as the steam rate was decreased. For the final air-blown mode, the H_2 decreased to 5.5 percent.

The CO_2 concentration decreased from 10 to 8 percent at the start of TC09. The 8-percent CO_2 was during the high air-blown steam rates at hours 52 and 57. The CO_2 then increased to about 9.5 percent for the rest of the air-blown mode. During the oxygen-blown mode, the CO_2 was steady at from 12 to 12.5 percent. The steam rate changes during the oxygen-blown mode did not effect the CO_2 concentration. When the system was returned to air-blown operation, the CO_2 returned to about 8.5 percent.

The CH_4 concentration started the run at 2 percent and then slowly decreased to 1.5 percent at hour 31. During the high air-blown steam rate operating periods at hour 52 and 57, the CH_4 decreased to about 0.5 percent. As the steam rate decreased during air-blown mode, the CH_4 slowly increased from 1 to 1.5 percent. During the oxygen-blown mode, the CH_4 also slightly increased from 2.0 to 2.4 percent. During the last air-blown mode operating period the CH_4 returned to 1.6 percent.

The C_2^+ concentrations were fairly constant during TC09 at 0.1 to 0.3 percent.

The CO/CO_2 ratios were calculated from the gas data for each operating period, and are listed on Table 4.3-4. The TC09 CO/CO_2 ratio varied from 0.2 to 0.8.

The LHV for each gas composition was calculated and is given on Table 4.3-4 and plotted on Figure 4.3-16.

The LHV value was calculated using the formula:

$$\mathrm{LHV(Btu/SCF)} = \left\{ \begin{matrix} 275\times(\mathrm{H_2\%}) + 322\times(\mathrm{CO\%}) + \\ 913\times(\mathrm{CH_4\%}) + 1641\times(\mathrm{C_2^+\%}) \end{matrix} \right\} / 100 \qquad (3)$$

The raw LHV was erratic at between 42 and 62 Btu/scf from the beginning of TC09 until hour 31. When the steam rate was increased at hour 52 and 57, the LHVs decreased to about 23 Btu/scf. For the rest of the air-blown mode, the LHVs slowly increased from 23 to 52 Btu/scf as the steam rate was slowly reduced. During oxygen-blown mode the raw LHVs also increased from 57 to 72 Btu/scf, again as the steam rate was decreased. For the final air-blown mode operating period, the LHVs returned to a typical air-blown mode value of 55 Btu/scf. As expected, the LHVs trends with steam rate followed the H_2 and CO concentration trends.

Past test runs have indicated that the LHV is most affected by the coal rate and steam rate. The LHV increases as the coal rate increases (see Figure 4.5-5 of the TC06 Final Report).

The coal rate effect is due to the way that the Transport Gasifier is operated in that the aeration and instrument nitrogen is maintained constant as coal rate increases. As coal rate increases the syngas rate increases, but the nitrogen rate remains constant. The pure nitrogen part of the syngas concentration is thus lessened (less nitrogen dilution) and the syngas LHV increases. When air is replace by oxygen in enhanced air- and oxygen-blown operation, the nitrogen content of the syngas is also decreased, increasing the LHV. The increase in steam produces lower LHV by the simple increased syngas dilution with H_2O. A way to combine the effects of changes in steam, mode of operation, and coal rates is to determine the overall percent of oxygen of all the gas that is fed to the Transport Gasifier. This compensates for the different amount of nitrogen and steam that are added to the gasifier. The overall percent O_2 is calculated by the following formula:

$$Overall\ \ percent O_2 = \frac{.21 * air + oxygen}{air + oxygen + (pure\ nitrogen) + steam} \qquad (4)$$

The air, oxygen, nitrogen, and steam flows are in moles per hour. At the PSDF, a large amount of pure nitrogen is fed to the gasifier for instrument purges, coal and sorbent transport, and equipment purges. In PSDF air-blown operation, about 50 percent of the synthesis gas nitrogen comes from air and 50 percent comes from the pure nitrogen system. In PSDF oxygen-blown operation, the removal of air nitrogen removes about the same amount of nitrogen as if the pure nitrogen was replaced by synthesis gas recycle.

The TC09 raw LHV data is plotted against overall percent O_2 on Figure 4.3-17. Also plotted on Figure 4.3-17 is the straight line correlation of TC06, TC07, and TC08 Powder River Basin (PRB) coal data, which contains air-, enhanced air-, and oxygen-blown mode data. The TC09 data is from 20 Btu/scf at 8.5-percent O_2 to 78 Btu/scf at 13.25-percent O_2 and follows a clear trend of increasing Btu/scf with percent O_2. Due to the higher steam rates used in TC09 than the earlier gasification runs, the percent O_2 has a lower range than the PRB percent O_2. This higher amount of TC09 dilution leads to lower Hiawatha bituminous LHV when compared to the PRB LHV. When the two coals are compared at the same level of percent O_2 (between 11- and 13- percent O_2), the Hiawatha bituminous has a higher LHV at the same percent O_2. This may be due to increased dilution of the PRB syngas due to the higher PRB coal moisture content (22.7 percent) when compared to Hiawatha bituminous moisture content (6.85 percent). The additional moisture in the PRB coal turns to steam and dilutes the syngas, but is not counted in the overall O_2 percent factor.

4.3.5 Nitrogen and Adiabatic Corrected Synthesis Gas Lower Heating Values

The PSDF Transport Gasifier produces syngas of a lower quality than a commercially sized gasifier due to the use of recycle gas (in a commercial gasifier) rather than nitrogen, (at the PSDF) for aeration and instrument purges, as well as the lower heat loss per pound coal gasified in a commercially sized gasifier when compared to the PSDF Transport Gasifier. To estimate the commercial synthesis LHV, the following corrections are made to the measured, raw synthesis gas composition:

1. All nonair nitrogen is subtracted from the syngas. This nitrogen is used for Transport Gasifier aeration and instrument purges. In a commercial plant, the instrument purges will be lower due to less commercial plant instrumentation and due to commercial instruments requiring the same purge rate independent of the plant size. This correction assumes that recycled syngas or steam will be used in a commercial plant for aeration and instrument purges to replace the nonair nitrogen. The nonair nitrogen was determined by subtracting the air nitrogen from the synthesis gas nitrogen. This correction increases all the nonnitrogen syngas compositions and decreases the nitrogen syngas composition. The syngas rate will decrease as a result of this correction. For oxygen-blown mode, this correction removes all nitrogen from the syngas and the oxygen-blown syngas will have 0 percent nitrogen. The water-gas shift equilibrium constant and the CO/CO_2 ratios will not change. This correction should be valid in that other gases should be able to replace the nonair nitrogen in the Transport Gasifier. One potential problem to this correction would be the use of recycle gas in Transport Gasifier locations where the recycle gas will combust in preference to the coal or recycle standpipe carbon, which could result in gasifier hot spots or decreased performance. A commercial plant might use some nitrogen for selected aeration and instrument locations.
2. Adjustments are made to account for the energy required to heat up the nonair nitrogen that has been eliminated by using steam or recycle gas for aeration or instrument purges. Once the nonair nitrogen is removed, the coal and air rates will decrease by the amount of energy no longer required to heat the nonair nitrogen to the maximum gasifier temperature. This results in decreased coal, air, and oxygen rates to the Transport Gasifier. It is assumed that this eliminated coal is combusted to CO_2 and H_2O to heat up the nonair nitrogen. Eliminating this additional coal reduces the syngas CO_2 and H_2O concentrations. The lower corrected air rates for air-blown mode also decreases the nitrogen in the corrected syngas. This correction decreases the synthesis gas flow rate. For this correction, the water-gas shift constant and the CO/CO_2 ratio both change due to the reduction in CO_2 and H_2O. This correction neglects the heat required to heat up the recycle gas replacing the nonair nitrogen used for aeration and instrument purges. The recycle gas will be available at a higher temperature than the nitrogen and less recycle gas will be required to replace the nonair nitrogen. This correction is more aggressive than it should be, but it is difficult to estimate the amount of recycle gas required in a commercial plant.
3. Corrections are included for the PSDF, which has a higher heat loss per pound of coal gasified than a commercially sized plant. Smaller scale pilot and demonstration units have higher surface area-to-volume ratios than their scaled up commercial counterparts, and hence the PSDF Transport Gasifier has a higher heat loss per pound of coal gasified than a commercial plant. Since the heat loss of a commercial plant is difficult to estimate, the corrected heat loss is assumed to be zero (adiabatic). The correction uses the same method to correct for the no-longer-required energy to heat up the nonair nitrogen. The coal, air, and oxygen rates are reduced; the syngas CO_2, H_2O, and N_2 concentrations are reduced; the water-gas shift equilibrium constant and the CO/CO_2 ratio change. This correction is probably good since the commercial

plant heat loss per pound of coal gasified is much larger than the PSDF Transport Gasifier heat loss per pound of coal gasified.

4. The steam rates are reduced for oxygen-blown operation, since in oxygen-blown operation, steam is added to control the gasifier temperature. In a commercial plant as the oxygen rate is decreased, the steam rate will also be decreased. It was assumed that the steam-to-oxygen ratio will be the same for the PSDF and the commercial Transport Gasifier, and hence the corrected steam rate will be lower than the original steam rate. The effect of lowering the steam rate was assumed to decrease the amount of H_2O in the syngas by the amount the steam rate was reduced. This correction reduces the steam rate and the H_2O content of the syngas and hence the LHV and water-gas shift equilibrium constant also changes. The steam-to-oxygen ratio is a function of the detailed design of the Transport Gasifier and it is difficult to estimate what the commercial steam-to-oxygen ratio will be.

The sum of all these four corrections is the adiabatic nitrogen corrected LHV. These calculations are an oversimplification of the gasification process. A more sophisticated model is required to correctly predict the effects of decreasing pure nitrogen and gasifier heat loss. It should be noted that the corrected syngas compositions are based on a corrected coal rate, corrected air rate, corrected oxygen rate, corrected steam rate, and a corrected syngas rate. Since the corrections change the syngas water-gas shift equilibrium constant, still another correction should be made to the corrected gas compositions since the water-gas shift constant should be a function of the gasifier mixing zone temperature, not whether recycle gas is used. The corrected syngas LHV is probably correct since the WGS reaction does not change the LHV much since H_2 is being replaced by CO (or vice versa). Due to correction #4, the corrected H_2O is probably too high. In a commercial plant, the WGS equilibrium will decrease H_2 to create more H_2O, which increases CO and decreases CO_2.

The corrections also change the equilibrium H_2S concentration, since as the H_2O and CO_2 concentrations increase, the equilibrium H_2S concentration increases. The corrected process conditions will result in higher equilibrium H_2S and could increase sulfur emissions if the sulfur emissions are equilibrium controlled.

The adiabatic N_2 corrected LHVs for each operating period are given in Table 4.3-5 and plotted on Figure 4.3-16. The N_2 corrected LHVs were between 37 and 106 Btu/scf for air-blown operation, and between 140 and 171 for oxygen-blown operation. The corrected air-blown LHVs were from 20 to 50 Btu/scf higher than the raw air-blown LHVs. The corrected oxygen-blown LHVs were 80 to 100 Btu/scf higher than the raw oxygen-blown LHV. The correction is higher for oxygen blown because there is less syngas in the raw oxygen-blown mode of operation, so taking about the same amount of pure nitrogen out the syngas has a larger effect.

For comparing the raw LHVs with the adiabatic N_2-corrected LHVs, an equivalent to the overall percent O_2 is defined as:

$$\text{Corrected Overall } \%O_2 = \frac{.21*(\text{corrected air}) + (\text{corrected oxygen})}{(\text{corrected air}) + (\text{corrected oxygen}) + (\text{corrected steam})} \quad (5)$$

All flow rates are expressed as moles per hour. The corrected air rate, corrected oxygen rate, and corrected steam rate are used in the determination of the corrected LHVs. The corrected overall percent O_2 rate for oxygen-blown mode is a direct function of the steam-to-oxygen ratio, since the corrected air rate is zero.

The adiabatic N_2-corrected LHVs are plotted against the adiabatic overall percent O_2 in Figure 4.3-18. The corrected air-blown LHVs and corrected oxygen-blown LHV form a single straight line with corrected overall O_2 percent in the feed gas. This indicates that the corrected oxygen-blown LHVs are consistent with the corrected air-blown LHVs.

A straight line fit of the raw LHVs and raw overall percent O_2 is also plotted on Figure 4.3-18. The corrected LHVs are 15 to 20 Btu/scf higher than the raw LHVs at the equivalent corrected O_2 percent.

A straight line fit of the corrected PRB LHVs and corrected percent O_2 from TC06, TC07, and TC08 is also shown on Figure 4.3-18. The PRB-corrected LHV were from 30 to 50 Btu/scf lower than the Hiawatha bituminous LHV at equivalent corrected overall feed percent O_2. Because it was possible to operate at a lower steam-to-coal ratio (higher corrected percent O_2) during PRB gasification as compared to Hiawatha bituminous gasification, higher LHVs were obtained with PRB than with Hiawatha bituminous. The PSDF Transport Gasifier was able to operate at a lower steam-to-coal ratio for PRB, than for Hiawatha bituminous because of the higher moisture content of PRB which acted as additional steam in the gasifier.

4.3.6 Synthesis Gas Water-Gas Shift Equilibrium

The water-gas shift equilibrium constants were calculated for the 14 in situ moisture measurements and are given on Table 4.3-6. The equilibrium constant varied from 0.54 to 0.63, which is a very tight range of equilibrium constants. The TC09 equilibrium constants had less variation and were lower than those in TC08, where the equilibrium constants varied from 0.7 to 1.0. Lower equilibrium constants would tend to have less H_2 and CO_2 and higher H_2O and CO. The WGS was constant despite the wide range of H_2O (12.3 to 38.6 percent), CO (3.2 to 10.2 percent), H_2 (5.2 to 14.7 percent), and CO_2 (10.0 to 19.7 percent) during TC09. This would indicate that the water-gas shift reaction is controlling the relative H_2, H_2O, CO, and CO_2 concentrations in the Transport Gasifier.

The thermodynamic equilibrium temperatures for each equilibrium constant were calculated from thermodynamic data and are shown on Table 4.3-6. The thermodynamic equilibrium temperature varied from 1,769 to 1,890°F. These temperatures are slightly higher than the mixing zone temperatures, which are listed in Table 4.3-6 for the sampling periods. The WGS constants calculated from the mixing zone temperatures are compared with the

measured WGS constants in Figure 4.3-19 using the same approach temperature used in Figure 4.3-13 (50°F).

The oxygen- and air-blown equilibrium constants were plotted separately on Figure 4.3-19. There is no difference in the comparison between measured and calculated equilibrium constants due to whether the Transport Gasifier is oxygen blown or air blown.

The WGS constants determined from the mixing zone temperature have slightly less variation than the measured WGS constants. Since the approach temperature of 50°F was used to curve fit the data, all points are centered around the 45 degree line on Figure 4.3-19.

4.3.7 Synthesis Gas Combustor Oxygen, Carbon, and Hydrogen Balance Calculations

The synthesis gas compositions and synthesis gas flow rate can be checked by oxygen balances, hydrogen balances, and carbon balances around the synthesis gas combustor (SGC) since the synthesis gas combustor flue gas composition is measured by the following syngas combustor flue gas analyzers (see Figure 4.3-1 for the analyzer location):

- AIT8775 - O_2
- AI476H - H_2O
- AI476D - CO_2

The synthesis gas combustor gas composition was calculated for each operating period by using synthesis gas composition synthesis gas flow rate, FI463, and the following syngas combustor flow rate tags:

- Primary air flow, FI8773
- Secondary air flow, FIC8772
- Quench air flow, FI8771
- Propane flow, FI8753

The measured and mass balance calculated O_2 values are shown in Figure 4.3-20 and Table 4.3-7. The measured and calculated synthesis gas combustor O_2 concentrations agreed very well for about half of the operating periods, with the other half up to about 1 percent difference. There was no consistent difference. The air-blown mode periods had both higher calculated oxygen and lower calculated oxygen when compared to the analyzer oxygen. The air-blown syngas combustor oxygen balances for TC07 and TC08 were better than TC09 with the differences between calculated and measured oxygen less than 0.5 percent. The air-blown syngas combustor oxygen content varied quite a bit during TC09, from 0- to 7-percent oxygen, with over 100 hours between 2- and 3-percent oxygen. For the air-blown operation, the calculated oxygen was usually higher than the measured oxygen up to hour 108. After hour 119 there was excellent agreement between the measured and calculated oxygen.

For the oxygen-blown operating periods, the calculated O_2 was from 0.5 to 0.0 percent lower than the analyzer O_2. The measured O_2 could indicate that the assumed synthesis gas

composition had more combustibles (higher LHV) than the actual synthesis gas. This was consistent with the TC08 oxygen-blown and enhanced air-blown operating periods. About half of the TC09 syngas combustor oxygen-blown mode oxygen balances were excellent. The syngas combustor oxygen balances showed that the syngas gas analyzer and syngas flow-rate data are consistent with the syngas combustor oxygen and flow-rate data.

The measured and mass balance synthesis gas combustor flue gas calculated CO_2 values are shown in Figure 4.3-21 and Table 4.3-7. The calculated CO_2 concentrations agreed well with the measured CO_2 up until hour 158, with the analyzer CO_2 up to 0.6 percent lower than the calculated CO_2. After hour 158, the difference between the measured and calculated CO_2 increased up to 2 percent during oxygen-blown mode. This implies that there is less carbon in the synthesis gas than indicated by the synthesis gas analyzers, and that the carbon conversion and LHVs may be lower than indicated by the synthesis gas analyzers. This is not consistent with the SGC O_2 analyzer data, which indicated the same amount of combustibles in the syngas than assumed from the syngas analyzers. This is the opposite of what was seen in the TC07 and TC08 SGC CO_2 analyzer and calculated CO_2 results, in that in TC07 and TC08 the SGC CO_2 analyzer was always higher than the calculated CO_2. The air-blown TC09 SGC CO_2 analyzer gave the best agreement with the calculated CO_2 in the last three runs - TC07, TC08, and TC09.

The AI475H measured and mass balance calculated H_2O values are shown in Figure 4.3-22 and Table 4.3-6. The calculated H_2O agreed very well with the analyzer H_2O for all air mode operating periods except for three periods (hours 31 to 57). For the oxygen-blown mode, the calculated H_2O was higher than the analyzer H_2O. This indicates that there was more hydrogen containing compounds (from H_2O, H_2, or CH_4) in the syngas than assumed from the gas analyzers. The good agreement between the H_2O analyzer and the calculated value is consistent with the H_2O analyzer performance in TC07 and TC08, in that the calculated and analyzer H_2O values usually agreed with each other. In the TC08 air-blown mode the H_2O calculated and analyzer values agreed with each other better than in the TC09 air-blown mode.

The results of the SGC flue gas analyzers indicate that the air-blown syngas compositions and flow rates are consistent with the syngas combustor flow rates and flue gas compositions. The oxygen-blown mode syngas combustor flow rates and flue gas compositions indicate that the syngas has less combustibles and lower LHVs than measured.

The synthesis gas LHV can be estimated by performing an energy balance around the synthesis gas combustor. The synthesis gas combustor energy balance is done by estimating the synthesis gas combustor heat loss by matching the synthesis gas LHV calculated by the synthesis gas combustor energy balance with the LHV calculated from the synthesis gas analyzer data. In some of the commissioning tests (GTC test series), the gas analyzers were not operational during the entire run, and the SGC energy balance determined LHV was used to estimate synthesis gas LHV during periods when there was no gas analyzer data. A comparison between the measured TC09 LHVs and the synthesis gas combustor energy balance LHVs using a synthesis gas combustor heat loss of 1.5×10^6 Btu/hr is given on Figure 4.3-23. This heating loss was consistent with previous test campaigns. The SGC

combustor energy balance LHVs and analyzer LHVs were very consistent with each other during both air- and oxygen-blown modes. Basically this indicates that the syngas combustor propane feed rate is consistent with the syngas LHVs.

4.3.8 Sulfur Emissions

The wet H_2S concentration measured by AI419J is plotted on Figure 4.3-24 and compared with the synthesis gas combustor SO_2 analyzer AI476N, and the synthesis gas total reduced sulfur (TRS). The sensydine H_2S measurements are also plotted on Figure 4.3-24. The AI419 analyzers measure the gas composition dry, so the values from AI419J were corrected to allow for the H_2O in the syngas. The synthesis gas combustor SO_2 analyzer, AI476N, measures the total sulfur emissions from the Transport Gasifier. The total sulfur emissions consist of H_2S, COS, and CS_2. The main sulfur species in coal gasification are considered to be H_2S and carbonyl sulfide (COS). There should also be a minor amount of carbon disulfide (CS_2). The sulfur emissions for the operating periods of TC09 are listed on Table 4.3-7. Since the synthesis gas combustor exit gas flow rate is about twice that of the synthesis gas rate during air-blown operations, the synthesis gas total reduced sulfur concentration is about twice that of the measured synthesis gas combustor SO_2 concentration during air-blown operations. During oxygen-blown operations the synthesis gas combustor flue gas rate is about three times the synthesis gas rate, so the syngas TRS is about three times the synthesis gas combustor SO_2 concentration. The H_2S analyzer AI419J was equal to or less than the TRS during air-blown mode. The operating periods when the AI419J was equal to the TRS would indicate zero COS and CS_2 emissions. Operating periods when the AI419J was less than the TRS would indicate that there was some COS and CS_2 emissions. During the oxygen-blown operation, AI419J was about equal to the TRS, which indicated no COS and CS_2 emissions. It is expected that there should be about 100 ppm of COS emissions, based on previous work on other gasifiers. Since TC09 AI419J readings are not always consistent with AI476N, H_2S analyzer AI419J data will not be used for the remainder of this report.

The Sensydine H_2S measurements were consistently higher than both the AI419J H_2S and the TRS data except for one data point at hour 56. The Sensydine H_2S was consistent with both the TRS and AI419J H_2S data up until hour 133 when it was 50 ppm higher. By the end of the air-blown testing, the Sensydine H_2S was 100 ppm higher than the TRS and the AI419J H_2S. During the oxygen-blown testing the Sensydine H_2S was 200 to 300 ppm higher than the AI419J H_2S and TRS. It would appear that the accuracy of the Sensydine H_2S decreases at higher H_2S concentrations.

TC09 was operated without sorbent addition for the entire run to determine the amount of sulfur removal that could be obtained by the Hiawatha bituminous ash alkalinity. This will be discussed further in Section 4.5.

The TRS emission began the run at about 350 ppm and then decreased to 200 ppm for two operating periods at 52 and 57 hours. The TRS was then constant at 300 ppm from hour 64 to 171. The TRS then increased to 375 ppm at hour 175 and was constant until the end of the air-blown mode. During the oxygen-blown mode testing, the TRS slowly increased from

450 to nearly 600 ppm. For the final periods of air-blown mode, the TRS decreased to 350 ppm.

In Figure 4.3-25, the Sensydine COS emissions are compared with the COS determined by the difference in the TRS and the AI419J H_2S measurements. Since the TRS is expected to consist of H_2S, COS, and CS_2, and the CS_2 is considered to be low, the difference between the TRS and the H_2S should give a good estimate of the COS concentration. The Sensydine COS data varied from 25 to 200 ppm during air-blown mode, and between 83 to 214 ppm in oxygen-blown mode. The COS by difference started TC09 at 175 ppm, quickly increased to 240 ppm at hour 13 and then decreased to 14 ppm at hour 52. The COS by difference remained below 50 ppm (with one outlier) until hour 199 when the COS by difference increased to 150 ppm. The COS by difference was less than zero from hour 226 to 281 because the AI419J H_2S was larger than the TRS. At the end of the oxygen-blown and the last air-blown operating periods, the COS by difference was less than 25 ppm.

Since the COS is expected to be about 10 percent of the TRS in the syngas, the COS by difference data looks reasonable when the COS is around 30 ppm. Periods when the COS by difference was higher than 50 ppm was when AI419J was reading much lower than the TRS, and probably was due to errors in the AI419J reading. Only two (hours 134 and 182) of the Sensydine COS readings seemed reasonable. It would appear that the Sensydine COS readings were high for most of TC09.

Table 4.3-1

Operating Periods

Operating Period	Start Time	End Time	Duration Hours	Operating Period Average Time	Operating Period Relative Hours
TC09A-1	9/5/2002 4:45	9/5/2002 6:45	2.00	9/5/2002 6:00	7
TC09A-2	9/5/2002 8:15	9/5/2002 10:00	1.75	9/5/2002 9:07	10
TC09A-3	9/5/2002 11:00	9/5/2002 12:30	1.50	9/5/2002 12:00	13
TC09A-4	9/5/2002 15:30	9/5/2002 17:45	2.25	9/5/2002 16:37	18
TC09B-1	9/9/2002 23:15	9/10/2002 0:45	1.50	9/10/2002 0:00	26
TC09B-2	9/10/2002 3:30	9/10/2002 6:30	3.00	9/10/2002 5:30	31
TC09B-3	9/10/2002 23:15	9/11/2002 5:15	6.00	9/11/2002 2:15	52
TC09B-4	9/11/2002 5:30	9/11/2002 8:45	3.25	9/11/2002 7:07	57
TC09B-5	9/11/2002 12:15	9/11/2002 15:15	3.00	9/11/2002 13:45	64
TC09B-6a	9/11/2002 20:00	9/12/2002 6:30	10.50	9/12/2002 1:15	75
TC09B-6b	9/12/2002 6:30	9/12/2002 17:30	11.00	9/12/2002 12:00	86
TC09B-7a	9/12/2002 22:15	9/13/2002 6:30	8.25	9/13/2002 2:22	100
TC09B-7b	9/13/2002 6:30	9/13/2002 14:30	8.00	9/13/2002 10:30	108
TC09B-8	9/13/2002 16:30	9/14/2002 2:00	9.50	9/13/2002 21:15	119
TC09B-8b	9/14/2002 2:00	9/14/2002 12:00	10.00	9/14/2002 7:00	129
TC09B-9	9/14/2002 19:00	9/15/2002 2:00	7.00	9/14/2002 22:45	144
TC09B-10	9/15/2002 3:00	9/15/2002 7:30	4.50	9/15/2002 5:15	151
TC09B-11	9/15/2002 8:00	9/15/2002 16:00	8.00	9/15/2002 12:00	158
TC09B-12	9/15/2002 23:15	9/16/2002 3:30	4.25	9/16/2002 1:22	171
TC09B-13	9/16/2002 4:30	9/16/2002 6:15	1.75	9/16/2002 5:37	175
TC09B-14	9/16/2002 11:00	9/16/2002 13:15	2.25	9/16/2002 12:07	182
TC09C-1	9/21/2002 22:15	9/22/2002 2:00	3.75	9/21/2002 23:45	196
TC09C-2	9/22/2002 2:15	9/22/2002 4:00	1.75	9/22/2002 3:07	199
TC09C-3	9/22/2002 9:30	9/22/2002 11:00	1.50	9/22/2002 10:45	206
TC09C-4	9/22/2002 12:30	9/22/2002 14:15	1.75	9/22/2002 13:22	209
TC09C-5	9/23/2002 4:00	9/23/2002 7:30	3.50	9/23/2002 5:45	226
TC09C-6	9/23/2002 7:45	9/23/2002 11:45	4.00	9/23/2002 9:45	230
TC09C-7	9/23/2002 19:15	9/24/2002 5:30	10.25	9/24/2002 0:22	244
TC09C-8	9/24/2002 11:00	9/24/2002 13:30	2.50	9/24/2002 12:15	256
TC09C-9	9/24/2002 13:45	9/25/2002 1:15	11.50	9/24/2002 20:22	264
TC09C-10	9/25/2002 1:30	9/25/2002 5:30	4.00	9/25/2002 3:15	271
TC09C-11	9/25/2002 9:00	9/25/2002 11:15	2.25	9/25/2002 10:07	278
TC09C-12	9/25/2002 11:30	9/25/2002 14:45	3.25	9/25/2002 13:07	281
TC09C-13	9/25/2002 21:15	9/26/2002 6:15	9.00	9/26/2002 2:07	294
TC09C-14	9/26/2002 8:00	9/26/2002 9:00	1.00	9/26/2002 8:30	301
TC09C-15	9/26/2002 9:15	9/26/2002 10:30	1.25	9/26/2002 9:52	302
TC09C-16	9/26/2002 13:30	9/26/2002 16:30	3.00	9/26/2002 14:30	307

Note: TC09A, TC09B, TC09C-1 to TC09C-4, and TC09C-16 were air blown;
TC09C-5 to TC09C-15 were oxygen blown.

Table 4.3-2

Operating Conditions

Operating Periods	Average Relative Hours	Mixing Zone Temperature TI368 °F	Pressure PI287 psig	PCD Inlet Temperature TI458 °F	Air Rate lb/hr	Oxygen Rate lb/hr	Synthesis Gas Rate lb/hr	Steam Rate lb/hr	Nitrogen Rate[1] lb/hr
TC09A-1	7	1,724	200	881	12,235	0	23,905	3,379	5,772
TC09A-2	10	1,754	200	845	12,466	0	22,955	2,238	5,653
TC09A-3	13	1,761	200	808	11,034	0	21,293	2,211	6,020
TC09A-4	18	1,792	202	796	10,093	0	18,847	1,540	5,573
TC09B-1	26	1,765	184	795	9,514	0	19,106	1,772	6,578
TC09B-2	31	1,789	200	796	10,893	0	20,701	1,988	6,051
TC09B-3	52	1,777	200	909	10,070	0	22,238	4,936	6,593
TC09B-4	57	1,775	200	921	10,350	0	22,965	5,424	6,231
TC09B-5	64	1,774	200	924	10,171	0	21,110	3,262	5,789
TC09B-6a	75	1,771	200	900	10,755	0	21,582	3,675	5,234
TC09B-6b	86	1,770	200	901	10,789	0	21,541	3,814	5,091
TC09B-7a	100	1,755	200	918	10,555	0	21,575	3,896	5,489
TC09B-7b	108	1,756	200	917	10,539	0	21,229	3,705	5,163
TC09B-8a	119	1,779	200	899	11,115	0	21,844	3,535	5,359
TC09B-8b	129	1,782	200	894	10,834	0	21,208	3,475	5,264
TC09B-9	144	1,787	200	916	11,935	0	24,278	4,204	6,035
TC09B-10	151	1,794	200	908	11,606	0	22,990	3,915	5,631
TC09B-11	158	1,782	200	902	11,335	0	22,626	3,862	5,554
TC09B-12	171	1,792	200	863	10,437	0	20,578	3,237	5,371
TC09B-13	175	1,786	200	876	11,352	0	22,056	3,646	5,403
TC09B-14	182	1,814	200	868	11,120	0	20,664	2,955	4,961
TC09C-1	196	1,795	200	821	11,214	0	21,819	3,168	6,052
TC09C-2	199	1,793	200	814	11,611	0	22,553	3,212	6,083
TC09C-3	206	1,806	220	798	11,338	0	21,226	2,923	5,388
TC09C-4	209	1,810	240	777	10,852	0	20,077	2,512	5,114
TC09C-5	226	1,774	150	811	0	2,015	15,528	4,639	6,377
TC09C-6	230	1,774	150	814	0	2,015	15,155	4,901	6,108
TC09C-7	244	1,781	160	789	0	1,857	14,389	4,627	6,007
TC09C-8	256	1,795	160	785	0	1,870	14,002	4,437	5,816
TC09C-9	264	1,812	160	765	0	1,869	13,879	4,233	5,972
TC09C-10	271	1,815	160	762	0	1,869	14,075	4,297	6,004
TC09C-11	278	1,824	160	771	0	2,061	14,511	4,417	5,810
TC09C-12	281	1,831	160	768	0	2,111	14,756	4,461	5,921
TC09C-13	294	1,826	160	773	0	2,060	14,617	4,251	6,065
TC09C-14	301	1,851	160	783	0	2,275	15,080	4,455	6,109
TC09C-15	302	1,848	160	779	0	2,139	14,592	4,401	5,908
TC09C-16	307	1,842	220	805	10,443	0	18,048	1,690	4,585

Notes:
1. Nitrogen feed rate reduced by 1,250 lb/hr for air blown and 0 lb/hr for oxygen blown to account for losses in feed systems and seals.
2. TC09A, TC09B, TC09C-1 to TC09C-16 were air blown; TC09C-5 to TC09C-15 were oxygen blown.

Table 4.3-3 Gas Analyzer Choices

Operating Periods	Average Relative Hours	Gas Compound					
		CO	H_2	CO_2	CH_4	C_2^+	N_2
TC09A-1	7	453	419	434	419	419	419
TC09A-2	10	425	419[2]	434[2]	419[2]	419	419
TC09A-3	13	425	419	434	419	419	419
TC09A-4	18	419	419	434	419	419	419
TC09B-1	26	453	419	419	419	419	419
TC09B-2	31	453	419	434	419	419	419
TC09B-3	52	453	464	419	419	419	419
TC09B-4	57	453	464[2]	419	419	419	419
TC09B-5	64	425	464	419	419	419	464
TC09B-6a	75	425	464	419	419	419	464
TC09B-6b	86	425	419	419	419	419	464
TC09B-7a	100	453	464	464	464	419	464[2]
TC09B-7b	108	425	464[2]	464	419	419	464
TC09B-8a	119	425	464	464	419	419	464
TC09B-8b	129	425	464	464	419	419	464
TC09B-9	144	425	464	464	419	419	464
TC09B-10	151	425	464	464	419	419	464
TC09B-11	158	425	464	464	419	419	464
TC09B-12	171	453	464	464	419	419	464
TC09B-13	175	453	464	464	419	419	464
TC09B-14	182	453	464	464	419	419	464
TC09C-1	196	453	464	464	419	419	419
TC09C-2	199	453	464	464	419	419	419
TC09C-3	206	453	464	464	419	419	419
TC09C-4	209	453	464	464	419	419	419
TC09C-5	226	425	419	464[2]	419	419	419
TC09C-6	230	425	419	419	419	464	419
TC09C-7	244	453	419	464	419	464	419
TC09C-8	256	453	419	464	419	464	419
TC09C-9	264	453	419	464	419	464	419
TC09C-10	271	464	419	464	419	464	419
TC09C-11	278	464	419	419	419	464	419
TC09C-12	281	464	419	419	419	464	419
TC09C-13	294	464	419	419	419	464	419
TC09C-14	301	464	419	419	419	464	419
TC09C-15	302	464	419	419	419	464	419
TC09C-16	307	464	419	419	419	464	419

Notes:
1. H_2O calculated from water-gas shift equilibrium using T1368, and H_2, CO, and CO_2 data.
2. Data interpolated from neighboring operating periods.

Table 4.3-4 Gas Compositions, Molecular Weight, and Heating Value

Operating Period	Average Relative Hour	H_2O Mole %	CO Mole %	H_2 Mole %	CO_2 Mole %	CH_4 Mole %	C_2H_6 Mole %	N_2 Mole %	Total Mole %	Syngas LHV Btu/SCF	Syngas TRS[1] ppm	Syngas MW lb./Mole	O_2 in Feed %	Syngas CO/CO_2 Ratio
TC09A-1	7	18.1	4.8	5.5	9.9	2.0	0.3	59.4	100.0	53	337	26.1	10.9	0.5
TC09A-2	10	12.0	7.3	5.8	9.1	2.1	0.3	63.6	100.0	62	294	26.5	11.9	0.8
TC09A-3	13	13.7	5.8	5.3	8.9	1.8	0.3	64.2	100.0	54	339	26.5	11.1	0.7
TC09A-4	18	12.1	5.8	4.6	8.7	1.4	0.3	67.2	100.0	49	306	26.8	11.5	0.7
TC09B-1	26	12.9	4.4	4.0	8.5	1.4	0.3	68.6	100.0	42	233	26.9	10.3	0.5
TC09B-2	31	13.5	5.7	4.9	8.9	1.6	0.2	65.1	100.0	50	332	26.6	11.1	0.6
TC09B-3	52	30.4	1.6	3.7	7.8	0.6	0.1	55.7	100.0	23	192	25.2	8.5	0.2
TC09B-4	57	32.4	1.4	3.4	7.8	0.5	0.2	54.2	100.0	22	195	25.1	8.5	0.2
TC09B-5	64	22.3	2.8	4.0	9.0	1.0	0.2	60.7	100.0	33	283	26.1	10.0	0.3
TC09B-6a	75	23.1	3.4	4.8	9.4	1.3	0.2	57.7	100.0	40	283	25.8	10.2	0.4
TC09B-6b	86	24.2	3.2	4.8	9.5	1.3	0.2	56.7	100.0	39	297	25.7	10.2	0.3
TC09B-7a	100	24.5	2.9	4.5	9.4	1.1	0.2	57.4	100.0	35	271	25.7	9.8	0.3
TC09B-7b	108	23.7	3.1	4.6	9.3	1.2	0.2	57.9	100.0	37	275	25.8	10.1	0.3
TC09B-8a	119	21.9	3.6	4.9	9.3	1.3	0.2	58.8	100.0	41	288	25.9	10.4	0.4
TC09B-8b	129	22.2	3.5	4.8	9.3	1.3	0.2	58.6	100.0	40	287	25.9	10.4	0.4
TC09B-9	144	23.6	3.2	4.8	9.1	1.2	0.2	57.8	100.0	38	302	25.7	10.0	0.3
TC09B-10	151	22.7	3.6	5.0	9.3	1.3	0.2	57.9	100.0	41	304	25.8	10.3	0.4
TC09B-11	158	23.1	3.5	5.0	9.3	1.4	0.2	57.5	100.0	41	312	25.7	10.2	0.4
TC09B-12	171	21.3	3.7	5.0	9.1	1.2	0.2	59.4	100.0	41	287	25.9	10.3	0.4
TC09B-13	175	21.3	4.2	5.5	9.3	1.6	0.2	57.9	100.0	47	372	25.7	10.4	0.4
TC09B-14	182	19.1	4.7	5.4	9.3	1.4	0.3	59.7	100.0	47	394	26.0	11.1	0.5
TC09C-1	196	19.0	4.4	5.2	9.2	1.4	0.2	60.5	100.0	45	373	26.1	10.4	0.5
TC09C-2	199	18.6	4.5	5.3	9.1	1.4	0.2	60.8	100.0	46	358	26.1	10.6	0.5
TC09C-3	206	18.0	5.1	5.6	9.2	1.5	0.2	60.3	100.0	49	356	26.0	11.0	0.6
TC09C-4	209	16.4	5.8	5.7	9.3	1.5	0.2	61.0	100.0	52	378	26.2	11.3	0.6
TC09C-5	226	36.2	4.5	7.5	12.6	2.1	0.2	36.9	100.0	57	462	24.2	11.5	0.4
TC09C-6	230	39.2	4.1	7.8	12.2	2.0	0.2	34.5	100.0	56	453	23.8	11.4	0.3
TC09C-7	244	37.9	4.4	8.1	11.9	2.0	0.2	35.6	100.0	58	475	23.8	11.0	0.4
TC09C-8	256	37.5	4.6	8.2	12.0	2.0	0.2	35.6	100.0	58	487	23.8	11.4	0.4
TC09C-9	264	36.2	4.9	8.4	11.8	1.9	0.2	36.7	100.0	60	483	23.9	11.5	0.4
TC09C-10	271	36.2	4.9	8.4	11.9	1.9	0.2	36.5	100.0	60	475	23.9	11.4	0.4
TC09C-11	278	35.7	6.0	9.2	12.7	2.2	0.2	34.0	100.0	68	524	23.8	12.5	0.5
TC09C-12	281	35.2	6.2	9.4	12.7	2.3	0.2	34.0	100.0	70	547	23.8	12.6	0.5
TC09C-13	294	33.8	6.4	9.4	12.6	2.3	0.2	35.3	100.0	71	532	23.9	12.4	0.5
TC09C-14	301	33.8	7.1	10.0	12.7	2.4	0.2	33.8	100.0	76	578	23.8	13.2	0.6
TC09C-15	302	34.7	6.6	9.6	12.6	2.2	0.2	34.1	100.0	72	524	23.8	12.8	0.5
TC09C-16	307	13.4	7.1	5.6	9.1	1.6	0.1	63.2	100.0	55	340	26.5	12.2	0.8

Notes:

1. Synthesis gas total reduced sulfur (TRS) estimated from Synthesis gas combustor SO_2 analyzer data.
2. TC09A, TC09B, TC09C-1 to TC09C-4, and TC09C-16 were air blown; TC09C-5 to TC09C-15 were oxygen blown.

Table 4.3-5 Corrected[1] Gas Compositions, Molecular Weight, and Heating Value

Operating Period	Average Relative Hour	H_2O Mole %	CO Mole %	H_2 Mole %	CO_2 Mole %	CH_4 Mole %	C_2H_6 Mole %	N_2 Mole %	Total Mole %	Syngas LHV Btu/SCF	Syngas MW lb./Mole	O_2 in Feed %	Syngas CO/CO_2 Ratio
TC09A-1	7	27.9	7.9	9.1	12.5	3.3	0.4	39.0	100.0	87	24.5	12.6	0.6
TC09A-2	10	18.5	12.4	9.8	11.3	3.5	0.4	44.0	100.0	106	25.0	14.7	1.1
TC09A-3	13	22.8	10.6	9.7	11.4	3.3	0.5	41.7	100.0	99	24.6	13.8	0.9
TC09A-4	18	20.7	11.2	8.9	11.1	2.8	0.5	44.9	100.0	94	25.1	14.9	1.0
TC09B-1	26	24.5	9.5	8.5	11.7	2.9	0.6	42.3	100.0	91	24.9	13.6	0.8
TC09B-2	31	22.5	10.5	9.1	11.5	2.9	0.4	43.1	100.0	92	24.9	14.3	0.9
TC09B-3	52	50.4	2.8	6.4	9.0	1.0	0.2	30.0	100.0	40	22.6	8.8	0.3
TC09B-4	57	52.2	2.3	5.7	9.0	0.9	0.3	29.5	100.0	37	22.6	8.6	0.3
TC09B-5	64	38.3	5.1	7.3	11.5	1.8	0.4	35.5	100.0	60	23.9	11.1	0.4
TC09B-6a	75	36.4	5.5	8.0	11.5	2.1	0.4	36.0	100.0	66	23.9	11.3	0.5
TC09B-6b	86	37.3	5.2	7.8	11.5	2.0	0.4	35.9	100.0	62	23.9	11.2	0.4
TC09B-7a	100	38.8	4.8	7.6	11.5	1.8	0.4	35.2	100.0	58	23.8	10.8	0.4
TC09B-7b	108	37.5	5.1	7.7	11.4	1.9	0.4	36.0	100.0	61	23.9	11.1	0.4
TC09B-8a	119	34.5	5.9	8.1	11.3	2.2	0.4	37.5	100.0	67	24.0	11.7	0.5
TC09B-8b	129	34.9	5.8	8.0	11.3	2.1	0.4	37.6	100.0	66	24.0	11.7	0.5
TC09B-9	144	37.2	5.3	7.8	11.2	2.1	0.4	36.1	100.0	63	23.8	11.2	0.5
TC09B-10	151	35.1	5.8	8.1	11.3	2.1	0.4	37.2	100.0	66	23.9	11.5	0.5
TC09B-11	158	35.8	5.7	8.2	11.3	2.2	0.4	36.6	100.0	67	23.8	11.4	0.5
TC09B-12	171	34.1	6.3	8.4	11.2	2.1	0.4	37.5	100.0	69	23.9	11.7	0.6
TC09B-13	175	32.6	6.7	8.9	11.2	2.6	0.4	37.7	100.0	75	23.9	11.8	0.6
TC09B-14	182	29.3	7.7	8.8	11.1	2.3	0.4	40.4	100.0	77	24.3	12.8	0.7
TC09C-1	196	30.4	7.5	8.8	11.4	2.4	0.4	39.1	100.0	76	24.2	12.3	0.7
TC09C-2	199	29.7	7.7	9.0	11.4	2.4	0.4	39.5	100.0	78	24.2	12.4	0.7
TC09C-3	206	27.8	8.4	9.2	11.2	2.4	0.4	40.6	100.0	80	24.3	12.9	0.7
TC09C-4	209	25.4	9.6	9.5	11.3	2.5	0.4	41.4	100.0	86	24.5	13.4	0.9
TC09C-5	226	37.6	12.0	20.1	24.2	5.6	0.5	0.0	100.0	153	22.2	19.6	0.5
TC09C-6	230	42.7	10.4	19.5	22.0	5.0	0.5	0.0	100.0	140	21.6	18.8	0.5
TC09C-7	244	40.5	11.3	21.0	21.5	5.2	0.5	0.0	100.0	150	21.3	19.0	0.5
TC09C-8	256	39.5	11.9	21.2	21.7	5.1	0.5	0.0	100.0	152	21.4	19.2	0.5
TC09C-9	264	36.8	13.1	22.5	21.7	5.3	0.5	0.0	100.0	161	21.3	19.8	0.6
TC09C-10	271	36.6	13.2	22.4	22.0	5.2	0.5	0.0	100.0	160	21.4	19.7	0.6
TC09C-11	278	37.1	14.0	21.4	21.8	5.2	0.5	0.0	100.0	160	21.6	20.8	0.6
TC09C-12	281	36.4	14.5	21.8	21.5	5.3	0.5	0.0	100.0	163	21.5	21.0	0.7
TC09C-13	294	34.2	15.3	22.6	21.8	5.6	0.5	0.0	100.0	171	21.5	21.4	0.7
TC09C-14	301	35.1	15.9	22.5	20.8	5.3	0.5	0.0	100.0	170	21.4	22.3	0.8
TC09C-15	302	35.8	15.2	22.3	21.1	5.1	0.5	0.0	100.0	165	21.4	21.5	0.7
TC09C-16	307	19.9	11.6	9.1	10.8	2.6	0.2	45.7	100.0	90	25.1	15.2	1.1

Notes:

1. Correction is to assume that only air nitrogen is in the synthesis gas and that the reactor is adiabatic
2. TC09A, TC09B, TC09C-1 to TC09C-4, and TC09C-16 were air blown; TC09C-5 to TC09C-15 were oxygen blown.

Table 4.3-6

Water-Gas Shift Equilibrium Constant

Table 4.3-6 Water Gas Shift Equilibrium Constant

In situ Start	In situ End	Average Run Time Hours	Operating Periods	CO %	H_2 %	CO_2 %	In-situ H_2O %	Kp	WGS Eqm. Temp. F	Mixing Zone Temp. F	Mixing Zone Kp^2
9/5/2002 9:00	9/5/2002 13:00	12	TC09A-2	7.37	6.25	9.98	12.3	0.60	1,801	1,761	0.60
9/10/2002 8:40	9/10/2002 10:40	36	(1)	3.22	5.62	13.38	30.3	0.54	1,890	1,787	0.58
9/11/2002 10:00	9/11/2002 14:00	62	TC09B-5	3.57	5.18	11.59	22.9	0.57	1,849	1,775	0.58
9/12/2002 9:00	9/12/2002 13:00	85	TC09B-6b	4.20	6.24	12.44	25.6	0.54	1,890	1,774	0.59
9/13/2002 10:00	9/13/2002 14:07	110	TC09B-7b	4.01	5.98	11.96	24.4	0.55	1,869	1,759	0.60
9/14/2002 8:30	9/14/2002 12:30	132	TC09B-8b	4.50	6.24	12.00	21.3	0.61	1,789	1,781	0.58
9/16/2002 9:00	9/16/2002 13:00	181	TC09B-14	5.57	6.51	11.40	18.5	0.59	1,822	1,808	0.56
9/22/2002 8:30	9/22/2002 12:30	207	TC09C-3	5.74	6.15	10.24	14.8	0.63	1,769	1,803	0.56
9/23/2002 8:30	9/23/2002 12:30	231	TC09C-6	7.19	12.83	19.27	38.5	0.55	1,873	1,774	0.59
9/24/2002 10:50	9/24/2002 12:50	256	TC09C-8	7.39	13.06	19.18	38.6	0.54	1,887	1,795	0.57
9/25/2002 8:30	9/25/2002 10:30	277	TC09C-11	8.99	14.07	19.72	34.5	0.59	1,823	1,822	0.55
9/25/2002 13:30	9/25/2002 15:30	283	TC09C-12	9.67	14.13	18.89	33.8	0.54	1,885	1,834	0.54
9/26/2002 8:50	9/26/2002 10:50	302	TC09C-15	10.19	14.73	18.88	32.2	0.57	1,838	1,846	0.53
9/26/2002 13:45	9/26/2002 14:45	306	TC09C-16	7.99	6.45	10.41	12.4	0.59	1,814	1,841	0.54

Notes:

1. Data not taken during operating period.
2. Equilibrium constant calculated at mixing zone temperature (TI368), with an 50ºF approach.
3. September 5 to 16 and 26 p.m. data taken during air operation. September 22 to 26 a.m. data taken during oxygen operation.

Table 4.3-7 Synthesis Gas Combustor Calculations

Operating Period	Average Relative Hour	AIT8775 SGC Exit O_2 M %	Calculated SGC Exit O_2 M %	AI476D SGC Exit CO_2 M %	Calculated SGC Exit CO_2 M %	AI476H SGC Exit H_2O M %	Calculated SGC Exit H2O M %	Gas Analyzer LHV Btu/SCF	Energy Balance LHV[1] Btu/SCF	Combustor SO_2 AI476N ppm	Syngas Total Reduced Sulfur[2] ppm
TC09A-1	7	5.9	6.4	7.6	8.2	15.3	14.4	54	57	145	337
TC09A-2	10	6.0	6.2	7.9	8.8	13.5	11.8	49	62	129	294
TC09A-3	13	5.9	6.7	7.8	7.9	13.3	12.1	42	59	143	339
TC09A-4	18	6.0	7.2	7.7	7.6	12.3	10.8	50	57	123	306
TC09B-1	26	6.0	6.3	7.0	7.8	12.4	11.9	23	37	85	233
TC09B-2	31	0.1	0.0	12.0	12.3	15.9	17.2	22	45	236	332
TC09B-3	52	6.0	5.9	6.3	6.7	17.6	19.7	33	22	84	192
TC09B-4	57	6.1	5.8	6.2	6.7	19.0	20.7	40	19	87	195
TC09B-5	64	5.8	6.6	7.2	7.3	16.2	15.5	39	37	117	283
TC09B-6a	75	6.0	6.4	7.1	7.6	16.7	16.4	35	41	120	283
TC09B-6b	86	6.0	6.7	7.3	7.4	17.1	16.6	37	43	124	297
TC09B-7a	100	6.1	6.7	6.8	7.3	16.9	16.4	41	38	110	271
TC09B-7b	108	6.0	6.6	6.9	7.4	17.3	16.2	40	39	112	275
TC09B-8a	119	3.7	3.7	8.5	9.1	19.1	18.9	38	41	162	288
TC09B-8b	129	3.0	2.7	9.0	9.6	20.2	20.2	41	39	176	287
TC09B-9	144	2.1	1.9	9.1	9.7	22.5	22.2	41	40	201	302
TC09B-10	151	2.0	1.7	9.4	10.1	21.8	22.0	41	41	205	304
TC09B-11	158	1.9	2.2	9.3	9.7	22.0	21.7	47	44	203	312
TC09B-12	171	2.0	1.7	9.2	10.1	20.5	20.9	47	42	193	287
TC09B-13	175	1.8	1.7	9.4	10.3	20.4	21.0	45	47	240	372
TC09B-14	182	2.0	2.5	9.8	10.2	18.7	18.6	46	49	242	394
TC09C-1	196	2.9	2.3	8.8	10.1	17.6	18.7	49	42	227	373
TC09C-2	199	2.8	2.1	8.9	10.2	17.6	18.6	52	44	224	358
TC09C-3	206	2.8	2.5	9.2	10.3	17.2	18.0	57	48	220	356
TC09C-4	209	3.0	2.6	9.4	10.5	16.4	16.8	56	50	227	378
TC09C-5	226	2.9	2.8	9.2	11.5	25.0	29.0	57	58	264	462
TC09C-6	230	5.5	5.5	8.4	9.3	24.1	26.0	58	57	208	446
TC09C-7	244	6.1	5.8	8.1	9.0	23.6	24.7	60	56	202	457
TC09C-8	256	6.0	5.5	8.1	9.3	23.3	24.9	60	56	210	470
TC09C-9	264	5.9	5.3	8.1	9.4	23.1	24.4	68	56	216	479
TC09C-10	271	5.9	5.3	7.9	9.5	22.9	24.4	70	57	213	472
TC09C-11	278	6.0	5.8	8.4	9.9	22.5	24.0	71	68	234	524
TC09C-12	281	6.2	6.0	8.2	9.7	21.6	23.3	76	70	237	547
TC09C-13	294	6.8	7.0	7.7	9.0	20.0	20.9	72	71	205	532
TC09C-14	301	6.1	6.3	8.2	9.7	20.9	22.2	55	75	242	578
TC09C-15	302	6.0	5.9	8.1	9.8	21.9	23.3	22	71	230	524
TC09C-16	307	4.8	5.0	8.5	9.5	13.5	13.0	62	55	172	340

Notes:

1. Energy LHV calcualted assuming the sythesis gas combustor heat loss was 1.5 x 10^6 Btu/hr.
2. Synthesis gas total reduced sulfur (TRS) estimated from Synthesis gas combustor SO_2 analyzer data
3. TC09A, TC09B, TC09C-1 to TC09C-4, and TC09C-16 were air blown; TC09C-5 to TC09C-15 were oxygen blown.

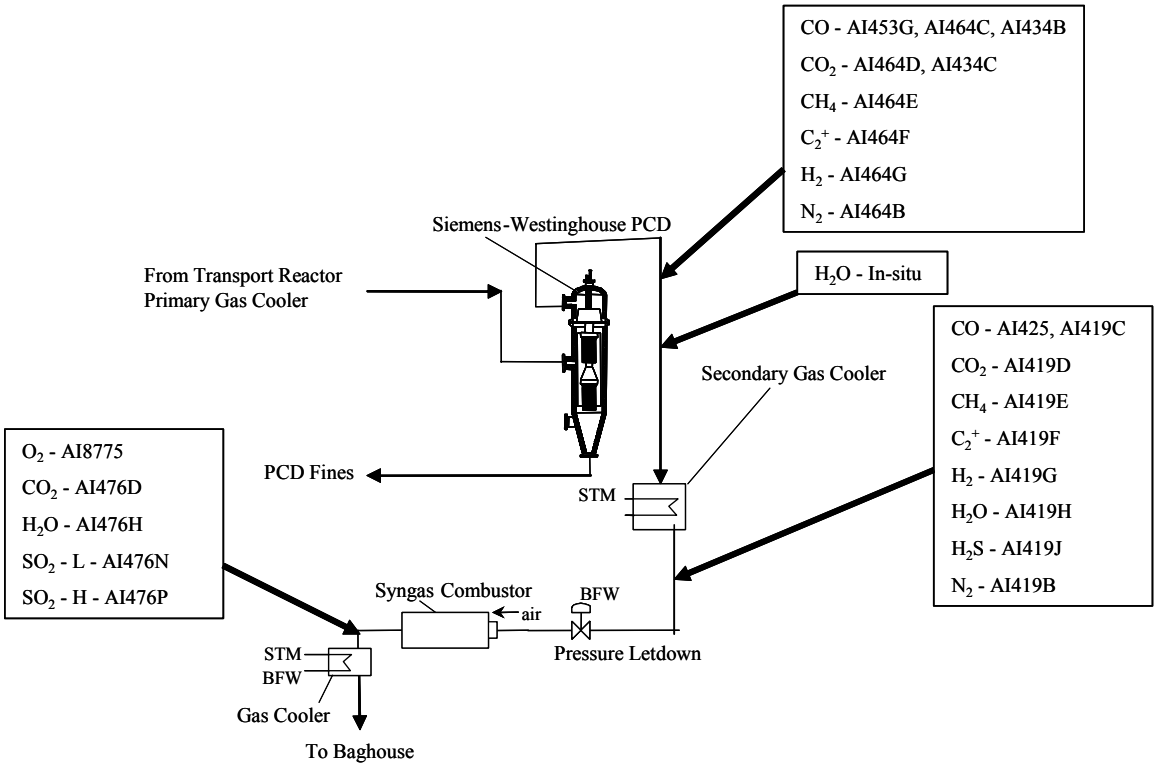

Figure 4.3-1 Gas Sampling Locations

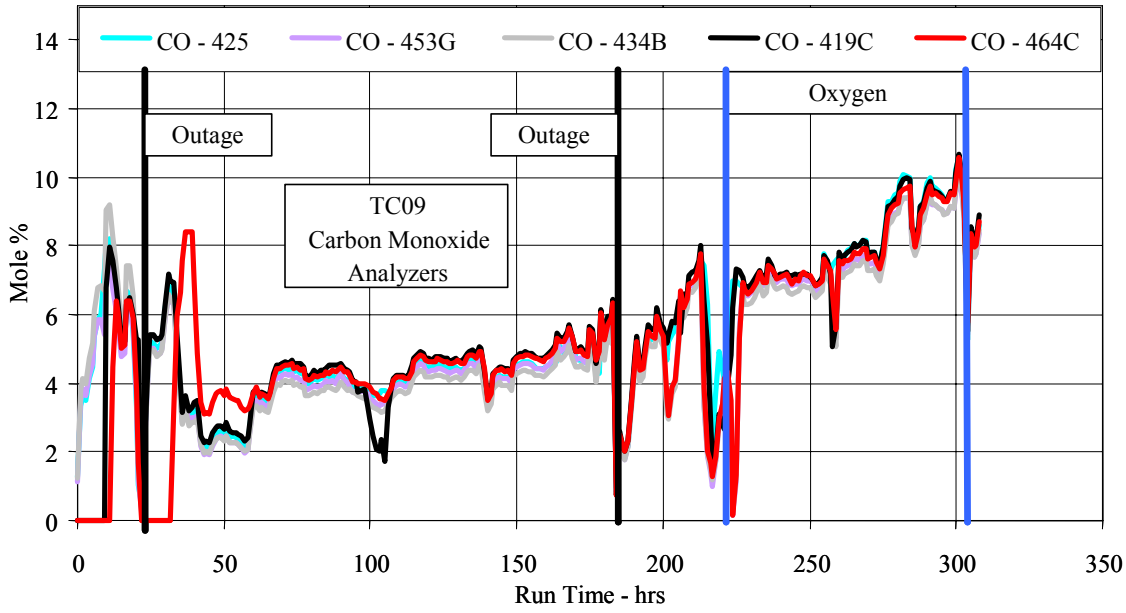

Figure 4.3-2 CO Analyzer Data

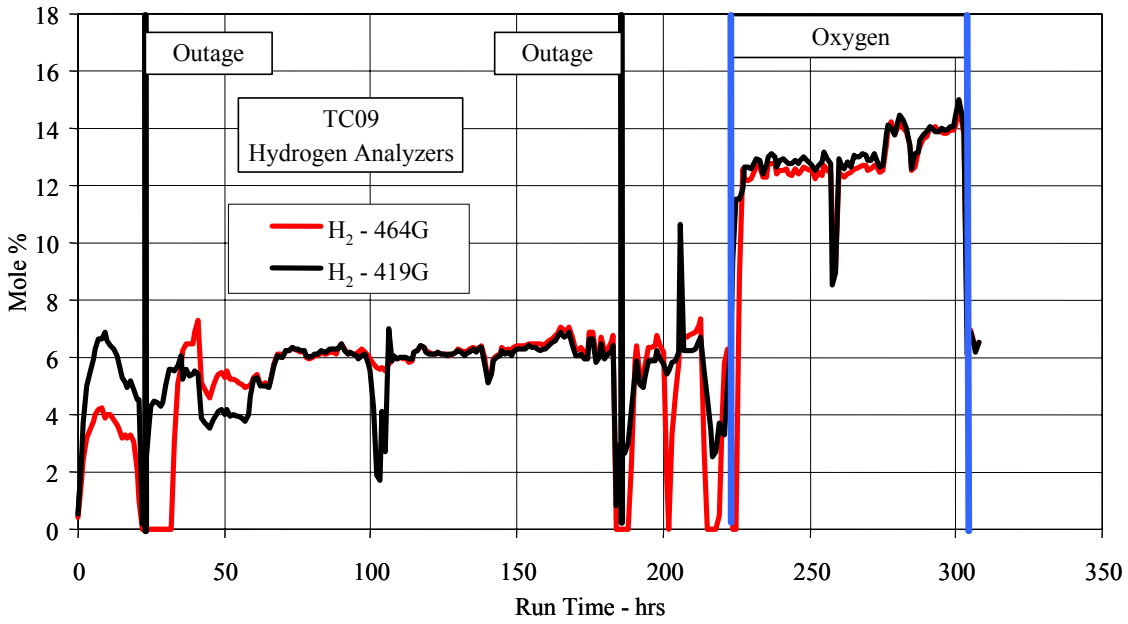

Figure 4.3-3 Analyzer H_2 Data

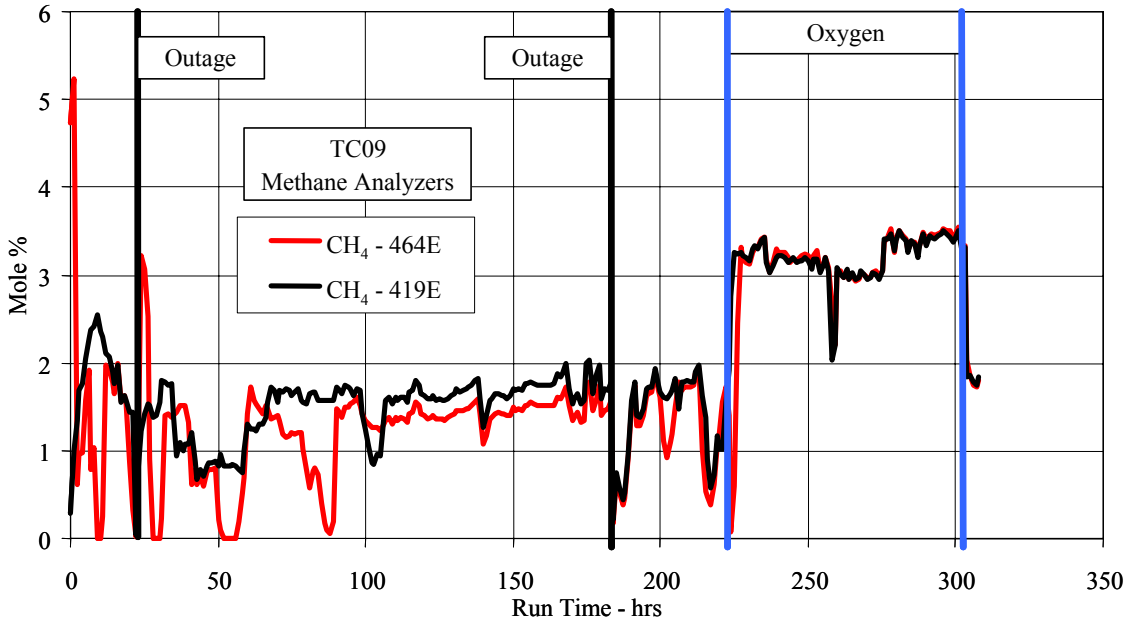

Figure 4.3-4 Analyzer CH_4 Data

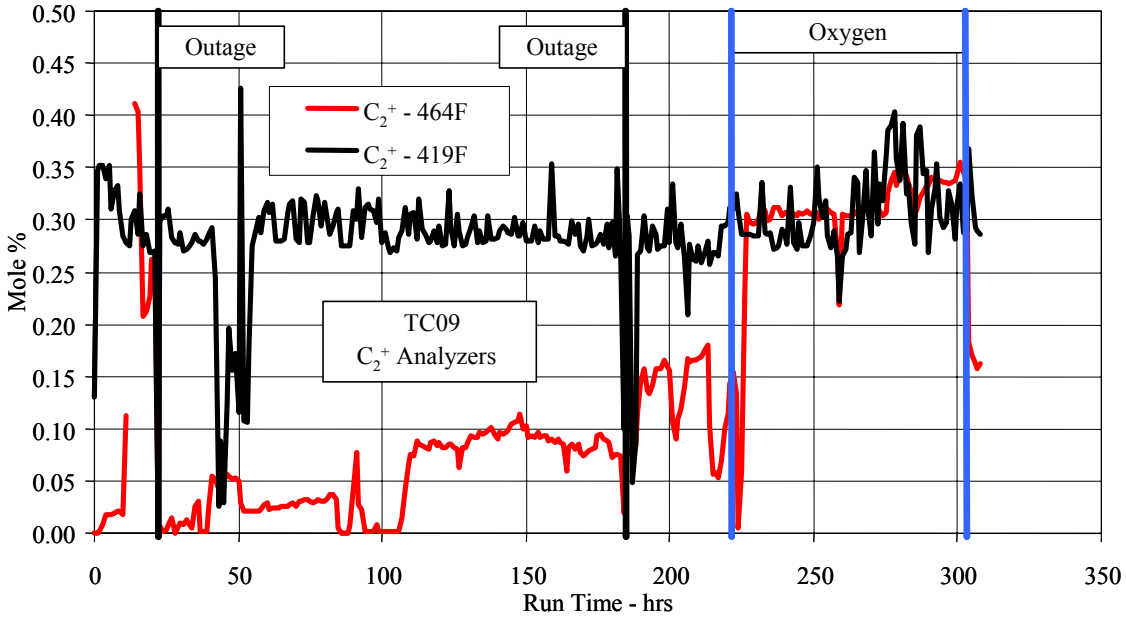

Figure 4.3-5 Analyzer C_2+ Data

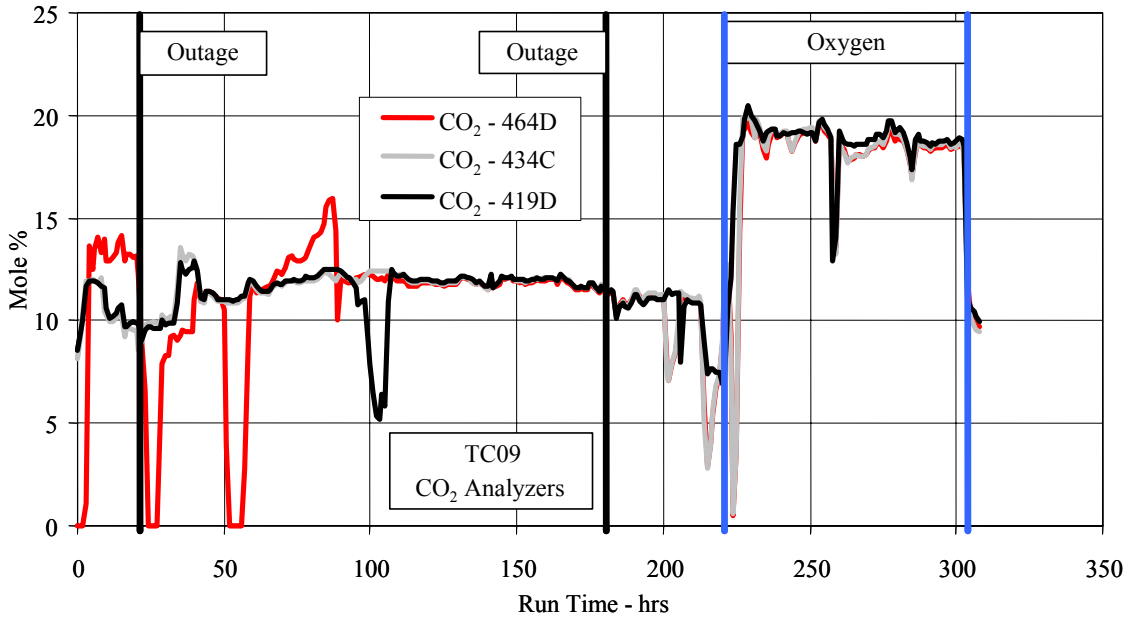

Figure 4.3-6 CO_2 Analyzer Data

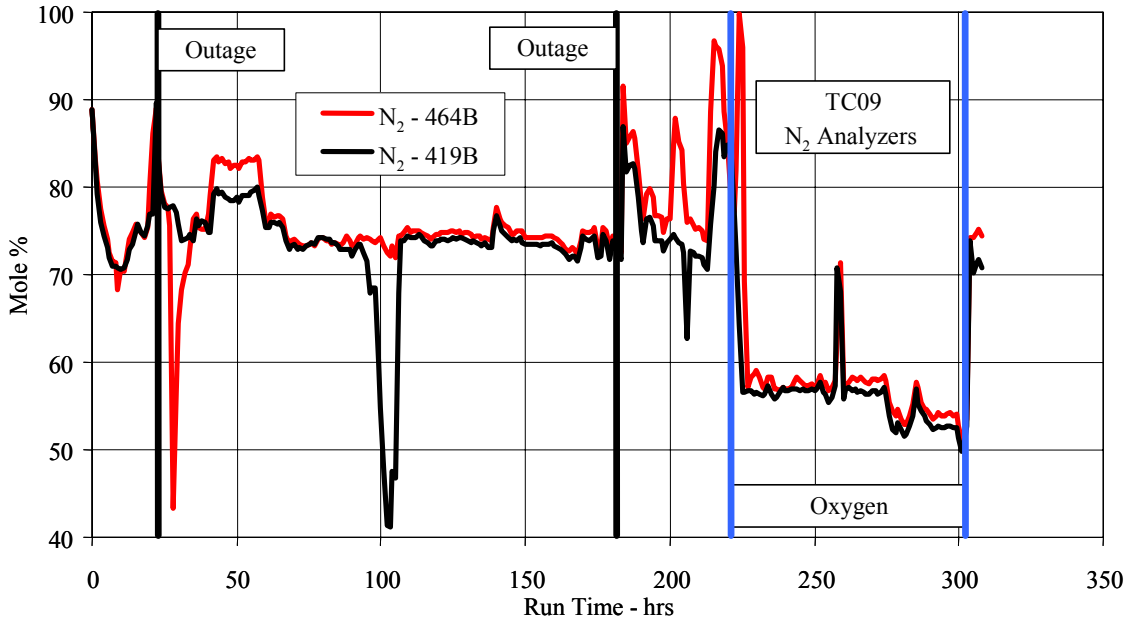

Figure 4.3-7 Analyzer Nitrogen Data

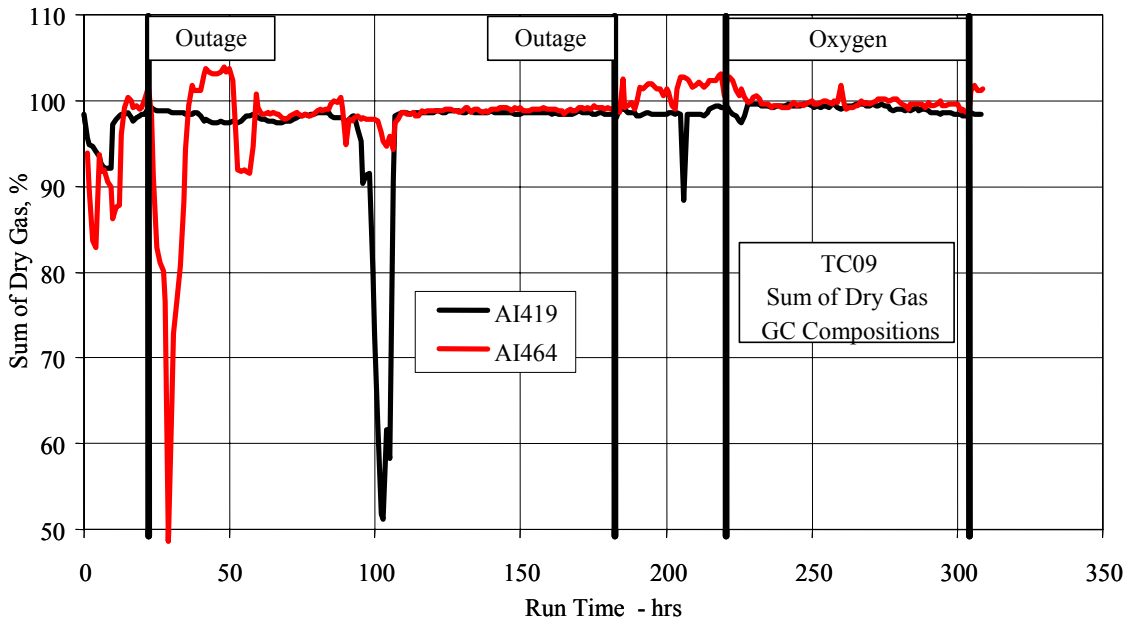

Figure 4.3-8 Sum of GC Gas Compositions (Dry)

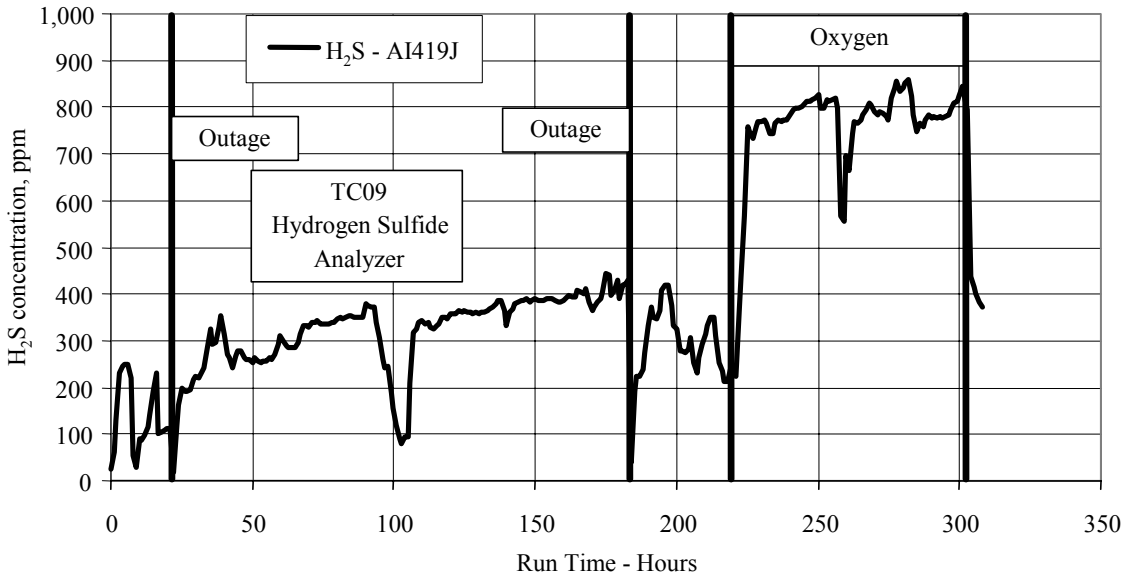

Figure 4.3-9 Hydrogen Sulfide Analyzer Data

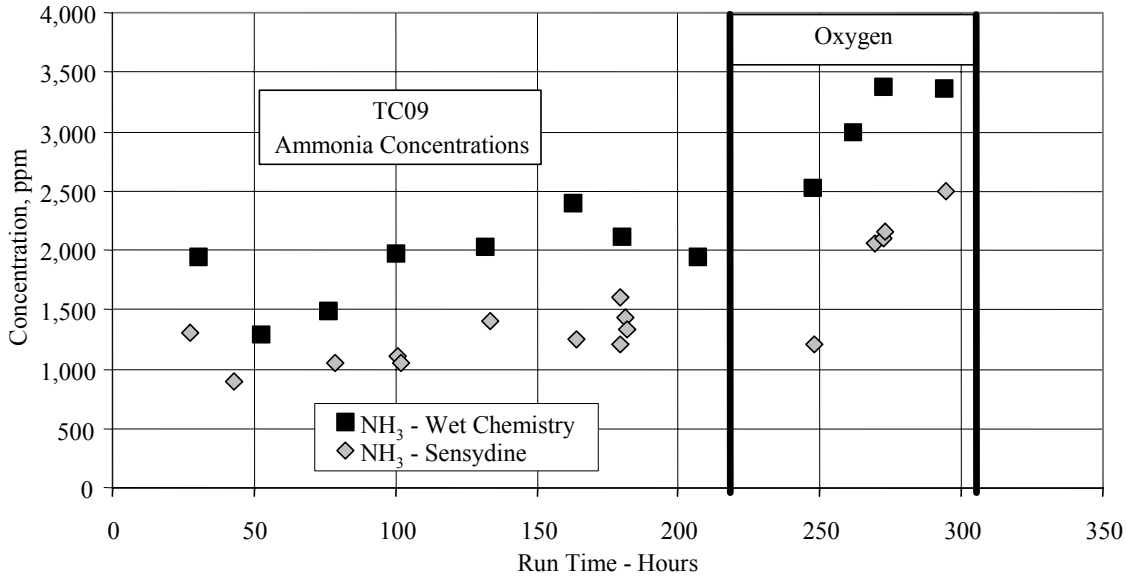

Figure 4.3-10 Ammonia Data

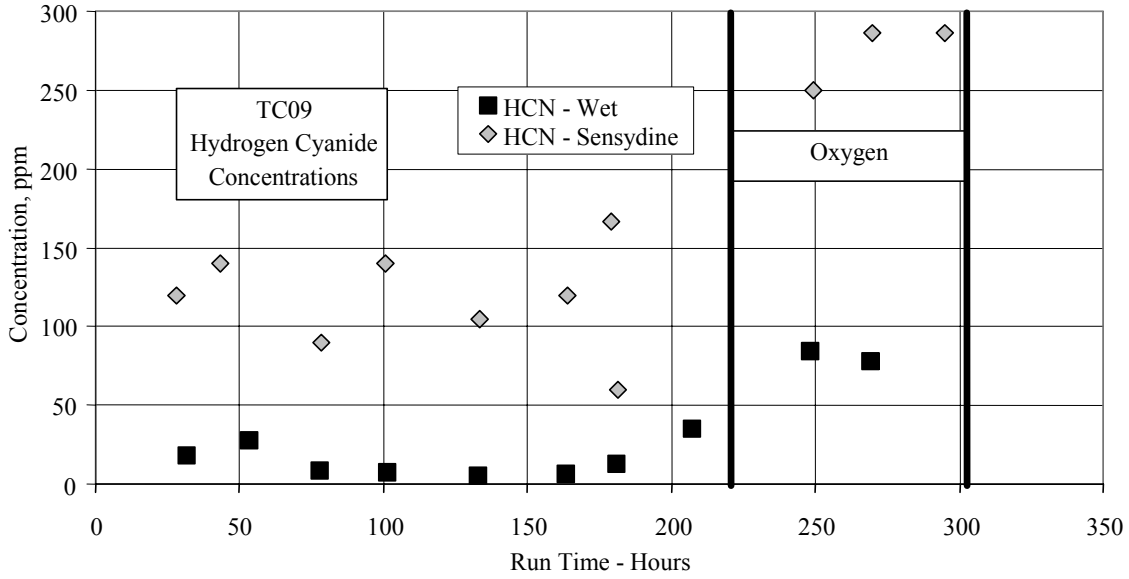

Figure 4.3-11 Hydrogen Cyanide Data

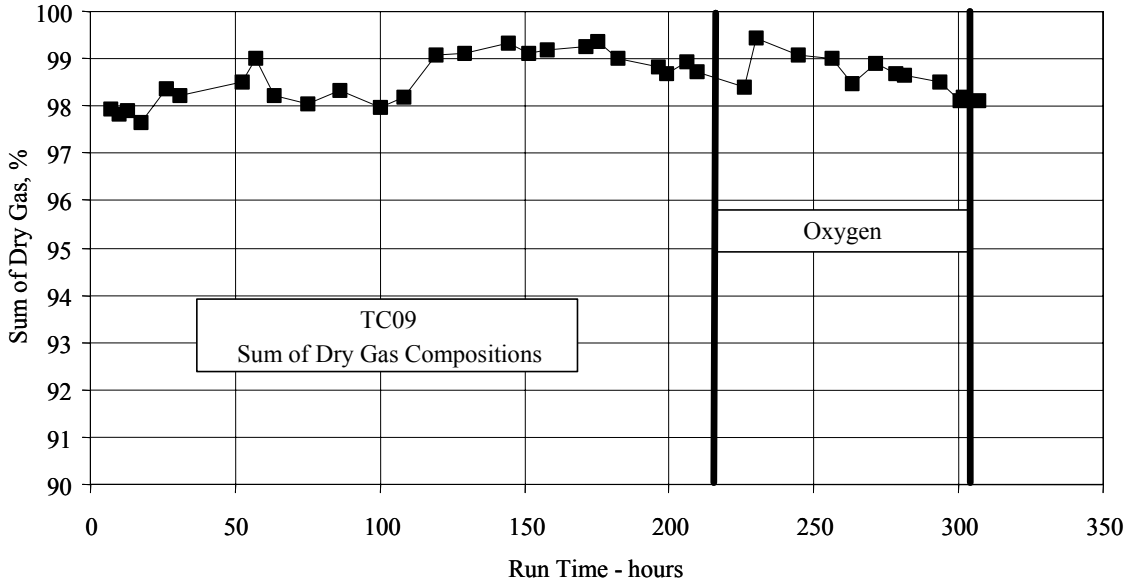

Figure 4.3-12 Sum of Dry Gas Compositions

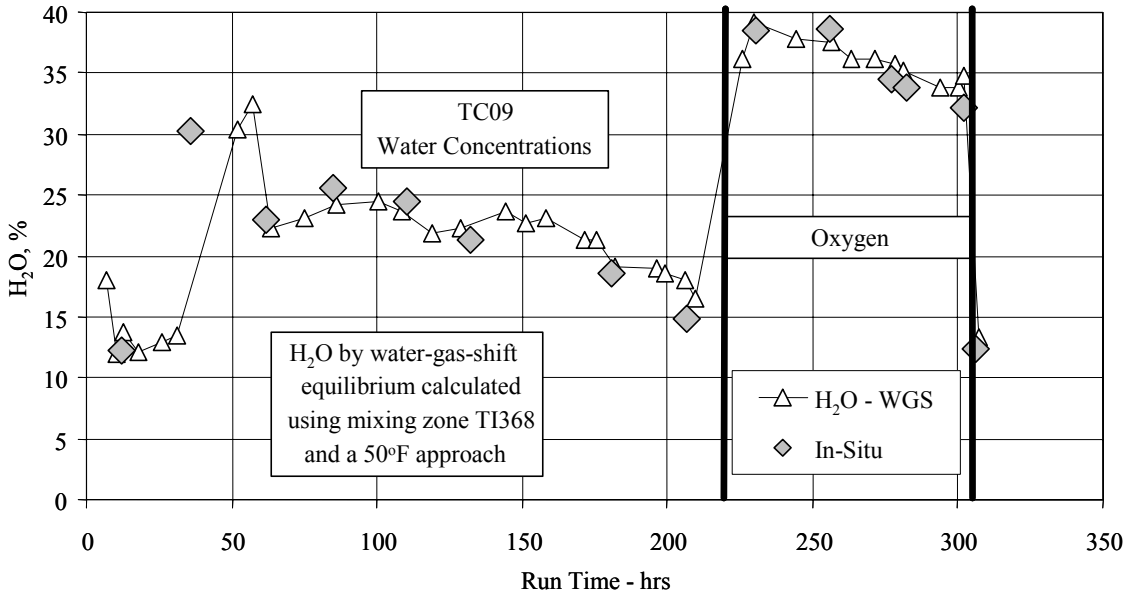

Figure 4.3-13 H_2O Data

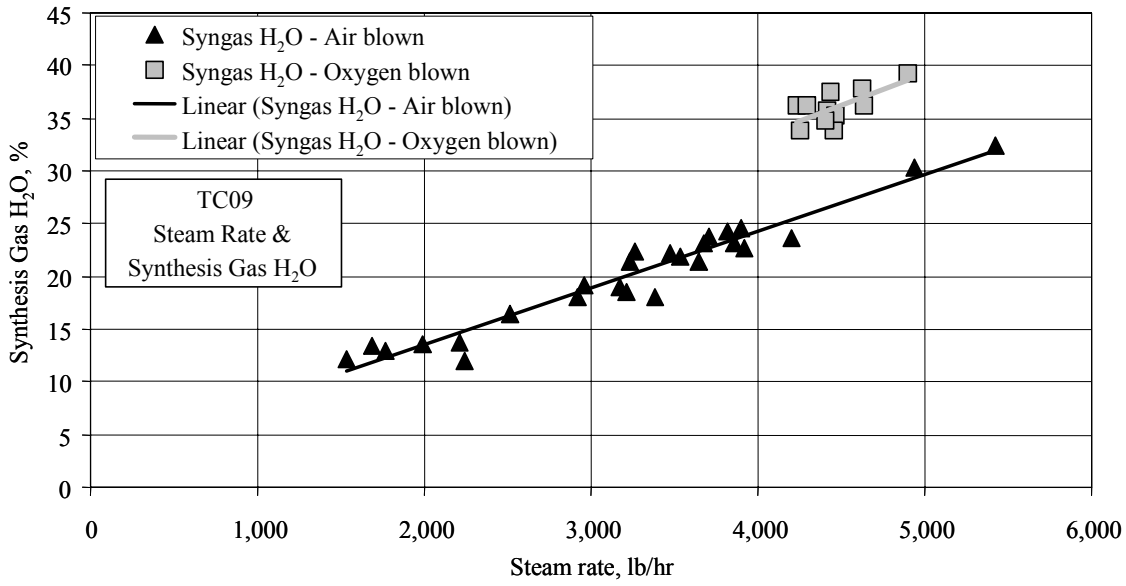

Figure 4.3-14 Steam Rate and Synthesis Gas H_2O

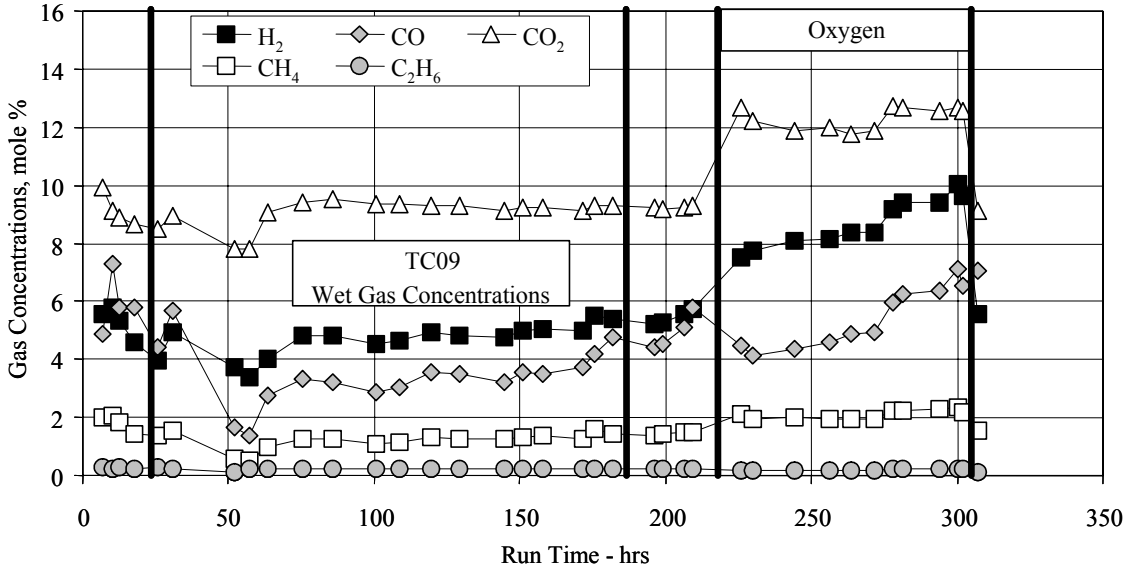

Figure 4.3-15 Wet Synthesis Gas Compositions

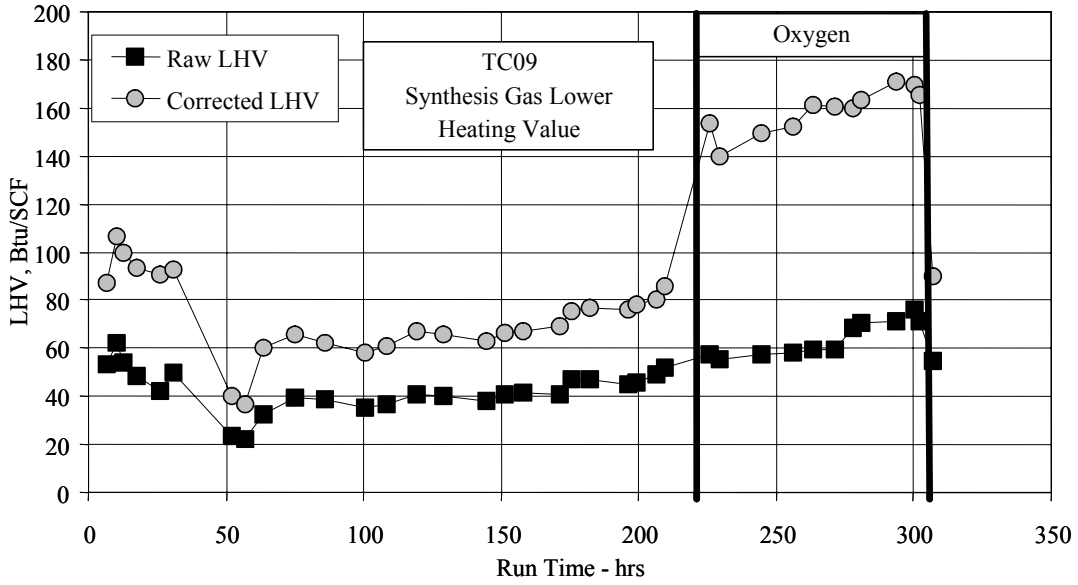

Figure 4.3-16 Synthesis Gas Lower Heating Values

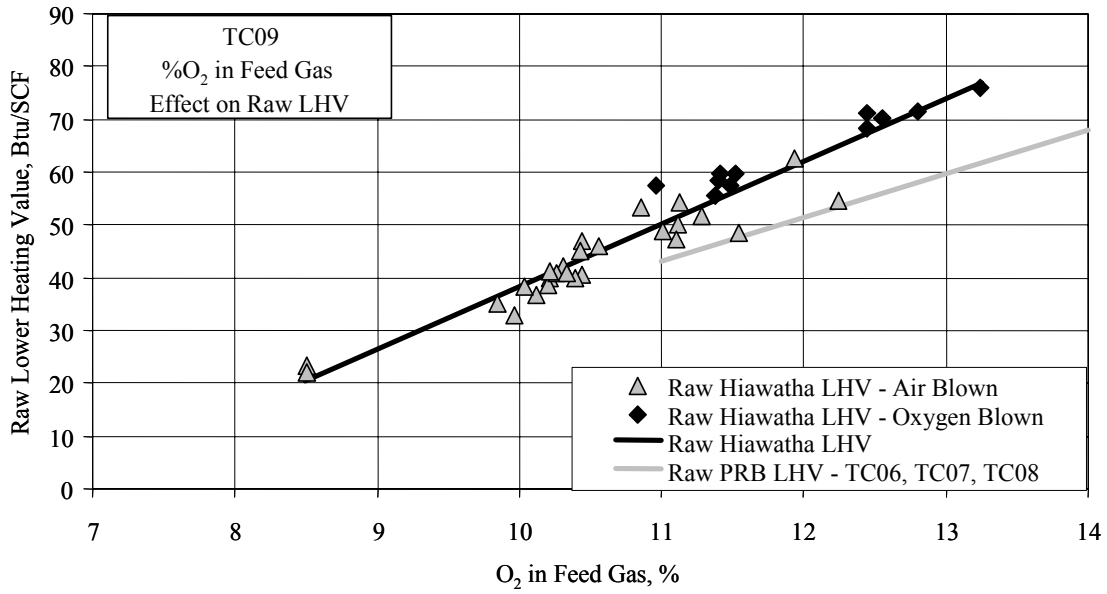

Figure 4.3-17 Raw Lower Heating Value and Overall Percent O_2

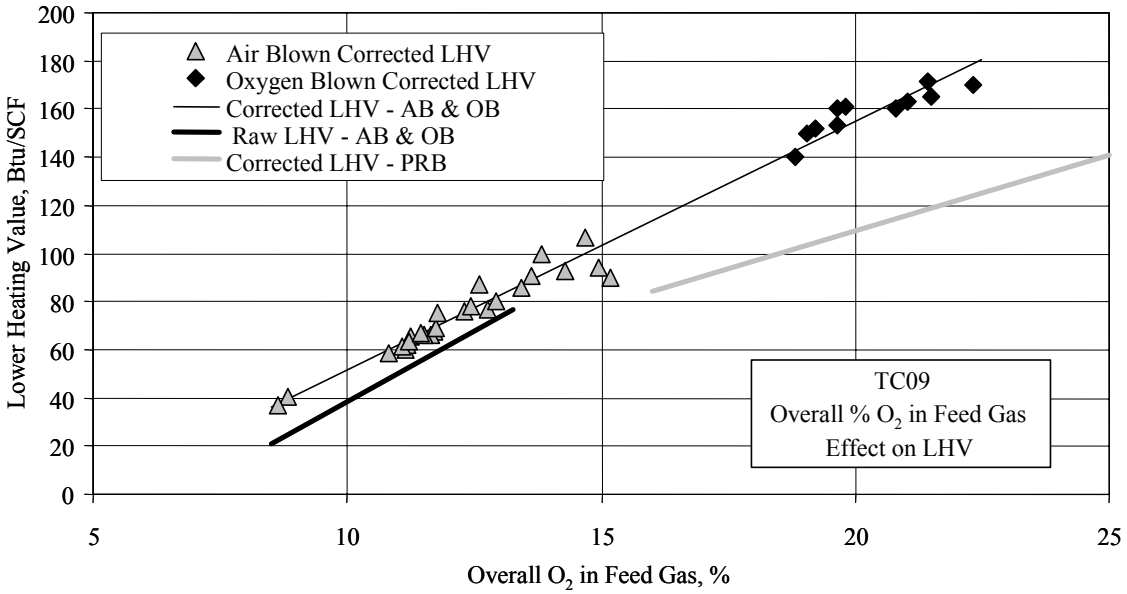

Figure 4.3-18 Corrected LHV and Overall Percent O_2

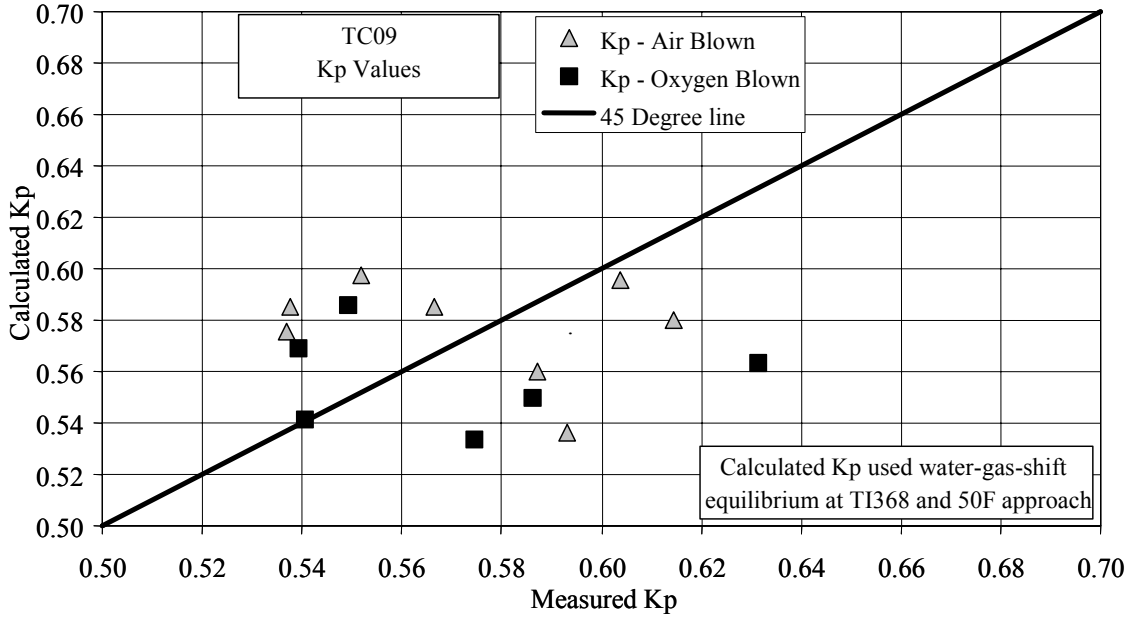

Figure 4.3-19 Water-Gas Shift Constant

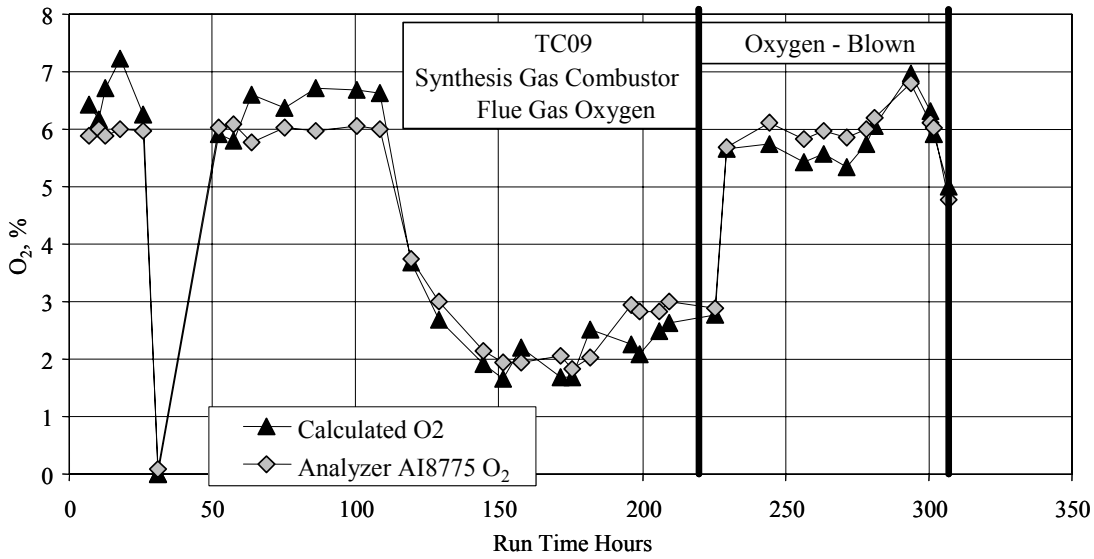

Figure 4.3-20 Synthesis Gas Combustor Outlet Oxygen

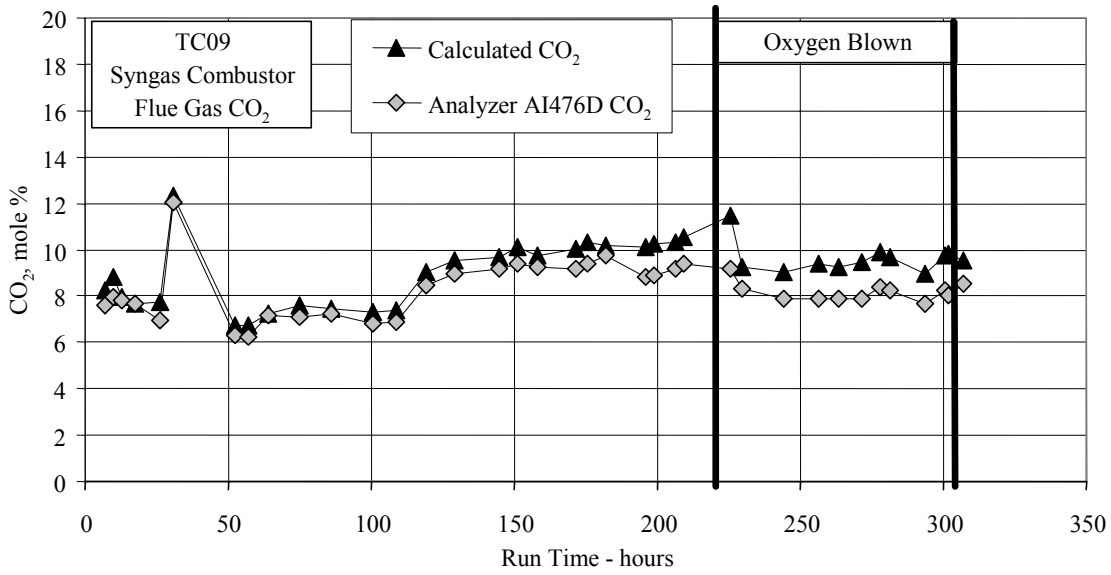

Figure 4.3-21 Synthesis Gas Combustor Outlet Carbon Dioxide

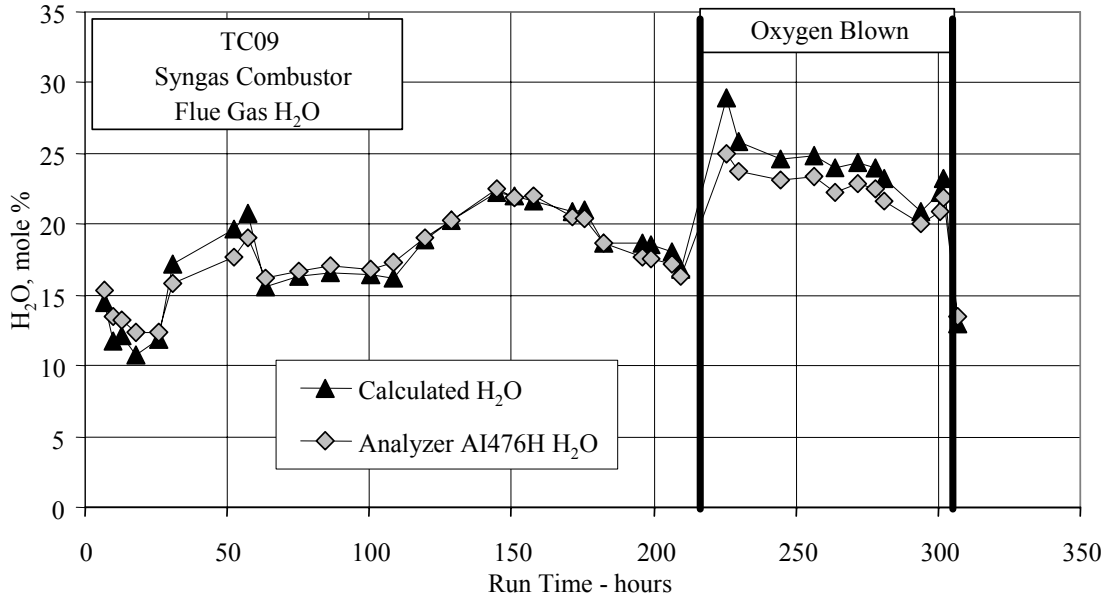

Figure 4.3-22 Synthesis Gas Combustor Outlet Moisture

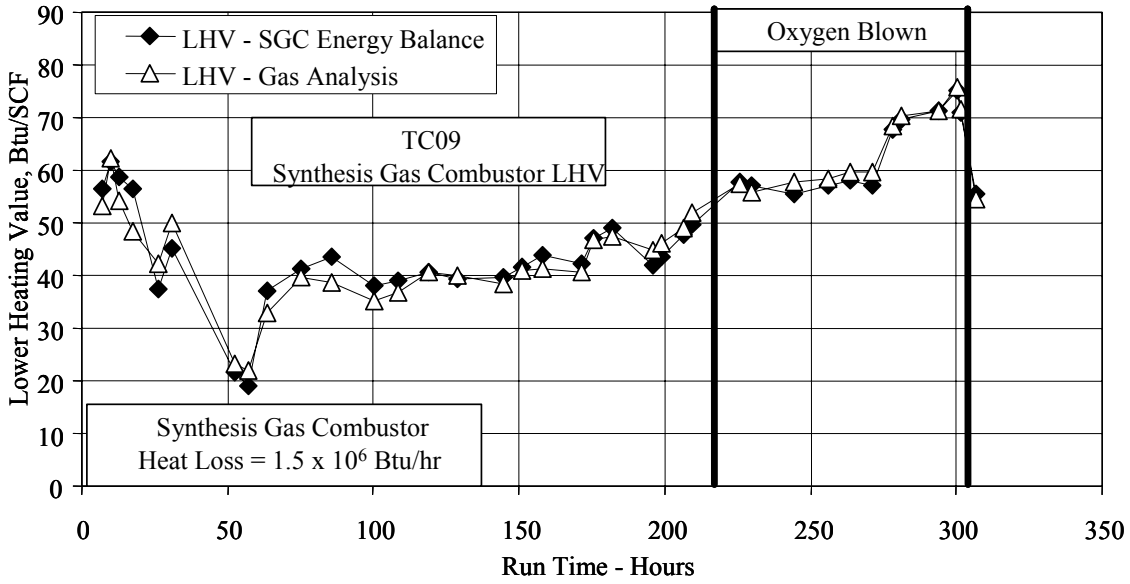

Figure 4.3-23 Synthesis Gas Combustor LHV

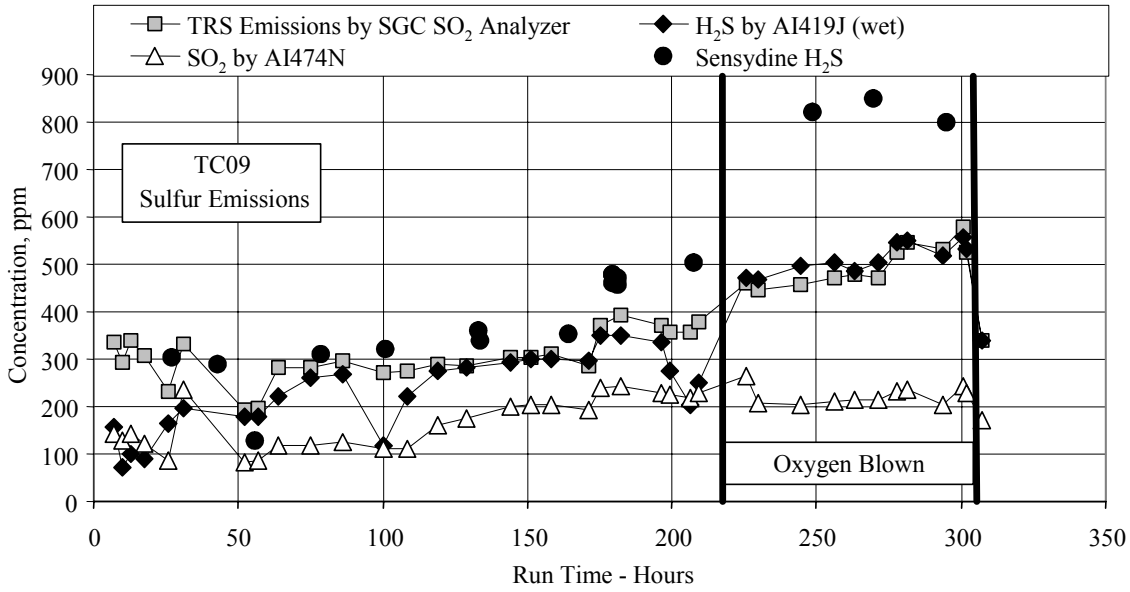

Figure 4.3-24 Sulfur Emissions

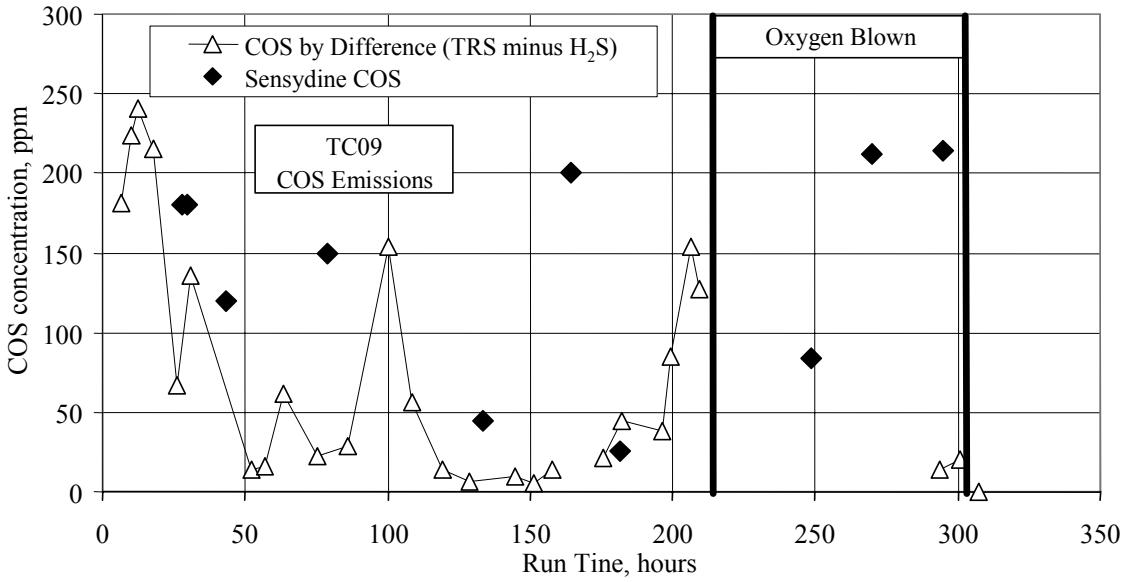

Figure 4.3-25 COS Emissions

4.4 SOLIDS ANALYSES

4.4.1 Summary and Conclusions

- Hiawatha bituminous coal composition was not constant during TC09 testing. There were slight variations in all of the coal properties.
- Standpipe carbon was as high as 1.0-weight percent for periods with coal feed. During coal and coke breeze feed the standpipe carbon was as high as 2.8-percent carbon.
- Standpipe solids did not reach steady compositions with respect to SiO_2, CaO, Al_2O_3, and MgO.
- Standpipe solids contained negligible amounts of CaS.
- Standpipe solids contained some $CaCO_3$; standpipe calcium was partially calcined.
- Carbon and CaS concentrations in PCD inlet in situ samples were higher than in FD0520 samples.
- $CaCO_3$ and SiO_2 concentrations in PCD inlet in situ samples were lower than in the FD0520 samples.
- CaO concentrations in PCD inlet in situ samples were about equal to those in the FD0520 samples.
- The PCD fines sulfur and standpipe solids sulfur content indicated very little overall Transport Gasifier sulfur capture.
- Use of coke breeze seemed to increase the carbon content of the PCD fines.
- The PCD fines calcium was 70- to 90- percent calcined.
- Lack of sorbent feed produced lower calcium concentrations of the standpipe solids and the PCD fines, when compared to test runs with sorbent feed and higher ash calcium coals (Powder River Basin).
- Coal feed particle size was constant at about 225 μ SMD, while the mass mean coal particle size increased from 250 to 350 μ.
- The coal feed did not have large amounts of fines; the percent fines increased during TC09.
- Standpipe solids particle size steadily increased between sand additions and never reached steady state.
- Standpipe solids bulk density decreased from 90 to 80 lb/ft^3.
- Standpipe solids particle sizes were larger than previous PRB air-blown testing.
- PCD solids particle size was constant at about 15 μ.
- In situ PCD fines particle sizes agreed well with the FD0520 samples particle sizes.
- PCD solids bulk density decreased from 40 to 20 lb/ft^3.
- In situ PCD fines bulk densities were lower than the FD0520 bulk densities at the beginning of TC09 and then slowly agreed with each other as TC09 progressed. At the end of TC09, the in situ and FD0520 bulk densities agreed with each other.

4.4.2 Introduction

During TC09, solid samples were collected from the fuel feed system (FD0210), the sorbent feed system (FD0220), the Transport Gasifier standpipe, and the PCD fine solids transport system (FD0520). In situ solids samples were also collected from the PCD inlet. The sample locations are shown in Figure 4.4-1. These solids were analyzed for chemical composition and particle size. During TC09, coke breeze and sand were added through FD0220. Sorbent was not added through FD0220.

4.4.3 Feeds Analysis

Table 4.4-1 gives the average coal composition for the samples analyzed during TC09. The coal carbon and moisture contents as sampled from FD0210 are shown in Figure 4.4-2. The average Hiawatha bituminous coal carbon was 66.4-weight percent and the average Hiawatha bituminous moisture was 6.85-weight percent. The carbon content of the coal varied slightly, while the moisture content was fairly constant.

Figure 4.4-3 shows the fuel sulfur and ash as sampled from the fuel feed system during TC09. The average values are given on Table 4.4-1; the Hiawatha bituminous coal average sulfur was 0.38 percent and the average ash was 10.3 percent. The Hiawatha bituminous coal sulfur and ash analyses show more variation than previous Powder River Basin analyses.

The coal higher heating value (HHV) and lower heating value (LHV) are given on Figure 4.4-4, with the TC09 average values given on Table 4.4-1. The LHV was determined from HHV by reducing the heating value to account for the coal moisture and hydrogen. The average HHV was 11,246 Btu/lb and the average LHV was 10,774 Btu/lb. There was a slight variation in the Hiawatha bituminous heating values during TC09.

Average values for TC09 coal moisture, carbon, hydrogen, nitrogen, sulfur, ash, oxygen, volatiles, fixed carbon, HHV, LHV, CaO, SiO_2, Al_2O_3, Fe_2O_3, and MgO are given in Table 4.4-1. Also given on Table 4.4-1 are the molar ratios for coal calcium to sulfur (Ca/S) and coal iron to sulfur (Fe/S). Hiawatha bituminous has sufficient alkalinity in the ash to remove all of the coal sulfur. The Hiawatha coal alkalinity has less relative alkalinity than the previously tested Powder River Basin.

FD0220 was used during TC09 to feed coke breeze or sand into the Transport Gasifier. Limestone sorbent was not fed to the Transport Gasifier during TC09.

4.4.4 Gasifier Solids Analysis

The chemical compositions of the solid compounds produced by the Transport Gasifier were determined using the solids chemical analysis and the following assumptions:

1. All carbon dioxide measured came from $CaCO_3$, hence moles CO_2 measured = moles $CaCO_3$.
2. All sulfide sulfur measured came from CaS.

3. All calcium not taken by CaS and $CaCO_3$ came from CaO.
4. All magnesium came from MgO.
5. Total carbon is measured, which is the sum of organic and inorganic (CO_2) carbon. The organic carbon is the total carbon minus the inorganic carbon (CO_2).
6. All iron reported as Fe_2O_3 is assumed to be present in the gasifier and PCD solids as FeO.
7. Inerts are the sum of the P_2O_5, K_2O, Na_2O, and TiO_2 concentrations.

It will be assumed that all iron in both the standpipe and PCD solids is in the form of FeO and not in the form of Fe_3O_4 or Fe_2O_3. Thermodynamically, the mild reducing conditions in the Transport Gasifier should reduce all Fe_2O_3 to FeO. The assumption of iron as FeO seemed to give solids compositions totals that add up to around 100 percent.

It will also be assumed that no FeS is formed in the Transport Gasifier and that all the sulfur in the standpipe and PCD fines solids is present as CaS. It is thermodynamically possible that some FeS is formed. Most of the captured sulfur should be in the form of CaS due to the larger amount of calcium than iron in the system.

Table 4.4-2 gives the results from the standpipe analyses. Times when standpipe solids were sampled before the start of steady period coal feed or sampled between periods of coal feed are noted.

The standpipe solids are solids that recirculate through the mixing zone, riser, and standpipe and change slowly with time, since a small amount of solids are taken out of the standpipe via FD0510. FD0510 was operated intermittently during TC09 to control the standpipe level. The flow rates for FD0510 and FD0520 solids during the stable operating periods will be given in Section 4.5.

On start-up, the standpipe solids mainly contained sand at 96.7-percent SiO_2. The standpipe did not contain pure sand at zero "run time" hours since there were several periods of coal and coke breeze operation prior to the starting of the clock for the test, which diluted the standpipe sand.

As the run progressed, the start-up sand was slowly replaced by CaO, Al_2O_3, Fe_2O_3, and other inerts. This is shown in Figure 4.4-5 which plots SiO_2, CaO, and Al_2O_3 and run time. The SiO_2 content slowly decreased and both the Al_2O_3 and the CaO increased to replace the SiO_2. There was one major sand addition to the gasifier during TC09 between hours 183 and 184 during the second outage. It is possible that the gasifier did reach constant conditions at the end of TC09 as the standpipe solids SiO_2, Al_2O_3, and CaO were all leveling out for the last two standpipe samples taken during oxygen-blown mode. It would appear that the solids did not reach steady composition prior to the second outage.

The standpipe organic carbon content is plotted in Figure 4.4-6. The average standpipe organic carbon content during coal operation was 0.6 percent and was higher than during previous PRB testing. One reason could be the occasional addition of coke breeze to the gasifier during coal operation. The samples that were taken during coal operation are noted on Figure 4.4-6. There were also several standpipe samples that were not taken during coke breeze addition that had organic carbon as high as 1.1 percent. The high standpipe carbon may also be a result of using a

less reactive coal than PRB. One standpipe sample had an organic carbon content of 19.5 percent (not plotted on Figure 4.4-6) since it was sampled during coke breeze – propane firing prior to coal feed.

The Table 4.4-2 standpipe solids sulfur level was very low, with all values essentially zero (except for one with 0.2-percent CaS), for all of the samples taken during coal feed. This indicates that all of the sulfur removed from the synthesis gas is removed via the PCD solids and is not accumulating in the gasifier or leaving with the gasifier solids.

The standpipe $CaCO_3$ was at 1 to 2 percent for most of TC09, indicating that there was some inorganic carbon in the gasifier. The standpipe calcium was about 80-percent calcined to CaO. Since there was no sorbent calcium, all the standpipe solids calcium came from the fuel calcium.

The MgO, Fe_2O_3, and other inerts contents are not plotted on Figure 4.4-5, but they follow the same trends as the CaO and Al_2O_3, that is, they are accumulating in the gasifier as the start-up sand is replaced by feed solids.

The standpipe analyses consistency was quite good as the total sum of the compounds in Table 4.4-2 averaged 100 percent with only two samples not between 98 and 102 percent.

4.4.5 Gasifier Products Solids Analysis

Figure 4.4-7 plots the organic carbon (total carbon minus CO_2 carbon) for the PCD solids sampled from FD0520. The organic carbon content for every PCD fines sample analyzed is also given on Table 4.4-3. Since FD0520 ran continuously during TC09, solid samples were taken often, with a goal of one sample every 4 hours. About half of the TC09 PCD solids that were sampled were analyzed. In situ PCD inlet particulate solids recovered were also analyzed.

The in situ carbon contents are compared with the FD0520 solids on Figure 4.4-7. The in situ solids organic carbon analyses were larger than the FD0520 solids for all of the 12 in situ solid samples. During oxygen-blown, in situ organic carbon samples were closer to the FD0520 organic carbon. This is consistent with about half of the TC08 FD0520 samples (see Figure 4.4-6 in the TC08 report) but different than the TC06 and TC07 in situ and FD0520 solids organic carbon which usually compared very well for most of the solids (see Figures 4.4-7 in the TC06 and TC07 reports). The in situ analyses would indicate a lower carbon conversion than the FD0520 analyses. It would appear that the in situ solids sampling is not capturing the particulates which contain lower amounts of organic carbon. The in situ and FD0520 particulate sizes will be compared in the Section 4.4.7. It is very unlikely due to the temperature and the residence time available for carbon conversion between the in situ sampling point and the FD0520 sampling point that there was any carbon conversion between the PCD inlet (in situ sampling) and the FD0520 sampling location. During TC09, two composite FD0520 samples were collected and compared well with the point FD0520 samples.

The periods of coke breeze addition are noted on Figure 4.4-7. There does not appear to be any effect of coke breeze addition on FD0520 samples organic carbon during the periods of coke

breeze addition prior to 50 hours. However, the period of coke breeze addition between hours 192 and 224 seemed to increase the PCD fines organic carbon.

The organic carbon varied between 20 and 50 percent for TC09, with a few outliers. The low carbon content at hours 38 and 150 were not used to determine the carbon conversion, while all the other points were used. The organic carbon was increasing at the end of the oxygen-blown mode, decreasing the carbon conversion. Carbon conversions will be determined in Section 4.5.5.

Figure 4.4-8 and Table 4.4-3 gives the amounts of SiO_2 and CaO in the PCD solids as sampled from FD0520. Also plotted on Figure 4.4-8 are the in situ solids concentrations for SiO_2 and CaO. The 12 in situ CaO concentrations showed good agreement with the FD0520 solids. The CaO concentrations were constant at around 5 to 7 percent until the second outage at hour 183, and then were constant at about 4 percent until the end of TC09. In TC06, TC07, and TC08, the in situ and FD0520 CaO analyses compared very well, as they did in TC09. The TC09 FD0520 solids CaO concentrations were about 1/4 of the TC06 and TC07 concentrations due to the lack of sorbent feed in TC09 because limestone sorbent feed was used in TC06 and TC07. The CaO concentrations in TC09 were about 1/2 of the CaO concentrations in TC08 due to the lower calcium in the TC08 fuel (PRB) when compared to Hiawatha bituminous.

The SiO_2 in situ and FD0520 solids analyses did not compare well during TC09. The in situ SiO_2 was lower than the FD0520 solids analyses by 5 to 30 percent. The lower in situ SiO_2 content is due to the higher in situ carbon content. During TC06 and TC07, there were periods of good agreement and periods of poor agreement between in situ and FD0520 SiO_2 analyses. During the first half of TC06 and TC08 and all of TC07, the in situ and FD0520 SiO_2 analyses compared very well. During the last half of TC06 and TC08, the in situ SiO_2 were lower than the FD0520 analyses, as in all SiO_2 analyses in TC09. During the last half of TC09 the in situ SiO_2 concentrations were also lower than the FD0520. The lower in situ TC09 SiO_2 compensates for some of the higher in situ organic carbon.

The SiO_2 concentrations decreased from 60 to 40 percent between the two outages. After the second outage the SiO_2 again decreased from 70 to 30 percent. Both SiO_2 decreases are expected as the start-up sand high in SiO_2 is replaced by coal ash.

Figure 4.4-9 and Table 4.4-3 give the amounts of $CaCO_3$ and CaS in the PCD solids as sampled from FD0520. Also plotted on Figure 4.4-9 are the in situ solids concentrations for $CaCO_3$ and CaS.

The first two in situ samples $CaCO_3$ concentrations agreed well with FD0520 solids $CaCO_3$. After hour 35, the in situ $CaCO_3$ concentrations were lower than the FD0520 concentrations by 0.5 to 2 percent to the end of TC09 with one exception at hour 255. In TC06, the in situ $CaCO_3$ concentrations were consistently higher than the FD0520 $CaCO_3$ concentrations, while in TC07 the in situ $CaCO_3$ concentrations were either equal to or slightly higher than the FD0520 $CaCO_3$ concentrations. In TC08, the in situ $CaCO_3$ agreed well with the FD0520 $CaCO_3$ until hour 100, when the in situ $CaCO_3$ was higher than the FD0520 $CaCO_3$ by 1 to 2 percent.

As expected, the TC09 PCD fines $CaCO_3$ (1.5 to 3 percent) was lower than the PBB tests with limestone (TC06 and TC07 at 2 to 10 percent) and the PRB test without limestone (TC08 at 1 to 4 percent limestone).

The FD0520 solids $CaCO_3$ concentration seemed to have an inconsistency at hour 50 when the $CaCO_3$ concentration jumped from around 0.7 to 2.5 percent and remained at 2.5 to 3 percent until the second outage. This was due to a sudden increase in solids CO_2 concentration, which may be due to the analytic error in the PD0520 solids CO_2 analysis. After the second outage, the $CaCO_3$ was constant at about 2.5 percent until it decreased to between 1.75 and 2.0 percent for the remainder of TC09.

Only two of the FD0520 solids CaS concentration agreed well with the in situ CaS concentration. This is not consistent with TC06 to TC08 data, where all of the in situ solids CaS analyses agreed with the FD0520 CaS analyses. The FD0520 CaS slowly varied from 0.5 to 0.0 percent from the start of TC09 until the second outage. From hour 250 until the end of TC09 during oxygen mode the CaS was consistent at about 0.4 percent CaS indicating some sulfur capture.

The PCD fines calcination is defined as:

$$\%\ \text{Calcination} = \frac{\text{M\% CaO}}{\text{M\% CaO} + \text{M\% CaCO}_3} \qquad (1)$$

The PCD fines calcination is plotted on Figure 4.4-10. The PCD fines calcination was fairly constant at 80 percent for long periods of operation during both air- and oxygen-blown modes. The calcination was at 90 percent for the first 46 hours of operation, but this was probably due to incorrect PCD fines CO_2 analyses. After the second outage the calcination dropped to between 55 and 70 percent. These results are close to TC06 to TC07 PCD fines calcinations, which averaged about 85 percent. Since the Hiawatha Bituminous coal ash had very little $CaCO_3$, the small amount of $CaCO_3$ is the result of CaO carbonation.

The calcium sulfation is defined as:

$$\%\text{Sulfation} = \frac{\text{M\%CaS}}{\text{M\%CaO} + \text{M\%CaCO}_3 + \text{M\%CaS}} \qquad (2)$$

The PCD fines sulfation is plotted on Figure 4.4-10 with the limestone calcination. The PCD fines sulfation started TC09 at about 8 percent and then decreased to nearly zero at hour 38. The calcium sulfation remained low for most of the rest of the air-blown operation. The sulfation increased at hour 250 during the oxygen-blown operation and ended TC09 at 8 percent.

Table 4.4-3 gives the PCD fines compositions for the samples collected in FD0520. The consistency is not as good as the standpipe solids in that the totals usually add up to between 96 and 108 percent with one outlier at 117 percent. The average of the totals was 100.2 percent, indicating no high or low bias. Additional components on Table 4.4-3, other than those plotted on Figures 4.4-6, -7, and -8, are MgO, FeO, and Al_2O_3. The MgO concentration was between 0.6 and 1.5 percent with a few outliers. The Al_2O_3 concentration was between 4 and 9 percent. Also

given on Table 4.4-3 are the HHV, LHV, and organic carbon for the PCD fines. As expected, the trend of heating values follows the carbon content of the PCD fines.

No FD0510 solid samples were analyzed during TC09 because the standpipe samples should give a more accurate view of the circulating solids composition.

4.4.6 Feeds Particle Size

The TC09 Sauter mean diameter (SMD) and mass mean diameter (D_{50}) particle sizes of the coal sampled from FD0210 are plotted on Figure 4.4-11. The Hiawatha Bituminous coal SMD particle size was fairly constant during TC09 with values between 200 and 250 μ. The Hiawatha bituminous coal mass mean diameter (D_{50}) was not constant during TC09, which is surprising since in previous test runs the D_{50} was usually larger than the SMD by a constant amount. The D_{50} decreased on startup from 287 to 239 μ at 54 hours. The D_{50} then increased slowly up to 294 μ at 158 hours. After the second outage the D_{50} increased to about 340 μ and was constant through oxygen-blown mode to the end of TC09. The change in the difference between SMD and D_{50} indicate that the coal-feed particle size distribution and D_{50} changed during TC09.

In past testing, high fines content resulted in an increased number of coal feeder outages due to coal feeder plugging caused by the packing of coal fines. A measure of the amount of fines in the coal is the percent of the smallest size fraction. To show the level of fines in the coal feed, the percent of ground coal less than 45 μ is plotted in Figure 4.4-12. The fines percent less than 45 μ was 3 to 8 percent during TC09. During TC09, the percent coal fines increased from 3 to about 6 percent at a steady rate independent of outages and mode of operation. The steady increase in coal fines was probably the cause of the increase in coal D_{50}. Keeping the percent fines under 15 percent for TC09 greatly helped the coal feeder performance. The coal feeder fines were less than during previous testing. Previous testing has indicated that when the percent fines are above 20 percent, there are numerous coal feeder trips. TC09 was relatively free of coal feeder trips caused by a high amount of coal fines.

4.4.7 Gasifier Solids Particle Size

The TC09 standpipe solids particle sizes are given in Figure 4.4-13. The particle size of the solids increased as the start-up sand is replaced by sorbent and coal ash. When the gasifier lost solids during gasifier excursions, the bed material was replaced by 122 μ D_{50} sand, which had a smaller particle size. This was done during the two outages. The standpipe particle size decreased as expected due to the sand addition during the outage. The SMD of the gasifier solids slowly increased from 135 μ at hour 160 to 180 μ at hour 110. The standpipe particle size was constant at 180 μ from hour 110 to hour 158. The last standpipe sample before the second outage had a SMD of 209 μ. After the second outage, the standpipe solids increased during both air- and oxygen-blown operations. The rate of particle size increase seemed to be faster during oxygen-blown operation. The final standpipe solid SMD was 233 μ. Unfortunately, the standpipe sampler collected enough solids to perform particle size distributions on only two standpipe samples after hour 248. The TC09 D_{50} was about 20 μ less than the TC09 SMD.

It is clear from Figure 4.4-13 that the standpipe solids never reached a steady-state particle size. The TC06 SMD steady-state particle size was about 160 μ (see TC06 report, Figure 4.4-14), and the steady-state TC07 SMD was about 170 μ (see TC07 report, Figure 4.4-14). The TC08 SMD steady-state particle size was about 160 μ during the initial air-blown testing. The TC08 oxygen-blown standpipe solids were generally increasing during oxygen-blown testing and reached as high as 250 μ SMD. This might be due to not injecting 10 μ sorbent during TC09 and TC08, which increased the standpipe particle size.

Figure 4.4-14 plots the SMD and D_{50} for the PCD solids sampled from FD0520 and the in situ solids recovered during the PCD inlet sampling. Ten of the twelve PCD inlet samples particle size agreed very well with particle size from the samples collected in FD0520. The close agreement in the particle sizes is surprising due to the lack of agreement in the chemical compositions. In TC06, TC07, and TC08, the FD0520 PCD fines particle size usually agreed with the in situ PCD inlet particle size.

The PCD fines SMD was fairly constant at about 15 μ for TC09 during both air-blown operation and oxygen-blown mode. PRB air-blown runs TC06 and TC07 PCD fines had 9 to 14 μ SMD (TC06 Report, Figure 4.4-15 and TC07 Report, Figure 4.4-15) and both were consistent with TC09. TC08 PRB air-blown mode SMD were lower than the TC09 PCD fines SMD (as well as TC06 and TC07), while the oxygen-blown TC08 PCD fines SMD were consistent with TC06, TC07, and TC09. The constant TC09 PCD particle sizes indicate that there are no changes in collection efficiencies of the disengager and cyclone system even with changing standpipe solids particle size during TC09.

The D_{50} was about 5 μ larger than the SMD and follows the same trends as the SMD particle sizes. The in situ PCD inlet D_{50} solids particle size also agreed with the FD0520 solids D_{50} particle size.

4.4.8 TC09 Particle Size Comparison

Figure 4.4-15 plots all the solids SMD particle sizes. The Transport Gasifier is fed approximately 250 μ SMD coal and produces 150 to 250 μ SMD gasifier solids and 15 μ SMD PCD fines. The FD0220 SMD was between 250 to 300 μ for the first four samples. The first four samples were coke breeze. The last two FD0220 samples were sand samples. Samples from FD0220 were taken only during the first 80 hours of TC09 since limestone was not being fed to the gasifier.

The D_{50} diameters were larger than the SMD for the FD210 (coal), and FD0520 (PCD fines), while the TC09 SMD particle sizes are larger than the D_{50} particle sizes for the standpipe solids. This trend was also seen in TC06, TC07, and TC08. The standpipe solids have a non-Gaussian distribution (bimodal) which probably caused the standpipe SMD to be larger than the standpipe D_{50}.

4.4.9 TC09 Standpipe and PCD Fines Bulk Densities

The TC09 standpipe bulk and PCD fines densities are given in Figure 4.4-16. The standpipe bulk density of the solids decreased slightly as the start-up sand was replaced by ash after both the original startup and the sand additions at hour 182. The standpipe solids bulk density decreased from 90 to 80 lb/ft^3 in about 50 hours after the first outage. The standpipe solids bulk density then remained constant at 80 lb/ft^3 until the second outage. After the sand addition at the second outage, the gasifier bulk density increased from 80 to 90 lb/ft^3. The gasifier solids bulk density then decreased from the second outage to the end of TC09. TC06, TC07, and TC08 standpipe solids bulk density behaved as did the TC09 standpipe bulk density, at 90 lb/ft^3 just after sand addition and then decreasing to about 80 lb/ft^3.

The bulk densities for the FD0520 PCD solids samples from both FD0520 and the in situ PCD inlet are plotted on Figure 4.4-16. The bulk densities of the FD0520 PCD fines were slowly decreased from about 40 lb/ft^3 at the start of TC09, to about 18 lb/ft^3 at the end of TC09. While there were spikes upward to nearly 50 lb/ft^3 during TC09, the trend downward is clear. The in situ PCD fines bulk densities were nearly constant at between 15 and 20 lb/ft^3 for TC09. The FD0520 PCD fines bulk density slowly approached the values of the in situ bulk densities and both measurements seemed to agree after hour 275.

TC06 fines bulk densities were in the range of 20 to 30 lb/ft^3. TC07 and TC08 bulk densities were constant at 22 lb/ft^3, with periods of wide variation in bulk density up to 60 lb/ft^3. In TC06, the in situ PCD inlet solids bulk density slowly decreased form 20 to 15 lb/ft^3 and agreed with the FD0520 bulk density during the first 600 hours of TC06. TC07 in situ and FD0520 PCD fines bulk densities agreed. TC08 in situ PCD inlet bulk densities were lower than the FD0520 bulk densities.

Table 4.4-1

Coal Analyses

	Hiawatha Bit.	
	Value	Standard Deviation
Moisture, wt%	6.85	0.39
Carbon, wt%	66.36	1.07
Hydrogen[2], wt%	4.34	0.09
Nitrogen, wt%	1.08	0.03
Oxygen, wt%	10.71	1.59
Sulfur, wt%	0.38	0.03
Ash, wt%	10.29	1.05
Volatiles, wt%	35.61	2.61
Fixed Carbon, wt%	47.25	2.52
Higher Heating Value, Btu/lb	11,246	151
Lower Heating Value, Btu/lb	10,774	147
CaO, wt %	1.29	0.33
SiO_2, wt %	5.23	0.89
Al_2O_3, wt %	1.43	0.24
MgO, wt %	0.33	0.09
Fe_2O_3, wt %	0.51	0.06
Ca/S, mole/mole	2.55	0.51
Fe/S, mole/mole	1.01	0.16

Notes:

1. All analyses are as sampled at FD0210.
2. Hydrogen in coal is reported separately from hydrogen in moisture.

Table 4.4-2 Standpipe Analysis

Sample Number	Sample Date & Time	Sample Run Time Hours	SiO_2 Wt. %	Al_2O_3 Wt. %	FeO Wt. %	Other Inerts[1] Wt. %	$CaCO_3$ Wt. %	CaS Wt. %	CaO Wt. %	MgO Wt. %	Organic Carbon Wt. %	Total Wt. %
AB11268	9/4/2002 16:00	(2)	94.0	2.3	0.0	1.5	0.1	0.0	0.1	0.0	0.9	98.9
AB11280	9/5/2002 12:00	13	88.1	3.9	0.2	2.0	0.3	0.0	3.1	0.5	0.5	98.8
AB11299	9/9/2002 13:00	(3)	80.6	1.8	0.4	0.9	1.6	0.2	0.0	0.1	19.5	105.0
AB11286	9/10/2002 04:00	30	85.5	5.3	1.2	1.3	2.0	0.0	0.6	0.4	0.4	96.9
AB11311	9/10/2002 12:00	38	90.1	3.5	1.1	1.7	1.5	0.0	1.9	0.5	1.1	101.4
AB11312	9/10/2002 20:00	46	85.0	4.3	1.4	1.9	1.8	0.0	2.5	0.7	2.8	100.5
AB11313	9/11/2002 04:00	54	85.2	4.6	1.6	2.2	2.0	0.0	3.2	0.8	0.3	100.0
AB11342	9/12/2002 04:00	78	81.3	5.5	2.1	2.8	2.1	0.0	5.0	1.1	0.8	100.8
AB11364	9/13/2002 04:00	102	77.3	6.7	2.5	3.4	1.6	0.0	6.8	1.4	0.0	99.7
AB11380	9/14/2002 04:00	126	74.4	7.6	2.8	3.7	1.9	0.0	7.9	1.6	0.3	100.1
AB11383	9/15/2002 04:00	150	72.9	9.0	2.8	4.2	1.8	0.0	7.8	1.7	0.9	101.1
AB11384	9/15/2002 12:00	158	71.7	9.0	2.8	4.2	1.8	0.0	8.1	1.7	0.3	99.6
AB11401	9/16/2002 12:00	182	68.8	10.9	3.0	4.2	1.9	0.0	8.2	1.8	0.3	99.0
AB11448	9/21/2002 20:00	192	89.3	4.1	1.0	2.0	1.5	0.0	1.5	0.5	0.8	100.6
AB11449	9/22/2002 12:00	208	86.0	5.3	1.5	2.3	1.5	0.0	2.4	0.7	0.2	100.0
AB11450	9/22/2002 20:00	216	83.6	6.3	1.9	2.4	1.7	0.0	3.4	1.0	0.6	100.8
AB11451	9/23/2002 04:00	224	82.4	6.6	2.0	2.4	2.0	0.0	3.4	1.1	1.3	101.1
AB11464	9/23/2002 12:00	232	81.5	6.9	2.1	2.6	1.6	0.0	4.3	1.1	0.1	100.3
AB11488	9/24/2002 12:00	256	77.4	8.5	2.6	2.7	1.8	0.0	5.6	1.6	0.0	100.2
AB11506	9/25/2002 12:00	280	69.2	12.7	3.2	3.1	1.9	0.0	7.2	2.3	0.4	100.0
AB11514	9/26/2002 00:00	292	68.8	12.8	3.4	3.3	0.0	0.0	8.7	2.1	0.4	99.5

Notes:

1. Other inerts consist of P_2O_5, Na_2O, K_2O, & TiO_2.
2. Sample AB11268 was taken prior to start of coal feed.
3. Sample AB11299 was taken prior to the restart of coal feed.
4. Samples taken prior to 9/23/02 are air blown; Samples taken after 9/22/02 are oxygen blown.

Table 4.4-3 PCD Fines From FD0520

Sample Number	Sample Date & Time	Sample Run Time Hours	SiO_2 Wt. %	Al_2O_3 Wt. %	FeO Wt. %	Other Insert[1] Wt. %	$CaCO_3$ Wt. %	CaS Wt. %	CaO Wt. %	MgO Wt. %	Organic C (C-CO_2) Wt. %	Total Wt. %	HHV Btu/lb.	LHV Btu/lb.
AB11273	9/5/2002 08:00	9	67.2	4.0	0.4	2.0	0.5	0.3	2.8	0.6	24.8	102.4	2,521	2,493
AB11278	9/5/2002 12:00	13	60.9	4.2	0.7	2.0	0.6	0.4	3.2	0.6	25.0	97.7	2,777	2,750
AB11281	9/5/2002 16:00	17	51.8	4.9	1.1	2.2	0.7	0.4	4.4	0.8	27.7	94.0	3,785	3,754
AB11290	9/10/2002 00:00	26	59.8	3.9	1.3	1.9	0.8	0.5	2.1	0.6	30.1	101.0	3,287	3,264
AB11291	9/10/2002 04:00	30	62.5	5.2	1.6	2.7	0.6	0.4	3.3	0.7	23.1	100.1	2,792	2,769
AB11301	9/10/2002 08:00	34	49.9	4.4	1.7	2.2	1.4	0.4	4.1	0.9	32.2	97.3	5,059	5,023
AB11308	9/10/2002 12:00	38	84.2	4.3	1.3	2.3	0.3	0.0	2.4	0.5	3.8	99.1	349	346
AB11321	9/10/2002 16:00	42	74.4	4.6	1.6	2.4	0.7	0.0	3.3	0.7	20.4	108.0	1,192	1,169
AB11322	9/10/2002 20:00	46	49.3	5.4	2.2	2.4	0.6	0.4	4.6	0.9	35.7	101.4	4,677	4,640
AB11323	9/11/2002 00:00	50	51.9	6.0	2.6	2.7	2.5	0.3	5.3	1.2	24.3	96.8	4,200	4,168
AB11326	9/11/2002 12:00	62	53.8	6.0	2.3	2.8	2.6	0.2	5.5	1.2	29.7	104.2	3,823	3,783
AB11345	9/11/2002 20:00	70	57.5	5.8	2.2	2.8	2.6	0.1	5.3	1.1	24.7	102.3	3,143	3,111
AB11346	9/12/2002 00:00	74	37.1	5.3	2.3	2.3	2.4	0.4	5.7	1.2	43.7	100.5	6,513	6,460
AB11348	9/12/2002 08:00	82	42.8	6.1	2.5	2.7	2.6	0.3	6.3	1.4	32.5	97.3	5,136	5,094
AB11360	9/12/2002 20:00	94	60.7	6.9	2.5	3.3	2.5	0.0	6.0	1.2	12.4	95.5	1,777	1,759
AB11361	9/13/2002 00:00	98	60.2	6.7	2.5	3.2	2.4	0.0	5.9	1.2	15.2	97.3	2,255	2,232
AB11363	9/13/2002 08:00	106	45.7	6.2	2.4	2.8	2.5	0.2	6.2	1.3	28.7	96.0	4,586	4,547
AB11369	9/13/2002 16:00	114	46.0	6.5	2.5	2.8	2.6	0.2	6.2	1.3	28.2	96.2	4,728	4,691
AB11391	9/14/2002 00:00	122	45.4	6.3	2.4	2.8	2.8	0.1	6.1	1.3	38.5	105.9	4,340	4,289
AB11392	9/14/2002 04:00	126	39.1	5.2	2.0	2.3	2.5	0.1	5.0	1.1	34.3	91.6	4,073	4,027
AB11393	9/14/2002 12:00	134	53.1	7.1	2.7	3.1	2.9	0.0	6.9	1.4	24.4	101.6	2,661	2,630
AB11394	9/14/2002 16:00	138	37.2	5.8	2.3	2.5	2.5	0.4	6.1	1.3	43.8	101.8	6,060	6,008
AB11396	9/15/2002 00:00	146	38.6	6.3	2.5	2.7	2.7	0.3	6.5	1.4	45.0	106.1	5,380	5,319
AB11397	9/15/2002 04:00	150	55.8	7.9	2.7	3.5	2.6	0.0	7.1	1.5	14.4	95.5	1,910	1,889
AB11398	9/15/2002 08:00	154	34.4	5.9	2.5	2.6	2.7	0.4	6.2	1.4	44.4	100.6	6,614	6,560
AB11400	9/15/2002 16:00	162	38.6	7.2	2.4	2.7	2.5	0.3	6.1	1.3	42.6	103.7	5,576	5,526
AB11402	9/16/2002 12:00	182	49.3	7.8	2.6	3.2	2.6	0.2	6.6	1.4	23.6	97.4	3,752	3,724
AB11432	9/21/2002 20:00	192	74.1	5.3	1.4	2.5	2.5	0.0	1.7	0.7	28.8	117.1	2,066	2,026
AB11435	9/22/2002 08:00	204	42.7	6.7	1.6	2.0	2.3	0.5	3.0	0.9	38.6	98.2	5,914	5,867
AB11437	9/22/2002 16:00	212	51.4	6.2	1.8	2.2	2.5	0.3	3.3	0.9	36.2	105.0	4,019	3,979
AB11440	9/23/2002 04:00	224	39.4	6.6	1.7	1.8	2.6	0.4	3.1	1.0	45.7	102.3	6,336	6,280
AB11461	9/23/2002 12:00	232	48.4	6.8	2.0	2.1	2.4	0.2	3.8	1.1	34.1	100.8	5,464	5,416
AB11470	9/23/2002 20:00	240	56.5	7.5	2.1	2.4	1.9	0.2	4.2	1.1	20.9	96.7	3,931	3,899
AB11479	9/24/2002 08:00	252	46.0	8.2	2.0	2.0	1.8	0.3	3.8	1.1	37.6	102.8	5,072	5,021
AB11493	9/24/2002 20:00	264	41.0	7.3	1.7	1.8	1.7	0.4	3.3	1.0	44.6	102.9	6,067	6,010
AB11501	9/25/2002 08:00	276	42.8	8.6	1.9	2.0	1.8	0.3	4.1	1.1	41.5	104.2	5,462	5,408
AB11507	9/25/2002 16:00	284	33.5	7.6	1.6	1.7	2.0	0.4	3.6	1.0	47.7	99.2	7,209	7,154
AB11512	9/26/2002 00:00	292	32.0	7.5	1.7	1.7	1.8	0.4	3.7	1.0	49.3	99.0	7,401	7,338
AB11517	9/26/2002 08:00	300	28.7	6.8	1.5	1.6	1.9	0.5	3.2	0.9	52.7	97.7	7,958	7,898

Notes:

1. Other inserts consist of P_2O_5, K_20, and TiO_2.
2. Hours 0 to 212 were air blown; hours 224 to 300 were oxygen blown.

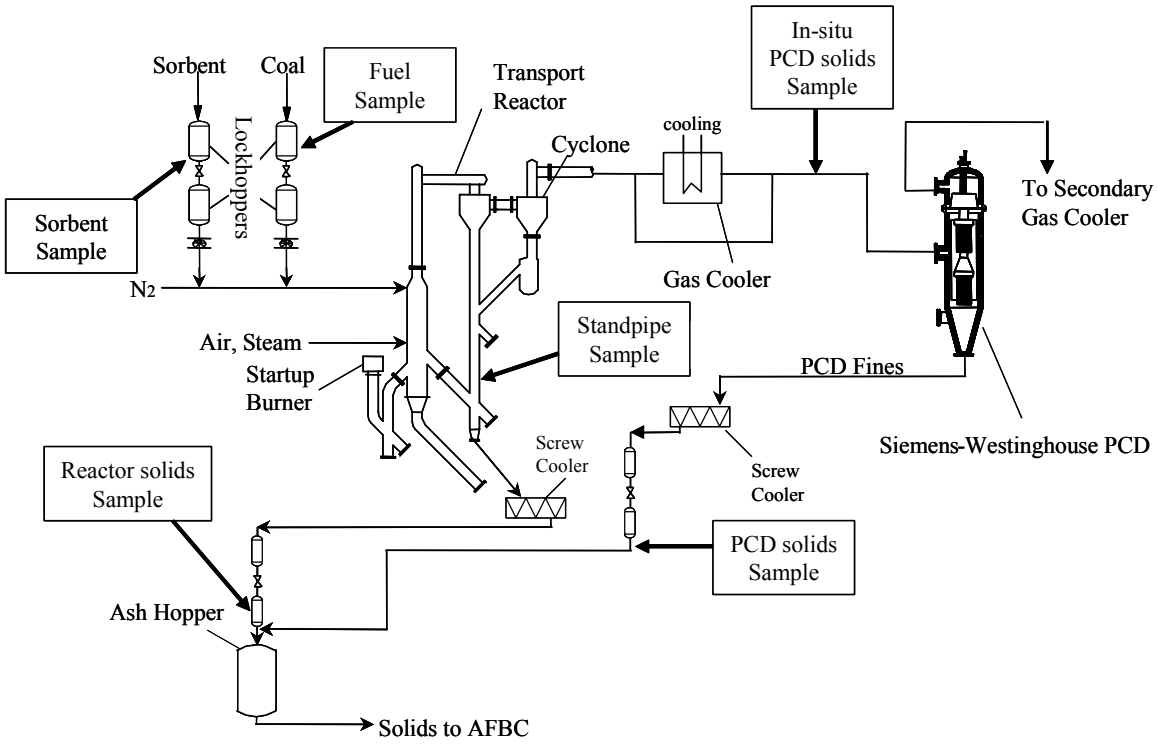

Figure 4.4-1 Solid Sample Locations

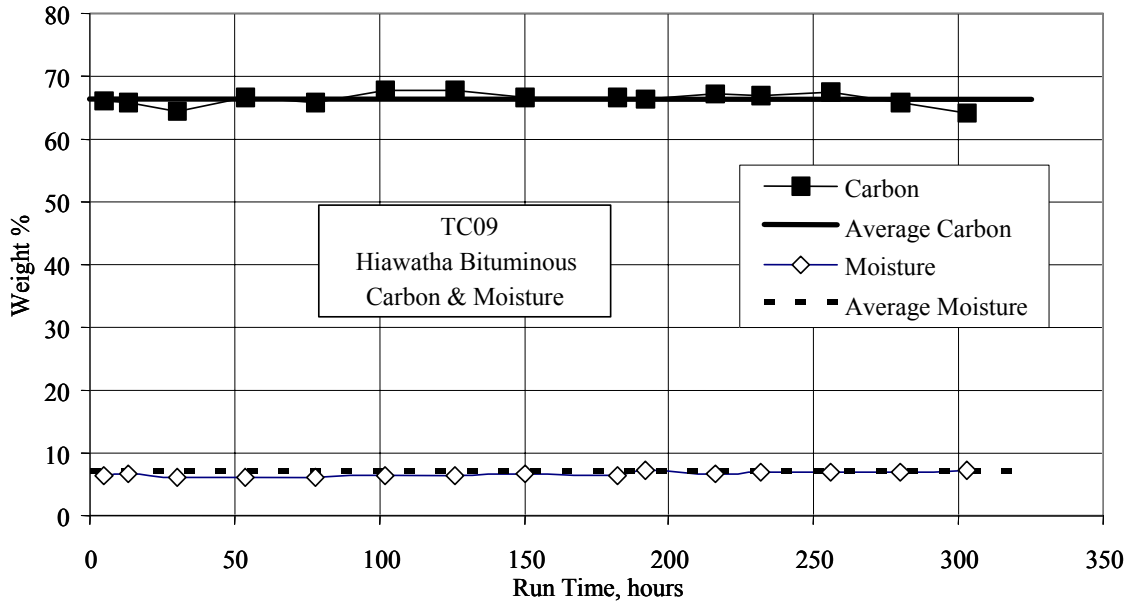

Figure 4.4-2 Coal Carbon and Moisture

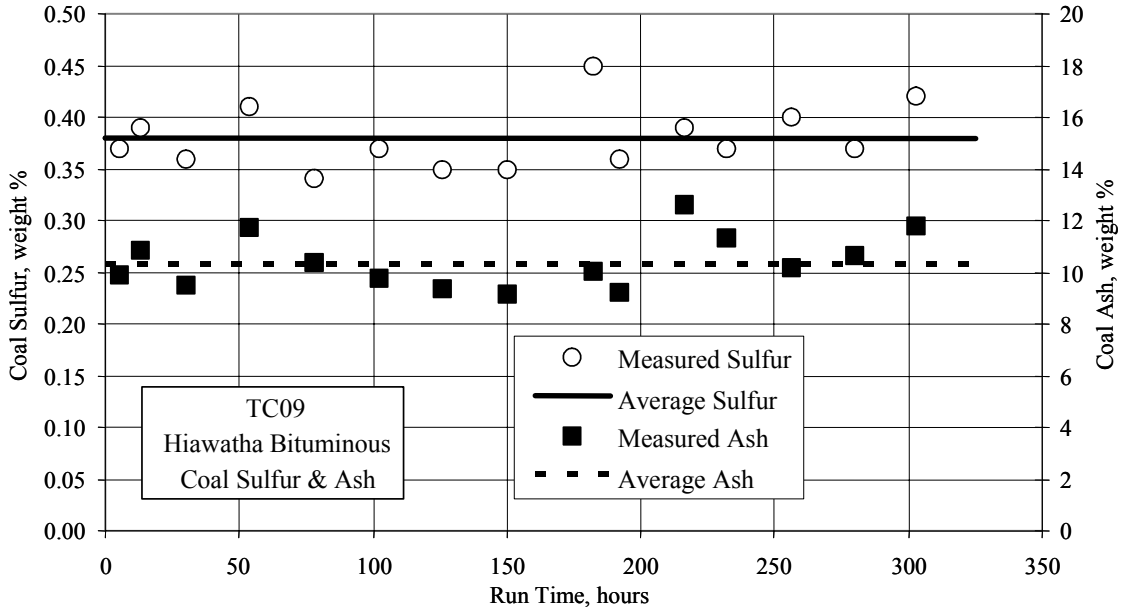

Figure 4.4-3 Coal Sulfur and Ash

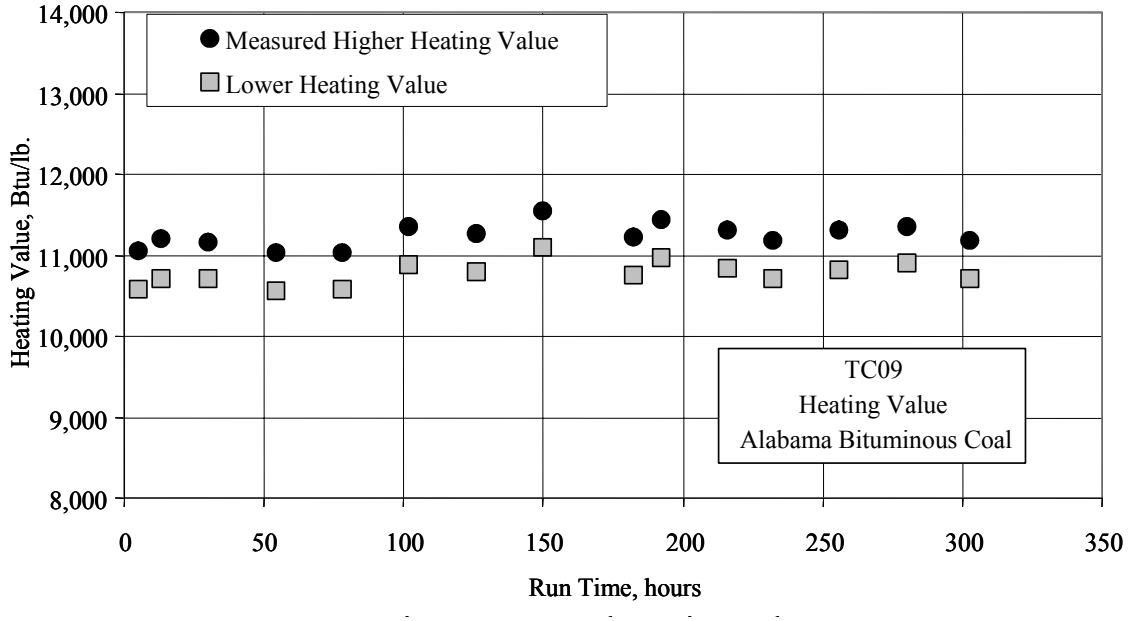

Figure 4.4-4 Coal Heating Value

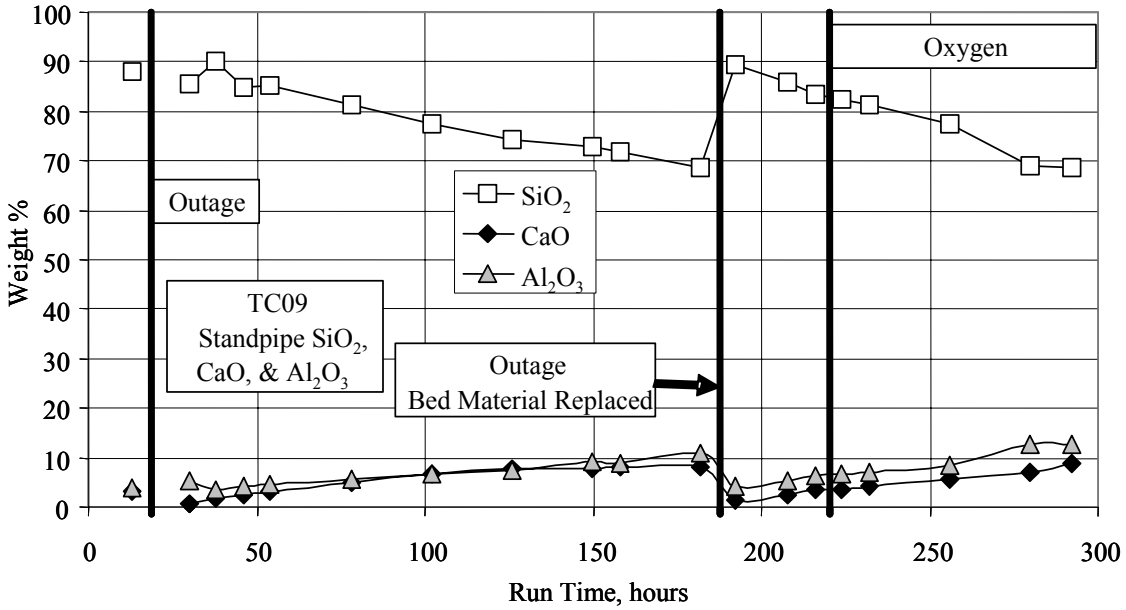

Figure 4.4-5 Standpipe SiO_2, CaO, and Al_2O_3

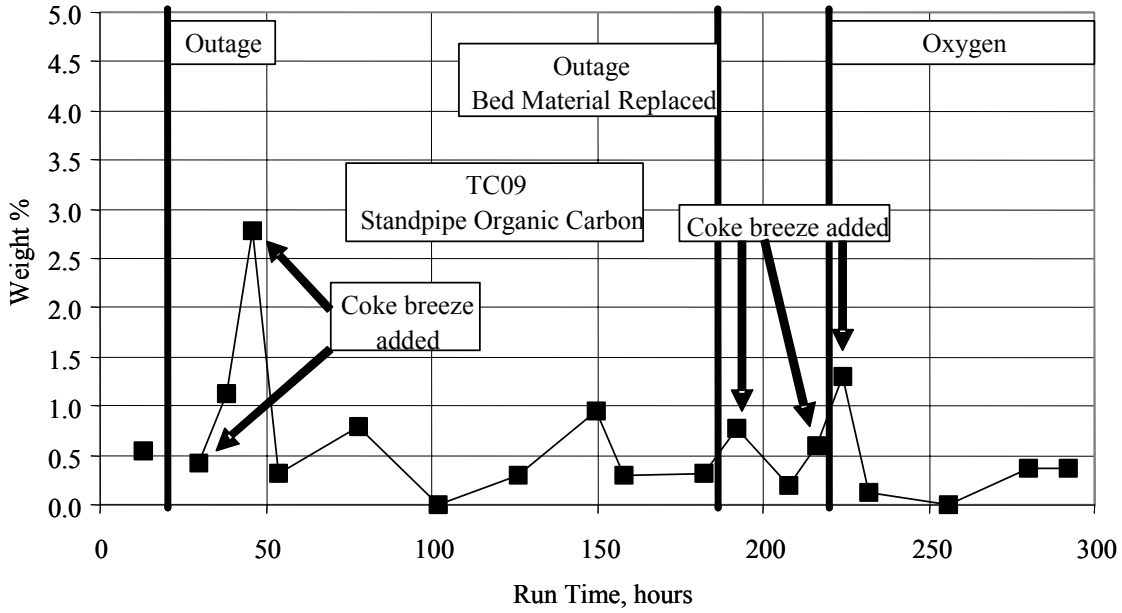

Figure 4.4-6 Standpipe Organic Carbon

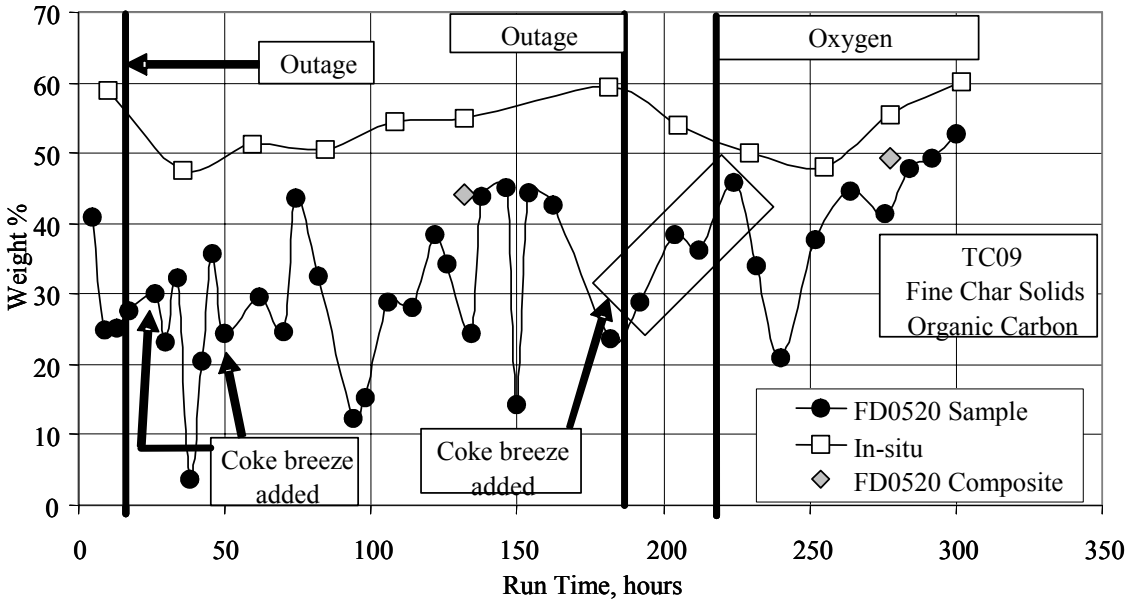

Figure 4.4-7 PCD Fines Organic Carbon

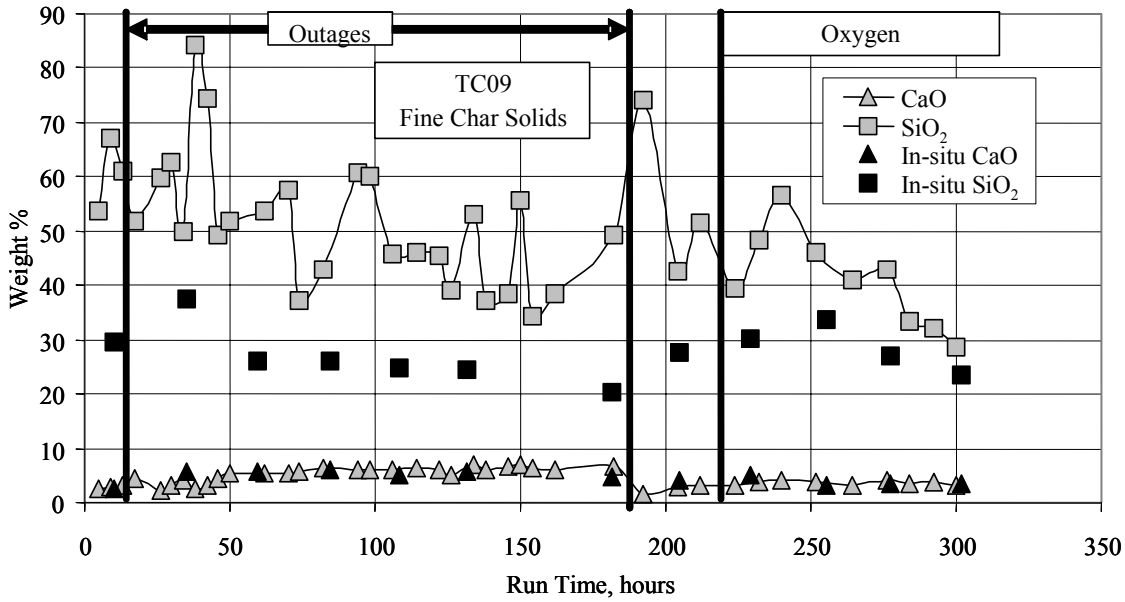

Figure 4.4-8 PCD Fines SiO_2 and CaO

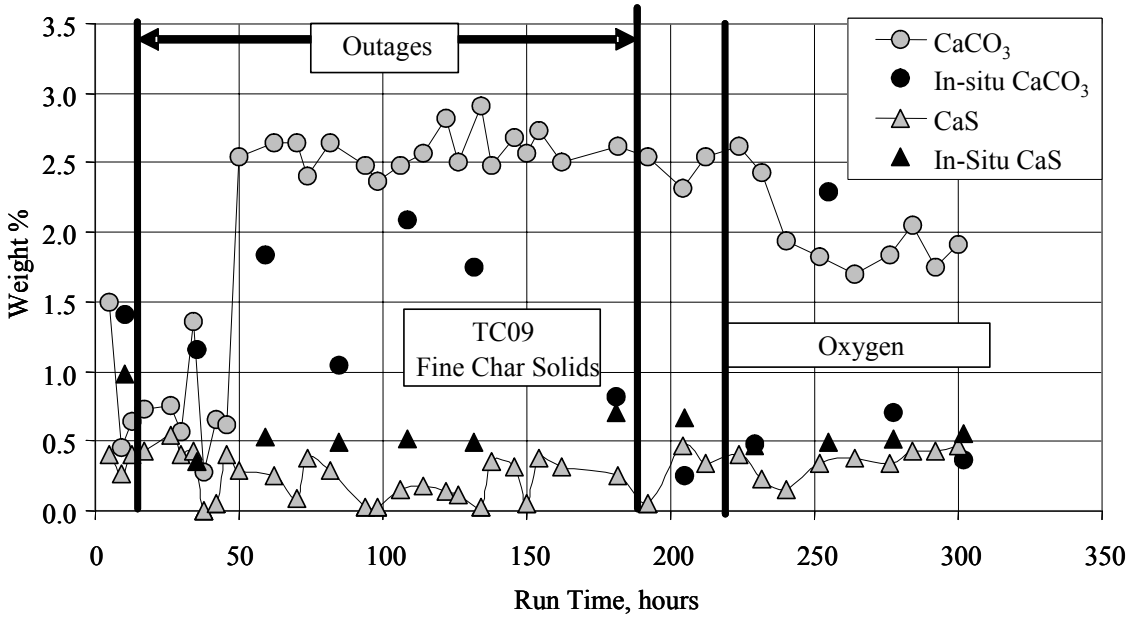

Figure 4.4-9 PCD Fines $CaCO_3$ and CaS

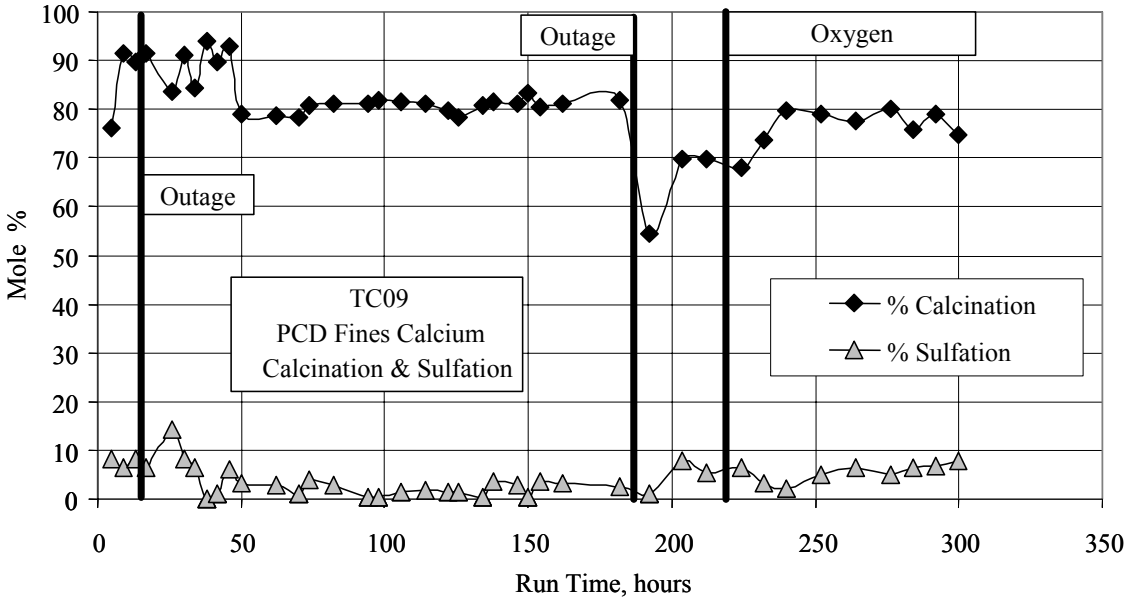

Figure 4.4-10 PCD Fines Calcination and Sulfation

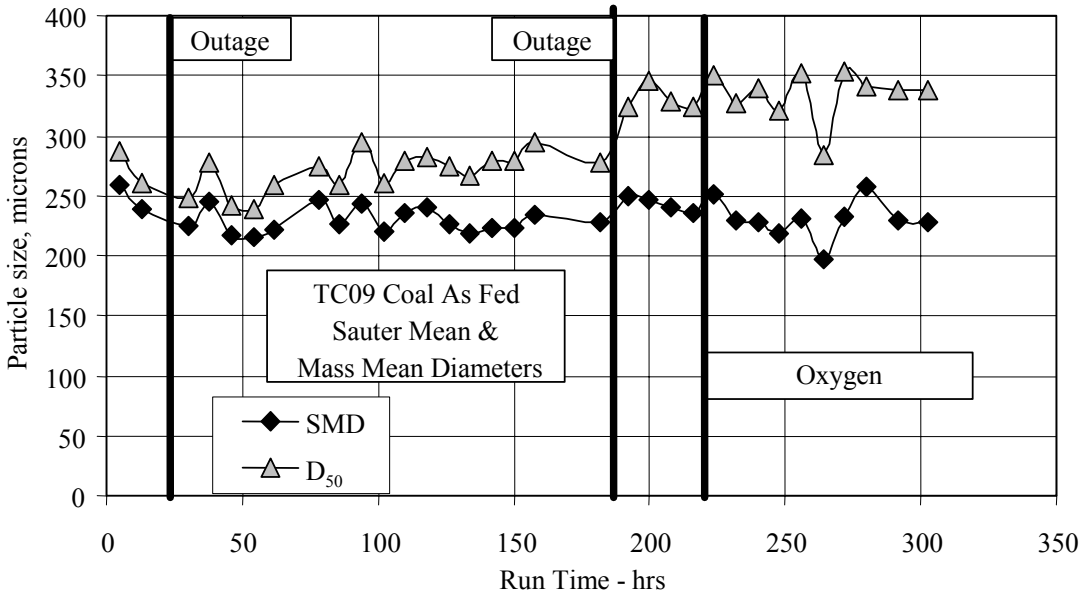

Figure 4.4-11 Coal Particle Size

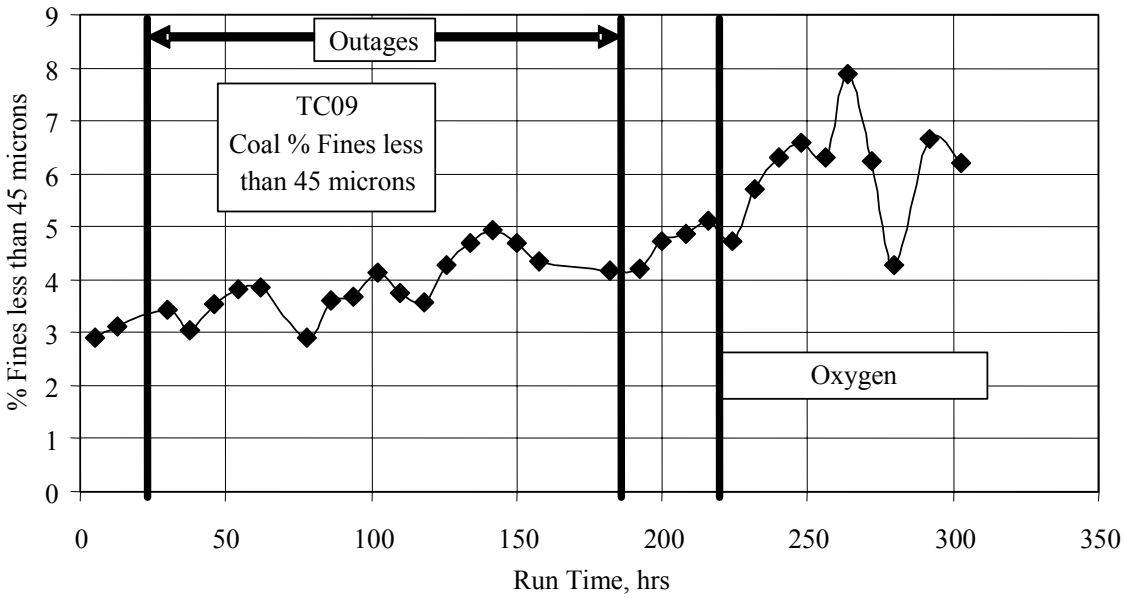

Figure 4.4-12 Percent Coal Fines

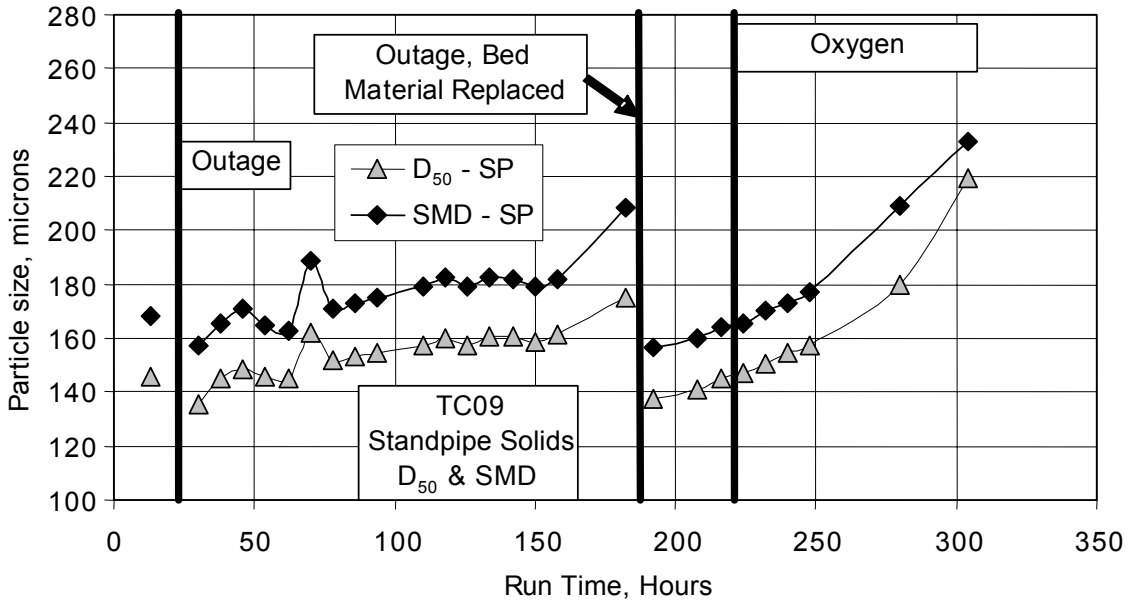

Figure 4.4-13 Standpipe Solids Particle Size

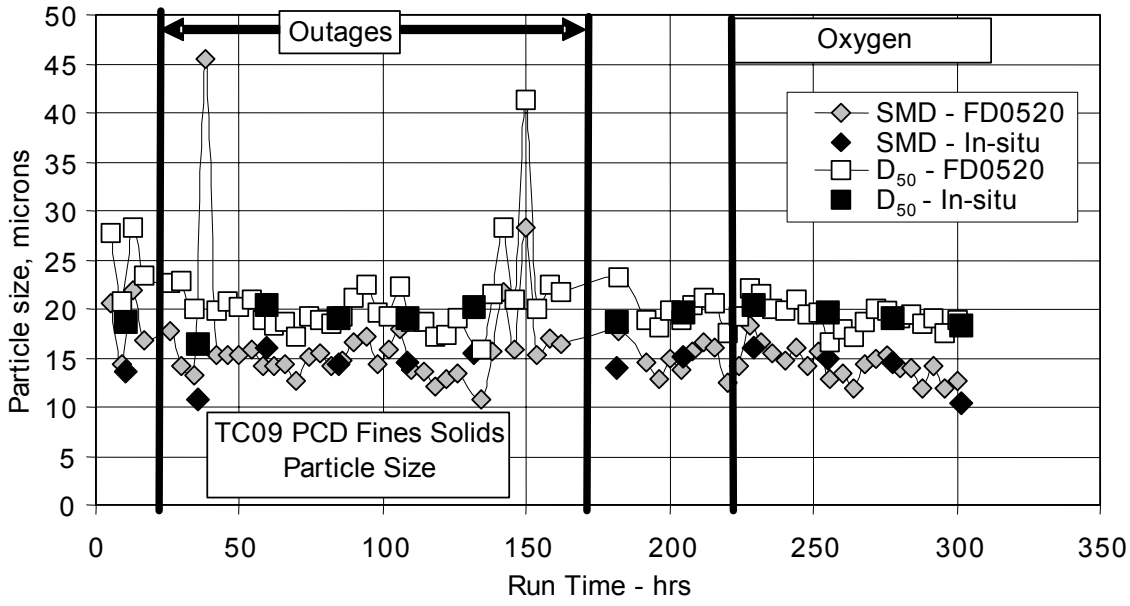

Figure 4.4-14 PCD Fines Particle Size

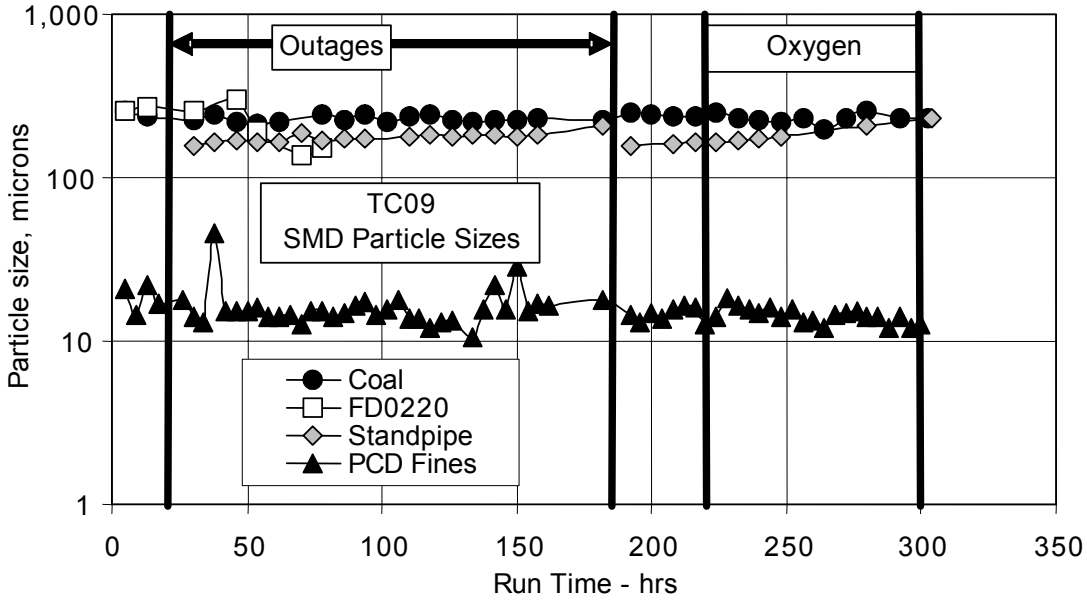

Figure 4.4-15 Particle Size Distribution

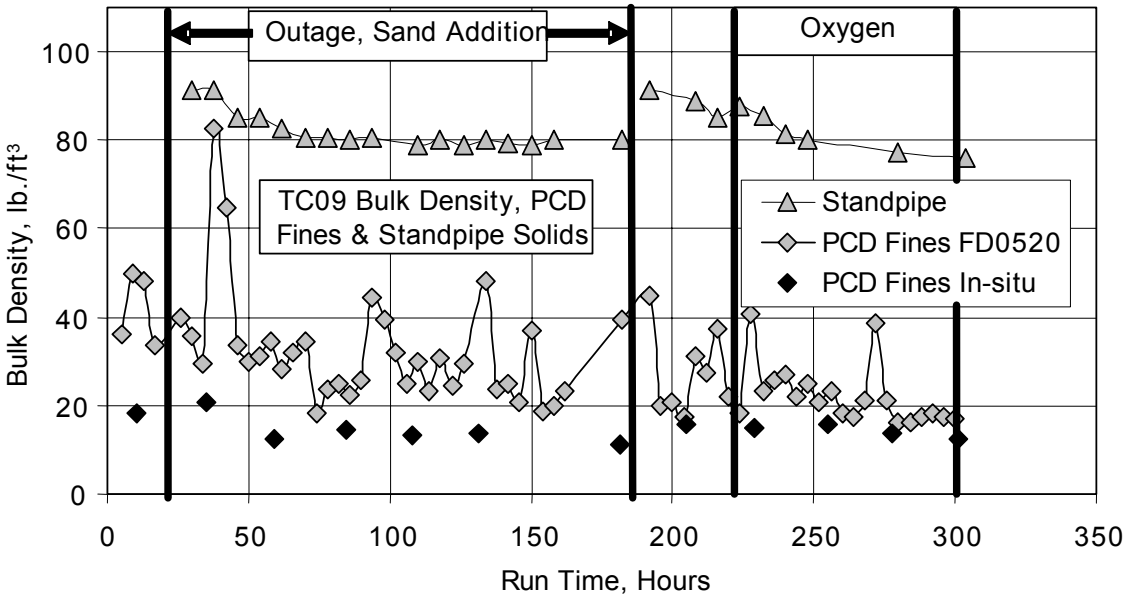

Figure 4.4-16 Standpipe and PCD Fines Solids Bulk Density

4.5 MASS AND ENERGY BALANCES

4.5.1 Summary and Conclusions

- Carbon conversions were between 87 and 95 percent in air-blown mode and between 85 and 90 percent in oxygen-blown mode.
- Carbon balances were acceptable for air-blown operation at -15 to 0 percent, with a negative bias. Carbon balances for oxygen-blown operation were acceptable, averaging about -17 percent, again with a negative bias.
- Coal rates were from 1,700 to 2,850 lb/hr.
- Oxygen-to-coal ratio (pound per pound) was 0.98 to 1.41 in air-blown mode and 0.86 to 0.96 in oxygen-blown mode.
- Overall mass balance was excellent at ±6 percent.
- Nitrogen balances were excellent at ±5 percent, assuming 1,250 lb/hr FI609 nitrogen did not enter the gasifier during air-blown mode and zero lb/hr FI609 nitrogen did not enter the gasifier during oxygen-blown mode.
- Sulfur balance was poor for air-blown mode at ±30 percent with no bias, and poor for oxygen-blown mode at about -13 to -30 percent with a negative bias.
- Sulfur removal was from 2 to 10 percent with one outlier at 18 percent. All removal came from the PRB coal alkalinity, since no sorbent was added.
- Sulfur emissions were from 0.60 to 1.01 lb SO_2/MBtu coal.
- Equilibrium H_2S calculations indicated that sulfur capture would not have been increased by the use of sorbent.
- Use of the measured steam rate did not produce acceptable hydrogen and oxygen balances, so the hydrogen balance was used to calculate the steam rate. Hydrogen balance steam rates were 30 to 50 percent higher than the measured steam rates.
- Oxygen balances were excellent for air-blown mode at ±3 percent and good for oxygen-blown mode at ±7 percent with a negative bias.
- Calcium balances were poor with about half of the calcium balances within ±40 percent.
- Energy balances were acceptable at 0 to 15 percent, with a positive bias in both modes.
- The raw cold-gasification efficiency was 34 to 60 percent for air-blown mode and 50 to 60 percent for oxygen-blown mode.
- The raw hot-gasification efficiency was between 82 and 92 percent for air-blown and 80 to 84 percent for oxygen blown.

- The corrected cold-gas efficiency was 44 to 71 percent for air-blown and 65 to 72 percent for oxygen blown.
- All three gasification efficiencies are strong functions of the steam-to-coal ratio.

4.5.2 Introduction

The process flows into the KBR Transport Gasifier are:

- Coal flow through FD0210.
- Coke breeze flow through FD0220.
- Air flow measured by FI205.
- Oxygen flow measured by FI726.
- Pure nitrogen flow measured by the sum of FI609 and FIC6080MEAS.
- Steam flow measured by the sum of FI204, FI727b, FI734, and FI733.

Sand was added through FD0220 to increase the Transport Gasifier bed height both during outages and coal feed. Limestone was not fed to the Transport Gasifier during TC09.

The process flows from the KBR Transport Gasifier process are:

- Synthesis gas-flow rate from the PCD measured by FI463.
- PCD solids flow through FD0520.
- Gasifier solids flow through FD0510.

The coal flow through FD0210 can be determined by three different methods:

- FD0210 surge bin weigh cell.
- Transport Gasifier carbon balance.
- Syngas Combustor carbon balance.

The FD0210 surge bin weigh cell uses the time between filling cycles and the weigh differential between dumps to determine the coal rate. This method was used to determine the coal rate in GCT4 and resulted in both the carbon and energy balance being 10 to 20 percent high. It appeared that the coal rates determined from the FD0210 weigh cell data were consistently higher than actual coal rate. For TC09, the energy balance based on the FD0210 weigh cells coal rate was 25 percent too high with 25 percent more energy entering the Transport Gasifier than accounted for in the product streams.

The Transport Gasifier carbon balance method uses the syngas carbon rate from the syngas flow rate and composition plus the PCD carbon rate from the PCD fines carbon concentration and PCD solids-flow rate. This method was used in TC06, TC07, and TC08. For TC09, the Transport Gasifier carbon balance was 12 percent high for air-blown and 20 percent high for oxygen-blown when using the coal rate from the Transport Gasifier carbon balance.

The syngas combustor carbon balance method uses the syngas combustor flue gas CO_2 analyzer and the syngas combustor flue gas rate to determine the carbon in the synthesis gas. The carbon in the PCD fines is added to the carbon in the synthesis gas to determine the coal rate. The syngas combustor carbon balance coal rates energy balance averaged 8.5 percent high for TC09. The TC09 energy balance was better for the syngas combustor carbon balance method than the other two coal rate methods so the syngas combustor carbon balance coal rate was used for TC09. The carbon balance using the syngas combustor carbon balance method is given on Table 4.5-1.

4.5.3 Feed Rates

The coke breeze flow through sorbent feeder FD0220 was determined from a correlation between feeder speed and dumps from the FD0220 storage bin between fills. The correlation is for data taken during the steady operating periods. This FD0220 flow rate - feeder speed data correlation is shown on Figure 4.5-1. The correlation for the sorbent feeder is:

$$\text{FD0220 rate} = 47.924(\text{rpm}) \quad (1)$$

The operating period coke breeze rates are shown on Table 4.5-2 and were from zero to 41 lb/hr. Coke breeze was fed to the Transport Gasifier during about 1/5 of the TC09 operating periods.

The operating period steam, oxygen, and nitrogen flow rates are shown in Figure 4.5-2 and on Table 4.5-2. It is estimated that during air-blown mode about 1,250 lb/hr nitrogen from FI609 does not enter the process but is used to seal valves, pressurized - depressurized feed and ash lock hopper systems, and in the seals for the screw coolers. During oxygen-blown mode, the nitrogen balance was better when it was assumed that no nitrogen leaked out of the process. Values on Table 4.5-2 and Figure 4.5-2 assume that 1,250 lb/hr of nitrogen from FI609 does not enter the Transport Gasifier during air-blown mode. In oxygen-blown mode, the actual FI609 nitrogen flow rate is used. In TC06, it was assumed that 1,000 lb/hr of nitrogen was lost, in TC07 it was assumed that 500 lb/hr was lost and in TC08 it was assumed that 1,000 lb/hr of nitrogen were lost. A small amount of nitrogen (~200 lb/hr) is added via FI6080 to the Transport Gasifier through the coke breeze feed line to keep the line clear between periods of coke breeze feed. This is included in the feed nitrogen.

Nitrogen rates were from 5,000 to 6,600 lb/hr during the first TC09 air-blown mode and were 4,600 for the second air-blown mode. The nitrogen rate was steady at about 6,000 lb/hr during oxygen-blown mode. Increasing the nitrogen rate decreases the LHV, so the air-blown mode LHV should have some variation, while the oxygen-blown mode LHV should be steady.

The oxygen rate was zero for air-blown mode. For oxygen-blown mode the oxygen rate was about 3,000 lb/hr.

The steam rate to the gasifier should be determined from the sum of FI204 (total steam flow to the UMZ), FI727 or FI727b (steam mixed with the air fed to the LMZ), FI734 (steam fed into the LMZ), and FI733 (steam fed to a shroud into the LMZ). FI727 and FI727b are two flow

meters on the same line and both should read the same. Since they did not, the decision was made to use one or the other. (In TC08, the hydrogen balance was used to decide which flow meter, FI727 to FI727b to use.) Using the TC09 steam rates from the steam flow meters resulted in poor Transport Gasifier hydrogen and oxygen balances, so the TC09 steam rate by hydrogen balance was used rather than the measured steam rate. A comparison of the hydrogen balance and measured steam rates will be given in Section 4.5.9.

TC09 began with 3,300 lb/hr steam for the first operating period, and then decreased to 1,500 from 2,000 lb/hr steam fed to the gasifier until hour 50, when the steam rate was increased to 5,000 lb/hr. The steam rate was then held steady at between 3,000 to 4,000 lb/hr until hour 200. The final two air-blown operating periods had steam rates between 2,500 and 3,000 lb/hr. All oxygen-blown mode operating periods had steam rates between 4,000 and 5,000 lb/hr. Steam was added during the oxygen-blown modes to control gasifier temperature. The steam rate was about 1,500 lb/hr during the final air-blown operating period.

Lower steam rates would tend to increase the synthesis gas LHV as shown in Figure 4.5-3. Air-blown mode tests show the trend clearly due to the large variation in air-blown steam rates.

The operating period air-feed rates are shown on Figure 4.5-4 and listed on Table 4.5-2. The air rate was between 9,500 and 12,500 lb/hr for the air-blown mode testing. During oxygen-blown mode there was no air fed to the Transport Gasifier. During the final period of air-blown mode, the air rate was about 10,000 lb/hr.

4.5.4 Product Rates

The operating period synthesis-gas rates are shown on Figure 4.5-4 and listed on Table 4.5-2. The synthesis-gas rates were taken from FI463.

The synthesis-gas rate was checked for all the operating periods using an oxygen, carbon, and hydrogen balance around the synthesis gas combustor and found to be in good agreement with the synthesis gas combustor data for most of the operating periods (see Figures 4.3-20, -21, and -22). The synthesis-gas rate was from 18,000 to 24,000 lb/hr for the first period of air-blown mode. During oxygen-blown mode the synthesis gas rate was from 14,000 to 15,000 lb/hr. The syngas rate was at 18,000 lb/hr for the final air-blown operating period. The synthesis gas rate is a strong function of the air and oxygen rates and a weak function of the steam and nitrogen rates.

The solids flow from the PCD can be determined from two different methods by using:

- In situ particulate sampling data upstream of the PCD.
- FD0530 weigh cell data.

The best measurements of the PCD solids flow are the in situ PCD inlet particulate determinations. Using the synthesis gas-flow rate and the in situ PCD inlet particulate measurement, the solids flow to the PCD can be determined, since the PCD captures all of the solids.

The FD0530 weigh cell data can be used to determine the PCD solids flow only if both the FD0530 feeder and the FD0510 feeder (standpipe solids) are off because FD0520 and FD0510 both feed into FD0530 and FD0530 feeds the sulfator. This method assumes that the PCD solids level in the PCD and FD0502 screw cooler are constant, that is the PCD solids level is neither increasing nor decreasing. A good check on the PCD fines rates is the calcium balance since the only calcium flows are the feed coal and the PCD fines since there was no standpipe flow in TC09. The two PCD fine rates methods are compared on Figure 4.5-5 where the twelve in situ rates are plotted against rates determined by the FD0530 weigh cells at about the same time. The in situ rates were higher than the FD0530 weigh cell rates for 10 of the 12 in situ samples. Only two samples gave excellent agreement. The three high in situ solids rates were either taken less than 24 hours after startup or were taken at a high coal rate prior to shutdown.

The results for all of the FD0530 weigh cell data are compared with the in situ data in Figure 4.5-6. The FD0530 weigh cell measurements had a large scatter and were usually lower than the in situ samples PCD fines rates. Also plotted on Figure 4.5-6 are the interpolated PCD solids rates used for the operating periods. The three high (above 800 pph) PCD solids rates were not used in estimating the PCD fines rates for the operating periods.

The operating periods PCD fines rates were from 400 to 600 lb/hr and did not change during oxygen-blown mode. The operating period's rates were used in mass balances shown on Table 4.5-2.

FD0510 was operated during 12 of the operating periods. The flow rates from those 12 periods are shown on Table 4.5-2. The amounts of solids removed from the gasifier were determined by differences in the standpipe level using LI339 before and after FD0206 and FD0510 operation. Since FD0510 was usually not operated for an entire operating period, the values shown on Table 4.5-2 and used in the mass balances have been prorated down from the FD0510 rates determined as if FD0510 had been operating continuously.

4.5.5 Coal Rates and Carbon Conversion

In GCT3 and GCT4, both the carbon balance and energy balance were off by 10 to 20 percent. It was speculated that this was due to FD0210 weigh cell data reading about 15 percent too high. Using coal rates determined by TC06 FD0210, weigh cell data would have produced a TC06 carbon balance that had 10 to 20 percent more carbon entering the Transport Gasifier than exiting the Transport Gasifier. The other large carbon flows (synthesis gas carbon flow and PCD solids carbon flow) were independently checked, so it is likely that the weigh cell coal rate was in error. The coal rate was determined in TC09 by a Synthesis Gas Combustor carbon balance, PCD carbon, standpipe carbon, and the PCD solids rate. Table 4.5-1 gives the TC09 Transport Gasifier carbon flows for each operating period.

The Transport Gasifier carbon balance coal rates, synthesis gas combustor carbon balance coal rates, and FD0210 weigh cells coal rates for the operating periods are compared on Figure 4.5-7. The FD0210 weigh cell coal rates were determined from a spreadsheet which calculated the coal

rate for every filling of the FD0210 surge vessel. The values for the FD0210 weigh cell were averaged for each operating period.

The weigh cell coal feed rate was higher than both the Transport Gasifier carbon balance coal rate and the syngas combustor carbon balance coal rate for all of TC09 during both air and oxygen mode. The coal rate by the syngas combustor carbon balance agrees well with the coal rate by the syngas analyzers for the first 86 hours of TC09. After the first 86 hours, the coal rate by syngas combustor carbon balance was consistently lower than the coal rate by the Transport Gasifier carbon balance. This was as expected since the syngas combustor has a good carbon balance with the synthesis gas rate and composition (see Figure 4.3-21) up to hour 86, and then the syngas combustor CO_2 analyzer was consistently lower than the CO_2 calculated from the Transport Gasifier gas composition.

The Syngas Combustor carbon balance coal rate will be used for all further data analysis in this section. This is because the energy balance is better for the lower Syngas Combustor carbon balance coal rates. The Transport Gasifier energy balance has more energy coming in than going out for all three coal rate methods, so using the Syngas Combustor carbon balance coal rate lowers the energy balance error. Use of the higher weigh cell coal rates decreases the carbon conversion when compared to using the coal rates by the Transport Gasifier or syngas combustor carbon balance.

The carbon balance coal-flow rates for the operating periods are given in Table 4.5-2. The coal rate was at about 2,800 lb/hr for the first two operating periods. The coal rate was slowly reduced to 1,700 lb/hr for hours 52 and 58. The coal rate was then increased to about 2,500 lb/hr at hour 144. The coal rate was then held steady at about 2,400 lb/hr until the start of oxygen mode at hour 226. For the oxygen-blown mode, the coal rate decreased to 1,950 lb/hr and then increased to 2,500 lb/hr.

The carbon balance is given on Figure 4.5-8. All of the air-blown carbon balances were between 0 and -15 percent error, while the oxygen-blown carbon balances were at about a -15 percent error. The carbon balance was sacrificed some to obtain the best possible energy balance by choosing the lowest coal rate.

Carbon conversion is defined as the percent fuel carbon that is gasified to CO, CO_2, CH_4, C_2H_6, and higher hydrocarbons. The carbon conversion is the measure of how much carbon is rejected by the gasifier with the PCD and gasifier solids. For the coke breeze addition periods of TC09, the coke breeze carbon was considered potential carbon for gasification. The rejected carbon to the gasifier or PCD fines solids is typically burned in a less efficient combustor (or disposed) and results in a less efficient use of fuel.

Due to errors in the carbon balance, the carbon conversion can be calculated at least three different ways. Since the carbon balance is off by up to 22 percent, each result could be different. If there were a perfect carbon balance, all three calculations would produce the same result (as in TC09A-4). Three calculation methods were used to determine carbon conversion with each:

1. Based on the feed carbon (coal plus coke breeze) and the carbon in the syngas. This assumes that the feed carbon and the synthesis gas carbon are correct. (Gas analyses method)
2. Based on the feed carbon and the synthesis gas carbon determined by a Transport Gasifier carbon balance, not the gas analyses. This assumes that the synthesis gas carbon is incorrect. (Solids analyses)
3. Based on the feed carbon determined by Transport Gasifier carbon balance and the synthesis gas carbon. This assumes that the coal feed is in error. (Products analyses)

The carbon conversion for all three methods is plotted on Figure 4.5-9. The carbon conversions for each operating period are given on Table 4.5-1. The carbon conversion by the gas method is larger than the carbon conversion by the products method, which is, in turn, larger than the solids method. The carbon conversion by the gas method has nearly half of the carbon conversions above 100 percent, which is a result of the syngas carbon being larger than the coal carbon for several operating periods. Clearly this is an unrealistic carbon conversions method. The products method is the most reasonable since it is not based on the coal rate, but on the syngas and PCD solids rates. The products method carbon conversion declined during the air-blown mode from 95 percent at the start of TC09 down to about 88 percent for most of the air-blown mode. During the oxygen-blown mode the products method carbon conversions was between 85 and 90 percent and was lower than during air-blown mode.

The carbon conversion should be a function of gasifier temperature, with the carbon conversion increasing as the temperature increases. The TC09 products method carbon conversions are plotted against riser exit temperature in Figure 4.5-10. Looking at the air-blown and oxygen-blown data individually, there is no effect of riser temperature on carbon conversions. Looking at all the data there appears to be a slight decrease of carbon conversion due to temperature because the lower oxygen mode carbon conversions are at a higher temperature than the air-blown carbon conversions. This is consistent with TC06, TC07, and TC08 data.

The carbon conversions of TC06 and TC07 gasifying PRB coal averaged 95-percent carbon conversions, indicating that the PRB is a more reactive coal than Hiawatha bituminous coal.

4.5.6 Overall Material Balance

Material balances are useful in checking the accuracy and consistency of data, as well as determining periods of operation where the data is suitable for model development or commercial plant design. Total material balances for each operating period are given on Figure 4.5-11 which compare the total mass in and the total mass out. The overall material balance was excellent, with all of the relative differences at ±6 percent. The relative difference (relative error) is defined as the Transport Gasifier feeds in minus products out divided by the feeds ({In-Out}/In). Note that the air-blown operating periods had higher overall mass-flow rates than the oxygen-blown operating periods.

The details of the overall mass balance are given in Table 4.5-2 with the relative differences and the absolute differences. The absolute difference (absolute error) is defined as the difference between the feeds and the products (In-Out).

The gas composition data in Section 4.3 and the solids composition data in Section 4.4 affect the mass balance through the coal rate determined by carbon balance. The main contributors to the material balance are the synthesis gas rate (13,900 to 23,000 lb/hr), air rate (0 to 12,500 lb/hr), oxygen rate (0 to 2,300 lb/hr), steam rate (1,550 to 4,900 lb/hr.), nitrogen rate (4,600 to 6,400 lb/hr), and coal rate (1,700 to 2,600 lb/hr).

The oxygen-to-coal ratios are listed on Table 4.5-2. The oxygen-to-coal ratio was 0.98 to 1.41 for air-blown operation and 0.86 to 0.96 for oxygen-blown operation. The differences in oxygen-to-coal ratios between air- and oxygen-blown is because less oxygen per pound of coal is required for oxygen-blown operation since air-blown operation requires more coal and air oxygen to heat up the air nitrogen.

4.5.7 Nitrogen Balance

TC09 operating period's nitrogen balances are plotted in Figure 4.5-12 by comparing the nitrogen in and the nitrogen out and are listed in Table 4.5-3. Nitrogen flows for air-blown test TC09A-3 are shown in Table 4.5-4 and nitrogen flows for oxygen-blown test TC09C-13 are shown on Table 4.5-5. Both the air- and oxygen-blown nitrogen balances were excellent with errors less than 5 percent for all operating periods. The nitrogen balances were made by assuming that 1,250 lb/hr of nitrogen was lost through seals and lock hopper purges for air-blown testing, while no nitrogen was lost for oxygen-blown testing. It is reasonable to expect that less nitrogen would be lost at lower pressure oxygen-blown operation than higher pressure air-blown operation. Note that air-blown mode nitrogen rates (13,000 to 16,000 lb/hr) were much higher than oxygen-blown nitrogen rates (6,000 to 7,000 lb/hr).

The nitrogen flows as shown in Tables 4.5-4 and -5 are dominated by the air, nitrogen, and synthesis gas flows. None of the solid streams contribute significantly to the nitrogen balance. TC06 nitrogen balances had a ±5-percent error, assuming 1,000 lb/hr of nitrogen lost, while TC07 had nitrogen balance errors of ±2 percent assuming 500 lb/hr of nitrogen lost. TC08 nitrogen balances were at 1 to 7 percent for air-blown mode, 2 to 4 percent for enhanced air mode, and -16 to 5 percent for oxygen-blown mode, assuming 1,000 lb/hr nitrogen did not enter the reactor. The TC09 air-blown nitrogen balances are consistent with TC06, TC07, and TC08 air-blown nitrogen balances, while the TC09 oxygen-blown mode had better nitrogen balances than TC08 oxygen-blown nitrogen balances.

4.5.8 Sulfur Balance and Sulfur Removal

Sulfur balances for all the TC09 operating periods are given in Figure 4.5-13 and Table 4.5-6. The synthesis gas sulfur compounds were not directly measured, but estimated from syngas combustor SO_2 analyzer data and synthesis gas combustor flue gas flow. The coal sulfur values were interpolated between the solids sampling times. The sulfur balances were poor for air-blown, with relative errors of less than ±30 percent for most of the air-blown operating periods

with no bias. The air-blown sulfur balances were much better than previous sulfur balances since 65 percent were with ±10 percent and there was no bias. The oxygen-blown sulfur balances were poor and between -13 and -30 percent. The air-blown sulfur balances were better than the sulfur balances for TC06, TC07, and TC08.

Most of the operating period's sulfur balances were biased high in TC06 and TC07. The first TC08 air-blown sulfur balance was neutral and the second air-blown sulfur balance was biased high. The TC08 enhanced air sulfur balances were biased high and the TC08 oxygen-blown sulfur balances were biased slightly negative.

With the errors in the sulfur balances, it is difficult to determine the correct sulfur removal. Similar to the coal conversions calculations, there are three different methods to determine Transport Gasifier sulfur removals:

1. From synthesis gas sulfur emissions (using the synthesis gas combustor flue gas rate and synthesis gas combustor flue gas SO_2 measurement) and the feed sulfur rate (using the feed-coal rate and coal sulfur content). (Gas analyses method)
2. From PCD solids analysis (using PCD solids flow rate and PCD solids sulfur content) and the feed-sulfur rate. (Solids analyses method)
3. From the gas analysis data and the PCD solids data. (Product analyses method)

The three sulfur removals are plotted on Figure 4.5-14 and given on Table 4.5-6. The sulfur in the fuel is an inaccurate measurement due to the multiplication of a very small number (coal sulfur) by a large number (coal-feed rate). The coal rate is determined by carbon balance rather than an actual measurement. The low coal sulfur contents (0.38 weigh percent sulfur) increases the error in feed sulfur. The gaseous sulfur flow should be accurate, although it is also the product of a small number (syngas combustor SO_2) and a large number (syngas combustor flue gas rate). The PCD fines sulfur rates have inaccuracies due to the low sulfur in the PCD solids. There is no accumulation of sulfur-containing solids in the gasifier during TC09 because the standpipe gasifier samples contained negligible amounts of sulfur.

The TC09 results indicate that the gas method is less accurate than the product and the solids methods. The solids and products methods usually agreed with each other and seemed to change slowly and consistently during the run. The gas method varied a lot during the run and there were several periods of negative gas method sulfur removals. The negative sulfur removals were because the sulfur flows out were larger than the sulfur flows in. The sulfur removal by the products is probably the most reliable sulfur removal.

The sulfur removal by-product varied from 2 to 10 percent during the air-blown mode, with one outlier at 18 percent. During oxygen-blown mode the products sulfur removal was more consistent at 6 to 10 percent than the air-blown mode sulfur removals. The solids method sulfur removal tracked the products method sulfur removal. The three methods agreed when the sulfur balance had less than about 0.1-percent error (TC09B-7a, TC09B-7b, and TC09B-8b).

The synthesis gas combustor SO_2 data was used for the sulfur emissions shown in Table 4.5-6. The sulfur emissions were from 0.60 to 1.01 lb SO_2/MBtu coal fed.

Figure 4.5-15 plots the measured sulfur emissions against the coal maximum reduced sulfur emissions. The coal maximum sulfur emissions are the maximum sulfur emissions possible based on the coal-feed rate, coal sulfur level, and syngas flow rate assuming zero percent sulfur capture. On Figure 4.5-15, the 45-degree line is the 0-percent sulfur removal line (sulfur emissions equal maximum coal sulfur emissions) and the X-axis is the 100-percent sulfur removal line (0-sulfur emissions). The area of the plot above the 45-degree line would indicate less than 0-percent removal; data that is in this region would be the result of errors in the sulfur balance that would have the data indicated more sulfur leaving the Transport Gasifier than in the feeds. This plot is a replotting of the gas method sulfur removal calculation since it is based on the coal feed sulfur and the syngas sulfur. The air-blown data indicates very little sulfur removal, with a few points above the 0-percent capture line. This is reflected in the air-blown gas method sulfur removal usually being above 0 percent and a few indicating above 20-percent sulfur capture. All the TC09 oxygen-blown data indicated less than 0-percent capture, due to errors in the coal feed-rate or sulfur levels. A higher coal rate or coal sulfur level would produce sulfur captures higher than the 0-percent capture calculated by the gas method from TC09 data.

The calculation of the minimum equilibrium synthesis H_2S concentration has been described in previous PSDF reports. In summary, the minimum equilibrium H_2S concentration is a function of the partial pressures of H_2O and CO_2 as long as there is calcium sulfide present in the solids. (The equilibrium H_2S concentration is a function of system temperature, while the minimum equilibrium H_2S concentration is not a function of temperature.) As the partial pressures of H_2O and CO_2 increase, the H_2S concentration should increase. Using Aspen simulations, the minimum equilibrium H_2S concentrations were determined for all of the operating periods and listed in Table 4.5-6.

Figure 4.5-16 plots the TRS and equilibrium H_2S directly against each other for TC09. The data is expected to all fall above the 45-degree line since the minimum equilibrium H_2S concentration should be the lowest H_2S concentration in a system with calcium sulfide present. All of the oxygen-blown data and nearly all of the air-blown data indicate sulfur emissions less than equilibrium, when in fact there was very little sulfur capture. The high H_2S equilibrium concentrations are a result of the high steam rates and resulting H_2O concentrations used in TC09. If the H_2S equilibrium concentrations are above the measured sulfur emissions, this indicates that no sulfur capture is possible. Put another way, the comparison of the equilibrium H_2S and measured sulfur emissions indicates that there is insufficient sulfur in the system to form CaS at the process conditions present in the reactor (low coal sulfur levels, high syngas H_2O concentrations). The equilibrium H_2S calculations reveal that there should be minimal sulfur capture for air-blown operation, and no sulfur capture for oxygen-blown operations, which is what the TC09 data indicated. Another conclusion of the equilibrium calculations is that the addition of sorbent would not have increased the sulfur capture, since the sulfur capture was not limited by insufficient sorbent, but by H_2S equilibrium.

4.5.9 Hydrogen Balance

In previous testing, the steam rate has been blamed for most of the errors in the hydrogen and oxygen balances. The TC09 hydrogen and oxygen balances were both poor if the measured stream rate was used in the material balances. For TC09, it was assumed that the steam rate determined by the hydrogen balance was more accurate than the measured steam rate. The steam rate for each operating period was calculated using a hydrogen balance, which is essentially the difference in hydrogen between the coal feed and synthesis gas rate. The hydrogen balance steam rate is compared with the measured steam rate on Figure 4.5-17. The measured steam rate is from a PI tag that sums the steam rate to the reactor from FI204 (total steam flow to the UMZ), FI727b (steam mixed with the air fed to the LMZ), FI734 (steam fed into the LMZ), and FI733 (steam fed to a shroud into the LMZ). The tag rejects any steam flows that are negative. The hydrogen balance steam rates were 30 to 50 percent higher than the measured steam rates. Using the measured steam rates would cause the hydrogen and oxygen balances to be severely in error.

Typical hydrogen flows for air-blown test TC09A-3 are shown in Table 4.5-4 and typical hydrogen flows for oxygen-blown test TC09C-13 are shown on Table 4.5-5. Note the lower steam rate in the air-blown mode example. The coal, steam, and synthesis gas streams dominate the hydrogen balance. The hydrogen balance was -20 to 0 percent for TC06 and -30 to 0 percent for TC07, and 0 to 12 percent in TC08.

In TC07 the hydrogen balance indicated that there was about 500 pounds more steam per hour than measured being fed to the Transport Gasifier. During TC08, the enhanced air- and oxygen-blown modes the steam rate by hydrogen balance was less than the measured steam rate by about 200 to 500 lb/hr of steam. The second air-blown mode indicates that about 500 pounds more steam per hour is being fed to the Gasifier than reported by the measured steam rate.

4.5.10 Oxygen Balance

Operating period oxygen balances are given in Figure 4.5-18 and Table 4.5-3. Typical oxygen flows for air-blown test TC09A-3 are shown in Table 4.5-4 and typical oxygen flows for oxygen-blown test TC09C-13 are shown on Table 4.5-5. The oxygen balance is determining if the steam and oxygen or air rates are consistent with the synthesis-gas rate and composition.

The TC09 operating period's oxygen balances for air-blown mode were excellent with all operating periods with less than ±3 percent relative error. The TC09 oxygen-blown mode oxygen balances were very good with all operating periods less than ±7-percent relative error with a low bias. Using the measured steam rates would have put the oxygen balances off by about 20 percent. The good oxygen balances indicate that the measured steam rates were not consistent with the rest of the TC09 data, while the hydrogen balance steam rates were consistent.

The TC06 oxygen balances were off by -20 to -4 percent and the TC07 oxygen balances were off by -20 to -5 percent. The TC08 oxygen balances were from 0 to 12 percent (0 to 859 pounds

oxygen/hr). The TC09 oxygen balances were better than the TC06 through TC08 oxygen balances, which used the measured steam rates.

4.5.11 Calcium Balance

Operating period calcium balances are given in Figure 4.5-19 and Table 4.5-3. Typical calcium flows for air-blown test TC09A-3 are shown in Table 4.5-4 and typical calcium flows for oxygen-blown test TC09C-13 are shown on Table 4.5-5. The calcium balances are essentially a comparison between the coal calcium and the PCD fines calcium, since there was no sorbent fed to the gasifier during TC09, minimal flow through FD0510, and the gasifier accumulation term was assumed to be small.

The calcium balances were acceptable during over half of the TC09 operating periods, when the calcium balance was from ±40 percent (±40 lb calcium/hr). Nearly all of the calcium balances had a positive bias. This is acceptable because essentially the comparison is between two solid streams that are difficult to measure. The calcium balances were the best during the middle of TC09, from hours 52 to 281, and the worst during the beginning and end of TC09. Note that the TC09 calcium rates are lower than TC06 and TC07 due to no sorbent feed in TC09. TC09 calcium rates were consistent with TC08 that also had no sorbent feed. In TC06 the calcium balances were off by -50 to +40 percent, in TC07 the calcium balances were off by -100 to +40 percent, and the TC08 calcium balances were off by ±40 percent.

Figure 4.5-20 plots TC09 sulfur removal by products method as a function of calcium to sulfur molar ratio (Ca/S, molecular weight) measured in the PCD solids samples from FD0520. The sulfur removals were 2 to 10 percent with one outlier at 18 percent. There removals were consistent with TC08 PRB sulfur removals with no sorbent addition. The trends in PCD solids Ca/S with sulfur emissions on Figure 4.5-20 are opposite of what are expected if the amount of excess sorbent is limiting sulfur capture. (It is expected that increased sorbent should lead to increased sulfur removal.) The sulfur removal should increase with Ca/S. Since the sulfur capture is in fact limited by gas-phase equilibrium, the amount of excess calcium is does not effect sulfur capture. The results seen on Figure 4.5-20 demonstrate that when the PCD solids contain very little sulfur (high Ca/S) the sulfur removals are low, which is reasonable by sulfur balance. The calcium sulfation percent is the reciprocal (times 100) of the Ca/S ratio based on the PCD fines solids. TC06 had 10- to 55-percent sulfur removal, TC07 had 5 to 50 percent sulfur removal, and TC08 had 0 to 17 percent sulfur removal. The lower sulfur removal during TC08 and TC09 were due to the absence of limestone feed and the high steam rates and resulting high syngas H_2O concentrations.

Figure 4.5-21 plots TC09 sulfur emissions (expressed as lb SO_2 emitted/MBtu coal fed) as a function of calcium-to-sulfur ratio (Ca/S) measured in the PCD solids sampled from FD0520. The sulfur emissions varied from 0.6 to 1.0 lb SO_2 emitted/MBtu coal fed with no trend with Ca/S ratio. The sulfur emissions were higher with oxygen-blown mode than air-blown mode, probably due to the higher steam rates during oxygen-blown mode, which would cause the H_2S equilibrium concentration to be higher. TC06 sulfur emissions were from 0.13 to 0.37 lb SO_2/MBtu, TC07 sulfur emissions were from 0.15 to 0.47 lb SO_2/MBtu, and TC08 were from 0.4 to

0.7 as lb SO_2 emitted/MBtu coal. TC08 and TC09 had similar sulfur emissions due to the higher steam rates than in TC06 and TC07.

4.5.12 Energy Balance

The TC09 Transport Gasifier energy balance is given in Figure 4.5-22 with standard conditions chosen to be 1.0 atmosphere pressure and 80°F. Table 4.5-7 breaks down the individual components of the energy balance for each operating period. The "energy in" consists of the coal, air, and steam fed to the Transport Gasifier. The nitrogen, oxygen, and sorbent fed to the gasifier were considered to be at the standard conditions (80°F) and hence have zero enthalpy. The "Energy out" consisted of the synthesis gas and PCD solids. The LHV of the coal and PCD solids were used in order to be consistent with the LHV of the synthesis gas. While the gasifier solids sampled from FD0510 flow had no latent heat, there was a small amount of sensible heat in the FD0510 solids. The energy of the synthesis gas was determined at the Transport Gasifier cyclone exit. About 1,200 pounds N_2/lb fed to the PCD inlet and outlet particulate sampling trains has been subtracted from the synthesis-gas rate to determine the actual syngas rate from the cyclone. The sensible enthalpy of the synthesis gas was determined by overall gas heat capacity from the synthesis gas compositions and the individual gas heat capacities. The synthesis gas and PCD solids energy consists of both latent and sensible heat. The heat loss from the Transport Gasifier was estimated to be 1.5 x 10^6 Btu/hr based on a previous combustion test. The assumption of 3.5 x 10^6 Btu/hr heat loss would put all of the TC09 energy balance error to be less than 10 percent. It is possible that the actual Transport Gasifier heat losses are higher than the 1.5 x 10^6 Btu/hr measured.

The TC09 energy balances had from 0 to +15-percent errors, with a consistent positive bias. There was more scatter in the air-blown energy balance errors while the oxygen-blown energy balance errors were about +10 percent. The negative carbon balance errors and the positive energy balance errors were both minimized by choosing the minimum coal rate. The use of the Syngas Combustor carbon balance coal rate produced a better energy balance than if the Transport Gasifier carbon balance or the FD0210 weigh cell data coal flow rates were used, since both the FD0210 weigh cell data and the Transport Gasifier carbon balance carbon balance would make the energy balance have a higher heat loss than the synthesis gas combustor carbon balance coal rates, because both methods had higher coal rates than the synthesis gas combustor carbon balance coal rates.

4.5.13 Gasification Efficiencies

Gasification efficiency is defined as the percent of the energy (coal energy and steam energy) that is converted to potentially useful synthesis gas energy. Two types of gasification efficiencies have been defined: the cold-gas efficiency and the hot-gas efficiency. The cold-gas efficiency is the amount of energy feed that is available to a gas turbine as synthesis gas latent heat.

Similar to sulfur removal and carbon conversion, the cold-gas efficiency can be calculated at least three different ways. Since the energy balance is off by up to 16 percent, each result could be different. If there were a perfect energy balance, all three calculations would produce the

same result. Three calculation methods were performed for cold-gasification efficiency consistent with the three methods of sulfur removal:

1. Based on the feed heat (coal latent heat plus steam heat) and the latent heat of the synthesis gas. This assumes that the feed heat and the synthesis gas latent heat are correct. (Gas analyses)
2. Based on the feed heat (coal latent heat plus steam heat) and the latent heat of the synthesis gas determined by a Transport Gasifier energy balance, not the gas analyses. This assumes that the synthesis gas latent heat is incorrect. (Solids analyses)
3. Based on the feed heat determined by Transport Gasifier energy balance and the synthesis gas sensible heat. This assumes that the coal feed or the steam rate is in error. (Products analyses)

The cold-gas gasification efficiencies for the three calculation methods are plotted in Figure 4.5-23. For all of the operating periods, the products method is between the solids and gas methods. The gas method is lower than the solids method and the products method for all TC09 operating period that the energy balances are biased high. The three methods agree with each other whenever the energy balance is perfect (hours 10 and 26). Only the products method is listed on Table 4.5-7 because the products method is the most accurate method since it does not use the coal rate determined by carbon balance.

The products analysis cold-gas gasification efficiencies started TC09 at nearly 60 percent due to the high coal rate and low steam rate. The cold-gas efficiency decreased as the steam rate was increased and the coal rate decreased. The lowest efficiency (35 percent) was during the higher steam rates and the lowest coal rates at hours 52 and 57. Between hours 75 and the end of the run, the cold-gas efficiency was between 45 and 55 percent and was mainly dependent on the steam and coal rates. The oxygen-blown cold-gas efficiencies slowly increased from 50 to 60 percent as the steam rate was decreased. The steam rate effect on cold-gas efficiency is not due to steam dilution but due to the increased loss in efficiency of heating steam up to the Transport Gasifier temperature. An increase in steam decreases the syngas LHV and increases the syngas rate such that the total syngas enthalpy remains the same.

The trend in cold-gas efficiency with steam-to-coal ratio is shown in Figure 4.5-24, whereas the steam-to-coal ratio increases, the cold-gas efficiency decreases. The same trend is shown for both air and oxygen-blown modes. The oxygen-blown tests had higher cold-gas efficiency than the air-blown modes at the same steam-to-coal ratio by about 10 percent because the air-blown modes had the inefficiency of heating up the air nitrogen.

The hot-gasification efficiency is the amount of feed energy that is available to a gas turbine plus a heat recovery steam generator. The hot-gas efficiency counts both the latent and sensible heat of the synthesis gas. Similar to the cold-gasification efficiency and the sulfur removal, the hot-gas efficiency can be calculated at least three different ways. The three calculation methods for hot-gasification are identical, with the three methods of cold-gasification efficiency calculation except for the inclusion of the synthesis gas sensible heat into the hot-gasification efficiency.

The hot-gasification efficiency assumes that the sensible heat of the synthesis gas can be recovered in a heat recovery steam generator, so the hot-gasification efficiency is always higher than the cold-gasification efficiency. The three hot-gasification calculation methods are plotted in Figure 4.5-25 and shown on Table 4.5-7.

The products method is essentially equal to the solids method for all of the operating periods. This is because the amount of inlet coal heat is about the same as the total synthesis gas heat, and it makes little difference whether the synthesis gas heat is corrected or the coal heat. The gas method is lower than the solids and products when the energy balance has a high bias.

As with the cold-gasification efficiencies, the hot-gasification efficiencies started TC09 high, at 92 percent due to low steam and high coal rates. Once the steam rates were increased at hour 53 the hot-gasification efficiencies decreased to between 83 and 87 percent for the remainder of the air-blown mode testing. During the oxygen-blown mode testing, the hot-gasification efficiencies were between 80 and 85 percent. The oxygen-blown hot-gasification efficiencies are lower than the air-blown hot-gasification efficiencies since the air-blown syngas sensible heat is higher than the oxygen-blown syngas sensible heat due to the higher air-blown syngas rate.

Figure 4.5-26 plots the hot-gas efficiency against the steam-to-coal ratio. The trend of decreasing gasification efficiency with increasing steam-to-coal ratio is clear, but not as pronounced as the cold-gasification efficiency trend. The oxygen-blown hot-gasification efficiency is lower than the air-blown hot-gasification by about 5 percent at the same steam-to-coal ratios, due to the sensible heat of the air nitrogen counted in the hot-gasification efficiency.

Two main sources of losses in efficiency are the gasifier heat loss and the latent heat of the PCD solids. The gasifier heat loss of 1.5 MBtu/hr was about 5 percent of feed energy, while the total energy of the PCD solids was about 8 percent of the feed energy. The heat loss percentage will decrease as the gasifier size is increased. While the Transport Gasifier does not recover the latent heat of the PCD solids, this latent heat could be recovered in a combustor. The total enthalpy of the PCD solids can be decreased by decreasing both the PCD solids carbon content (heating value) and the PCD solids rate.

Gasification efficiencies can be calculated from the adiabatic nitrogen-corrected gas heating values and corrected flow rates that were determined in Section 4.3. The products adiabatic nitrogen-corrected cold-gasification efficiencies are plotted on Figure 4.5-27 against the corrected steam-to-coal ratio and are listed on Table 4.5-7 for all of the operating periods. Only the cold-gasification efficiencies based on the products are given in Figure 4.5-27 and Table 4.5-7 because they are the most representative of the actual gasification efficiencies. Since the nitrogen and adiabatic syngas LHV corrections reduce the coal rate and the steam rate (for oxygen-blown only), the corrected coal rates and the corrected steam rates were used in Figure 4.5-27. The corrected efficiencies are calculated assuming an adiabatic reactor, since zero heat loss was one of the assumptions in determining the corrected LHV in Section 4.3. The corrected cold-gas efficiencies were from 44 to 71 percent for air-blown mode and from 65 to 72 percent for oxygen-blown mode, with a decreasing trend of efficiency with increasing steam-to-coal ratio. As for the raw cold-gas efficiencies, the oxygen-blown mode was higher than the air-blown mode at equivalent steam-to-coal ratios. The nitrogen and adiabatic corrections

increased the cold-gasification efficiencies by about 10 percent in air-blown mode and by about 15 percent in oxygen-blown mode due to the use of recycle gas rather than nitrogen for aeration and instrument purges.

The adiabatic nitrogen correction does not increase the hot-gasification efficiency because the deleted nitrogen lowers the synthesis gas sensible heat and increases the synthesis gas latent heat. Both changes effectively cancel each other out.

Table 4.5-1

Carbon Rates

Operating Period	Average Relative Hours	Carbon In (Feed)			Carbon Out (Products)				In - Out	(In- Out)/In	Carbon Conversion[4]
		Coal[1] lb/hr	Coke B. lb/hr	Total lb/hr	Syngas lb/hr	Standpipe[2] lb/hr	PCD Solids lb/hr	Total lb/hr	lb/hr	%	%
TC09A-1	7	1,893	0	1,893	1,900	0.0	146	2,046	-153	-8	92.9
TC09A-2	10	1,875	0	1,875	1,970	0.0	110	2,080	-205	-11	94.7
TC09A-3	13	1,720	0	1,720	1,645	0.0	111	1,756	-36	-2	93.7
TC09A-4	18	1,489	0	1,489	1,384	0.0	99	1,483	7	0	93.3
TC09B-1	26	1,202	28	1,230	1,267	0.0	146	1,413	-183	-15	89.7
TC09B-2	31	1,618	26	1,644	1,556	0.0	129	1,685	-41	-2	92.4
TC09B-3	52	1,111	0	1,111	1,091	0.0	124	1,216	-104	-9	89.8
TC09B-4	57	1,130	0	1,130	1,116	0.0	134	1,250	-121	-11	89.3
TC09B-5	64	1,419	0	1,419	1,291	0.0	141	1,432	-14	-1	90.1
TC09B-6a	75	1,514	0	1,514	1,459	0.1	188	1,647	-134	-9	88.6
TC09B-6b	86	1,546	0	1,546	1,452	0.0	137	1,589	-43	-3	91.4
TC09B-7a	100	1,365	0	1,365	1,384	0.0	105	1,490	-125	-9	92.9
TC09B-7b	108	1,415	0	1,415	1,384	0.1	152	1,536	-121	-9	90.1
TC09B-8a	119	1,562	0	1,562	1,482	0.0	182	1,664	-102	-7	89.1
TC09B-8b	129	1,492	0	1,492	1,431	0.1	158	1,588	-96	-6	90.1
TC09B-9	144	1,705	0	1,705	1,589	0.0	212	1,801	-95	-6	88.2
TC09B-10	151	1,583	0	1,583	1,562	0.0	132	1,694	-111	-7	92.2
TC09B-11	158	1,681	0	1,681	1,538	0.1	222	1,760	-79	-5	87.4
TC09B-12	171	1,447	0	1,447	1,387	0.0	187	1,574	-127	-9	88.1
TC09B-13	175	1,610	0	1,610	1,596	0.0	166	1,762	-152	-9	90.6
TC09B-14	182	1,595	0	1,595	1,523	0.0	134	1,657	-62	-4	91.9
TC09C-1	196	1,487	31	1,519	1,555	0.0	177	1,733	-214	-14	89.8
TC09C-2	199	1,560	31	1,591	1,618	0.0	191	1,809	-218	-14	89.5
TC09C-3	206	1,593	30	1,622	1,591	0.0	210	1,800	-178	-11	88.4
TC09C-4	209	1,573	30	1,603	1,568	0.0	208	1,776	-173	-11	88.3
TC09C-5	226	1,424	26	1,450	1,509	0.0	254	1,763	-313	-22	85.6
TC09C-6	230	1,501	0	1,501	1,430	0.0	225	1,655	-154	-10	86.4
TC09C-7	244	1,307	0	1,307	1,352	0.2	148	1,500	-193	-15	90.1
TC09C-8	256	1,313	0	1,313	1,337	0.1	205	1,542	-229	-17	86.7
TC09C-9	264	1,338	0	1,338	1,325	0.1	229	1,554	-216	-16	85.3
TC09C-10	271	1,337	0	1,337	1,353	0.2	229	1,583	-245	-18	85.5
TC09C-11	278	1,550	0	1,550	1,562	0.1	235	1,797	-247	-16	86.9
TC09C-12	281	1,597	0	1,597	1,609	0.5	240	1,849	-253	-16	87.0
TC09C-13	294	1,558	0	1,558	1,590	0.2	222	1,813	-255	-16	87.7
TC09C-14	301	1,662	0	1,662	1,721	0.0	210	1,931	-269	-16	89.1
TC09C-15	302	1,512	0	1,512	1,606	0.0	207	1,812	-300	-20	88.6
TC09C-16	307	1,509	0	1,509	1,473	0.0	207	1,680	-170	-11	87.7

Notes:

1. Coal carbon determined by Syngas Combustor carbon balance.
2. Standpipe carbon flow intermittent. Rate shown is average FD0510 rate during operating period.
3. TC09A, TC09B, TC09C-1 to TC09C-4, and TC09C-16 were air blown; TC09C-5 to TC09C-15 were oxygen blown.
4. Carbon conversion based on products method.

Table 4.5-2 Feed Rates, Product Rates, and Mass Balance

		Feeds (In)							Products (Out)						
Operating Period	Average Relative Hours	Coal[4] lb/hr	Coke Br. FD0220 lb/hr	Air FI205 lb/hr	Oxygen FI426 lb/hr	Nitrogen FI609[1] lb/hr	Steam[5] lb/hr	Total lb/hr	Syngas FI465 lb/hr	PCD Solids FD0520 lb/hr	SP Solids FD0510[2] lb/hr	Total lb/hr	In - Out lb/hr	(In- Out)/In %	Oxygen to Coal Ratio lb/lb
TC09A-1	7	2,865	0	12,235	0	5,772	3,379	24,251	23,905	443	0	24,348	-97	-0.4	0.99
TC09A-2	10	2,844	0	12,466	0	5,653	2,238	23,201	22,955	443	0	23,398	-196	-0.8	1.02
TC09A-3	13	2,613	0	11,034	0	6,020	2,211	21,877	21,293	443	0	21,736	141	0.6	0.98
TC09A-4	18	2,263	0	10,093	0	5,573	1,540	19,469	18,847	357	0	19,204	265	1.4	1.03
TC09B-1	26	1,867	37	9,514	0	6,578	1,772	19,767	19,106	483	0	19,589	177	0.9	1.18
TC09B-2	31	2,509	33	10,893	0	6,051	1,988	21,474	20,701	483	0	21,184	289	1.3	1.01
TC09B-3	52	1,670	0	10,070	0	6,593	4,936	23,269	22,238	483	0	22,721	547	2.4	1.40
TC09B-4	57	1,695	0	10,350	0	6,231	5,424	23,700	22,965	483	0	23,448	252	1.1	1.41
TC09B-5	64	2,137	0	10,171	0	5,789	3,262	21,358	21,110	491	0	21,601	-243	-1.1	1.10
TC09B-6a	75	2,291	0	10,755	0	5,234	3,675	21,955	21,582	509	14	22,105	-150	-0.7	1.09
TC09B-6b	86	2,323	0	10,789	0	5,091	3,814	22,017	21,541	524	0	22,065	-48	-0.2	1.08
TC09B-7a	100	2,017	0	10,555	0	5,489	3,896	21,957	21,575	531	0	22,106	-148	-0.7	1.21
TC09B-7b	108	2,088	0	10,539	0	5,163	3,705	21,495	21,229	532	13	21,773	-278	-1.3	1.17
TC09B-8a	119	2,308	0	11,115	0	5,359	3,535	22,316	21,844	521	9	22,373	-57	-0.3	1.12
TC09B-8b	129	2,209	0	10,834	0	5,264	3,475	21,782	21,208	510	20	21,738	44	0.2	1.14
TC09B-9	144	2,548	0	11,935	0	6,035	4,204	24,722	24,278	507	0	24,785	-63	-0.3	1.09
TC09B-10	151	2,372	0	11,606	0	5,631	3,915	23,524	22,990	507	0	23,497	27	0.1	1.13
TC09B-11	158	2,519	0	11,335	0	5,554	3,862	23,270	22,626	507	17	23,150	120	0.5	1.04
TC09B-12	171	2,167	0	10,437	0	5,371	3,237	21,212	20,578	552	0	21,130	82	0.4	1.12
TC09B-13	175	2,412	0	11,352	0	5,403	3,646	22,813	22,056	552	0	22,608	205	0.9	1.09
TC09B-14	182	2,389	0	11,120	0	4,961	2,955	21,424	20,664	552	0	21,216	208	1.0	1.08
TC09C-1	196	2,235	41	11,214	0	6,052	3,168	22,710	21,819	548	0	22,367	343	1.5	1.16
TC09C-2	199	2,341	40	11,611	0	6,083	3,212	23,287	22,553	548	0	23,101	187	0.8	1.15
TC09C-3	206	2,380	39	11,338	0	5,388	2,923	22,068	21,226	552	0	21,778	290	1.3	1.10
TC09C-4	209	2,349	39	10,852	0	5,114	2,512	20,867	20,077	556	0	20,632	235	1.1	1.07
TC09C-5	226	2,123	34	0	2,015	6,377	4,639	15,187	15,528	588	0	16,117	-930	-6.1	0.95
TC09C-6	230	2,238	0	0	2,015	6,108	4,901	15,262	15,155	591	0	15,746	-483	-3.2	0.90
TC09C-7	244	1,944	0	0	1,857	6,007	4,627	14,435	14,389	540	43	14,973	-538	-3.7	0.96
TC09C-8	256	1,947	0	0	1,870	5,816	4,437	14,070	14,002	507	16	14,525	-455	-3.2	0.96
TC09C-9	264	2,001	0	0	1,869	5,972	4,233	14,074	13,879	521	20	14,420	-346	-2.5	0.93
TC09C-10	271	2,016	0	0	1,869	6,004	4,297	14,186	14,075	534	43	14,652	-466	-3.3	0.93
TC09C-11	278	2,353	0	0	2,061	5,810	4,417	14,641	14,511	543	13	15,067	-426	-2.9	0.88
TC09C-12	281	2,432	0	0	2,111	5,921	4,461	14,925	14,756	527	86	15,368	-443	-3.0	0.87
TC09C-13	294	2,405	0	0	2,060	6,065	4,251	14,781	14,617	439	35	15,091	-310	-2.1	0.86
TC09C-14	301	2,584	0	0	2,275	6,109	4,455	15,422	15,080	397	0	15,477	-55	-0.4	0.88
TC09C-15	302	2,352	0	0	2,139	5,908	4,401	14,800	14,592	391	0	14,983	-183	-1.2	0.91
TC09C-16	307	2,351	0	10,443	0	4,585	1,690	19,069	18,048	391	0	18,439	630	3.3	1.03

Notes:

1. Nitrogen feed rate reduced by 1,250 pounds per hour for air blown and 0 pounds per hour for oxygen blown to account for losses in feed systems and seals.
2. FD0510 rates determined by change of standpipe level while FD0510 was operated; rates are prorated to time of operating period.
3. TC09A, TC09B, TC09C-1 to TC09C-4, and TC09C-16 were air blown; TC09C-5 to TC09C-15 were oxygen blown.
4. Coal Rate by Syngas Combustor carbon balance.
5. Steam rate by the Transport Gasifier hydrogen balance.

Table 4.5-3 Nitrogen, Oxygen, and Calcium Mass Balances

Operating Period	Average Relative Hours	Nitrogen[1]		Oxygen		Calcium	
		(In- Out) / In	In - Out	(In- Out) / In	In - Out	(In- Out) / In	In - Out
		%	lb/hr	%	lb/hr	%	lb/hr
TC09A-1	7	-0.6	-87	-2.1	-130	81.4	49
TC09A-2	10	-1.4	-215	-0.3	-14	82.1	49
TC09A-3	13	-0.1	-11	-0.1	-6	77.8	43
TC09A-4	18	0.7	93	-0.5	-18	72.1	34
TC09B-1	26	2.9	405	1.7	68	65.0	19
TC09B-2	31	2.7	398	-1.3	-61	61.7	24
TC09B-3	52	3.5	505	2.3	160	16.4	5
TC09B-4	57	1.7	236	1.8	136	16.8	5
TC09B-5	64	-1.4	-184	-2.2	-121	31.6	11
TC09B-6a	75	-0.5	-70	-1.3	-76	27.3	10
TC09B-6b	86	0.3	34	-1.8	-109	18.2	7
TC09B-7a	100	0.7	90	-1.2	-73	-1.2	0
TC09B-7b	108	-0.9	-115	-0.7	-43	-7.1	-2
TC09B-8a	119	-0.3	-36	0.0	-3	2.9	1
TC09B-8b	129	0.7	90	0.1	4	1.3	0
TC09B-9	144	-0.8	-117	-0.7	-47	2.7	1
TC09B-10	151	0.3	37	0.1	10	-7.8	-2
TC09B-11	158	0.4	51	-0.6	-39	5.1	2
TC09B-12	171	1.0	140	0.1	8	-12.4	-3
TC09B-13	175	1.4	199	1.2	72	-0.9	0
TC09B-14	182	1.3	178	0.8	44	-1.6	-1
TC09C-1	196	3.0	442	0.6	33	45.3	12
TC09C-2	199	1.6	237	0.9	55	41.8	11
TC09C-3	206	2.1	301	0.7	41	29.8	8
TC09C-4	209	2.4	315	-0.4	-20	26.6	7
TC09C-5	226	-3.6	-229	-6.5	-414	5.1	1
TC09C-6	230	-0.3	-20	-4.8	-320	4.2	1
TC09C-7	244	-0.2	-9	-3.7	-226	-18.0	-3
TC09C-8	256	-0.4	-22	-3.4	-207	-1.5	0
TC09C-9	264	0.3	20	-3.0	-178	3.2	1
TC09C-10	271	0.0	2	-3.9	-230	-8.8	-2
TC09C-11	278	0.6	38	-5.1	-318	8.2	2
TC09C-12	281	0.7	42	-4.8	-303	4.6	1
TC09C-13	294	0.7	45	-5.0	-303	33.5	8
TC09C-14	301	2.1	130	-3.5	-225	52.5	14
TC09C-15	302	1.4	81	-3.7	-234	48.9	12
TC09C-16	307	4.1	518	-1.1	-47	49.0	12

Notes:
1. Nitrogen feed rate reduced by 1,250 lb/hr for air blown and 0 lb/hr for oxygen blown to account for losses in feed systems and seals.
2. TC09A, TC09B, TC09C-1 to TC09C-16 were air blown; TC09C-5 to TC09C-15 were oxygen blown.

Table 4.5-4

Typical Air-Blown Component Mass Balances

	Nitrogen[1]	Hydrogen[2]	Oxygen	Calcium
Operating Period	TC09A-3	TC09A-3	TC09A-3	TC09A-3
Date Start	9/5/2002	9/5/2002	9/5/2002	9/5/2002
Time Start	11:30	11:30	11:30	11:30
Time End	12:30	12:30	12:30	12:30
Fuel	Hia. Bit.	Hia. Bit.	Hia. Bit.	Hia. Bit.
Riser Temperature, ^{O}F	1,782	1,782	1,782	1,782
Pressure, psig	200	200	200	200
In, pounds/hr				
Fuel	28	133	280	55
Coke Breeze				
Air	8,416		2,557	
Nitrogen[1]	6,021			
Steam[2]		246	1,965	
Total	14,465	379	4,802	55
Out, pounds/hr				
Synthesis Gas	14,475	377	4,796	
PCD Solids	1	2	12	12
Reactor				
Total	14,476	379	4,808	12
(In-Out)/In, %	-0.1%	0.0%	-0.1%	77.8%
(In-Out), pounds per hour	-11	0	-6	43

Notes:
1. Feed nitrogen decreased by 1,250 lb/hr.
2. Steam rate by hydrogen balance.

Table 4.5-5

Typical Oxygen-Blown Component Mass Balances

	Nitrogen	Hydrogen[1]	Oxygen	Calcium	SiO_2
Operating Period	TC09C-13	TC09C-13	TC09C-13	TC09C-13	TC09C-13
Date Start	9/25/2002	9/25/2002	9/25/2002	9/25/2002	9/25/2002
Time Start	22:00	22:00	22:00	22:00	22:00
Time End	6:15	6:15	6:15	6:15	6:15
Fuel	Hia. Bit.	Hia. Bit.	Hia. Bit.	Hia. Bit.	Hia. Bit.
Riser Temperature, ^{O}F	1,814	1,814	1,814	1,814	1,814
Pressure, psig	160	160	160	160	160
In, pounds/hr					
Fuel	26	123	258	37	152
Coke Breeze					
Oxygen			2,060		
Nitrogen	6,066				
Steam[1]		472	3,779		
Total	6,092	595	6,097	25	152
Out, pounds/hr					
Synthesis Gas	6,047	593	6,387		
PCD Solids	1	2	12	15	136
Reactor				1	29
Total	6,048	595	6,398	17	165
(In-Out)/In, %	0.7%	0.0%	-5.0%	33.5%	-8.6%
(In-Out), pounds per hour	45	0	-302	8	-13

Note:
1. Steam rate by hydrogen balance.

Table 4.5-6 Sulfur Balance

Operating Period	Average Relative Hours	Feeds (In) Coal lb/hr	Products (Out) Syngas lb/hr	PCD Solids lb/hr	Reactor lb/hr	Total lb/hr	In - Out lb/hr	(In- Out)/In %	Sulfur Removal Gas[4] %	Products %	Solids %	Sulfur Emissions lb $SO_2/10^6$Btu	Equilibium H_2S ppm	Measured TRS ppm
TC09A-1	7	10.7	9.9	0.7	0.0	10.5	0.2	1.9	8	6	6	0.73	415	337
TC09A-2	10	10.9	8.1	0.6	0.0	8.7	2.1	19.7	25	7	5	0.61	266	294
TC09A-3	13	10.2	8.7	0.8	0.0	9.5	0.7	6.4	14	8	8	0.71	301	339
TC09A-4	18	8.8	6.9	0.7	0.0	7.6	1.3	14.4	22	9	8	0.65	265	306
TC09B-1	26	6.7	5.3	1.2	0.0	6.5	0.3	4.0	21	18	17	0.60	272	233
TC09B-2	31	9.1	8.3	0.9	0.0	9.2	-0.1	-1.1	9	10	10	0.70	298	332
TC09B-3	52	6.8	5.4	0.6	0.0	6.0	0.7	10.5	19	10	9	0.69	637	192
TC09B-4	57	6.8	5.7	0.6	0.0	6.3	0.5	7.5	16	9	8	0.72	681	195
TC09B-5	64	8.1	7.3	0.5	0.0	7.8	0.3	4.2	10	6	6	0.73	494	283
TC09B-6a	75	8.0	7.6	0.7	0.0	8.3	-0.2	-3.0	5	8	8	0.70	521	283
TC09B-6b	86	8.1	8.0	0.5	0.0	8.4	-0.3	-3.9	2	6	6	0.73	548	297
TC09B-7a	100	7.4	7.3	0.2	0.0	7.4	0.0	-0.1	2	2	2	0.77	551	271
TC09B-7b	108	7.6	7.3	0.4	0.0	7.7	0.0	-0.5	5	5	5	0.74	533	275
TC09B-8a	119	8.2	7.8	0.3	0.0	8.1	0.1	0.8	5	4	4	0.72	491	288
TC09B-8b	129	7.7	7.5	0.2	0.0	7.7	0.0	0.0	2	2	2	0.73	498	287
TC09B-9	144	8.9	9.1	0.7	0.0	9.8	-0.9	-9.6	0	7	7	0.76	526	302
TC09B-10	151	8.4	8.7	0.4	0.0	9.1	-0.7	-7.9	0	4	5	0.78	509	304
TC09B-11	158	9.4	8.8	0.8	0.0	9.6	-0.1	-1.5	7	8	8	0.74	518	312
TC09B-12	171	9.0	7.3	0.7	0.0	8.0	1.0	11.6	19	9	8	0.72	475	287
TC09B-13	175	10.4	10.2	0.7	0.0	10.8	-0.5	-4.7	2	6	6	0.90	479	372
TC09B-14	182	10.7	10.0	0.6	0.0	10.6	0.1	0.9	7	6	6	0.89	429	394
TC09C-1	196	8.2	10.0	0.5	0.0	10.5	-2.3	-28.1	0	4	6	0.95	427	373
TC09C-2	199	8.6	9.9	0.7	0.0	10.6	-2.0	-23.2	0	7	8	0.90	415	358
TC09C-3	206	9.0	9.3	1.0	0.0	10.3	-1.3	-14.4	0	10	11	0.83	418	356
TC09C-4	209	9.0	9.3	1.0	0.0	10.2	-1.3	-14.2	0	9	11	0.84	391	378
TC09C-5	226	8.0	9.5	0.9	0.0	10.4	-2.4	-29.9	0	9	12	0.95	828	462
TC09C-6	230	8.4	9.2	0.7	0.0	10.0	-1.6	-19.5	0	7	9	0.88	888	453
TC09C-7	244	7.5	9.2	0.5	0.0	9.8	-2.3	-30.3	0	6	7	1.01	863	475
TC09C-8	256	7.8	9.2	0.8	0.0	10.0	-2.2	-28.3	0	8	10	1.00	859	487
TC09C-9	264	7.8	9.0	0.9	0.0	9.9	-2.1	-26.7	0	9	11	0.96	822	483
TC09C-10	271	7.7	9.0	0.8	0.0	9.8	-2.2	-28.1	0	9	11	0.95	826	475
TC09C-11	278	8.8	10.2	0.9	0.0	11.1	-2.3	-26.5	0	8	10	0.92	835	524
TC09C-12	281	9.1	10.9	0.9	0.1	11.8	-2.8	-30.8	0	8	10	0.95	822	547
TC09C-13	294	9.7	10.4	0.9	0.0	11.3	-1.6	-17.0	0	8	9	0.92	787	532
TC09C-14	301	10.7	11.7	0.8	0.0	12.6	-1.8	-17.1	0	7	8	0.97	789	578
TC09C-15	302	9.8	10.3	0.8	0.0	11.1	-1.3	-13.1	0	7	8	0.93	809	524
TC09C-16	307	9.9	7.4	0.8	0.0	8.2	1.6	16.7	25	10	8	0.67	306	340

Notes:

1. Synthesis gas sulfur emissions determined from synthesis gas combustor SO_2 analyzer.
2. TC09A, TC09B, TC09C-1 to TC09C-4, and TC09C-16 were air blown; TC09C-5 to TC09C-15 were oxygen blown.
3. Negative sulfur removals were assumed to actually be 0% sulfur removal.

Table 4.5-7 Energy Balance

Operating Period	Average Relative Hours	Feeds (In)				Products (Out)						In - Out	(In- Out)/In	Efficiency		
						Latent	Sensible	PCD	Reactor	Heat				Raw[2]		Corrected[2,4]
		Coal	Air	Steam	Total	Syngas	Syngas	Solids	Solids	Loss	Total			Cold	Hot	Cold
		10^6 Btu/hr	10^6 Btu/hr	10^6 Btu/hr	10^6 Btu/hr	10^6 Btu/hr	10^6 Btu/hr	10^6 Btu/hr	10^6 Btu/hr	10^6 Btu/hr	10^6 Btu/hr	10^6 Btu/hr	%	%	%	%
TC09A-1	7	30.4	0.8	4.4	35.6	18.5	11.7	1.7	0.00	1.5	33.4	2.2	6.2	55.5	90.3	66.2
TC09A-2	10	30.3	0.8	3.0	34.2	20.5	11.1	1.3	0.00	1.5	34.4	-0.2	-0.7	59.6	91.7	71.1
TC09A-3	13	28.0	0.7	2.9	31.7	16.6	10.1	1.4	0.00	1.5	29.5	2.1	6.7	56.1	90.1	68.8
TC09A-4	18	24.3	0.7	2.1	27.0	12.9	8.8	1.5	0.00	1.5	24.7	2.2	8.3	52.3	87.8	66.5
TC09B-1	26	20.0	0.6	2.4	23.0	11.4	8.7	1.8	0.00	1.5	23.4	-0.4	-1.7	48.7	85.8	64.1
TC09B-2	31	26.8	0.7	2.7	30.2	14.8	9.8	2.0	0.00	1.5	28.1	2.0	6.7	52.6	87.6	65.3
TC09B-3	52	17.6	0.6	6.8	25.0	7.8	11.1	2.2	0.00	1.5	22.6	2.4	9.7	34.6	83.6	45.4
TC09B-4	57	17.9	0.6	7.4	26.0	7.7	11.5	2.1	0.00	1.5	22.8	3.2	12.4	33.6	84.0	43.8
TC09B-5	64	22.6	0.6	4.4	27.6	10.1	10.3	2.0	0.00	1.5	23.9	3.8	13.6	42.3	85.3	55.1
TC09B-6a	75	24.2	0.7	5.1	30.0	12.6	10.6	3.0	0.01	1.5	27.7	2.3	7.7	45.6	83.8	55.8
TC09B-6b	86	24.8	0.7	5.1	30.6	12.3	10.6	2.3	0.00	1.5	26.7	3.9	12.7	46.1	85.7	56.4
TC09B-7a	100	21.9	0.7	5.3	27.9	11.2	10.3	1.8	0.00	1.5	24.8	3.1	11.2	45.2	86.6	56.4
TC09B-7b	108	22.7	0.7	5.1	28.4	11.5	10.1	2.7	0.01	1.5	25.8	2.6	9.3	44.7	83.8	55.2
TC09B-8a	119	25.0	0.7	4.8	30.5	13.0	10.3	2.5	0.00	1.5	27.3	3.1	10.3	47.6	85.2	58.2
TC09B-8b	129	23.9	0.7	4.8	29.4	12.4	9.9	2.0	0.01	1.5	25.8	3.6	12.1	48.2	86.4	59.1
TC09B-9	144	28.1	0.8	5.6	34.4	13.7	10.9	2.8	0.00	1.5	29.0	5.4	15.8	47.4	85.2	57.3
TC09B-10	151	26.3	0.7	5.4	32.4	13.9	10.6	2.1	0.00	1.5	28.1	4.3	13.4	49.4	87.3	60.0
TC09B-11	158	27.7	0.7	5.4	33.8	13.8	10.4	3.3	0.01	1.5	29.0	4.8	14.2	47.5	83.5	57.1
TC09B-12	171	23.5	0.7	4.4	28.6	12.3	9.2	2.8	0.00	1.5	25.8	2.7	9.6	47.5	83.3	58.1
TC09B-13	175	26.1	0.7	4.9	31.6	15.2	9.9	2.6	0.00	1.5	29.3	2.4	7.5	52.1	85.9	61.9
TC09B-14	182	25.7	0.7	4.0	30.4	14.3	9.4	2.3	0.00	1.5	27.5	2.9	9.5	52.0	86.1	62.6
TC09C-1	196	24.5	0.7	4.5	29.6	14.3	10.4	2.1	0.00	1.5	28.3	1.3	4.5	50.5	87.4	61.7
TC09C-2	199	25.6	0.7	4.5	30.8	15.1	10.7	2.6	0.00	1.5	30.0	0.8	2.7	50.4	86.3	61.2
TC09C-3	206	25.9	0.7	4.1	30.6	15.1	10.2	3.1	0.00	1.5	29.9	0.7	2.3	50.5	84.6	60.5
TC09C-4	209	25.5	0.7	3.5	29.7	15.1	9.4	2.9	0.00	1.5	28.9	0.7	2.5	52.2	84.9	62.3
TC09C-5	226	22.8	0.0	6.4	29.2	14.0	8.1	3.8	0.00	1.5	27.3	1.9	6.4	51.0	80.5	65.6
TC09C-6	230	23.8	0.0	6.5	30.3	13.3	8.0	3.6	0.00	1.5	26.5	3.8	12.5	50.4	80.6	64.8
TC09C-7	244	21.8	0.0	6.3	28.1	13.3	7.6	2.6	0.02	1.5	25.0	3.2	11.3	53.2	83.6	69.2
TC09C-8	256	22.0	0.0	6.2	28.2	13.3	7.4	3.0	0.01	1.5	25.1	3.1	11.0	52.8	82.2	68.2
TC09C-9	264	22.1	0.0	5.9	28.0	13.4	7.2	3.3	0.01	1.5	25.4	2.6	9.1	52.9	81.1	67.9
TC09C-10	271	21.8	0.0	5.9	27.7	13.4	7.1	3.2	0.02	1.5	25.3	2.5	8.9	53.0	81.1	68.0
TC09C-11	278	25.6	0.0	6.0	31.6	15.8	7.5	3.4	0.01	1.5	28.2	3.4	10.7	55.9	82.6	69.2
TC09C-12	281	26.5	0.0	6.0	32.5	16.5	7.6	3.7	0.04	1.5	29.4	3.1	9.7	56.4	82.3	69.2
TC09C-13	294	25.9	0.0	5.8	31.7	16.5	7.3	3.5	0.02	1.5	28.8	2.9	9.1	57.2	82.6	70.3
TC09C-14	301	27.7	0.0	6.0	33.8	18.3	7.6	3.3	0.00	1.5	30.6	3.1	9.3	59.6	84.3	71.8
TC09C-15	302	25.2	0.0	6.0	31.2	16.7	7.4	3.3	0.00	1.5	28.8	2.4	7.8	57.9	83.5	70.9
TC09C-16	307	25.2	0.6	2.3	28.1	14.1	7.6	3.3	0.00	1.5	26.5	1.6	5.7	53.3	82.1	63.1

Notes:

1. Nitrogen and sorbent assumed to enter the system at ambient temperature and therefore have zero enthalpy.
2. Using total inlet heat.
3. Reference conditions are 80°F and 14.7 psia.
4. Correction is to assume that only air nitrogen is in the synthesis gas and that the reactor is adiabatic.
5. TC09A, TC09B, TC09C-1 to TC09C-4, and TC09C-16 were air blown; TC09C-5 to TC09C-15 were oxygen blown.

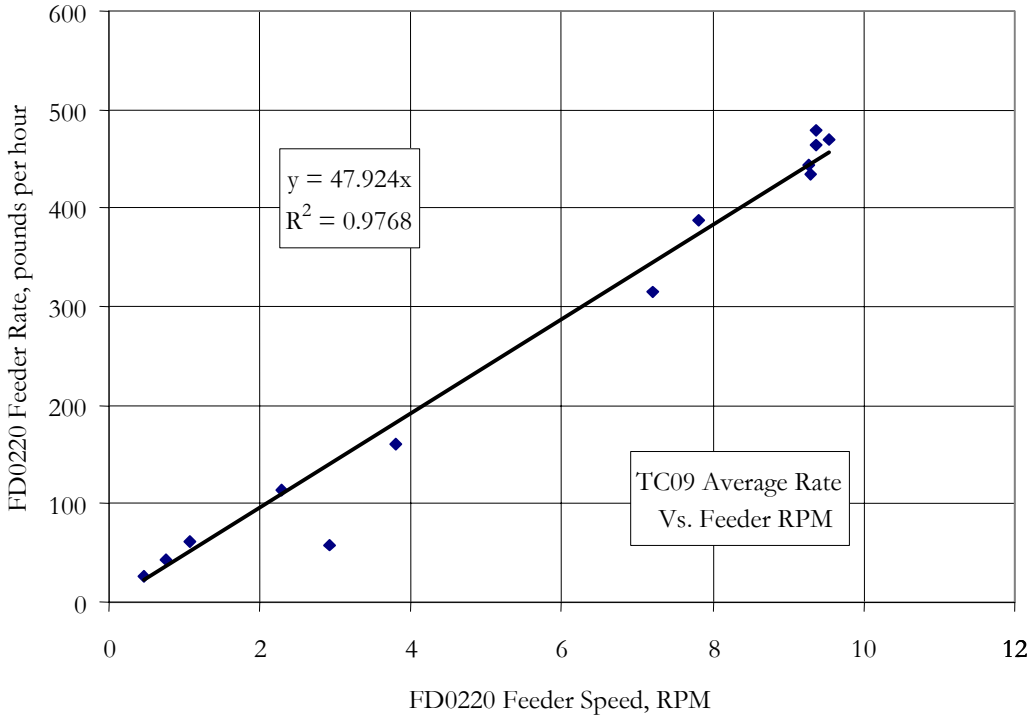

Figure 4.5-1 Sorbent Feeder Correlation

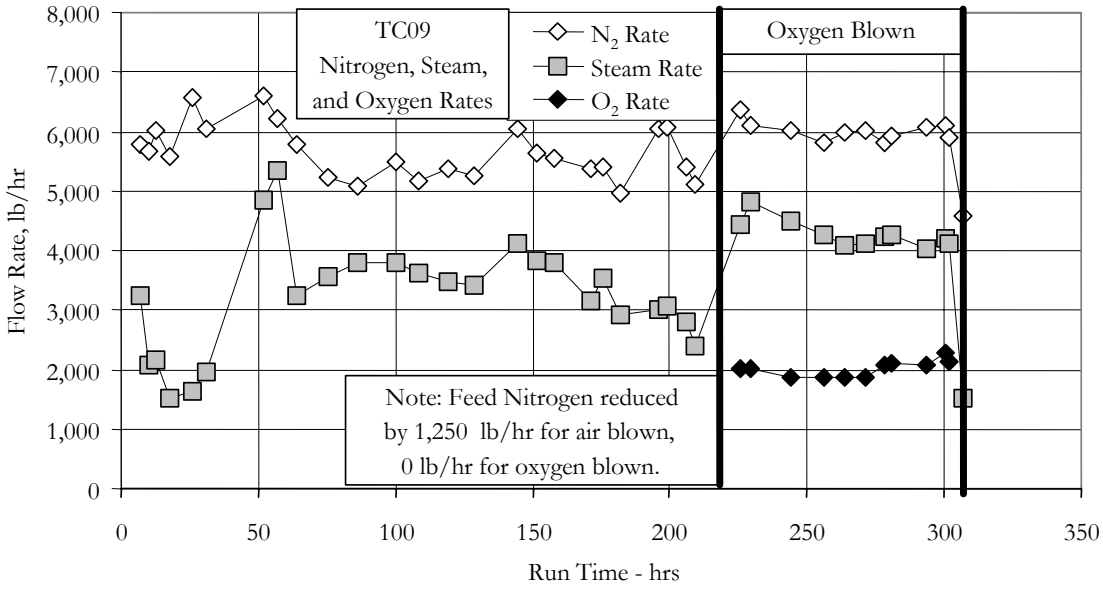

Figure 4.5-2 Nitrogen, Oxygen, and Steam Rates

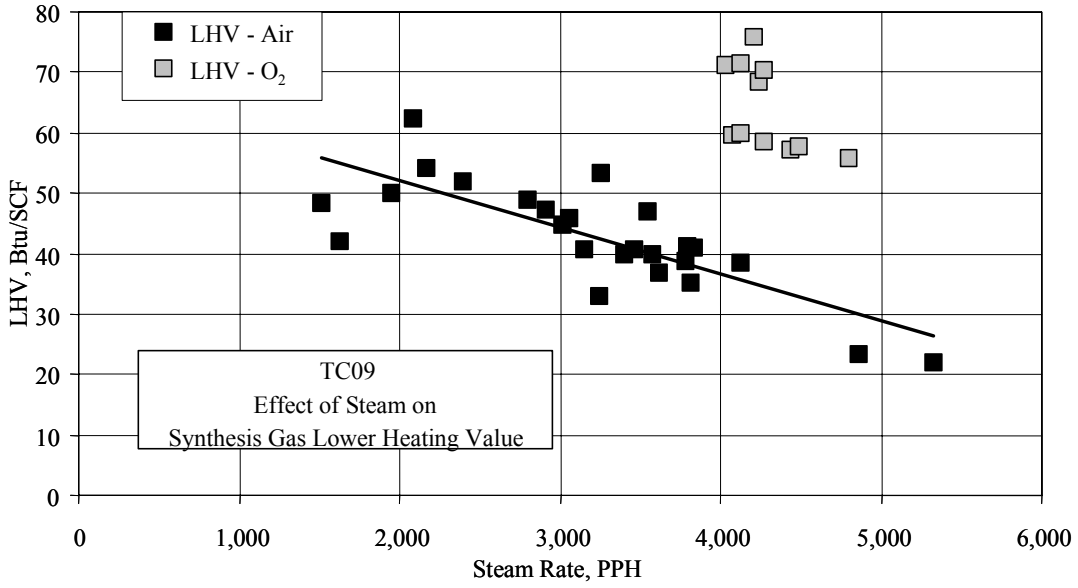

Figure 4.5-3 Effect of Steam on Syngas LHV

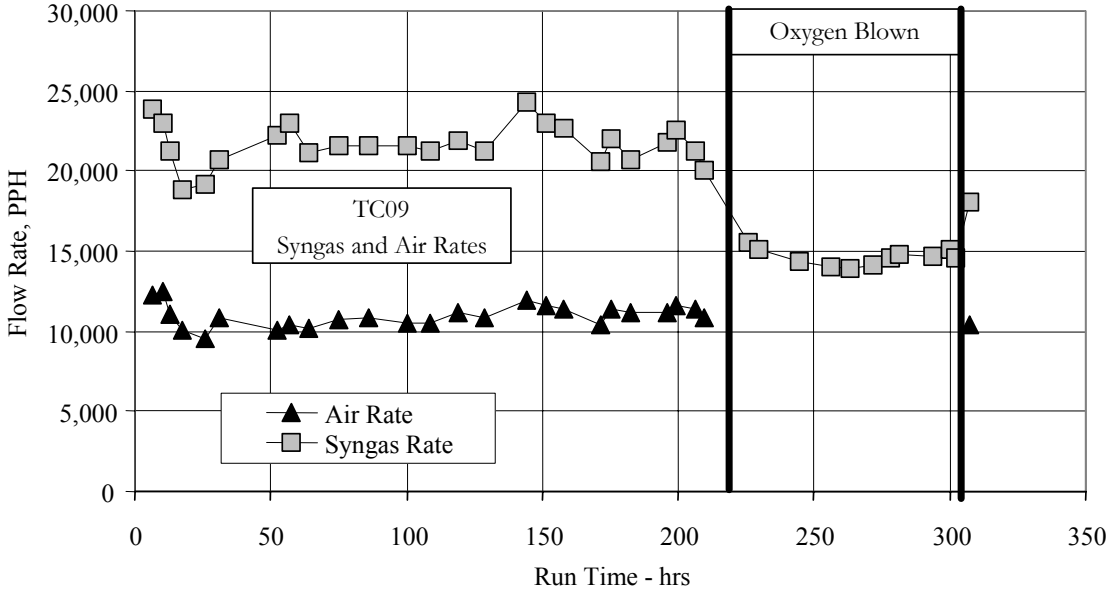

Figure 4.5-4 Air and Synthesis Gas Rates

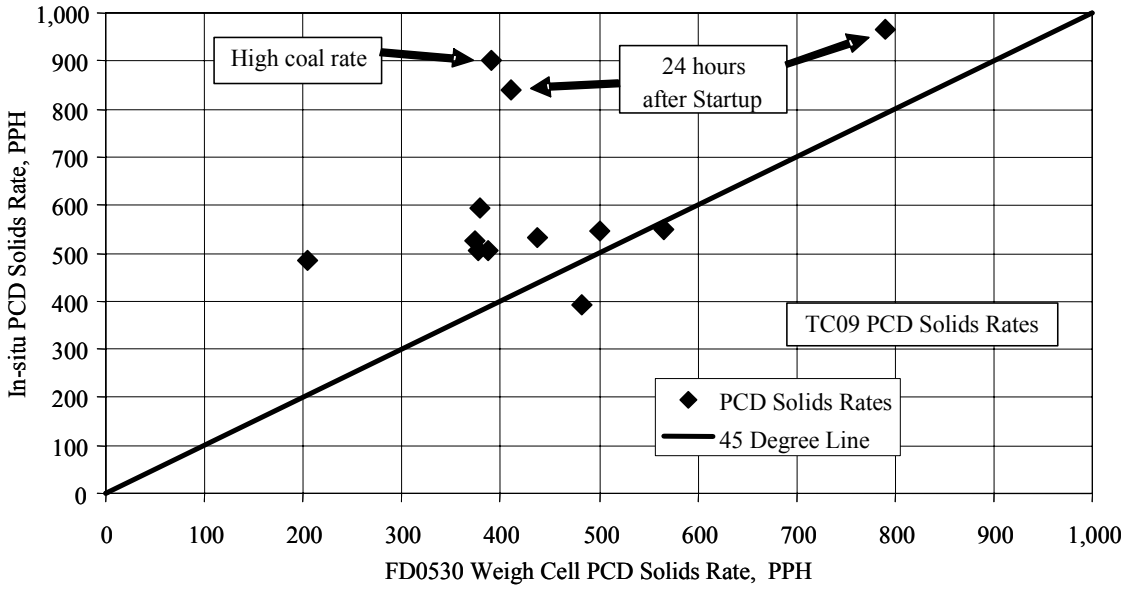

Figure 4.5-5 PCD Fines Rates

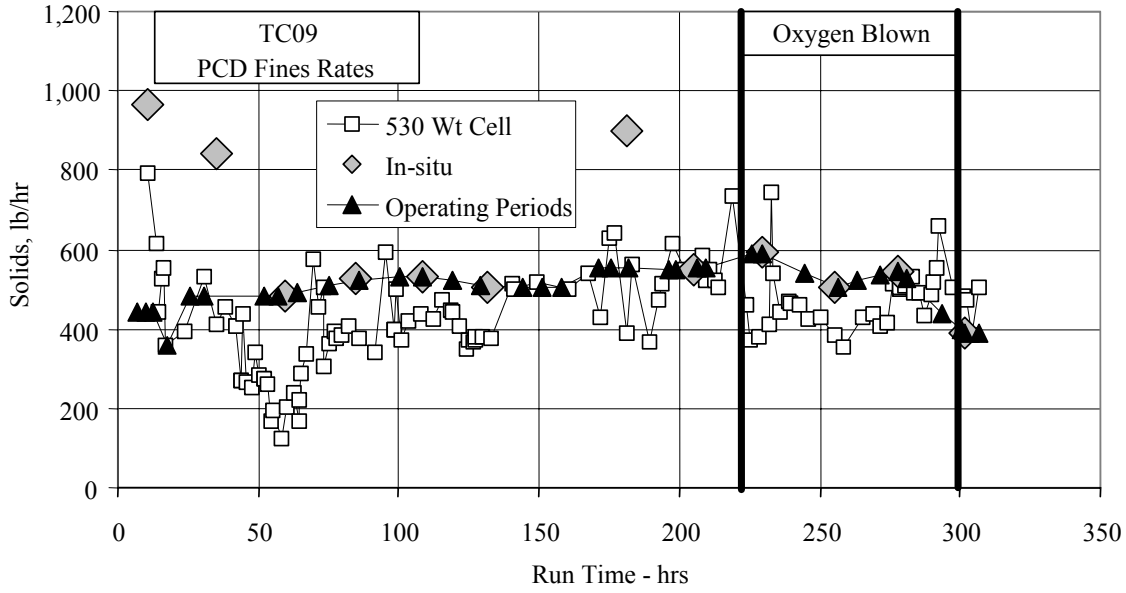

Figure 4.5-6 PCD Fines Rates

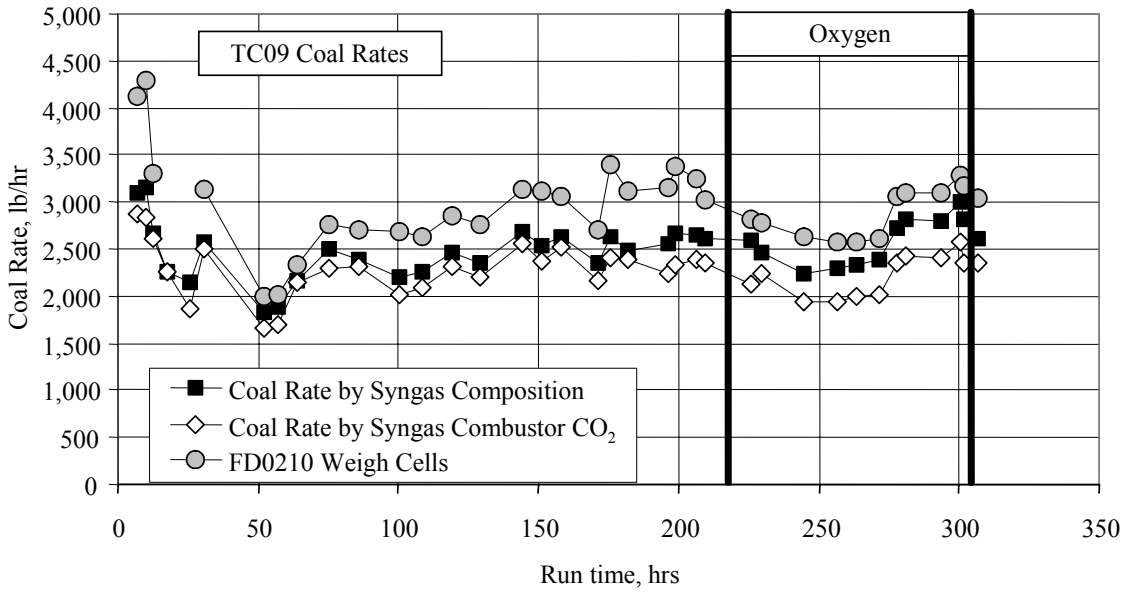

Figure 4.5-7 Coal Rates

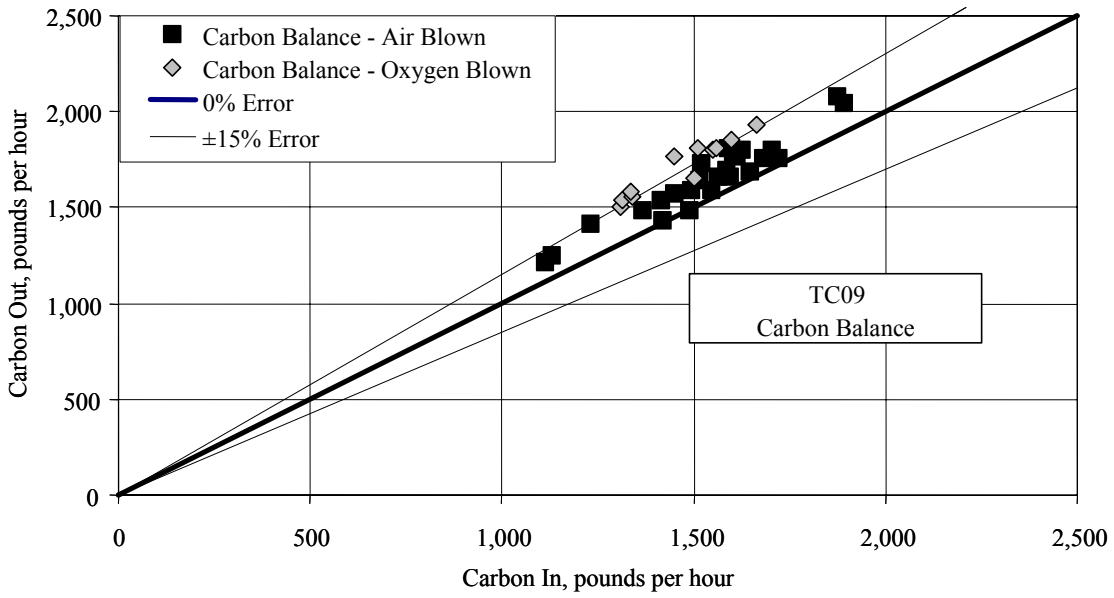

Figure 4.5-8 Carbon Balance

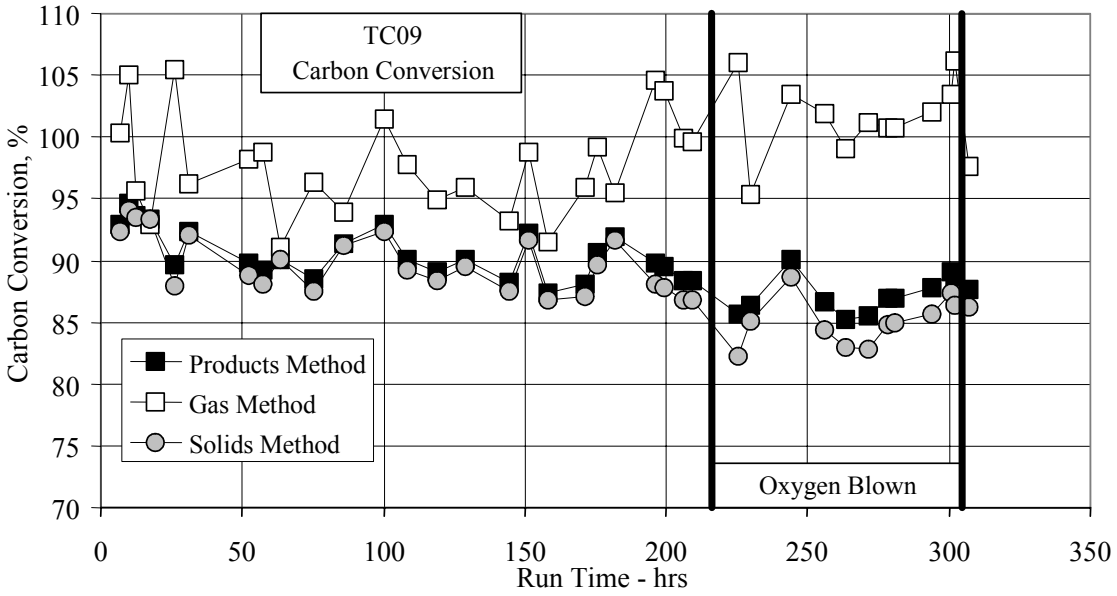

Figure 4.5-9 Carbon Conversion

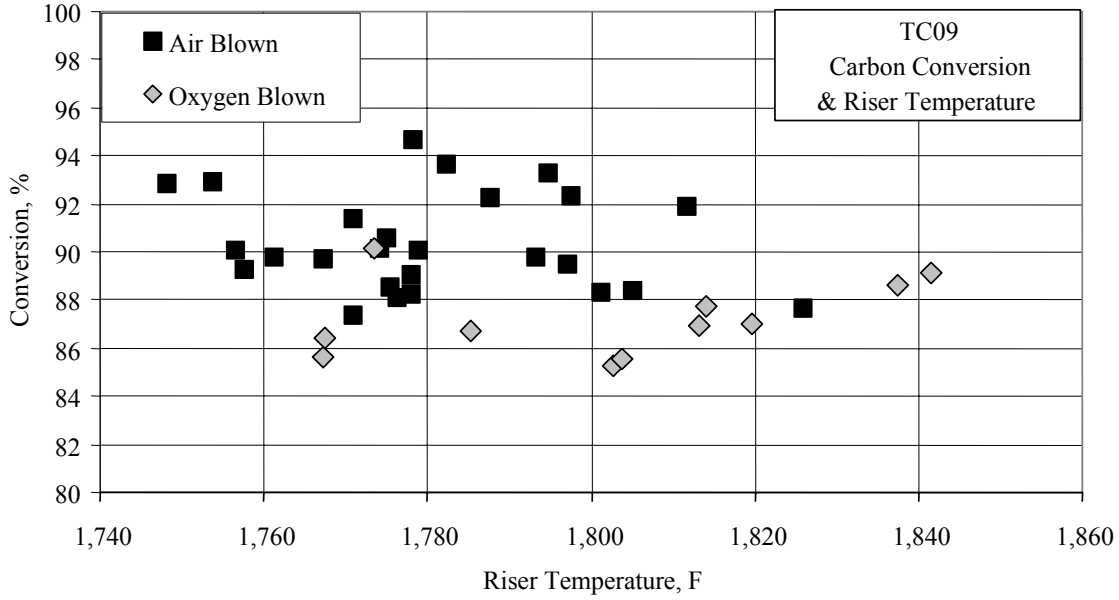

Figure 4.5-10 Carbon Conversion and Riser Temperature

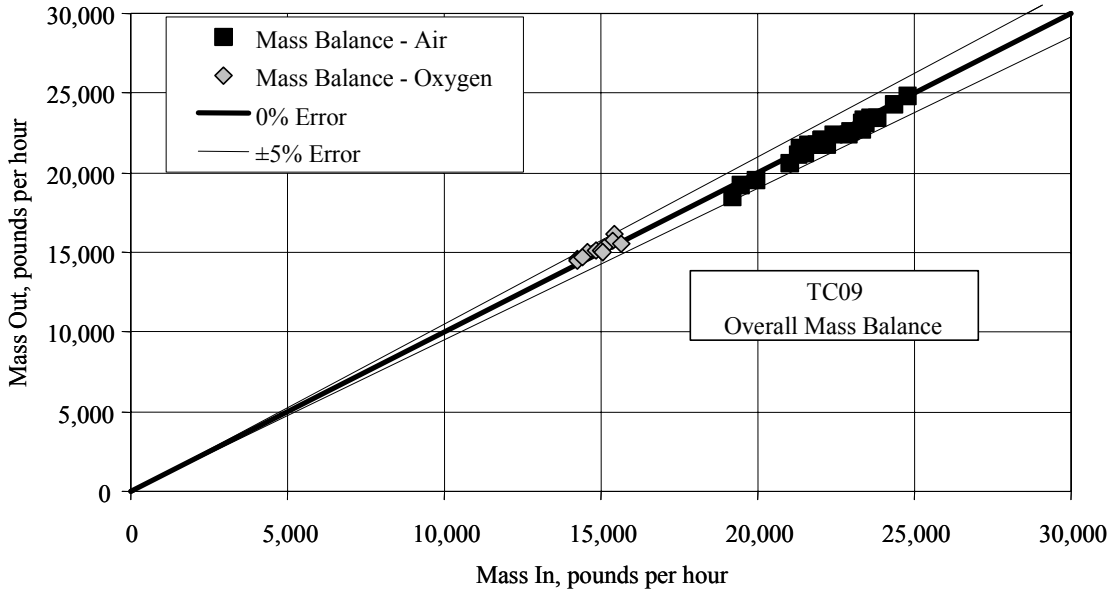

Figure 4.5-11 Overall Material Balance

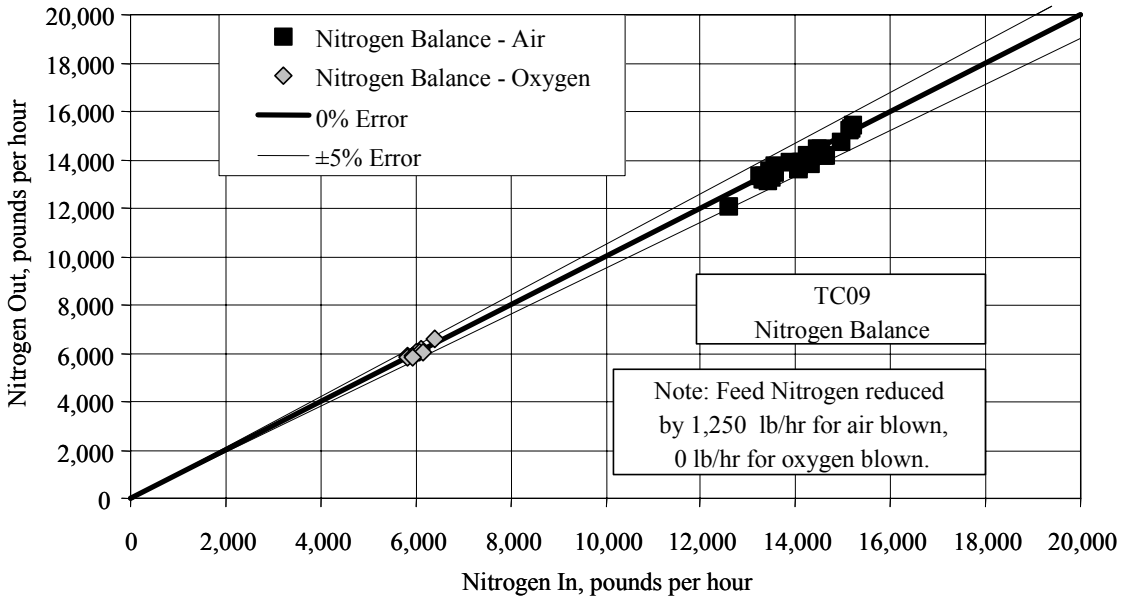

Figure 4.5-12 Nitrogen Balance

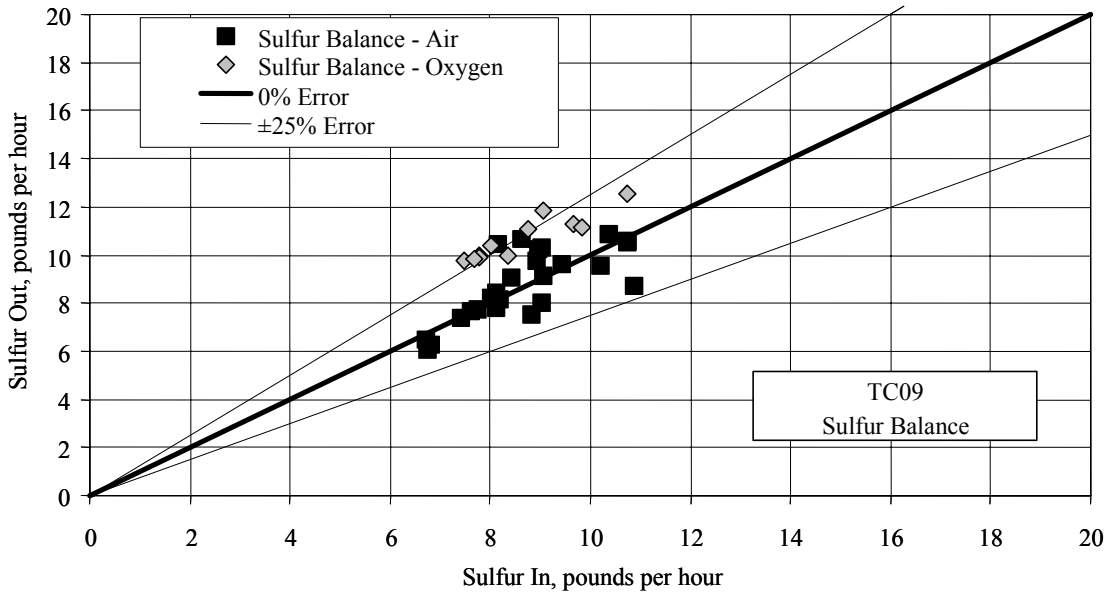

Figure 4.5-13 Sulfur Balance

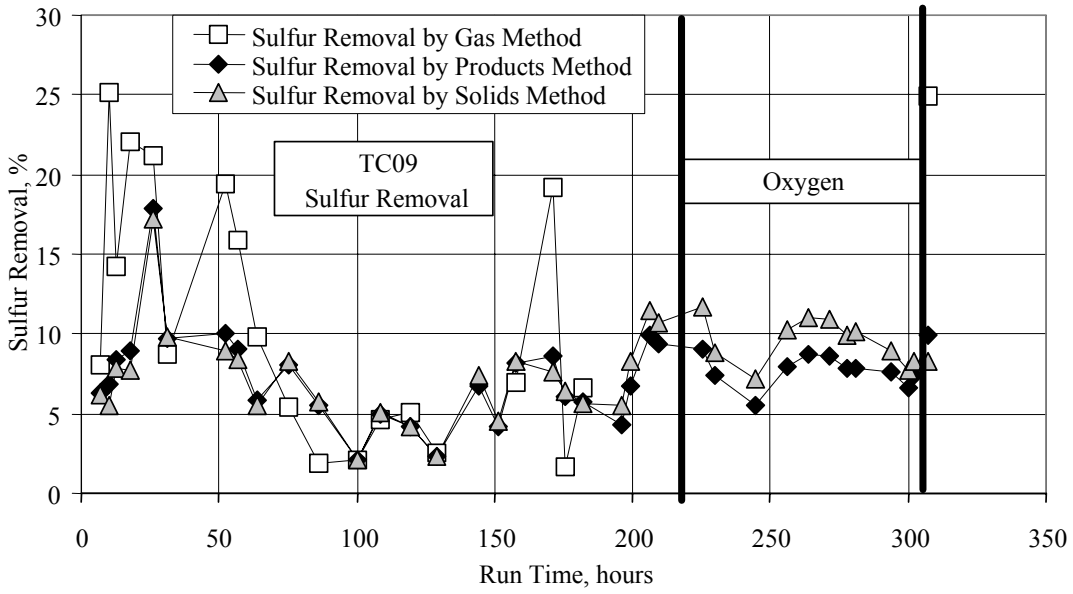

Figure 4.5-14 Sulfur Removal

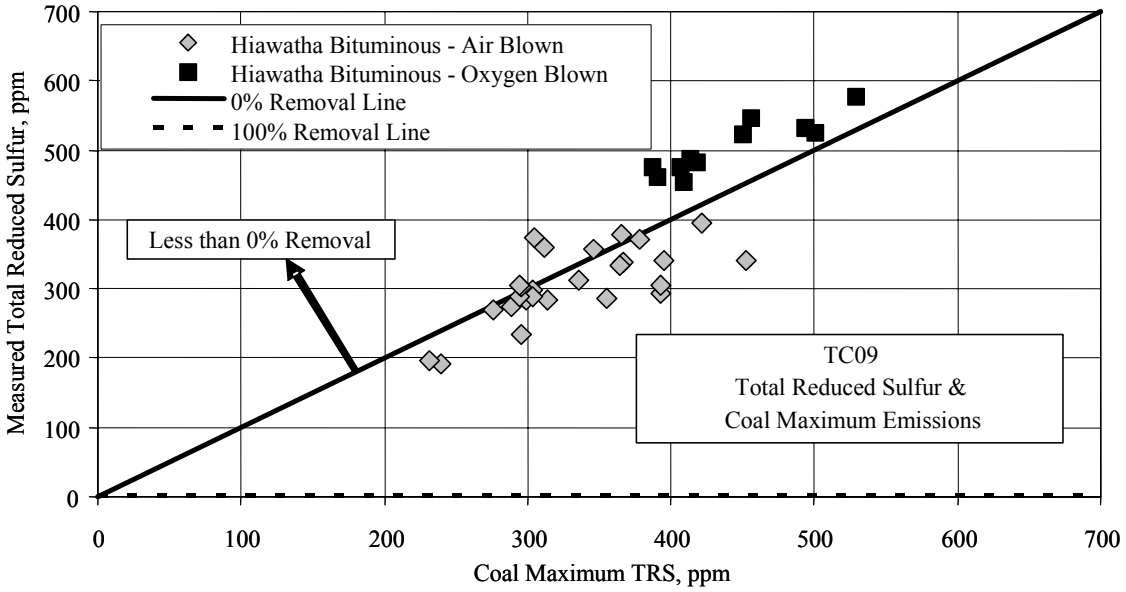

Figure 4.5-15 Measured and Maximum Sulfur Emissions

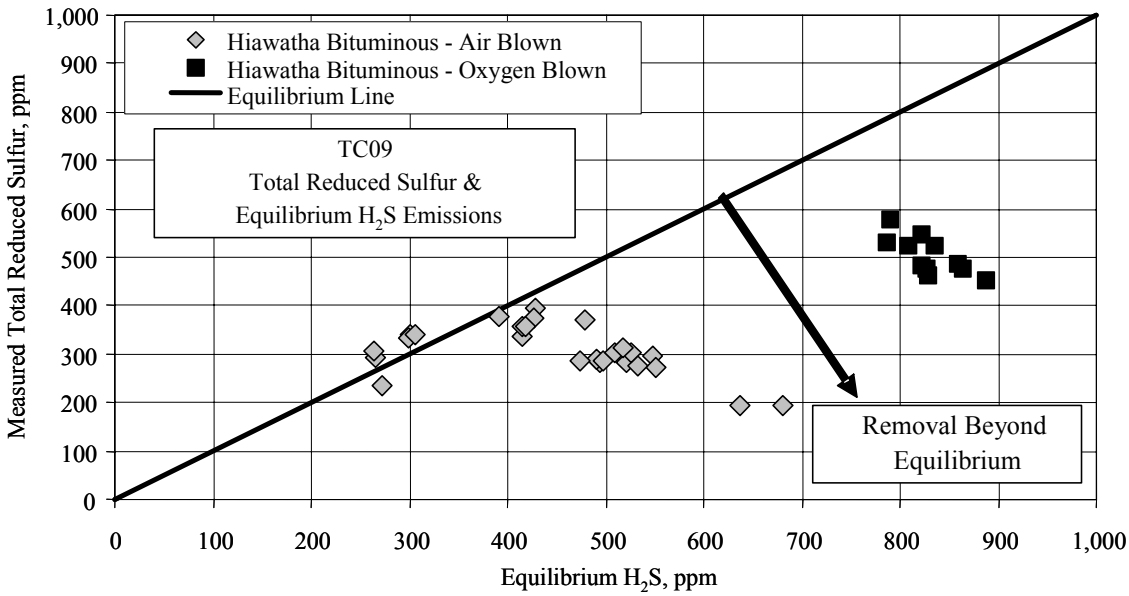

Figure 4.5-16 Measured and Equilibrium Sulfur Emissions

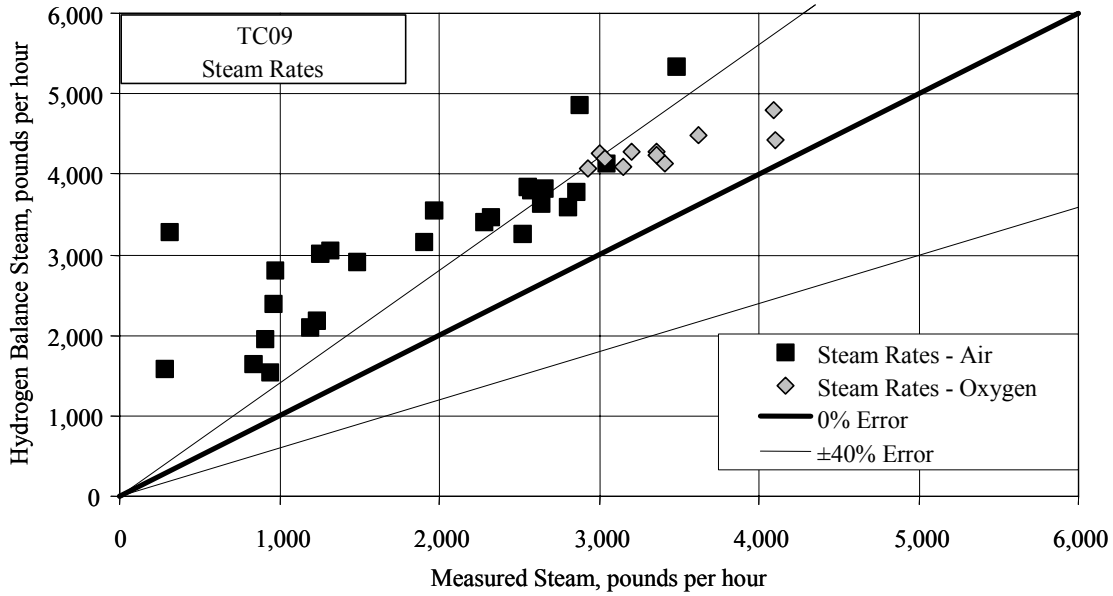

Figure 4.5-17 Steam Rates

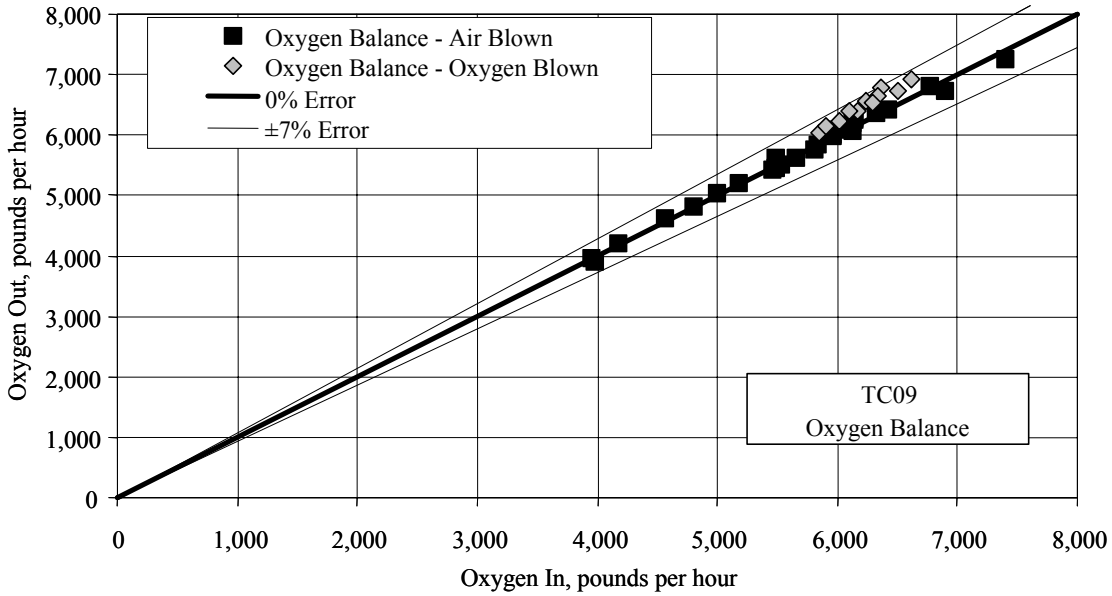

Figure 4.5-18 Oxygen Balance

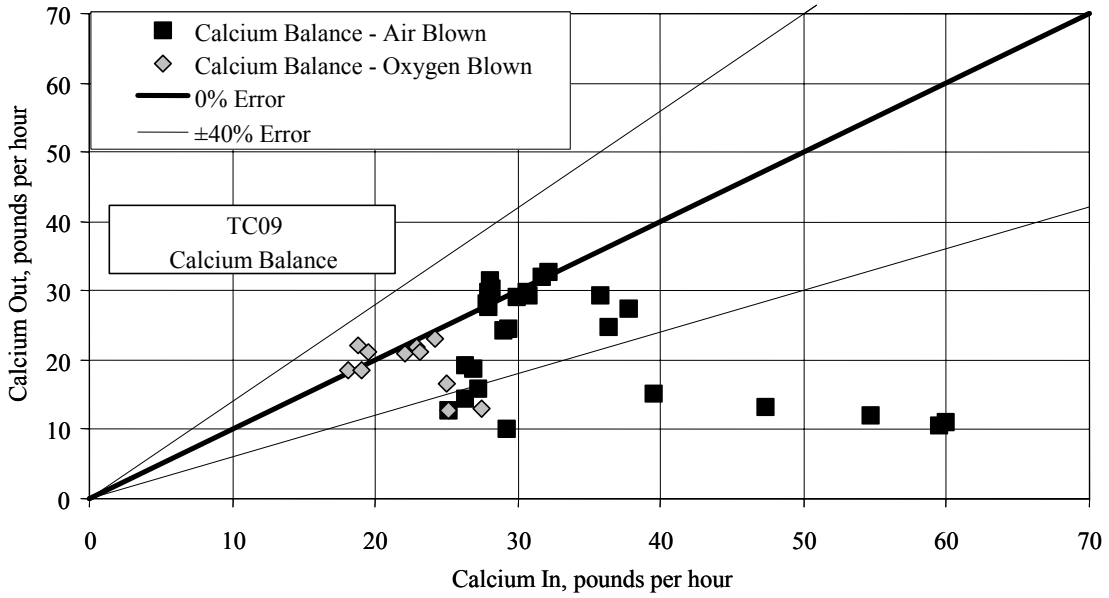

Figure 4.5-19 Calcium Balance

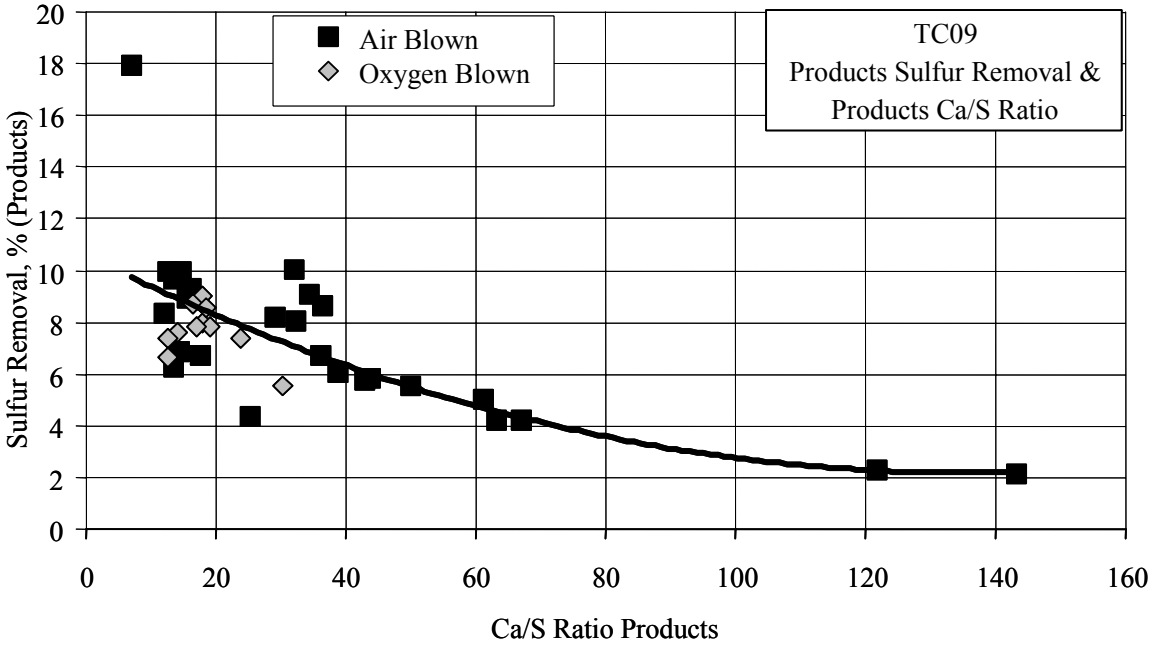

Figure 4.5-20 Sulfur Removal and PCD Solids Ca/S Ratio

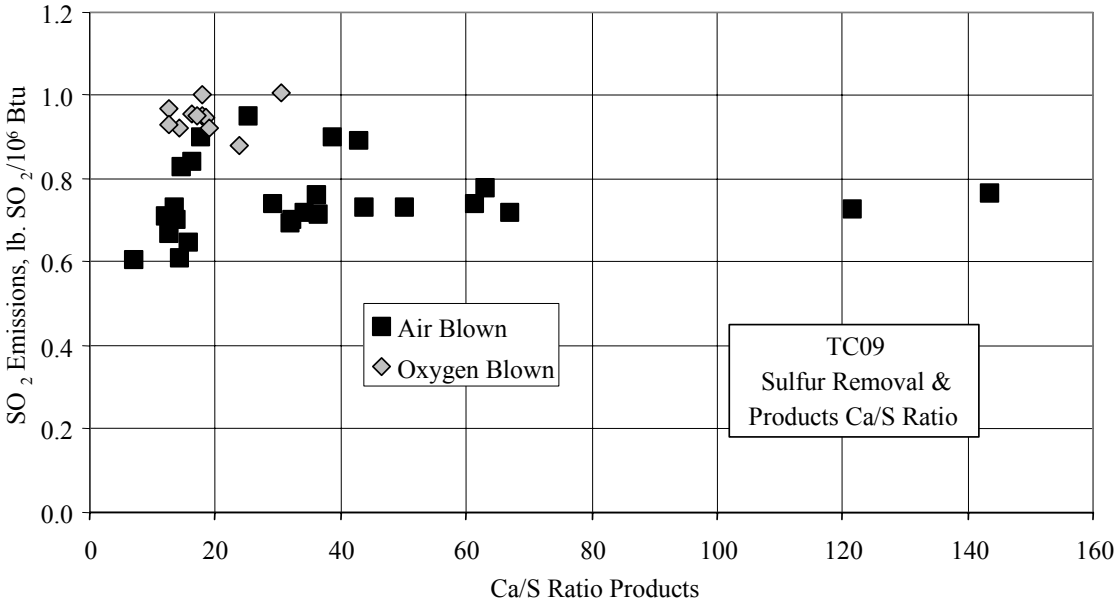

Figure 4.5-21 Sulfur Emissions and PCD Solids Ca/S Ratio

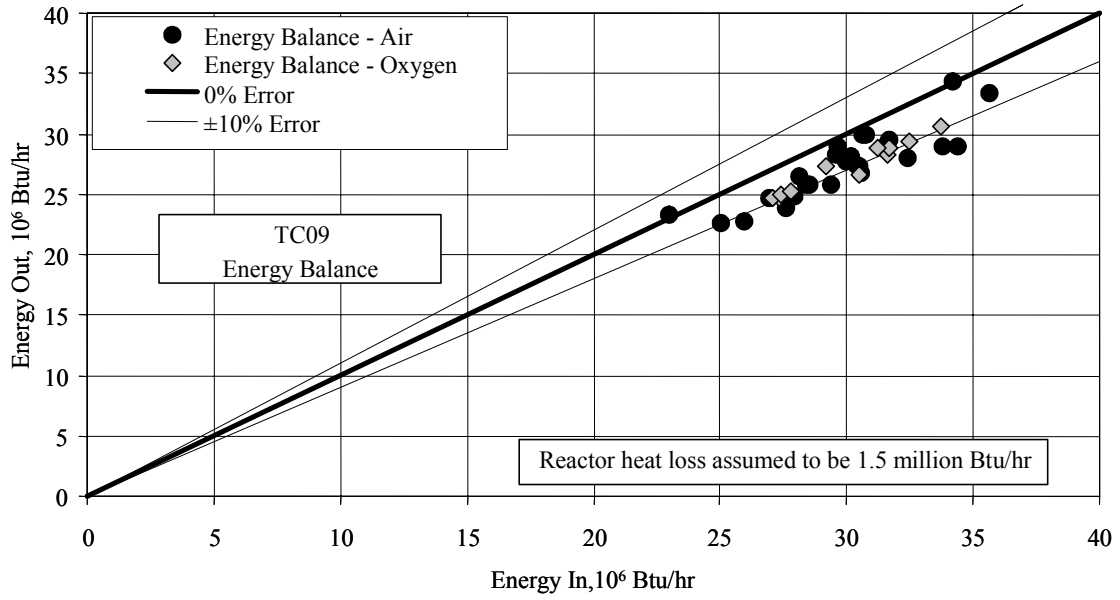

Figure 4.5-22 Energy Balance

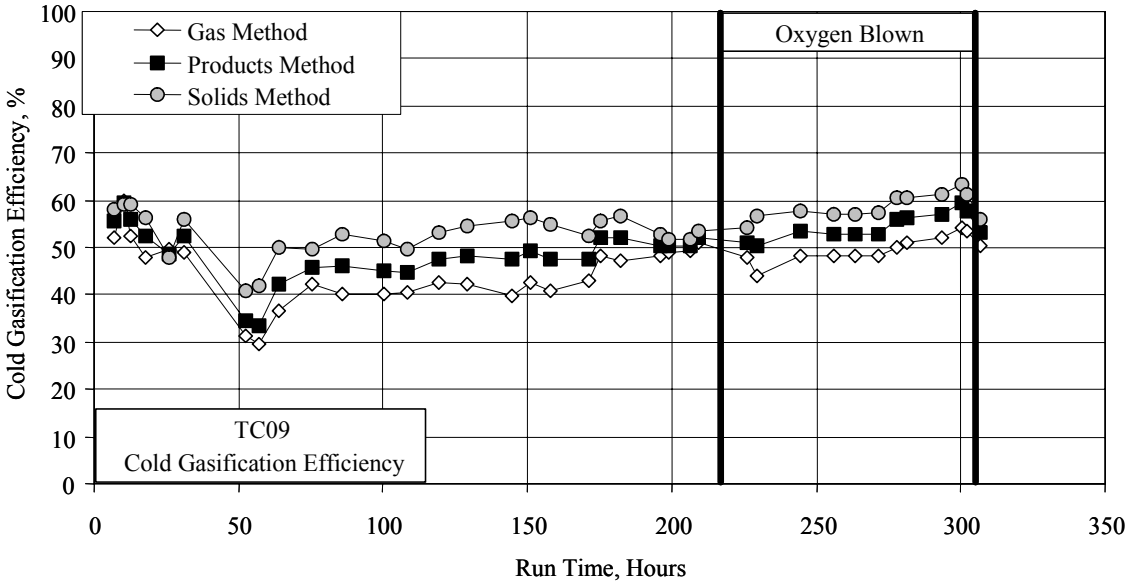

Figure 4.5-23 Cold-Gasification Efficiency

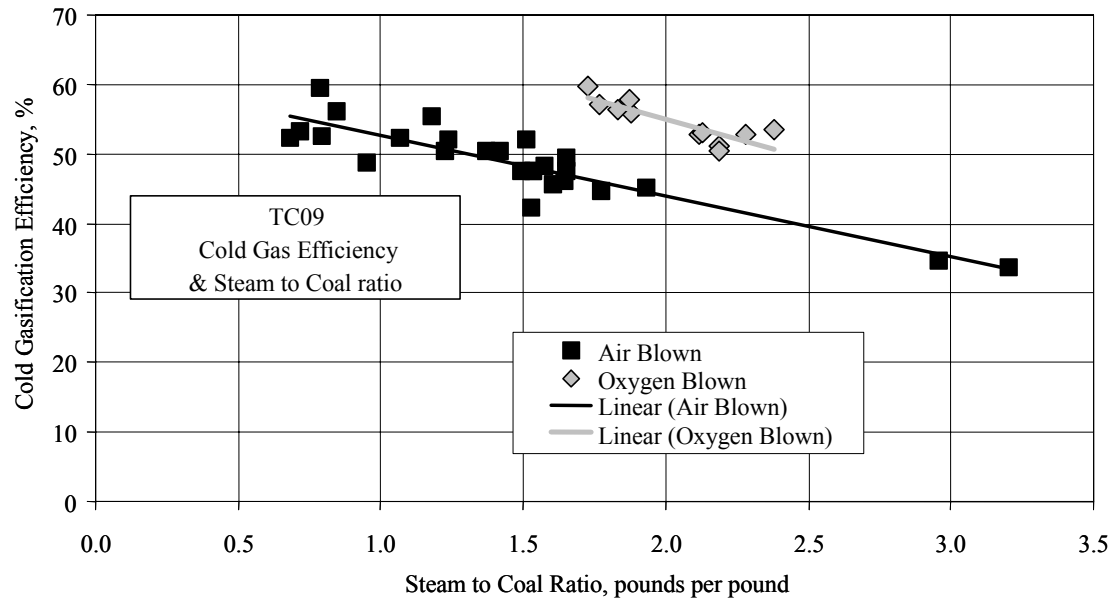

Figure 4.5-24 Cold-Gasification Efficiency and Steam-to-Coal Ratio

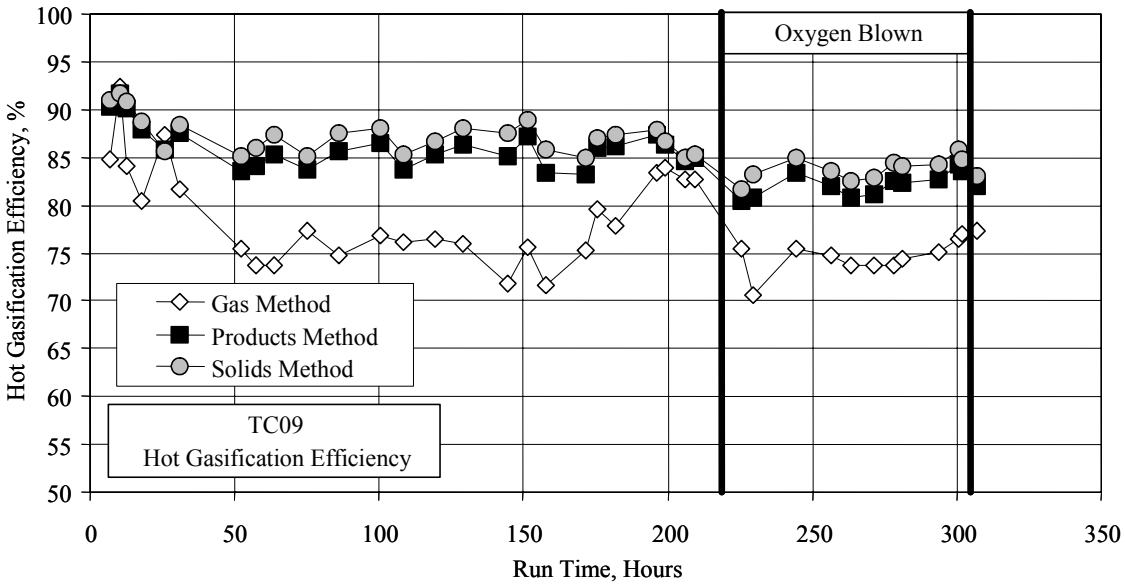

Figure 4.5-25 Hot-Gasification Efficiency

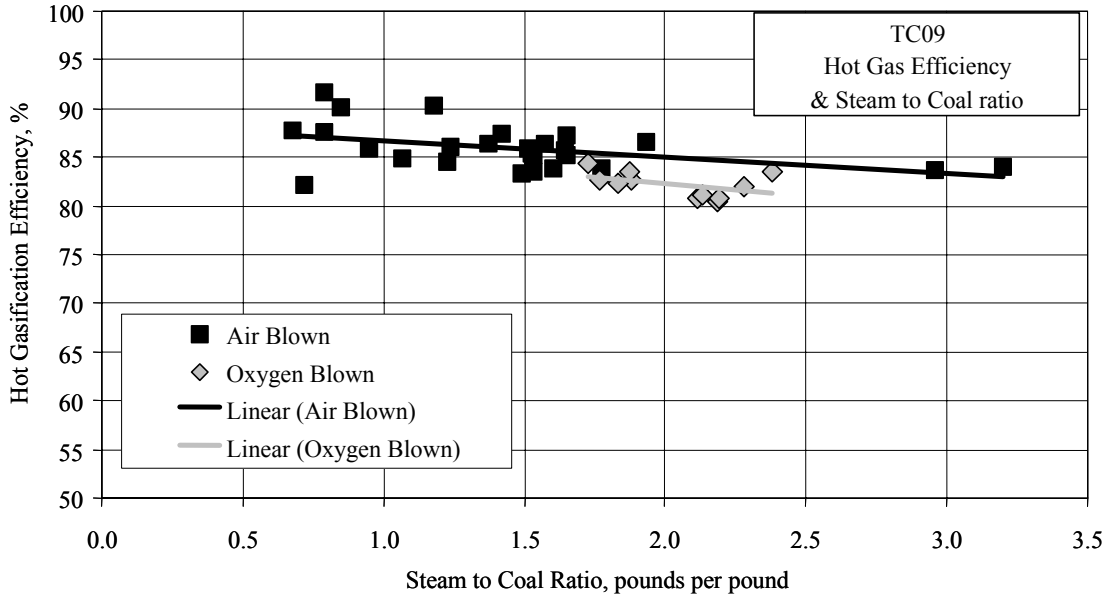

Figure 4.5-26 Hot-Gasification Efficiency and Steam-to-Coal Ratio

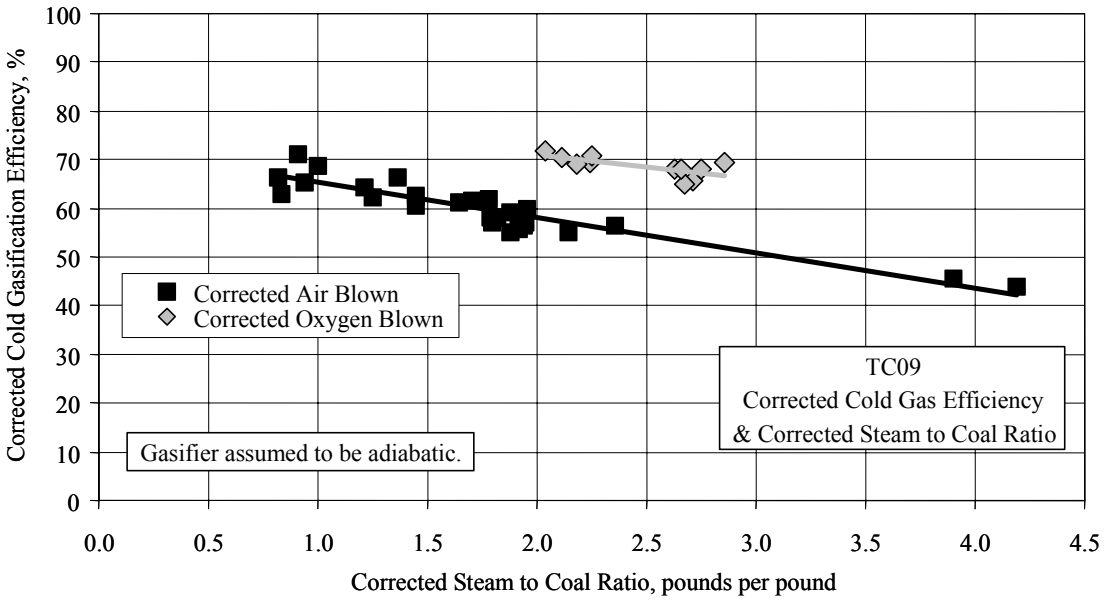

Figure 4.5-27 Nitrogen-Corrected Cold-Gasification Efficiency

4.6 ATMOSPHERIC FLUIDIZED-BED COMBUSTOR (AFBC) OPERATIONS

The Atmospheric Fluidized-Bed Combustor (AFBC) system operated for a total of 457 hours during TC09. While all hours included propane-firing with indirect heating, there were also 161 hours of g-ash feed to the AFBC and 193 hours of diesel firing. The average bed temperature during TC09 was 1,380°F, less than the design temperature of 1,600 to 1,650°F, but sufficient for g-ash combustion and sulfation.

At the beginning of TC09, there was a problem with the combustion air supply to the AFBC. The pressure drop across the air distribution grid was excessive. This was causing the AFBC compressor to run at higher than normal discharge pressures and resulted in compressor trips and difficulty in maintaining proper alignment of the drive belt. The cause was determined to be bed material plugging the grid. The bed material was forced into the grid during the preceding outage when the outlet valve was inadvertently closed and increasing pressure forced solids into the grid. The problem was fixed by lining up the main air compressor to the AFBC and using the higher pressure to blow the solids out of the grid. The compressor, distribution grid, and AFBC worked well for the rest of the run.

TC09 was a typical AFBC run. The bed temperature profile from TC09 is shown in Figure 4.6-1. As stated above, the bed temperature was a bit lower than design for the run. The temperature profile shows that the bed is well mixed. A related and interesting effect of operating the bed at a lower temperature is shown in Figure 4.6-2. Temperature profiles indicate that much of the combustion in the AFBC takes place in the freeboard space above the bed. The difference in temperature between the bed and the cyclone exit decreases with increasing temperature.

Some excess bed material continues to be lost to the baghouse during operation. Figure 4.6-3 shows the pressure drop across the bed for TC09. In general, an increase in pressure drop across the bed is indicative of an increase in bed height due to sand addition. Additional sand was added to the AFBC nine times during TC09 to replace the bed material. The extra sand needed during TC09 was partially influenced by collecting drums of g-ash for research purposes rather than feeding it to the AFBC.

The last few days of TC09 also saw the unexpected increase of unburned carbon in the solids leaving the AFBC. Figure 4.6-4 plots the LOI of the g-ash and of the AFBC ash in TC09. The plot also shows LOI of g-ash in the feed (FD0520 sample) to the AFBC. It ranges from about 10 to 50 percent. During most of the operating periods, the LOI of the fine ash in the AFBC exit stream (FD0820 sample) is near zero. The last 3 days show a sharp rise from about 0 to 10 percent in the LOI of the AFBC ash captured in the baghouse and transported to the ash silo via FD0820.

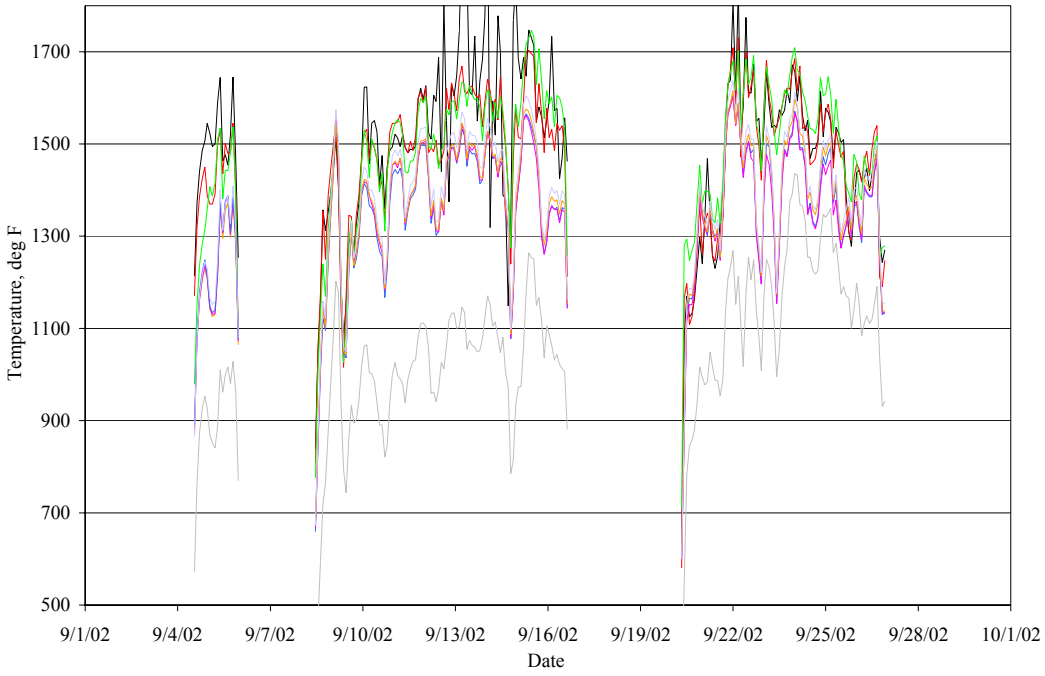

Figure 4.6-1 Temperature Profile of Bed

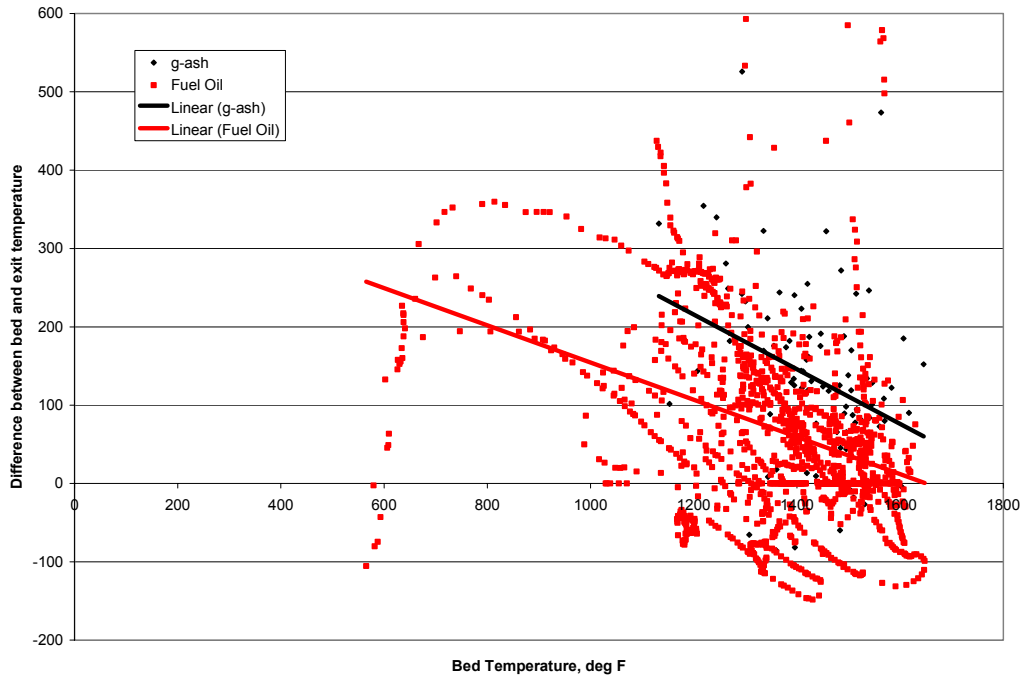

Figure 4.6-2 Effect of Bed Temperature on Difference Between Freeboard and Bed Temperatures

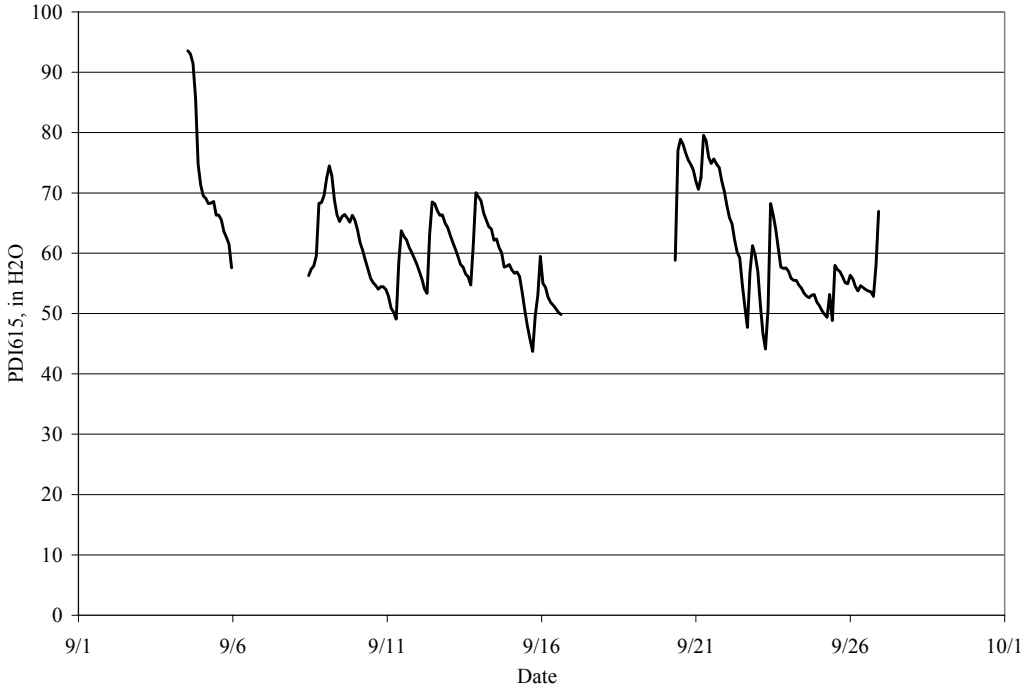

Figure 4.6-3 Pressure Profile of Bed

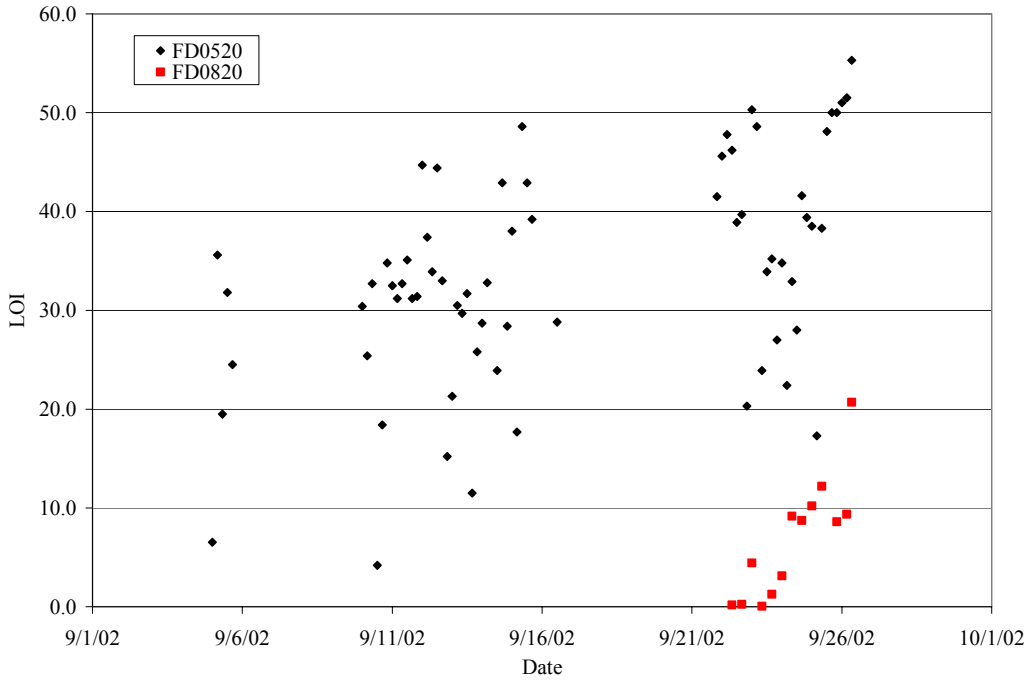

Figure 4.6-4 LOI of Gasification and AFBC Ash

4.7 PROCESS GAS COOLERS

Heat transfer calculations were done on the Primary Gas Cooler, HX0202, and the Secondary Gas Cooler, HX0402, to determine if their performance had deteriorated during TC09 due to tar or other compounds depositing on the tubes.

The Primary Gas Cooler, HX0202, is between the Transport Gasifier cyclone, CY0201, and the Siemens Westinghouse PCD, FL0301. During TC09, HX0202 was not bypassed, and took the full gas flow from the Transport Gasifier. The Primary Gas Cooler is a single flow heat exchanger with hot gas from the Transport Gasifier flowing through the tubes and the shell side operating with the plant steam system. The pertinent equations are:

$$Q = UA\Delta T_{LM} \tag{1}$$

$$Q = c_p M(T_1 - T_2) \tag{2}$$

$$\Delta T_{LM} = \frac{(T_1 - t_2) - (T_2 - t_1)}{\ln \frac{(T_1 - t_2)}{(T_2 - t_1)}} \tag{3}$$

Q = Heat transferred, Btu/hour
U = Heat transfer coefficient, Btu/hr/ft^2/°F
A = Heat exchanger area, ft^2
ΔT_{LM} = Log mean temperature difference, °F
c_p = Gas heat capacity, Btu/lb/°F
M = Mass flow of gas through heat exchanger, lb/hr
T_1 = Gas inlet temperature, °F
T_2 = Gas outlet temperature, °F
t_1 = t_2= Steam temperature, °F

Using Equations (1) through (3) and the process data, the product of the heat transfer coefficient and the heat exchanger area (UA) can be calculated. The TC09 HX0202 UA is shown on Figure 4.7-1 as 4-hour averages, along with the design UA of 5,200 Btu/hr/°F and the pressure drop across HX0202. If HX0202 is plugging, the UA should decrease and the pressure drop should increase. The UA deterioration is a better indication of heat exchanger plugging because the pressure drop is calculated by the difference of two pressure transmitters that generally have numbers of about the same size, usually from 150 to 240 psig, resulting in pressure drops of 1 to 3 psi.

The TC09 UA was elevated 5,700 to 6,700 Btu/hr/°F, during the first 16 hours of operation. After that, the UA settled down to a very steady 4,700 to 5,200 Btu/hr/°F for the next 144 hours until the unit was shut down to inspect the PCD before beginning

oxygen-blown operation. During the 40 hours of air-blown operation after the restart, the UA was again up in the 5,800 to 6,800 Btu/hr/°F range. When the gasifier transitioned to oxygen-blown operation around hour 200, the UA dropped and remained in the range of 3,900 to 4,400 Btu/hr/°F for the remainder of the run, excluding a few hours of air-blown operation immediately before shutting down. During all except about 60 hours of the test, HX0202 operated below the design UA of 5,200 Btu/hr/°F.

Early in TC09, the pressure drop across HX0202 increased until reaching a maximum of 2.9 psi after 16 hours. After that, the pressure drop declined to 1.6 psi and stayed in the range of 1.5 to 2.3 psi until the unit was shut down to inspect the PCD. When the gasifier was restarted, the pressure drop was very unsteady, swinging from as low as 1.9 psi up to 4.0 psi. After moving to oxygen-blown operation, the pressure drop was 1.5 to 2.1 psi for the rest of the run. The periods of higher pressure drop and higher UA values both coincided with each other and with periods of higher syngas flow. There was not any evidence of plugging in HX0202 during TC09.

During most of TC09, the UA hovered just below the design UA of 5,200 Btu/hr/°F, while in TC08, the UA hovered just above design for most of the run. The pressure drop in TC09, 1.5 to 2.3 psi for most of the run, was higher than the pressure drop in TC08 of 0.5 to 1.5 psi, but comparable or slightly lower than the 1.0 to 3.3 psi pressure drop in TC07.

The Secondary Gas Cooler, HX0402, is a single flow heat exchanger with hot gas from the PCD flowing through the tubes and the shell side operating with plant steam system. Some heat transfer and pressure drop calculations were done around HX0402 to determine if there was any plugging or heat exchanger performance deterioration during TC09. HX0402 is not part of the combustion gas turbine commercial flow sheet. In the commercial gas turbine flow sheet, the hot synthesis gas from the PCD would be directly sent to a combustion gas turbine. HX0402 would be used commercially if the synthesis gas was to be used in a fuel cell or as a chemical plant feedstock.

Using Equations (1) through (3) and the process data, the product of the heat transfer coefficient and the UA can be calculated. The UA for TC09 testing is shown on Figure 4.7-2 as 2-hour averages, along with the design UA of 13,100 Btu/hr/°F and the pressure drop across HX0402. If HX0402 is plugging, the UA should decrease and the pressure drop should increase.

During the first 200 hours of TC09, the air-blown portion, the UA of HX0402 was around or just above the design UA of 13,100 Btu/hr/°F. The range of values in this time was 12,600 to 15,100 Btu/hr/°F. Once the gasifier started oxygen-blown operations, the UA decreased to a range of 10,200 to 10,800 Btu/hr/°F.

The pressure drop across HX0402 was also tied to the operating environment of the gasifier. During the first 200 hours of air-blown operation, the pressure drop was 2.2 to 3.3 psi although it generally increased as the run progressed. During the oxygen-blown operation the pressure drop decreased to 1.2 to 1.8 psi with the lower gas flows.

The UA of TC09 compared closely to that of TC08. During the air-blown part of TC09, the UA for HX0402 was 12,600 to 15,100 Btu/hr/°F, and during TC08 the UA was 13,300 to 14,400 Btu/hr/°F. In oxygen-blown mode, TC09 saw a UA of 10,200 to 10,800 Btu/hr/°F, and TC08 of 11,000 to 11,800 Btu/hr/°F, both below the design value. The pattern was the same for the pressure drop with air-blown operation having pressure drops around 3.0 psi and oxygen-blown operation having a pressure drop around 1.6 psi.

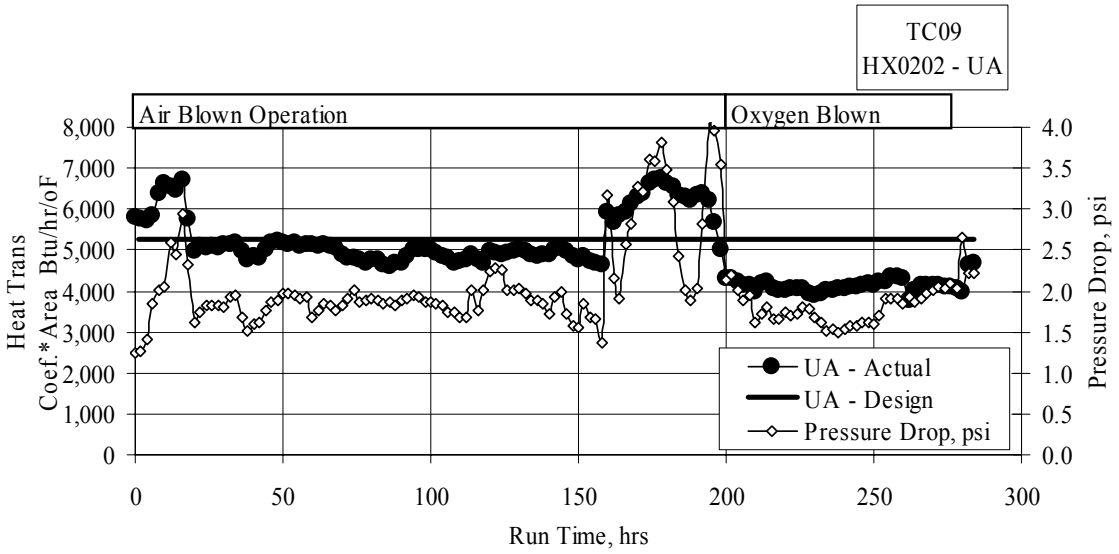

Figure 4.7-1 HX0202 Heat Transfer Coefficient and Pressure Drop

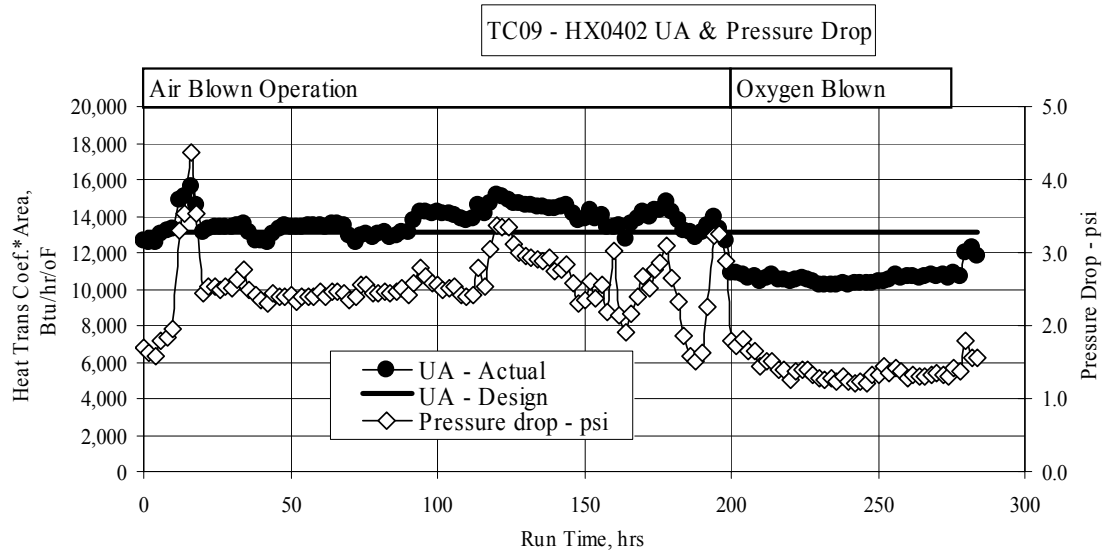

Figure 4.7-2 HX0402 Heat Transfer Coefficient and Pressure Drop

TERMS

Listing of Abbreviations

AAS	Automated Analytical Solutions
ADEM	Alabama Department of Environmental Management
AFBC	Atmospheric Fluidized-Bed Combustor
APC	Alabama Power Company
APFBC	Advance Pressurized Fluidized-Bed Combustion
ASME	American Society of Mechanical Engineers
AW	Application Workstation
BET	Brunauer-Emmett-Teller (nitrogen-adsorption specific surface technique)
BFI	Browning-Ferris Industries
BFW	Boiler Feed Water
BMS	Burner Management System
BOC	BOC Gases
BOP	Balance-of-Plant
BPIR	Ball Pass Inner Race, Frequencies
BPOR	Ball Pass Outer Race, Frequencies
BSF	Ball Spin Frequency
CAD	Computer-Aided Design
CAPTOR	Compressed Ash Permeability Tester
CEM	Continuous Emissions Monitor
CFB	Circulating Fluidized Bed
CFR	Code of Federal Regulations
CHE	Combustor Heat Exchanger
COV	Coefficient of Variation (Standard Deviation/Average)
CPC	Combustion Power Company
CPR	Cardiopulmonary Resuscitation
CTE	Coefficient of Thermal Expansion
DC	Direct Current
DCS	Distributed Control System
DHL	DHL Analytical Laboratory, Inc.
DOE	U.S. Department of Energy
DSRP	Direct Sulfur Recovery Process
E & I	Electrical and Instrumentation
EDS or EDX	Energy-Dispersive X-Ray Spectroscopy
EERC	Energy and Environmental Research Center
EPRI	Electric Power Research Institute
ESCA	Electron Spectroscopy for Chemical Analysis
FCC	Fluidized Catalytic Cracker
FCP	Flow-Compacted Porosity
FFG	Flame Front Generator
FI	Flow Indicator
FIC	Flow Indicator Controller
FOAK	First-of-a-Kind
FTF	Fundamental Train Frequency

FW	Foster Wheeler
GBF	Granular Bed Filter
GC	Gas Chromatograph
GEESI	General Electric Environmental Services, Inc.
HHV	Higher Heating Valve
HP	High Pressure
HRSG	Heat Recovery Steam Generator
HTF	Heat Transfer Fluid
HTHP	High-Temperature, High-Pressure
I/O	Inputs/Outputs
ID	Inside Diameter
IF&P	Industrial Filter & Pump
IGV	Inlet Guide Vanes
IR	Infrared
KBR	Kellogg Brown & Root, Inc.
LAN	Local Area Network
LHV	Lower Heating Valve
LIMS	Laboratory Information Management System
LMZ	Lower Mixing Zone
LOC	Limiting Oxygen Concentration
LOI	Loss on Ignition
LPG	Liquefied Propane Gas
LSLL	Level Switch, Low Level
MAC	Main Air Compressor
MCC	Motor Control Center
MMD	Mass Median Diameter
MS	Microsoft Corporation
NDIR	Nondestructive Infrared
NETL	National Energy Technology Laboratory
NFPA	National Fire Protection Association
NO_X	Nitrogen Oxides
NPDES	National Pollutant Discharge Elimination System
NPS	Nominal Pipe Size
OD	Outside Diameter
ORNL	Oak Ridge National Laboratory
OSHA	Occupational Safety and Health Administration
OSI	OSI Software, Inc.
P&IDs	Piping and Instrumentation Diagrams
PC	Pulverized Coal
PCD	Particulate Control Device
PCME	Pollution Control & Measurement (Europe)
PDI	Pressure Differential Indicator
PDT	Pressure Differential Transmitter
PFBC	Pressurized Fluidized-Bed Combustion
PI	Plant Information
PLC	Programmable Logic Controller
PPE	Personal Protection Equipment

PRB	Powder River Basin
PSD	Particle Size Distribution
PSDF	Power Systems Development Facility
ΔP or DP or dP	Pressure Drop or Differential Pressure
PT	Pressure Transmitter
RAPTOR	Resuspended Ash Permeability Tester
RFQ	Request for Quotation
RO	Restriction Orifice
RPM	Revolutions Per Minute
RSSE	Reactor Solid Separation Efficiency
RT	Room Temperature
RTI	Research Triangle Institute
SCS	Southern Company Services, Inc.
SEM	Scanning Electron Microscopy
SGC	Synthesis Gas Combustor
SGD	Safe Guard Device
SMD	Sauter Mean Diameter
SRI	Southern Research Institute
SUB	Start-up Burner
TCLP	Toxicity Characteristic Leaching Procedure
TR	Transport Reactor
TRDU	Transport Reactor Demonstration Unit
TRS	Total Reduced Sulfur
TSS	Total Suspended Solids
UBP	Uncompacted Bulk Porosity
UMZ	Upper Mixing Zone
UND	University of North Dakota
UPS	Uninterruptible Power Supply
UV	Ultraviolet
VFD	Variable Frequency Drive
VOCs	Volatile Organic Compounds
WGS	Water-Gas Shift
WPC	William's Patent Crusher
XRD	X-Ray Diffraction
XXS	Extra, Extra Strong

Listing of Units

acfm	actual cubic feet per minute
Btu	British thermal units
°C	degrees Celsius or Centigrade
°F	degrees Fahrenheit
ft	feet
FPS	feet per second
gpm	gallons per minute
g/cm^3 or g/cc	grams per cubic centimeter
g	grams
GPa	gigapascals
hp	horsepower
hr	hour
in.	inches
inWg (or inWc)	inches, water gauge (inches, water column)
in.-lb	inch pounds
°K	degrees Kelvin
kg	kilograms
kJ	kilojoules
kPa	kilopascals
ksi	thousand pounds per square inch
m	meters
MB	megabytes
min	minute
mm	millimeters
MPa	megapascals
msi	million pounds per square inch
MW	megawatts
m/s	meters per second
MBtu	Million British thermal units
m^2/g	square meters per gram
μ or μm	microns or micrometers
dp_{50}	particle size distribution at 50 percentile
ppm	parts per million
ppm (v)	parts per million (volume)
ppm (w)	parts per million (weight)
lb	pounds
pph	pounds per hour
psi	pounds per square inch
psia	pounds per square inch absolute
psid	pounds per square inch differential
psig	pounds per square inch gauge
ΔP	pressure drop
rpm	revolutions per minute
s or sec	seconds
scf	standard cubic feet

scfh	standard cubic feet per hour
scfm	standard cubic feet per minute
V	volts
W	watts